THEORETICAL CHEMISTRY INSTITUTE

THE UNIVERSITY OF WISCONSIN

INTERATOMIC FORCES FROM SPECTRAL DATA, AND UTILIZATION OF POTENTIAL CURVES IN SPECTROSCOPY, SCATTERING AND KINETICS

Robert James Le Roy

WIS-TCI-428

15 January 1971

MADISON, WISCONSIN

INTERATOMIC FORCES FROM SPECTRAL DATA, AND UTILIZATION OF POTENTIAL CURVES IN SPECTROSCOPY, SCATTERING AND KINETICS

by

Robert James Le Roy

A thesis submitted in partial fulfillment of the requirements

for the degree of

Doctor of Philosophy

(Chemistry)

at the

University of Wisconsin

1971

INTERATOMIC FORCES FROM SPECTRAL DATA, AND UTILIZATION OF POTENTIAL CURVES IN SPECTROSCOPY, SCATTERING AND KINETICS*

by

Robert James Le Roy†

(under the supervision of Professor Richard B. Bernstein)

ABSTRACT

Part I considers divers means of determining diatomic potential curves, placing particular emphasis on utilization of the spectroscopically-observed distribution of vibrational-rotational energy levels. The widely-used RKR procedure is applied to ground-state $(X\ ^1\Sigma_g^+)I_2$. A new approach is introduced which allows the determination of the dissociation limit and long-range potential tail from the distribution of the uppermost vibrational levels. It also yields a simple expression for the vibrational spacings which leads to a "better than Birge-Sponer" plot for determining the dissociation limit. These procedures were applied successfully to $B(^3\Pi_{0u}^+)$-state $C\ell_2$, Br_2 and I_2. Other methods for the determination of diatomic potentials are reviewed, including one utilizing 3-body atomic recombination rate

- - - - - - - - - - - - - - - - - - -

*Work supported by National Science Foundation Grant GB-16665 and National Aeronautics and Space Administration Grant NGL 50-002-001.

†National Research Council of Canada Scholarship holder, 1969-71.

constants.

The best known ab initio diatomic potential is that calculated by Kołos and Wolniewicz (KW) for ground-state molecular hydrogen. Nevertheless, a comparison of the calculated and observed vibrational energy levels indicated that a small correction is required by the KW potential; this is evaluated empirically.

Part II of the thesis considers a number of problems in which a knowledge of the appropriate potential curves allows a better understanding of certain physical phenomena. Application of the new method of Part I leads to a reassignment of some I_2 uv lines emitting into a shallow van der Waals excited state with a potential hump.

A study was made of spectroscopic and scattering-theory manifestations of the quasibound diatomic levels which lie above the dissociation limit, but are bound by a potential barrier. Results of illustrative computations are presented for ground-state molecular hydrogen, showing extensive barrier penetration. This implies that Bernstein's method of extracting long-range potentials from rotational predissociation data should not be applied to hydridic diatomics. The eigenvalues, and the expectation values of R, R^2, R^{-2} and kinetic energy are calculated for all bound and quasibound levels of ground-state H_2, HD and D_2, using the ab initio relativistic-adiabatic potential of Kołos and Wolniewicz.

A method for calculating exact tunnelling probabilities for one-dimensional potential barriers is presented and used to test Bell's approximate tunnelling factor formulae for truncated parabolic barriers.

Most of the results in this thesis have by now been published.

to Virginia

who makes so much possible

ACKNOWLEDGEMENTS

It is a great pleasure to acknowledge my immense debt to Professor Richard B. Bernstein, whose astute and ebullient approach to research has so guided and matured my own. His friendship and generosity have contributed considerably to making my stay in Madison pleasant, as well as profitable.

I would like to express my gratitude to Professor George Burns, who introduced me to the rewarding rigors of independent research.

I must register a tremendous debt of thanks to my parents, who managed in the course of a happy upbringing to confront me with the realization that hard intellectual effort is an appealing pastime.

I am greatly beholden to Professor J. O. Hirschfelder for providing the extensive facilities and stimulating atmosphere of the Theoretical Chemistry Institute, and for a number of illuminating discussions. In addition, I have benefitted considerably over the past four years from interactions with Professors S. T. Epstein and J. P. Walters, and correspondence with Professors W. C. Stwalley, R. D. Verma and J. I. Steinfeld. Concurrently, I have gained a great deal from my contacts with my fellow students and postdoctoral fellows, particularly Drs. A. S. Dickinson, M. T. Marron, M. D. Pattengill and J. T. Muckerman, and Messrs. J. R. Miller and R. A. La Budde, and all members of the molecular beam research group.

I am also very grateful to the staff of the Theoretical Chemistry Institute, particularly Sheila Battle and Candy Spencer, for their many favors and considerable tolerance over the past quadrennium.

TABLE OF CONTENTS

1. INTRODUCTION

Knowledge of intermolecular forces is a prerequisite to a basic understanding of most of the physical and chemical properties of matter. However, although the formal theory for the calculation of many observable properties is well known,[1-3] accurate potentials are available for a relatively limited number of systems. It now appears as if the need for such potentials will not be answered by a priori calculations in the near future. Only for the two simplest molecular systems, H_2 and He_2, have such theoretical potentials achieved accuracy as good as, or better than that of potentials obtained empirically by inverting experimental data.[4] On the other hand, a growing number of routes to the potential function from experimental data are being developed.[2,3]

The present discussion is concerned only with the simplest class of interactions, those which may be treated mathematically as one-dimensional problems. This means, in effect, the isotropic interactions of isolated pairs of atoms, although applications to complicated problems which are only approximately reducible to one mathematical dimension are also considered.

The presentation is divided into two parts, the first of which is concerned with the determination of interatomic potentials by "inversion" of experimental data. The greatest emphasis here is on the utilization of the spectroscopically-measured distribution of vibrational-rotational diatomic energy levels. Considered are the already widely used RKR procedure,[9] and a new method which focuses attention on the uppermost vibrational levels, yielding an estimate of the long-range potential

tail and accurately locating the dissociation limit. Other approaches are reviewed, including an indirect method based on measured rate constants for atomic recombination. In a slightly different vein, the accuracy of Kołos and Wolniewicz's[5] *à priori* potential for ground-state H_2 is examined by comparing calculated and observed vibrational energy levels. This leads to the suggestion of an empirical correction to be added to the theoretical potential.

The second part of the thesis considers a number of problems which implicitly assume knowledge, of different degrees of completeness, about the potential function. First, application of the new method of Part I is coupled with theoretical knowledge of long-range interatomic forces to facilitate the untangling of some hitherto confused spectroscopic assignments. Next, a study is presented of the manifestations, spectroscopically and via scattering, of the quasibound diatomic vibrational-rotational levels which lie above the dissociation limit, but are partially bound by a potential barrier. Significant tunneling is found for ground-state H_2, HD, and D_2, implying that Bernstein's[10] method of extracting long-range potentials from rotational predissociation data should not be applied to hydrides (or deuterides). The Kołos and Wolniewicz[5] potential for ground state molecular hydrogen is then utilized in the calculation of the eigenvalues, and expectation values of kinetic energy and various powers of R for all the bound and quasibound levels of H_2, HD, and D_2. Finally, a method of calculating exact tunneling probabilities for arbitrary one-dimensional potential barriers is presented. It is then used to delineate

the range of validity of Bell's[11] widely used[12] approximate formulae for tunneling through inverted parabolic barriers.

Much of the following consists of reprints of already published material, or reports; some of the latter will be submitted for publication. As a result, each section is self-contained with its own figures, tables, and footnotes and references.

FOOTNOTES

1. J. O. Hirschfelder, C. F. Curtiss, and R. B. Bird, Molecular Theory of Gases and Liquids (John Wiley and Sons, Inc., New York, 1964).
2. J. Ross (editor), Adv. Chem. Phys. 10 (Molecular Beams, Interscience Publishers, New York, 1966).
3. J. O. Hirschfelder (editor), Adv. Chem. Phys. 12 (Intermolecular Forces, Interscience Publishers, New York, 1967).
4. The Kołos and Wolniewicz[5] variational potential for ground-state H_2 has a better dissociation energy than the best spectroscopic value existing[6] when it was published. Although this situation has since been reversed by Herzberg's[7] new measurements, the theoretical value is still within one cm^{-1} of experiment. For He_2, two groups[8] recently simultaneously published independent calculations in good agreement with each other and with the best empirical potentials.
5. a) W. Kołos and L. Wolniewicz, J. Chem. Phys. 41, 3663 (1964); b) ibid. 43, 2429 (1965); ibid. 49, 404 (1968).

6. G. Herzberg and A. Monfils, J. Mol. Spectry. 5, 482 (1960).

7. G. Herzberg, J. Mol. Spectry. 33, 147 (1970); see also the reanalysis of his data by W. C. Stwalley, Chem. Phys. Lett. 6, 241 (1970).

8. a) H. F. Schaefer, III, D. R. McLaughlin, F. E. Harris, and B. J. Alder, Phys. Rev. Lett. 25, 988 (1970); b) P. Bertoncini and A. C. Wahl, Phys. Rev. Lett. 25, 991 (1970).

9. See, e.g., the discussion by E. A. Mason and L. Monchick in Chapter 7 of Ref.(3).

10. R. B. Bernstein, Phys. Rev. Lett. 16, 385 (1966).

11. R. P. Bell, Trans. Faraday Soc. 55, 1 (1959).

12. See, e.g., E. F. Caldin, Chem. Rev. 69, 135 (1969).

PART I

THE EMPIRICAL DETERMINATION OF INTERATOMIC POTENTIALS

2. THE RKR METHOD: POTENTIALS FROM VIBRATIONAL-ROTATIONAL DATA

2.1 DISCUSSION OF THE METHOD

The Rydberg-Klein-Rees (RKR) procedure[1] allows the determination of an attractive diatomic potential below the dissociation limit from its known vibrational-rotational energy level spectrum. It is the simplest and most accurate method known for determining the "bowl" of a potential, and in the past decade it has been very successfully applied to a wide variety of systems.[2,3]

In this approach, pairs of classical turning points lying on the potential are calculated at energies corresponding to chosen values (usually integer) of the vibrational index, v . The inner (R_-) and outer (R_+) turning points at the energy corresponding to a given value of v are

$$R_{\pm}(v) = K \left\{ \left[\bar{f}(v)^2 + \bar{f}(v)/\bar{g}(v) \right]^{\frac{1}{2}} \pm \bar{f}(v) \right\} \quad [\text{Å}] , \qquad (1)$$

where

$$\bar{f}(v) = \int_{-\frac{1}{2}}^{v} [G(v) - G(x)]^{-\frac{1}{2}} \, dx , \qquad (2a)$$

$$\bar{g}(v) = \int_{-\frac{1}{2}}^{v} B_x \, [G(v) - G(x)]^{-\frac{1}{2}} \, dx , \qquad (2b)$$

and

$$K = \left\{ \hbar/4\pi c\mu \right\}^{\frac{1}{2}} = \left\{ 16.85803/\mu \right\}^{\frac{1}{2}} \, [\text{Å}^2 \ \text{cm}^{-1}]^{\frac{1}{2}} \qquad (3)$$

Here the standard vibrational energies G(v) and rotational constants B_v are both in cm^{-1}, and the reduced mass of the nuclei, μ, is in amu (^{12}C). The physical constants collected in the numerical factor in Eq.(3) were taken from Ref.(4).

Nuclear vs Atomic Reduced Mass

There is some disagreement in the literature over whether the reduced mass used in Eq.(3) should be that of the two nuclei, or of the two atoms.[5] This is equivalent to the question of which mass should be used in the radial Schrödinger equation, of which Eqs.(1-3) is a WKB-based inversion. Consideration of the separation of electronic and nuclear motion in the total Hamiltonian shows that in the clamped nuclei (simple Born-Oppenheimer) and adiabatic approximations, the resulting radial Schrödinger equation depends only on the nuclear reduced mass.[6,7] On the other hand, Herman and Asgharian's[8] perturbation treatment of the exact Hamiltonian for nuclei and electrons yielded a separable effective radial Schrödinger equation depending mainly on the atomic reduced mass, but with correction terms depending on the ratio of the atomic to the nuclear reduced mass. While this question is not yet fully resolved, the work presented here (in Section 2.2) uses the nuclear reduced mass.

Corrections to Calculated Turning Points

It is apparent from consideration of Eqs.(1-3) that any error in the assumed values of the physical constants or reduced mass affects calculated RKR turning points only through the multiplicative factor

K in Eq.(1). This is particularly important in view of the uncertainty as to which reduced mass (atomic or nuclear) should be used.[9] Clearly, such errors are simply removed by multiplying all the calculated turning points by the numerical factor

$$K(\text{corrected}) \;/\; K(\text{initial}).$$

This approach will be found useful in Section 2.2 .

Combined Isotope RKR Calculation

A fact apparently not previously noted is that experimental data for different isotopes of a particular species can be used together in an RKR calculation of the internuclear potential for a given electronic state. The necessary assumption, valid within the clamped nuclei approximation,[6] is that the different isotopes are subject to precisely the same internuclear potential. For all non-hydrogenic molecules this is a very good approximation, and in any case, disagreement with it is probably less than the error implicit in the use of the WKB approximation on which the RKR method is based.[11]

According to the WKB approximation,[13] in a given potential well the energy corresponding to vibrational index v_i of isotope-i precisely corresponds to index

$$v_j(i) = (\mu_j/\mu_i)^{\frac{1}{2}}\, v_i \qquad (4)$$

of isotope-j. Thus the experimental G(v) and B_v data for isotope-i ($i \neq j$) may be treated simply as additional isotope-j data at the (usually non-integer) vibrational index $v_j(i)$.[14] Combining the data

in this manner should give smoother and more accurate G(v) and B_v functions, covering a wider range than for any of the isotopes considered alone. This means that more accurate and extensive $\overline{f}(v)$ and $\overline{g}(v)$ functions and turning points will be obtained. In addition, the quadratures will only have to be evaluated once for a given state of a particular chemical species.

An example of the type of situation in which this "combining isotopes" approach may be particularly fruitful is the $B(^3\Pi^+_{0u})$ state of Br_2. Here there exist fairly accurate vibrational energies (reported to 0.01 cm^{-1}) and B_v values for levels v' = 1-9 of $^{79,79}Br_2$,[15] and for v' = 9-19 and 50-53 of both of the pure isotopes $^{79,79}Br_2$ and $^{81,81}Br_2$.[16,17] In addition much less accurate band-head energies ("not accurate to better than 2 cm^{-1}") for the mixed isotope $^{79,81}Br_2$ are available for the intermediate region v' = 20-48.[19] Combining these data as suggested above should give the best RKR curve currently obtainable for this state. This approach could also be very profitably applied to $Br_2(X\ ^1\Sigma^+_g)$ for which the existing data are quite analogous to those for the B-state.[15]

FOOTNOTES

1. a) R. Rydberg, Z. Physik 73, 376 (1931); ibid, 80, 514 (1933); b) O. Klein, Z. Physik 76, 226 (1932); c) A. L. G. Rees, Proc. Phys. Soc. (London) 59, 998 (1947).

2. See, e.g.; a) E. A. Mason and L. Monchick, Adv. Chem. Phys. 12 (Intermolecular Forces), 329 (1967), §IIIA and references mentioned therein; b) J. I. Steinfeld, R. N. Zare, L. Jones, M. Lesk, and W. Klemperer, J. Chem. Phys. 42, 25 (1965); c) R. J. Spindler, Jr., J. Quant. Spectry. Radiat. Transf. 9, 597, 627, 1041 (1970); d) J. A. Coxon, J. Quant. Spectry. Radiat. Transf. (in press).

3. R. J. Le Roy, J. Chem. Phys. 52, 2683 (1970); see Section 2.2 .

4. B. N. Taylor, W. H. Parker, and D. N. Langenberg, Rev. Mod. Phys. 41, 375 (1969).

5. The nuclear reduced mass was used in Ref.(3), while atomic reduced masses were definitely used in Ref.(2d), and probably also in the other work referred to in footnote (2).

6. See, e.g., J. O. Hirschfelder and W. J. Meath, Adv. Chem. Phys. 12, (Intermolecular Forces), 3 (1967).

7. L. Wolniewicz, J. Chem. Phys. 45, 515 (1966), and references therein.

8. R. M. Herman and A. Asgharian, J. Mol. Spectry. 19, 305 (1966).

9. For the inverse problem of determining vibrational-rotational eigenvalues from a known potential, it is readily shown that the first-order error in an eigenvalue arising from use of the wrong reduced mass is the product of the relative error in the mass used, times the expectation value of the kinetic energy of the level considered:

$$\Delta E = \left\{\frac{\mu(\text{right})}{\mu(\text{wrong})} - 1\right\} \langle T_{v,j} \rangle$$

For ground-state H_2, a change from atomic to nuclear reduced mass yields level shifts as large as 5.6 cm^{-1}.[10]

10. R. J. Le Roy and R. B. Bernstein, J. Chem. Phys. 49, 4312 (1968); see Section 5.

11. The dominant correction to the clamped nuclei approximation, the diagonal correction for nuclear motion (adiabatic correction) is relatively small and varies directly as the inverse of the isotopic nuclear reduced mass. For the worst possible case, H_2 , Kołos and Wolniewicz[12] have calculated this quantity for the ground electronic state. In this case, below the dissociation limit the effective correction has a maximum of 25 cm^{-1}, a minimum of -18 cm^{-1}, and approached zero at large R .

12. W. Kołos and L. Wolniewicz, J. Chem. Phys. 41, 3663 (1964).

13. See, e.g., a) E. Merzbacher, Quantum Mechanics (John Wiley and Sons, New York, 1961), Chapter 7; b) A. S. Davydov, Quantum Mechanics Pergamon Press, London, 1965), §25; c) D. R. Bates, Quantum Theory: I. Elements (Academic Press, New York, 1961), Chapter 7.

14. This assumes that the vibrational energies are all expressed on the same absolute scale, such as relative to the potential minimum.

15. J. A. Coxon, J. Mol. Spectry. (in press).

16. J. A. Horsley and R. F. Barrow, Trans. Faraday Soc. 63, 32 (1967).

17. The four highest observed levels have recently been reassigned as v' = 50-53, increasing the experimentalists'[16] numbering by one.[15,18]

18. R. J. Le Roy and R. B. Bernstein, J. Mol. Spectry. (1971, in press); see Section 3.2 .

19. W. G. Brown, Phys. Rev. 38, 1179 (1931).

2.2 RKR POTENTIAL FOR GROUND-STATE $I_2(X\ ^1\Sigma_g^+)$

A detailed reanalysis of existing spectroscopic data for ground-state I_2 was performed, yielding improved molecular constants and RKR turning points. This work, reprinted below, was published in the Journal of Chemical Physics, Volume 52, pp. 2683-2689 (American Institute of Physics, New York, 1970).

Unfortunately, when this work was done the best existing values of the physical constants[1] and the reduced mass of the nuclei[2] were not used in the RKR calculation. However, as discussed in Section 2.1, the reported turning points (in Table III, below) may be corrected by multiplying them all by the factor

$$\frac{K(\text{corrected})}{K(\text{initial})} = \left\{\frac{16.85803}{16.85749} \times \frac{63.437700}{63.437697}\right\}^{\frac{1}{2}} = 1.0000160 .$$

FOOTNOTES

1. B. N. Taylor, W. H. Parker, and D. N. Langenberg, Rev. Mod. Phys. 41, 375 (1969).

2. J. H. E. Mattauch, W. Thiele, and A. H. Wapstra, Nucl. Physics 67, 1 (1965).

Reprinted from THE JOURNAL OF CHEMICAL PHYSICS, Vol. 52, No. 5, 2683–2689, 1 March 1970
Printed in U. S. A.

Molecular Constants and Internuclear Potential of Ground-State Molecular Iodine*

ROBERT J. LEROY

Theoretical Chemistry Institute and Department of Chemistry, University of Wisconsin, Madison, Wisconson 53706

(Received 3 September 1969)

A reanalysis of the spectroscopic data for ground-state iodine yields improved rotational constants and vibrational energies which are used to compute a new RKR potential. Polynomial representations of the vibrational energies and rotational constants are presented which fit all the data to within the respective experimental precision of Verma and of Rank and Baldwin. New approaches are introduced for separately obtaining the rotational B_v and D_v constants and for estimating error bounds for computed RKR turning points.

INTRODUCTION

In 1960 Verma[1] reported some remarkable measurements of several series of uv-resonance emission doublets in the spectrum of I_2, excited in an electric discharge. Although the final state of one of these resonance series has recently been reassigned as $0_g^+(^3\Pi)$,[2] the remaining lines thoroughly catalogue the levels of ground-state $X\ 0_g^+(^1\Sigma)I_2$ up to within 4% of the dissociation limit. Because of this remarkably complete set of data, the ground state of I_2 has become almost a touchstone of RKR potential calculations.[1,3–5]

In the present work, the data for the ground state are handled somewhat differently than was done previously, and discrepancies of up to 6.6 cm^{-1} were found between the vibrational energies obtained here and the earlier results.[1] Since the reported ground-state RKR potential curves[1,3–5] are based on this earlier energy spectrum,[1] all will be somewhat in error. Furthermore, most of these curves[1,3,4] were calculated all the way to the dissociation limit by utilizing the energies of a set of levels which recently has been reassigned to another electronic state.[2] An improved energy spectrum and RKR potential will be presented which are based on both the uv-resonance data[1] and the more accurate, but restricted (to $v\leq 22$), green-line resonance data of Rank and Baldwin.[6]

SELECTION OF EXPERIMENTAL DATA

The raw data used in the present analysis consisted of the green-line resonance doublets measured by Rank and Baldwin[6], and five of the six uv-resonance doublet series reported by Verma.[1,8] The former measurements are relatively accurate, being reported to 0.001 cm^{-1}, though they only describe levels $v=0$–22. On the other hand, while the uv measurements span the region from $v=0$–84, they were reported only to an accuracy of 0.01 cm^{-1}. Because of this difference in precision, only the green-line data were used in determining the vibrational energies and rotational B_v constants for $v\leq 22$. In addition, all of the blended uv lines were omitted from consideration[9], as well as three lines which the present analysis suggests were misassigned.[10]

THE ROTATIONAL CONSTANTS

Values of B_v constants are obtained from the experimental P–R doublet branch splittings

$$\Delta\nu_{P-R}(v,J_r)=(4J_r+2)[B_v-2(J_r^2+J_r+1)D_v], \quad (1)$$

where $\Delta\nu_{P-R}(v,J_r)$ is the observed doublet splitting for vibrational level v, in the resonance series characterized by rotational quantum number J_r. In the original analysis of the uv data,[1] Verma tried to obtain a polynomial representation for the D_v constants by fitting the splittings for different J_r directly to (1). However, in Ref. 7 it was pointed out that this approach is not very meaningful, because the effect of the D_v values on the splittings is less than the experimental precision. On the other hand, significant information on the D_v's can still be obtained, because while the effect of this term on the doublet splittings varies as $\approx 8\times J_r^3$, its effect on the vibrational energies varies as $\approx J_r^4$. For the $J_r=87$ resonance series this difference is particularly significant.

Since the D_v constants are known to be small,[1,7] they will affect the observed splittings only slightly. Hence, to a first approximation they can be replaced by any plausible set of trial values $\{D_v^{(n)}\}$, yielding

$$B_v^{(n)}=[\Delta\nu_{P-R}(v;J_r)/(4J_r+2)]+2(J_r^2+J_r+1)D_v^{(n)}$$
$$=B_v-2(J_r^2+J_r+1)(D_v-D_v^{(n)})\approx B_v. \quad (2)$$

These estimates of the exact D_v and B_v values may then be applied to the data for resonance series $J_r=J_2$ to yield an apparent vibrational energy for level v, $G_{J_2}^{(n)}(v)$. Comparison of the apparent vibrational energies obtained from the data for two different resonance series then yields improved estimates of D_v:

$$D_v^{(n+1)}=D_v^{(n)}+\left(\frac{G_{J_1}^{(n)}(v)-G_{J_2}^{(n)}(v)}{(J_2^2+J_2)^2-(J_1^2+J_1)^2}\right)$$
$$=D_v-(D_v-D_v^{(n)})\left(\frac{2\langle J_r^2+J_r+1\rangle_v}{J_2^2+J_2+J_1^2+J_1}\right). \quad (3)$$

Here $\langle J_r^2+J_r+1\rangle_v$ is an average for the different resonance series contributing splittings at levels near v.[11]

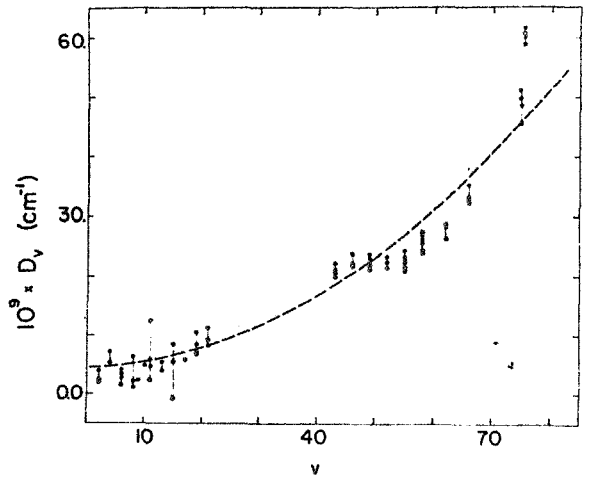

FIG. 1. D_v vs v for ground-state $X\,{}^1\Sigma_g^+$ I_2. ●, empirical points; - - -, curve from expression (5).

These $D_v^{(n+1)}$ values may then be substituted into the first part of (2) to yield improved $B_v^{(n+1)}$ values, ··· etc. The error in a $D_v^{(n)}$ value obtained after n such iterations is

$$D_v^{(n)} - D_v = (D_v^{(0)} - D_v)\left(\frac{2\langle J_r^2+J_r+1\rangle_v}{J_2^2+J_2+J_1^2+J_1}\right)^n.$$

Clearly the sequence $\{D_v^{(0)}, B_v^{(0)}\}$, $\{D_v^{(1)}, B_v^{(1)}\}$, ··· etc. will converge to the exact $\{D_v, B_v\}$ as long as

$$f \equiv 2\langle J_r^2+J_r+1\rangle_v/(J_2^2+J_2+J_1^2+J_1) < 1.$$

In applying (3), apparent vibrational energies from the $J_2=87$ resonance series were compared in turn to those yielded by each of the $J_1=49$, 46, 25, and 23 series, for all levels $0 \leq v \leq 82$.[12] In applying (2), for $v<22$ only the green-line resonance splittings were used (i.e., $J_r=34$ only)[13]; therefore, in this region $f \lesssim 0.3$ and the $\{D_v^{(n)}, B_v^{(n)}\}$ sequence will converge quite quickly. Analogously, for $v \geq 43$ the $J_r=87$, 49, and 46 splittings are weighted about equally; hence $f \approx 0.85$, and the sequence will converge here also. However, $f \approx 2$ for $22<v<43$, since in this region only the $J_r=87$ splittings were measured with high precision.[14] Therefore, Eq. (3) was only applied to the data for $v \leq 22$ and $v \geq 43$, while $D_v^{(n)}$ values in the intermediate region were obtained by interpolation.

In applying the above stepwise convergence procedure, the individual values of $D_v^{(n)}$ and $B_v^{(n)}$ were always represented by polynomials in $(v+\frac{1}{2})$ before utilizing them in the next step. The values of $D_v^{(n)}$ were represented by

$$D_v^{(n)} = D_e^{(n)} + \beta_e^{(n)}(v+\tfrac{1}{2}) + d_2^{(n)}(v+\tfrac{1}{2})^2,$$

where $D_e^{(n)}$ and $\beta_e^{(n)}$ were calculated from the other spectroscopic constants using the expressions given by Herzberg,[15] and $d_2^{(n)}$ was obtained from a least-squares fit to the data.[16] The convergence of $d_2^{(n)}$ to an asymptotic value was used as the criterion of convergence for the $\{D_v^{(n)}, B_v^{(n)}\}$ sequence.

The high accuracy of the green-line splitting for $v<22$ relative to the uv splittings used for $v>22$ was retained in the polynomial representation of the $B_v^{(n)}$ constants. First, a second-order least-squares fit to the green-line data for $v<22$[17] yielded approximate values of the three lowest-order polynomial coefficients, B_e, α_e, and γ_e. Next, the contributions of these terms [i.e., $B_e - \alpha_e(v+\frac{1}{2}) + \gamma_e(v+\frac{1}{2})^2$] were subtracted from the 79 individual $B_v^{(n)}$ values[18] and the remainders fitted to an expression of the form

$$R(v) = \delta_e(v+\tfrac{1}{2})^3 + \epsilon_e(v+\tfrac{1}{2})^4.$$

Then the contributions of these initial δ_e and ϵ_e values were subtracted from the $B_v^{(n)}$ values for $v<22$ and these remainders fitted to a quadratic, yielding improved estimates of B_e, α_e, and γ_e. This cycle was then repeated until the polynomial coefficients converged.[19]

The above $\{D_v^{(n)}, B_v^{(n)}\}$ convergence procedure was applied three times, using polynomial representations of the $B_v^{(n)}$ constants with maximum order $M=3$, 4, and 5, respectively.[19] In each case, the initial trial D_v values were $\{D_v^{(0)}=0\}$. The results are shown in Table I.

In the above manner, the following mutually consistent expressions were found to best represent the rotational constants B_v and D_v (in cm^{-1}):

$$B_v = 3.7395\times10^{-2} - 1.2435\times10^{-4}(v+\tfrac{1}{2}) + 4.498\times10^{-7}(v+\tfrac{1}{2})^2 - 1.482\times10^{-8}(v+\tfrac{1}{2})^3 - 3.64\times10^{-11}(v+\tfrac{1}{2})^4, \quad (4)$$

$$D_v = 4.54\times10^{-9} + 1.7\times10^{-11}(v+\tfrac{1}{2}) + 7\times10^{-12}(v+\tfrac{1}{2})^2. \quad (5)$$

Expression (4) represents the experimental B_v values [obtained by substituting (5) into (1)] within a standard error of $\pm0.24\times10^{-4}$ cm^{-1} for $v<22$, and $\pm3.2\times10^{-4}$ for $v \geq 22$. Figure 1 contrasts a plot of expression (5) with the final D_v values obtained from expression (3). Utilizing the first term of (4) in the

TABLE I. Results of $\{D_v^{(n)}, B_v^{(n)}\}$ convergence using different polynomial fits to the $B_v^{(n)}$ values.[19] ERR is the standard error of the D_v representation. All quantities are in cm^{-1}.

B_v representation			D_v representation	
Order M	$10^2\times B_e$	$10^4\times\alpha_e$	$10^9\times$ERR	$10^9\times d_2$
3	3.7397	1.2519	6.7	0.004_3
4	3.7395	1.2435	4.4	0.007_2
5	3.7399	1.2652	4.4	0.007_0

TABLE II. Absorption lines exciting observed resonance series. $R(33)$ is for the green-line series[6] and the others for the uv series.[1]

Line	$R(33)$	$P(47)$	$R(48)$	$P(23)$	$R(24)$
ν_e (cm^{-1})	18 307.487	54 633.216	54 633.155	54 633.203	54 633.182

usual manner,[15] one obtains an equilibrium internuclear distance of $R_{EQ}=2.665_7$ Å for ground state I_2.

THE VIBRATIONAL CONSTANTS

A shift of B_v values for $v>22$ generated from expression (4) by one standard error, $\pm 3.2\times 10^{-4}$ cm^{-1}, changes vibrational energies obtained from the resonance series characterized by $J_r=87$ by $\approx\mp 2.5$ cm^{-1}, while affecting energies obtained from the other (uv) series by between ∓ 0.15 and ∓ 0.8 cm^{-1} (corresponding to $J_r=22$ and 49, respectively). In view of this, the $J_r=87$ data were not utilized at all in the determination of the vibrational spectrum and constants for the ground state. This means that the highest level fitted is $v=82$, although the highest level observed is $v=84$.

Utilizing expressions (4) and (5), a vibrational ladder may be constructed from the data for each of the five remaining resonance series, $J_r=49$, 46, 34, 25, and 22. Unfortunately, the emission lines corresponding to the inverse of the five molecular transitions exciting the various series are masked by the intense atomic lines. Also, the atomic emission and molecular absorption lines have a significant width,[20] so that the peaks of the latter need not coincide with those of the former.

In the present work, improved values for the peak energies of the exciting molecular transitions were obtained by shifting the five independent vibrational ladders so as to minimize disagreement,[21] yielding the frequencies given in Table II. A weighted average value for the 4 uv series is 54 633.18 cm^{-1}. This lies between the center of the atomic line which is the source of the uv light, 54 633.46 cm^{-1},[22] and the value $\nu_e=54\,632.93$ cm^{-1} used in the original analysis[1] as the single excitation frequency for all 6 uv resonance series.

The above procedure, combined with the method of obtaining the D_v values,[12] yields a fairly high degree of internal consistency between the results for different resonance series. The statistical scatter in the B_v values for $v>22$, $\pm 3.2\times 10^{-4}$ cm^{-1}, could give rise to differences of ∓ 0.6 cm^{-1} between vibrational energies calculated from the $J_r=49$ and 22 series. However, the disagreement actually found is always less than 0.15 cm^{-1} for $v<74$, while for $74\leq v\leq 82$, where the rotational data is least reliable, the spread never exceeds 0.5 cm^{-1}.

Vibrational energies obtained by applying expressions (4) and (5) to the data were fitted to a polynomial in $(v+\frac{1}{2})$ to yield the customary representation (ω_e, $\omega_e x_e\cdots$ etc.). An iterative procedure was used to obtain a single self-consistent set of constants which reflected the higher accuracy of the green-line data used for $v\leq 22$. The approach was similar to that used for obtaining the B_v representation. The coefficients of terms of order up to five were based mainly on the $v\leq 22$ data and those of order six to nine mainly on the uv data ($22\leq v\leq 82$). In addition, an external constraint[23] was applied to force the vibrational constants to yield roughly the known dissociation limit.[2]

The final expression obtained for the vibrational energies is[24] (in cm^{-1})

$$G(v)=214.5481(v+\tfrac{1}{2})-0.616259(v+\tfrac{1}{2})^2+7.507\times 10^{-5}(v+\tfrac{1}{2})^3-1.263643\times 10^{-4}(v+\tfrac{1}{2})^4+6.198129\times 10^{-6}(v+\tfrac{1}{2})^5-2.0255975\times 10^{-7}(v+\tfrac{1}{2})^6+3.9662824\times 10^{-9}(v+\tfrac{1}{2})^7-4.6346554\times 10^{-11}(v+\tfrac{1}{2})^8+2.9330755\times 10^{-13}(v+\tfrac{1}{2})^9-7.61000\times 10^{-16}(v+\tfrac{1}{2})^{10}. \quad (6)$$

This fits the 30 green-line data for $v\leq 22$ with a standard error of $\pm 0.004_6$ cm^{-1}, and the 146 (uv) data for $22<v\leq 82$ with a standard error of ± 0.14 cm^{-1}, within the ranges of the respective experimental uncertainties. However, the extrapolated eigenvalues are probably not reliable much beyond $v\approx 85$.

RKR POTENTIAL FOR GROUND STATE I_2

RKR calculations reported here were performed using a slightly modified version of the computer program reported by Zare.[25] This program was previously tested and found to yield a potential which reflects the input vibrational energies and rotational B_v's with an accuracy better than that warranted by the data used here.[26] Values of the physical constants, taken from Cohen and DuMond,[27] yielded

$$\hbar/(4\pi c\mu)=16.85749/\mu\ (\text{(Å)}^2\text{cm}^{-1}),$$

where $\mu=63.4377$ amu[28] is the reduced mass of the two nuclei.[29]

A check of the plausibility of the potential by evaluating its first and second derivatives over the range of the inner turning points[23] showed the second derivatives to be negative for $v>56$. This must be due to inaccuracy in the B_v constants in this region,

TABLE III. RKR turning points (in angstroms) for ground-state I_2. The energies $G(v)$ are in cm^{-1}.

v	$G(v)$	$R_1(v)$	$R_2(v)$	v	$G(v)$	$R_1(v)$	$R_2(v)$
0	107.120	2.61784	2.71750	30	5 932.60	2.3689	3.2176
1	320.435	2.58504	2.75807	32	6 274.60	2.3618	3.2443
2	532.515	2.56348	2.78741	34	6 610.06	2.3550	3.2713
3	743.356	2.54653	2.81214	36	6 938.78	2.3487	3.2986
4	952.952	2.53228	2.83419	38	7 260.56	2.3427	3.3264
5	1 161.296	2.51983	2.85444	40	7 575.21	2.3370	3.3546
6	1 368.379	2.50871	2.87339	42	7 882.51	2.3316	3.3835
7	1 574.194	2.49862	2.89134	44	8 182.20	2.3265	3.4132
8	1 778.731	2.48933	2.90850	46	8 474.05	2.3217	3.4436
9	1 981.980	2.48072	2.92502	48	8 757.78	2.3171	3.4751
10	2 183.932	2.47268	2.94101	50	9 033.11	2.3128	3.5076
11	2 384.577	2.46511	2.95655	52	9 299.72	2.3087	3.5413
12	2 583.905	2.45796	2.97172	54	9 557.29	2.3049	3.5765
13	2 781.904	2.45119	2.98656	56	9 805.50	2.3012	3.6133
14	2 978.564	2.44473	3.00113	58	10 043.98	2.2978	3.6520
15	3 173.874	2.43857	3.01545	60	10 272.39	2.2946	3.6928
16	3 367.822	2.43268	3.02958	62	10 490.37	2.2916	3.7360
17	3 560.397	2.42702	3.04352	64	10 697.57	2.2888	3.7819
18	3 751.586	2.42159	3.05732	66	10 893.66	2.2862	3.8310
19	3 941.377	2.41635	3.07099	68	11 078.35	2.2837	3.8837
20	4 129.756	2.41130	3.08454	70	11 251.40	2.2815	3.9406
21	4 316.709	2.40643	3.09801	72	11 412.60	2.2794	4.0021
22	4 502.223	2.40172	3.11140	74	11 561.84	2.2775	4.0689
24	4 868.87	2.3927	3.1380	76	11 699.11	2.275_8	4.142
26	5 229.58	2.3843	3.1645	79	11 882.75	2.273_4	4.264
28	5 584.20	2.3764	3.1910	82	12 040.40	2.271_5	4.406

since they largely determine the absolute positioning of the pair of turning points for a given level, while the distance between a pair of turning points depends only on the relatively more accurate vibrational spacings. However, a good approximation to the potential may still be obtained by adding the relatively more accurate differences between the pairs of turning points $[R_2(v)-R_1(v)]$ to inner turning points obtained by extrapolation from the region in which the two derivatives are acceptable. Consideration of the derivatives of the repulsive branch of the potential for $22\leq v\leq 50$ showed that the best (integer) inverse-power fit to it corresponded to R^{-12}.[30] The expression $A/R^{12}+B$ was then fitted to the computed inner turning points at $v=49$ and 50, yielding

$$V(R)=2.921166\times 10^{8}/R^{12}-3438.00. \qquad (7)$$

Expression (7) was then used with expression (6) to generate "extrapolated" inner turning points $R_1(v)$ for $v>50$ (i.e., $R<2.313$ Å). The differences between the extrapolated and RKR turning points increased from 0.00016 Å at $v=60$, to 0.0020 at $v=70$, to 0.0094 at $v=82$. Because of the magnitude of this correction and the steepness of the potential, the probable errors in the resulting inner turning points are insignificant.

Table III gives the RKR turning points computed from expressions (4) and (6) for $0\leq v\leq 50$, and the adjusted turning points for $v>50$ obtained by combining the extrapolated $R_1(v)$ values with the computed quantities $[R_2(v)-R_1(v)]$. The differences $[R_2(v)-R_1(v)]$ depend solely on the vibrational spectrum and have approximate error bounds of $\pm 0.8\times 10^{-5}$ Å for levels $v\leq 22$, and bounds ranging from ± 0.0003 to ± 0.003 Å as v increases from 23 to 82. On the other hand, the average of a pair of turning points $\frac{1}{2}[R_1(v)+R_2(v)]$ depends mainly on the less accurately known B_v constants. These averages have approximate error bounds of ± 0.0009 Å for $v\leq 22$, and bounds ranging from 0.01_3 to $\pm 0.02_8$ Å for v increasing from 23 to 82.[31] These bounds were obtained by applying the statistical standard errors of the fits of (4) and (6) to the data, to the expressions derived in the Appendix. It is important to note that the accuracies of the turning-point differences are significant, despite the relatively large uncertainties in the average values.

Consideration of the derivatives of the outer branch of the RKR potential for $v=80$–82 shows that in this region it is converging to the dissociation limit as $R^{-8.4}$.[30] On the other hand, the theoretical asymptotic long-range behavior of the potential for this state is R^{-6}.[2] Therefore, the experimental results do not extend far enough to either confirm the long-range R^{-6} behavior or yield a value for the C_6.[32]

DISCUSSION

Vibrational energies generated from expression (6) differ significantly from those obtained by Verma in his original analysis of the uv spectrum.[1] His level spacings (see Table VI of Ref. 1)[33] yield energies relative to $v=0$ which are too high. The error ranges from 0.2 cm^{-1} at $v=10$ up to 6.6 cm^{-1} at $v=54$ and then decreases to 4.3 cm^{-1} by $v=82$. Verma appears to have based his vibrational spectrum on the spacings

TABLE IV. Comparison of calculated and observed disagreements with Zare's[3] turning points. In all cases, δ represents subtraction of the present value from the previous value. $\Delta G_{v-1/2}$ and B_v are in cm^{-1}, while lengths are in angstroms.

			$10^4\times\delta[R_2(v)-R_1(v)]$		$10^4\times\frac{1}{2}\delta[R_2(v)+R_1(v)]$	
v	$-\delta(\Delta G_{v-1/2})$	$10^3\times\delta B_v$	From (A1) and (A3)	Obs	From (A2) and (A4)	Obs
9	0.07	−2.4	0.8	0.0	8.	−2.2
19	−0.17	−1.0	−2.9	−2.4	4.	0.3
29	−0.24	−2.4	−5.7	−4.3	10.	1.4
39	−0.20	−6.9	−6.3	−7.5	31.	−1.6
49	−0.14	−14.2	−5.9	−6.4	65.	−3.4
59	0.21	−23.2	12.5	1.0	125.	9.7
69	−0.02	−31.9	−1.8	0.6	200.	60.0

of the 17 pairs of adjacent levels in the P branch of resonance series $J_r=49$. On the other hand, the present analysis fits 176 vibrational energies directly. The discrepancies between the results of these two approaches shows how a relatively large error can accumulate when attention is focused on the individual vibrational spacings, rather than on the vibrational ladder as a whole. These errors in the previously reported vibrational spectrum[1] are reflected in the previous RKR potentials[1,3,5] in two ways. First of all, the differences $[R_2(v)-R_1(v)]$ are slightly in error (see Appendix); and more seriously, the turning points are correlated with incorrect energies.

The shift of the computed turning points above $v=50$, in the present work, has implications with regard to the accuracy of the B_v, D_v, and $G(v)$ representations [expressions (4)–(6)]. These shifts in the turning points actually correspond to small changes in the B_v values in this region. To be entirely consistent, new B_v values corresponding to the shifted turning points should have been derived and applied to yield new D_v values and vibrational energies. The maximum effect, occurring at $v=82$, would be a decrease of 1.04×10^{-4} cm^{-1} (0.5%) in B_{82}, and a concomitant decrease of 10×10^{-9} cm^{-1} (19%) in D_{82} and increase of 0.18 cm^{-1} in $G(82)$. However, aside from the change in D_{82}, these changes are effectively within the statistical standard error of the representations, and their effect on the turning point differences $[R_2(v)-R_1(v)]$ will be well within the stated bounds. Furthermore, these errors will drop quite sharply for lower vibrational levels and should be completely negligible for levels below $v\approx74$.

Rotational B_v constants generated from (4) also differ with those reported previously.[1,7] While the discrepancies are quite small for the lower levels, they increase steeply above $v\approx60$. At $v=82$ the present $B_v=0.02190$ cm^{-1} is 1.4% larger than Verma's value and 5.7% larger than that of Rank and Rao.[7] The main reason for this disagreement is the fact that the previous analyses used significantly smaller estimates for the D_v constants for the higher levels, while basing their B_v values in this region solely on the $J_r=87$ doublet splittings, which are relatively the most sensitive to errors in D_v. While the preceding paragraph suggests that the present $B_{v=82}$ is too large by ≈0.5%, it will still be more accurate than values yielded by the previous analyses.

ACKNOWLEDGMENT

The author would like to thank Professor R. B. Bernstein for his encouragement and support.

APPENDIX: ACCURACY OF RKR TURNING POINTS

RKR turning points for a $J=0$ potential curve are obtained from the spectroscopic data through the expressions

$$f(v)=\left(\frac{\hbar}{4\pi c\mu}\right)^{1/2}\int_{-1/2}^{v}[G(v)-G(x)]^{-1/2}\,dx$$
$$=\tfrac{1}{2}[R_2(v)-R_1(v)],$$
$$g(v)=\left(\frac{4\pi c\mu}{\hbar}\right)^{1/2}\int_{-1/2}^{v}B_x[G(v)-G(x)]^{-1/2}\,dx$$
$$=\tfrac{1}{2}\{[R_1(v)]^{-1}-[R_2(v)]^{-1}\},$$

where B_x and $G(x)$ are the rotational constant and vibrational energy for level x. Hence, to a first approximation, errors δE_x in $G(x)$ yield an apparent value of $f(v)$:

$$\left(\frac{\hbar}{4\pi c\mu}\right)^{1/2}\int_{-1/2}^{v}[G(v)-G(x)-\delta E_x]^{-1/2}\,dx$$
$$\approx\left\{1+\frac{1}{2}\left\langle\frac{\delta E_x}{G(v)-G(x)}\right\rangle\right\}\tfrac{1}{2}[R_2(v)-R_1(v)].$$

Similarly, combining this effect with errors δB_x in the rotational constant B_v, the apparent value of $g(v)$ is

$$\left(\frac{4\pi c\mu}{\hbar}\right)^{1/2}\int_{-1/2}^{v}(B_x+\delta B_x)[G(v)-G(x)-\delta E_x]^{-1/2}\,dx$$
$$\approx\left\{1+\left\langle\frac{\delta B_x}{B_x}\right\rangle+\frac{1}{2}\left\langle\frac{\delta E_x}{G(v)-G(x)}\right\rangle\right\}$$
$$\times\tfrac{1}{2}\{[R_1(v)]^{-1}-[R_2(v)]^{-1}\}$$

The average of a pair of turning points is

$$\tfrac{1}{2}[R_1(v)+R_2(v)]=f(v)[1+f(v)^{-1}g(v)^{-1}]^{1/2},$$

where the portion in parenthesis is dominated by the last term. Therefore, the errors in the difference and average of the turning points calculated for level v are

$$\delta[R_2(v)-R_1(v)] \approx \tfrac{1}{2}\langle \delta E_x/[G(v)-G(x)]\rangle [R_2(v)-R_1(v)], \quad \text{(A1)}$$

and

$$\tfrac{1}{2}\delta[R_1(v)+R_2(v)] \approx -\tfrac{1}{2}\langle \delta B_x/B_x\rangle \tfrac{1}{2}[R_1(v)+R_2(v)]. \quad \text{(A2)}$$

In cases where the errors δE_x and δB_x are small, the average values in (A1) and (A2) may be replaced by

$$\langle \delta E_x/[G(v)-G(x)]\rangle \approx -\delta(\Delta G_{v-1/2})/\Delta G_{v-1/2}, \quad \text{(A3)}$$

and

$$\langle \delta B_x/B_x\rangle \approx \delta B_v/B_v. \quad \text{(A4)}$$

Also, approximate turning point error bounds are obtained if the numerators on the right-hand sides of (A3) and (A4) may be replaced by $\langle \delta E_x\rangle$ and $\langle \delta B_x\rangle$.

Expressions (A1)–(A4) were tested by comparing the turning points calculated in the present work with those reported by Zare.[5] The latter were calculated using essentially the same computer program as was used here, and are probably the most accurate previous results.[26] However, Zare utilized Verma's reported vibrational spacings and B_v representation which are believed to be slightly in error (see Discussion, above). The comparison is shown in Table IV. For the differences $[R_2(v)-R_1(v)]$ the agreement is quite good except for $v=59$ and 69, and there the discrepancy is anomalously large only because $\delta(\Delta G_{v-1/2})$ changes sign at $v=55$ and at $v=68$. On the other hand, there is no readily apparent reason for the relatively large discrepancies between the calculated and observed errors in the turning point averages, other than the fact that Eq. (A4) is a relatively much worse approximation than is Eq. (A3).

* Research supported by National Science Foundation Grant GP-7409 and National Aeronautics and Space Administration Grant NGL 50-002-001.

[1] R. D. Verma, J. Chem. Phys. 32, 738 (1960).

[2] R. J. LeRoy, J. Chem. Phys. 52, 2678 (1970), preceding paper.). See Chapter 6.

[3] S. Weissman, J. T. Vanderslice, and R. Battino, J. Chem. Phys. 39, 2226 (1963).

[4] W. G. Richards and R. F. Barrow, Trans. Faraday Soc. 60, 797 (1964).

[5] R. N. Zare, J. Chem. Phys. 40, 1934 (1964).

[6] D. H. Rank and W. M. Baldwin, J. Chem. Phys. 19, 1210 (1951). While this reference did not list the raw data, they were presented later by Rank and Rao.[7]

[7] D. H. Rank and B. S. Rao, J. Mol. Spectry. 13, 34 (1964).

[8] The sixth series is the portion of Verma's IVb (listed in his Table V) which was reassigned in Ref. 2.

[9] In addition to the lines so designated in Ref. 1, this includes 29 other lines which appear to be blended, based on comparison of the data in Tables I–IV of Ref. 1.

[10] It appears that $R(21)$ was inadvertently set equal to $P(50)$, and consequently the actual $R(21)$ and $P(23)$ lines were misassigned as $R(24)$ and $P(26)$, respectively.

[11] This averaging is introduced by smoothing the individual $B_v^{(n)}$ values by representing them by a polynomial in $(v+\frac{1}{2})$ before using them to compute the $G_{J_2}^{(n)}(v)$ values. The individual $D_v^{(n)}$ values were similarly smoothed before use.

[12] The green-line ($J_r=34$) resonance data were omitted from these comparisons, since accurate relative positioning of these levels relative to those obtained from the uv measurements is impossible until good rotational constraints are obtained. $\nu_e=54\,633.18$ cm^{-1} was used here as the single frequency exciting all the uv resonance series. Although this is slightly in error, the spread shown in Table II is considerably smaller than 0.27 cm^{-1}, the minimum effect of the D_v constant on $G(v)$ values.

[13] This is on account of the higher accuracy of the green-line ($J_r=34$) as compared to the uv ($J_r=87$, 49, 46, 25, and 22) measurements.

[14] At least one branch of every doublet of the other uv resonance series is blended in this region,[1] while the accurate green-line ($J_r=34$) data do not extend past $v=22$.[7]

[15] G. Herzberg, *Spectra of Diatomic Molecules* (D. Van Nostrand Co., Inc., Toronto, Canada, 1950), 2nd. ed.

[16] This rather simple representation was used because the scatter of the data both makes the theoretical values of D_e and β_e [15] somewhat more reliable than those obtained from a fit, and also precludes the use of a higher order fit.

[17] Since the analysis of Ref. 7 indicated that the uncertainties of the green-line splittings at $v=5$, 8, and 22 were considerably greater than those of other levels, the first two were omitted entirely from these fits, while the latter was included with the less precise uv splittings.

[18] As was stated previously, the uv resonance data for $v<22$ were excluded from these fits.

[19] This approach of coupling a fit of order 0–N to the $B_v^{(n)}$ values based on the green-line data for $v<22$, with a fit of order $(N+1)$ to M to the residuals for $0\leq v\leq 82$, was tried for $N=1$, 2, and 3 and $M(>N)=3$, 4, 5, 6, and 7. For all M, $N=2$ was much better than $N=1$ or 3, while with $N=2$ the results were roughly equally good for $M=3$, 4, or 5.

[20] Microphotometer traces of some uv emission lines (see Ref. 1) indicate that the reported molecular lines have a width at half-maximum of ≈ 0.8 cm^{-1}. Of this, the contribution from the Doppler effect is calculated to be 0.02 cm^{-1} (cf. 0.035 cm^{-1} for the absorbed atomic line). The remainder of the broadening must be due to collisional effects and Stark broadening in the discharge. Despite these effects, Verma was able to measure the peak positions of the molecular lines with an accuracy of ± 0.02 cm^{-1} for sharp nonoverlapped lines, and from ± 0.07 to ± 0.14 cm^{-1} for others.[1]

[21] In this procedure, the uv data for the whole range $0\leq v\leq 82$ were used. On the other hand, the uv data for $v\leq 22$ were omitted from the analysis when the vibrational energies were being obtained.

[22] C. C. Kiess and C. H. Corliss, J. Res. Natl. Bur. Std. 63A, 1 (1959).

[23] R. J. LeRoy and G. Burns, J. Mol. Spectry. 25, 77 (1968).

[24] The numbers of significant digits in the constants were chosen so that Eq. (6) would reproduce energies up to $v=82$ with a precision of ± 0.01 cm^{-1}, and energies up to $v=22$ with a precision of ± 0.001 cm^{-1}.

[25] R. N. Zare, University of California Lawrence Radiation Laboratory Rept. UCRL-10925, 1963.

[26] A given RKR potential may be tested by substituting it into the radial Schrödinger equation, solving exactly to get the vibrational energies $G(v)$ and expectation values $\langle v|R^{-2}|v\rangle$, and comparing these to the energies and B_v constants used as input in the RKR computations. Zare tested his program in this manner[5] using Verma's results for the ground state of I_2 as the test case. He found that for the first thirty levels, the deviations of the vibrational energies were ≤ 0.09 cm^{-1}, while the deviations in the B_v values were $<1.\times 10^{-6}$ cm^{-1}.

[27] E. R. Cohen and J. W. M. DuMond, Rev. Mod. Phys. 37, 537 (1965).

[28] *Handbook of Chemistry and Physics*, R. C. Weast, Ed. (Chemical Rubber Publ. Co., Cleveland, Ohio, 1966), 47th ed.

[29] Using inexact values of the physical constants can have a real effect on the accuracy (through not the precision) of the RKR calculation. It was recently shown [R. J. LeRoy and R. B. Bern-

See Section 5.

stein, J. Chem. Phys. 49, 4312 (1968)] that for the inverse problem of obtaining eigenvalues from a given potential, different authors obtained results differing by up to 0.7 cm^{-1} for the eigenstates of H_2, on this account. Furthermore, use of the atomic reduced mass for H_2 rather than the nuclear reduced mass introduced errors of over 6. cm^{-1}.

[30] The potential was fitted to the expression A/R^n+B.

[31] The actual errors in the $[R_1(v)\pm R_2(v)]$ values are probably somewhat smaller than is indicated by these bounds. The results in the Appendix suggest that this may be especially true for the average values $\frac{1}{2}[R_2(v)+R_1(v)]$.

[32] The previously reported "experimental" C_6 values[1,4] were based on the data for the levels which have recently been reassigned to the $0_g^+(^3\Pi)$ state. Furthermore, even ignoring this reassignment, they appear to have been rather inconsistently obtained. Verma[1] obtained the asymptotic C_6 from his RKR curve in the interval $4.6<R<6.4$ Å, while his potential for $6.4<R<8.8$ Å converges significantly more slowly than his C_6/R^6. On the other hand, the deviation between the observed (RKR) and calculated (based on their C_6) curves of Richards and Barrow[4] shows that their RKR potential has distinctly sharper curvature than is explained by their C_6.

[33] As reported previously,[5] the $G(v)$ values given in Table VII of Ref. 1 are all 5 cm^{-1} too small.

2.3 LONG-RANGE POTENTIALS OF $Br_2(B\ ^3\Pi_{0u}^+)$ AND $Cl_2(B\ ^3\Pi_{0u}^+)$ FROM COMBINING RKR RESULTS WITH THEORY

Improved RKR potentials for the $B(^3\Pi_{0u}^+)$ states of Br_2 and Cl_2, extending to within a few cm^{-1} of the dissociation limit, have recently been calculated by Coxon.[1] They are combined here with the theoretical C_5 potential constants to yield estimates of the C_6 constants for these states. The approach used is analogous to that applied by Stwalley to the ground $(X\ ^1\Sigma_g^+)$ state of Mg_2.[2]

It is theoretically known that for the $B(^3\Pi_{0u}^+)$-state halogens the long-range potential may be expanded as:[3-5]

$$V(R) = D - C_5/R^5 - C_6/R^6 - C_8/R^8 - \ldots \qquad (1)$$

Values of the C_5 constants may be readily calculated for most species,[5,7,8] and those for the states in question are given in Table I. Like the C_5's, the C_6 and C_8 dispersion coefficients for these molecular states are also almost certainly positive (attractive), although they are much harder to obtain theoretically.[10] A question raised by the use of Eq. (1) is whether the turning points considered lie at sufficiently large internuclear distances for it to be valid. This point has been discussed by Stwalley in relation to ground state Mg_2.[2] He pointed out that for the $b(^3\Sigma_u^+)$ state of H_2, Eq. (1) breaks down for $R \lesssim 5$ Å, and he suggested that it should not be used in this region for any diatomic. Assuming his criterion is sufficient, the present treatment

TABLE I

Asymptotic potential coefficients of the $B(^3\Pi^+_{0u})$-state halogens.

	C_5 [cm^{-1} Å^5] (theoretical)[a]	C_6 [cm^{-1} Å^6] [b] (empirical)[c]
Cl_2	1.44×10^5	$0.42 (\pm 0.02) \times 10^6$
Br_2	2.39×10^5	$1.01 (\pm 0.24) \times 10^6$

a) See Footnote 7 .

b) The uncertainties here represent 95% statistical confidence intervals on the slopes of the lines through the highest four points.

c) From Figs. 1 and 2.

- - - - - - - - - -

is viable, since the outer RKR turning points for the levels considered all lie in the region $5.5 < R < 9.5$ Å.[1]

It has recently been shown[12] that the distribution of highest observed vibrational levels for each of the B-state halogens corresponds to the outer branch of the potential in this region being dominated by the leading (R^{-5}) term in Eq.(1). On the other hand, the turning points in question are not particularly large ($R \lesssim 9.2$ Å) so that it seems quite possible that some of the higher-power terms also contribute significantly. This would appear to suggest a direct least-squares fit of the outer turning points to Eq.(1); however, this approach is not advisable for a number of reasons. One of these is the uncertainty as to how many of the terms in the expansion of

Eq. (1) should actually be retained in a given case. This difficulty is accentuated by the fact that the competing powers are fairly similar, so that in the absence of data spanning a very wide interval, relatively small errors in the turning points could grossly distort the apparent relative contributions of the different terms. A more serious problem is that the outer turning point for the highest observed level is relatively much less accurate than those for somewhat deeper levels,[13] while having a dominant voice in the determination of the relative importance of the contributing terms.

In the present case the difficulties inherent in a general least-squares fit to Eq. (1) may be avoided because accurate theoretical C_5 constants are known (see Table I).[5,7,8] Following the approach Stwalley applied to ground-state Mg_2,[2] plots of $\{E(v) + C_5/[R_2(v)]^5\}$ vs $[R_2(v)]^{-6}$ were made, where E(v) are the energies and $R_2(v)$ Coxon's[1] outer RKR turning points for the highest observed vibrational levels of B-state Br_2 and $C\ell_2$. These are shown in Figs. 1 and 2.[14] Consideration of Eq. (1) shows that the limiting slopes of these plots yield the C_6 coefficients; the values thus obtained are listed in Table I together with the C_5 coefficients on which they are based. In both cases these slopes were constrained to yield the dissociation energies obtained in Refs. (6) and (12), since the plots did not appear capable of yielding more reliable values. In particular, a best straight line through the four highest points for Br_2 in Fig. 2 would yield an estimate of the dissociation energy significantly larger than that obtained in Ref. (12) when the R^{-5} term was ignored and the potential assumed to be purely R^{-6}.[18] This is quite unacceptable, and suggests that there

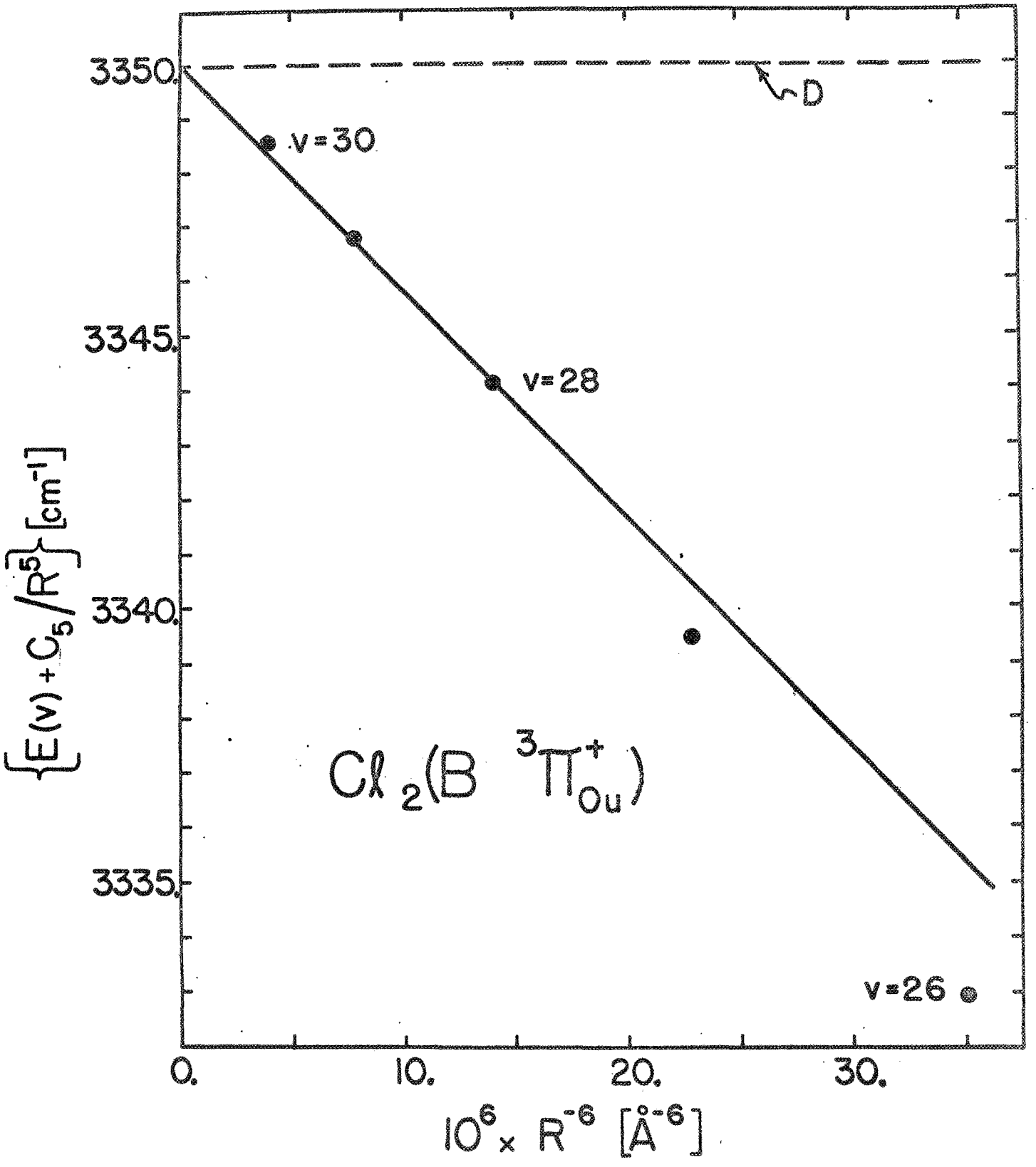

Figure 1: $\{E(v) + C_5/[R_2(v)]^5\}$ vs $[R_2(v)]^{-6}$ for $Cl_2(B\ ^3\Pi^+_{0u})$.

The solid line is a least-squares fit to the four highest points, constrained to have its intercept at the previously obtained[6,12] value of D (horizontal dashed line).

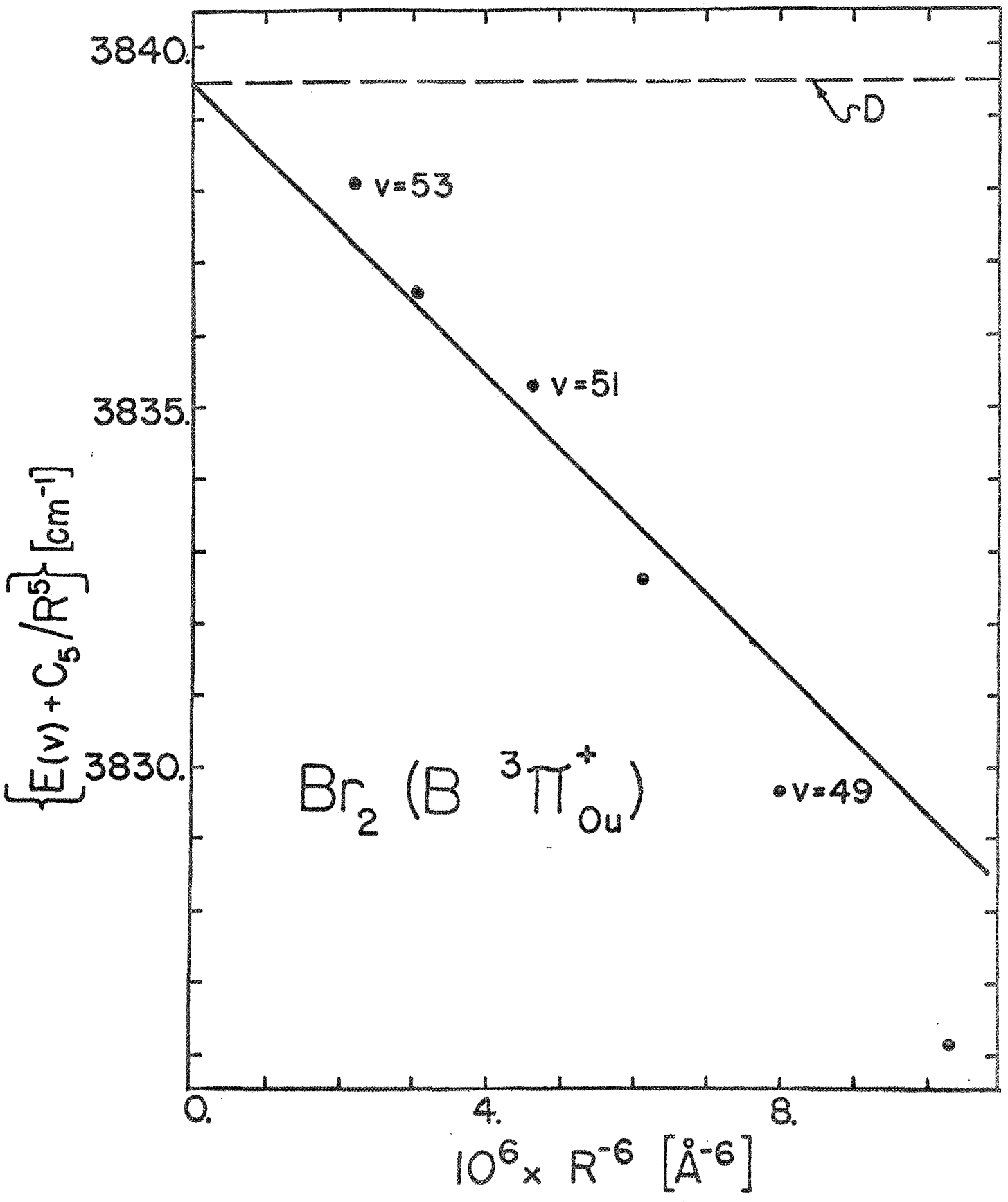

Figure 2: $\left\{E(v) + C_5/[R_2(v)]^5\right\}$ vs $[R_2(v)]^{-6}$ for Br_2 ($B\ ^3\Pi^+_{0u}$). The solid line is a least-squares fit to the four highest points, constrained to have its intercept at the previously obtained[6,12] value of D (horizontal dashed line).

are small errors in these RKR turning points.[13,19] As expected, the points for the deeper levels fall below the lines in Figs. 1 and 2, indicating the increasing importance of the R^{-8} and other terms.

In addition to the inherent interest in the C_6 constants in Table I, a most significant feature of the present results is in the ease with which they were obtained. While this is due in large part to the simplicity of calculating theoretical C_5 coefficients,[5,7,8] it also attests to the utility of Stwalley's[2] graphical method. These results also have implications concerning the method presented in Chapter 3, and hence will be discussed further in Section 3.3 .

FOOTNOTES

1. J. A. Coxon, "The Calculation of Potential Energy Curves of Diatomic Molecules: Application to Halogen Molecules", J. Quant. Spectry. Radiat. Transfer (to be published).
2. W. C. Stwalley, "Long-Range Analysis of the Internuclear Potential of Mg_2", Chem. Phys. Lett. (1970, to be published).
3. The derivation of this expression is discussed in a number of sources, including Refs. (4-5). The lowest-power term contributing to Eq. (1) is determined by the nature of the atoms to which the molecular state dissociates; a summary of the theoretical rules governing this is given in Appendix B of Ref. (6).
4. J. O. Hirschfelder, C. F. Curtiss, and R. B. Bird, Molecular Theory of Gases and Liquids (John Wiley and Sons, Inc., New York, 1964), Part III.
5. T. Y. Chang, Rev. Mod. Phys. 39, 911 (1967).
6. R. J. Le Roy and R. B. Bernstein, J. Chem. Phys. 52, 3869 (1970); see Section 3.1.
7. It was shown by Knipp[8] that interatomic C_5 coefficients may be expressed as the product of an angular factor and the expectation value of the square of the electron radii in the unfilled valence shell of each of the interacting atoms. Knipp[8] also presented values of these angular factors and approximate expectation values for a few systems. Recently, Chang[5] extended the tables of angular factors considerably, and Fischer[9] reported Hartree-Fock values of the necessary expectation values for all atoms from He to Rn.

8. J. K. Knipp, Phys. Rev. 53, 734 (1938).

9. C. F. Fischer, Can. J. Phys. 46, 2336 (1968).

10. The second-order perturbation theory expressions for interatomic dispersion forces[4] show that in the present case, where the molecular state dissociates to one ground ($^2P_{3/2}$) and one excited ($^2P_{1/2}$) atom, there is only one repulsive contribution to each of the C_6 and C_8 terms. Its magnitude depends on a matrix element coupling the $^2P_{3/2}$ and $^2P_{1/2}$ atomic states; this is known to be very small because of the forbiddenness of this atomic transition,[11] and it is certain to be overwhelmed by the contributions from terms corresponding to allowed transitions to higher excited states.

11. a) R. H. Garstang, J. Res. Natl. Bur. Std. (U.S.) 68A, 61 (1964);
b) R. J. Donovan and D. Husain, Chem. Rev. 70, 489 (1970).

12. R. J. Le Roy and R. B. Bernstein, "Dissociation Energies and Long-Range Potentials of Diatomic Molecules from Vibrational Spacings: The Halogens," J. Mol. Spectry. 37 (1971, in press); see Section 3.2.

13. This may be seen from consideration of the two quadratures required for the calculation of a pair of turning points (see Eqs. (1-3) in Section 2.1). The integrand of each always has an integrable singularity at the energy of the level whose turning points are being calculated, and hence the largest contribution to the integral comes from this neighborhood. For all but the highest level this presents little difficulty, as a smooth interpolation between the data for the surrounding levels should yield highly accurate inte-

grands at these singularities. However, for the very highest observed level, the absence of data for yet higher levels introduces a relatively large uncertainty into this interpolation, and hence into the resulting turning points.

14. A point for v = 32 was omitted from Fig. 1 because of its completely unreasonable disagreement with the others; it would have lain 0.8 cm^{-1} below the point for v = 31, at an abscissa of $10^6/R^6 = 0.07$. This omission is justified on the basis of possible errors in the RKR calculation for the highest level,[13] and probable error in the data on which the calculation was based. The only reported observation of this level is in the thesis of Richards,[15] and it was not observed in the later analyses of Refs. (16) and (17). The discrepancy is qualitatively that expected if the v = 31-32 level spacing used in Coxon's[1] RKR calculation was too small, as is suggested by the fact that it is 33% smaller than that predicted in Ref. (6).

15. W. G. Richards, Ph.D. thesis, Oxford University (1962).

16. A. E. Douglas, Chr. Kn. Møller, and B. P. Stoicheff, Can. J. Phys. 41, 1174 (1963).

17. M. A. A. Clyne and J. A. Coxon, J. Mol. Spectry. 33, 381 (1970).

18. This suggested a dissociation energy only 0.5 cm^{-1} higher than the best estimate (the latter corresponding to the assumption of a pure R^{-5} potential tail).[12]

19. This is also suggested by the scatter in the points, and would not be surprising in view of the interpolations Coxon[1] had to perform between data for different isotopes with markedly different accuracies.

3. DISSOCIATION ENERGIES AND LONG-RANGE POTENTIALS FROM THE VIBRATIONAL LEVEL DISTRIBUTION NEAR THE DISSOCIATION LIMIT

While the RKR method (discussed in the previous chapter) is the most accurate way of determining the bowl of an attractive potential curve, it has definite limitations. One problem is that accurate turning points for a given level may be obtained only if both the energies and rotational B_v constants are known for all of the deeper vibrational levels of the given state. This restricts consideration to cases for which these data are available about the potential minimum, and means that in most other cases the curves obtained may not extend very close to the dissociation limit. Another drawback of the RKR method is that it implicitly includes no simple way of accurately placing the dissociation limit. This is fairly serious, as the dissociation energy is perhaps the most interesting single property of a potential well.

This chapter presents a new method which yields more accurate values of molecular dissociation energies than were previously obtainable. It also yields an estimate of the long-range potential tail, and predicted eigenvalues for vibrational levels lying above the highest one observed.

3.1 DERIVATION AND DEMONSTRATION OF THE METHOD

This section is reprinted from the Journal of Chemical Physics, Volume 52, pp. 3869-3879 (American Institute of Physics, New York, 1970).

Reprinted from THE JOURNAL OF CHEMICAL PHYSICS, Vol. 52, No. 8, 3869–3879, 15 April 1970
Printed in U. S. A.

Dissociation Energy and Long-Range Potential of Diatomic Molecules from Vibrational Spacings of Higher Levels*

ROBERT J. LEROY AND RICHARD B. BERNSTEIN

Theoretical Chemistry Institute and Chemistry Department, University of Wisconsin, Madison, Wisconsin 53706

(Received 12 December 1969)

An expression is derived which relates the distribution of vibrational levels near the dissociation limit D of a given diatomic species to the nature of the long-range interatomic potential, in the region where the latter may be approximated by $D-C_n/R^n$. Fitting experimental energies directly to this relationship yields values of D, n, and C_n. This procedure requires a knowledge of the relative energies and relative vibrational numbering for at least four rotationless levels lying near the dissociation limit. However, it requires no information on the rotational constants or on the number and energies of the deeply bound levels. D can be evaluated with a much smaller uncertainty than heretofore obtainable from Birge–Sponer extrapolations. The formula predicts the energies of all vibrational levels lying above the highest one measured, with uncertainties no larger than that of the binding energy of the highest level. The validity of the method is tested with model potentials, and its usefulness is demonstrated by application to the precise data of Douglas, Møller, and Stoicheff for the $B\,^3\Pi_{0u}^+$ state of Cl_2.

I. INTRODUCTION

For more than four decades the Birge–Sponer[1] extrapolation procedure has been employed, with only minor modifications,[2,3] for the determination of values for dissociation limits of diatomic molecules from experimental vibrational spacings $\Delta G_{v+1/2}$.[4] One of the great virtues of this method is its simplicity, as exemplified by the exact linear relationship between $\Delta G_{v+1/2}$ and v for a Morse potential. In this case, $\Delta G(v)$ [5] extrapolates to zero at $v_D=[(\omega_e/2\omega_e x_e)-\frac{1}{2}]$, where v_D is the noninteger "effective" vibrational index of the dissociation limit.[4] For more realistic potentials it is well known that the Birge–Sponer (B–S) plot shows positive curvature in the region just prior to dissociation, due to the dominating influence of the long-range "tail" of the interatomic potential.[2–4,6] Graphical extrapolation to the dissociation limit is therefore less reliable, and uncertainties of several cm^{-1} are common in values so obtained for the dissociation limit D.

The WKB-based method to be described takes advantage of the dominating influence of the long-range portion of the potential on the uppermost vibrational levels. It requires only the energies and relative vibrational numbering of four or more rotationless levels lying close to the dissociation limit D (i.e., less than $\approx$10% of the well depth below D). These are fitted to an analytical approximation formula, yielding "best" estimates of D and of the long-range interatomic potential. Although a proper RKR analysis yields a much more accurate estimate of the potential,[7] it is much more restrictive than the present method since it requires as additional information the energies and B_v constants of *all* levels below the one whose turning points are being calculated. Furthermore, the RKR approach provides no estimate of D or of the energies or even of the total number of vibrational levels above the highest one observed, and offers no direct means of extrapolating beyond the observed levels.

II. METHOD

A. Derivation

The starting point of the present treatment is the first-order WKB quantum condition for the eigenvalues of a potential $V(R)$:

$$v+\tfrac{1}{2}=\frac{(2\mu)^{1/2}}{\pi\hbar}\int_{R_1(v)}^{R_2(v)}[E(v)-V(R)]^{1/2}dR, \quad (1)$$

where $E(v)$ is the energy of level v and $R_1(v)$ and $R_2(v)$ are its classical turning points: $E(v)=V[R_1(v)]=V[R_2(v)]$. Although the allowed eigenvalues correspond to integer v, it is convenient to treat v as a continuous variable.

Differentiation of Eq. (1) with respect to $E(v)$ yields

$$\frac{dv}{dE(v)}=(\pi\hbar)^{-1}(\tfrac{1}{2}\mu)^{1/2}\int_{R_1(v)}^{R_2(v)}[E(v)-V(R)]^{-1/2}dR. \quad (2)$$

Consideration of the nature of the integrand in Eq. (2) suggests that the integral will be very nearly unchanged if the exact $V(R)$ is replaced by an approximate function which is accurate near the outer turning point $R_2(v)$. This is illustrated in Fig. 1 for the case of a model potential, chosen to be of the Lennard-Jones (12,6) form.[8] Using the asymptotic approximation for $V(R)$,

$$V(R)=D-C_n/R^n, \quad (3a)$$

where D is the dissociation limit of the potential, C_n is given by

$$E(v)=D-C_n/[R_2(v)]^n. \quad (3b)$$

Changing the variable of integration to $y\equiv R_2(v)/R$, Eq. (2) becomes

$$\frac{dv}{dE(v)}=(\pi\hbar)^{-1}(\tfrac{1}{2}\mu)^{1/2}\frac{C_n^{1/n}}{[D-E(v)]^{1/2+1/n}}\times\int_1^{R_2/R_1}y^{-2}(y^n-1)^{-1/2}dy.$$

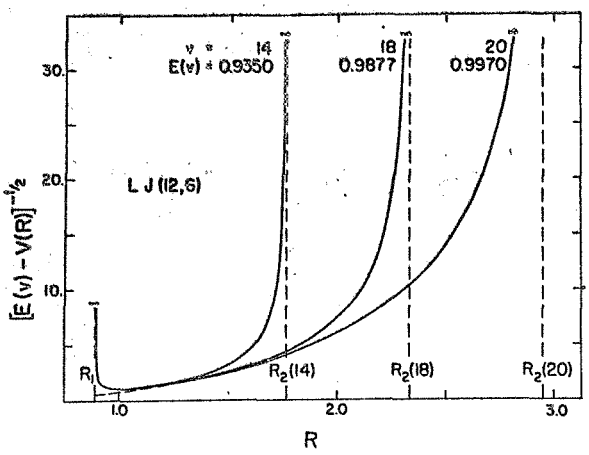

FIG. 1. Exact integrand (solid curves) of Eq. (2) for three levels of a "standard" 24-level LJ (12,6) potential.[8] The dashed segment of curve near R_1 is the approximate integrand $[E(v)-(1-2/R^6)]^{-1/2}$ for $v=20$. The dashed vertical lines are the turning points, where the exact integrand is singular.

In the limit $R_1(v)\to 0$ [i.e., $R_2(v)/R_1(v)\to\infty$] this integral is well known.[9] This yields an approximate analytical expression for $dE(v)/dv$ near the dissociation limit:

$$\frac{dE(v)}{dv}=\hbar\left(\frac{2\pi}{\mu}\right)^{1/2}\frac{\Gamma(1+1/n)}{\Gamma(\frac{1}{2}+1/n)}\frac{n}{C_n^{1/n}}[D-E(v)]^{[(n+2)/2n]}$$
$$=K_n[D-E(v)]^{[(n+2)/2n]}, \quad (4)$$

where K_n is an obvious collection of constants and $\Gamma(x)$ is the gamma function.[10] Note that $dE(v)/dv$ is closely related to the conventional Birge–Sponer ordinate[5]; cgs units are used throughout.

Equation (4) shows that for the uppermost vibrational levels of a given diatomic species, the spacings depend only upon the long-range potential parameters D, n, and C_n. Thus, for electronic states with the same long-range potential, B–S plots for levels near D will be precisely superimposable upon shifting of their abscissa (v) scales. This result is discussed further in Appendix A.

For sets of vibrational levels which can be described by Eq. (4), the curvature of the B–S plot must be positive since[8]

$$d^2E(v)/dv^2=[(n+2)/n^2]K_n^2[D-E(v)]^{2/n-1/2}$$
$$=d^2\Delta G(v)/dv^2$$
$$\cong\tfrac{1}{2}[d^2(\Delta G_{v-1/2}+\Delta G_{v+1/2})/dv^2]. \quad (5)$$

For $n=6$, this curvature is a constant; for $n>6$, it increases with increasing v, becoming infinite at the dissociation limit; for $n<6$, it decreases to zero at D. Positive curvature of a B–S plot for a set of experimental vibrational energies is therefore a necessary (though not sufficient) condition for the applicability of the present method.

In practical applications it is most convenient to employ the integrated form of Eq. (4),[11] which for $n\neq 2$ is

$$E(v)=D-[(v_D-v)H_n]^{[2n/(n-2)]}, \quad (6)$$

where $H_n=[(n-2)/2n]K_n$ and v_D is an integration constant.[12,13] For $n>2$, v_D takes on physical significance as the effective (noninteger) vibrational index at the dissociation limit, provided that the potential is well approximated by Eq. (3) from the highest observed levels up to D. In this case, truncation of v_D to an integer yields the vibrational index of the uppermost rotationless level, say N_D. It is interesting to note that the "natural" dependent and independent variables in Eq. (6) are, respectively, the binding energy $D-E(v)$ and the vibrational "index" counted down from D (for $n>2$). Applications of the present method are based upon the fitting of experimental energies $E(v)$ to Eq. (6) to yield values of the four quantities D, n, C_n, and v_D. This is discussed further in Secs. II.D and III.

B. Special Cases

While the potentials considered above ($n>2$) are of most practical interest, results for $n<2$ will be noted. Here the integration constant v_D must be *smaller* than any of the v values of the levels being fitted (and may even be negative) since K_n is positive and $(n-2)$ is negative [see Eq. (6)]. For $n=1$, Eq. (6) becomes

$$D-E(v)=(\mu/2\hbar^2)C_1^2/(v-v_D)^2,$$

which is the exact quantum result for a pure R^{-1} potential if one sets $v_D=-1$.[14] For $n=2$, integration of Eq. (4) yields

$$D-E(v)=[D-E(0)]\exp[-\pi\hbar v(2/\mu C_2)^{1/2}]. \quad (7)$$

Here the assignment of any given level as $v=0$ is arbitrary since the levels cannot be enumerated either down from D or up from a lowest level.[15] Equation (7) is identical to the exact quantal result[14] except that it omits the (usually small) effect on the apparent C_2 constant of the Langer correction[16] to the WKB integral, Eq. (1).

The present approach can also be applied to potentials whose long-range tails are not of the inverse-power form. For example, consider any potential with an attractive exponential tail,[17] such that at large R, $V(R)=D-Ae^{-\beta R}$. Applying the same approximations [replacing the full potential in Eq. (2) by its tail and letting $R_1\to 0$], an expression analogous to Eq. (4) is obtained:

$$\frac{dE(v)}{dv}=\frac{(2/\mu)^{1/2}\hbar\beta[D-E(v)]^{1/2}}{1-(2/\pi)\sin^{-1}\{[D-E(v)]/A\}^{1/2}}. \quad (8)$$

As with Eq. (4), in this case the vibrational spacings near D depend only on the potential parameters (here D, β, and A), and to a first approximation (ignoring the arcsin term) they are independent of A. Integra-

tion of this expression yields

$$\left(\frac{D-E(v)}{A}\right)^{1/2}\left[1-\frac{2}{\pi}\sin^{-1}\left(\frac{D-E(v)}{A}\right)^{1/2}\right]$$
$$+\frac{2}{\pi}\left[1-\left(1-\frac{D-E(v)}{A}\right)^{1/2}\right]=\frac{\hbar\beta}{(2\mu A)^{1/2}}(v_D-v),$$

where the integration constant v_D has the same physical significance as in the inverse power ($n>2$) case. Upon expanding the left-hand side as a power series in $\{[D-E(v)]/A\}^{1/2}$, reversion of the series yields

$$D-E(v)=(\hbar^2\beta^2/2\mu)(v_D-v)^2[1+(v_D-v)Y$$
$$+\tfrac{5}{6}(v_D-v)^2Y^2+\cdots], \quad (9)$$

where

$$Y=(2/\mu A)^{1/2}\hbar\beta/\pi. \quad (10)$$

As with the inverse-power potential, the B–S plot will show positive curvature; however here the curvature is quite small, and to first order (setting $Y=0$) it is zero.[18]

This result [Eq. (9)] for potentials with an exponential tail is particularly useful since it allows a test of the approximations underlying the present treatment. One may compare Eq. (9) with the exact quantal results for one realistic model potential with an exponential tail, the Morse potential[19]: $V_M(R)=D_e\{1-\exp[-\beta(R-R_e)]\}^2$, whose eigenvalues are given by[4,14]

$$D-E(v)=(\hbar^2\beta^2/2\mu)(v_D-v)^2=\omega_e x_e(v_D-v)^2, \quad (11)$$

where v_D is, as before, the effective vibrational index at D. Clearly, in the limit $Y\to 0$, the distribution of vibrational levels predicted by Eq. (11) agrees with that of Eq. (9). This is true despite the different v_D's, which merely correspond to a change in vibrational numbering and a small shift in the eigenvalues (arising from the small change in v_D-N_D). In effect, this merely shifts the abscissa scale in the B–S plot. The influence of the short-range portion of the Morse potential is thus merely to remove the small "correction" terms in $(v_D-v)Y$ from Eq. (9), yielding Eq. (11). The value of Y depends on both β and the coefficient of the long-range (attractive) exponential term in $V_M(R)$, $A=2D_e\exp(\beta R_e)$. Substituting the latter into Eq. (10) and using known relations among the Morse parameters,[4] one identifies

$$Y=(8^{1/2}/\pi)(\omega_e x_e/\omega_e)\exp(-\tfrac{1}{2}\beta R_e), \quad (12)$$

which shows that for typical diatomics $Y\ll 1$.

C. Significance of Parameters and Sources of Error

Perturbation theory suggests[20] that near the dissociation limit, the internuclear interaction may be expressed as a sum of inverse (integer) power terms in R:

$$V(R)=D-\sum_m C_m/R^m. \quad (13)$$

Over any small interval, Eq. (3a) is a close approximation to Eq. (13), if one considers n to be an "effective" or "local" power which corresponds to a weighted average of the different m values,[21] e.g.,

$$n=\frac{\sum_m (m+1)mC_m/[R_2(v)]^{m+1}}{\sum_m mC_m/[R_2(v)]^{m+1}}-1. \quad (14)$$

In the limit $v\to v_D$, as $R_2(v)$ reaches the asymptotic region, the effective noninteger power $n\to\tilde{n}$, the (integer) smallest power contribution to Eq. (13). As long as the potential for the state in question is well behaved,[22] fits of Eq. (6) to different subsets of a given energy spectrum should all yield essentially the same value of D, though the "local" values of n, C_n, and v_D differ slightly.

At somewhat shorter separations, exponential-type exchange forces replace the inverse-power terms in dominating the interaction[20]; thus, the B–S plot becomes increasingly linear for the deeper levels.[18] However, the approximations of the present treatment are worse for these more deeply bound levels, so only the region dominated by the long-range inverse-power terms (positive curvature of the B–S plot) should be treated by the present method.

There are two main sources of error inherent in the approximations represented by Eq. (3). First and most obvious is the neglect of the singularity at $R_1(v)$ in the exact integrand of Eq. (2) (see Fig. 1). This omission tends to make the estimate of the integral used to obtain Eq. (4) somewhat small, and since the relative magnitude of this error decreases for the higher levels, the effect will be to yield values of both n and C_n which are somewhat too large.

The second source of error arises from the fact that a realistic long-range interatomic potential is a sum of attractive inverse-power terms [see Eq. (13)], in contrast to the single attractive term in the model LJ (12,6) potential. This means that whatever the effective inverse-power precisely at a given $R_2(v)$ [from Eq. (14)], terms with higher powers contribute relatively more to the potential for $R<R_2(v)$, so that the exact integrand of Eq. (2) is smaller than that for the single C_n/R^n function which best fits the potential at $R_2(v)$. This error has the opposite effect of the first, tending to produce values of n and C_n which are slightly too small. The former error is most serious for the deeper levels, while the latter dominates the situation as n [see Eq. (14)] approaches its asymptotic value $\tilde{n}$.[23]

A third potential source of error arises from use of the first-order WKB approximation [given by Eq. (1)], compounded by the omission of the Langer correction.[16] However the effect of this approximation is expected to be negligible.[24]

Values of D, n, and C_n obtained on fitting any given set of vibrational energies to Eq. (6) yield a "local" estimate of the potential in the form of Eq. (3). Be-

cause of the errors described above, this estimate of the potential will be somewhat too deep when using data for the deeper levels and slightly too shallow when considering only the highest levels. This is illustrated by the examples considered in Sec. III.

Next in importance to D are the power $\tilde{n}$ and coefficient C_n of the longest-range ($\tilde{n}$th-power) term in the expansion for the potential [see Eq. (13)]. The errors in n (see above) which induce slight errors in D, may also weaken the accuracy of $\tilde{n}$. However, for many electronic states $\tilde{n}$ is known from theoretical considerations[25]; the only question is whether the levels being fitted lie close enough to the dissociation limit D to be governed mainly by the asymptotic R^{-n} ($n=\tilde{n}$) term of the potential. If this is so, it is desirable to constrain n to be equal to $\tilde{n}$ and employ a three parameter fit to Eq. (6) [or if $\tilde{n}=2$, a two parameter fit to Eq. (7)]. This should yield improved accuracy in D and provide significant values of the theoretically interesting C_n ($n=\tilde{n}$) and v_D.

D. Implementation

In this section, a procedure is described for the practical application of the present method to experimental data in a manner intended to yield the best possible estimates of the parameters D, n, C_n, and (for $n\neq 2$) v_D. The general case of $n\neq 2$ will be considered first, followed by a brief discussion of the situation for $n=2$.

A least-squares fit of experimental energies directly to Eq. (6) is the most general way of obtaining the best values of the four quantities.[26] However, since this expression is nonlinear in the parameters, the general regression problem may have no unique solution since the sum of squares may show local minima which do not correspond to the best parameter values. This problem can be avoided if the initial trial parameter values (required by nonlinear regression procedures) are sufficiently accurate. The necessary trial values for n and v_D may be obtained from a fit to a linear expression obtained on combining derivatives from Eq. (6)[27]:

$$E'(v)/E''(v)=-[(n-2)/(n+2)](v_D-v). \quad (15)$$

Holding fixed the n and v_D values thus obtained, Eq. (6) becomes linear in a new independent variable, $w\equiv\{[(n-2)/2n](v_D-v)\}^{[2n/(n-2)]}$:

$$E(v)=D-wK_n^{[2n/(n-2)]}. \quad (16)$$

This yields trial values of D and K_n [which gives C_n via Eq. (4)]. The four parameter values thus obtained are good starting approximations for the direct nonlinear fit of the experimental energies to Eq. (6)[28]; the linearity of Eqs. (15) and (16) makes this approach particularly straightforward.[29,30]

While Eq. (16) may be used only for $n\neq 2$, Eq. (15) is also valid for $n=2$ since combining the derivatives of Eq. (7) shows that

$$E'(v)/E''(v)=-(\pi\hbar)^{-1}(\tfrac{1}{2}\mu C_2)^{1/2}.$$

Thus, even though $v_D(n=2)=\infty$,

$$\lim_{n\to 2}[(n-2)/(n+2)]v_D(n)=(\pi\hbar)^{-1}(\tfrac{1}{2}\mu C_2)^{1/2}.$$

Manipulating Eq. (4) and its derivatives, one obtains simple expressions yielding trial values of D and C_n:

$$D=E(v)-[(n+2)/2n][E'(v)]^2/E''(v) \quad (17a)$$

and

$$K_n=E'(v)/[D-E(v)]^{[(n+2)/2n]}, \quad (17b)$$

where, as before, C_n is obtained from K_n. While Eqs. (17) are valid for all n, in practice they are somewhat less accurate and more difficult to use than is Eq. (16).[31]

III. APPLICATIONS

A. Dissociation Limit and Potential Tail from Eigenvalues of a Model Potential

The method is first applied to the exact eigenvalues of the previously mentioned (Sec. II.A) 24-level LJ (12,6) potential[8]: $V(R)=1+1/R^{12}-2/R^6$ (here $D=1$, $\tilde{n}=6$, $C_6=2$). A B-S plot of the eigenvalues of any LJ (12,6) potential has positive curvature everywhere.[6] However, as discussed in Sec. II, consideration of the deeper levels by the present method is inappropriate, so the following analysis deals only with the eleven levels lying less than 10% of the well depth below the dissociation limit [i.e., $D-E(v)\leq 0.1D_e$].[19] Throughout this section, energies are expressed in units of the well depth (i.e., set $D_e=1$), length in units of the equilibrium distance (i.e., set $R_e=1$), and the zero of energy is set at the potential minimum.

The calculated eigenvalues[8] for the eleven highest levels were smoothed by fitting them to a 5th order polynomial in v, in order to obtain the derivatives on

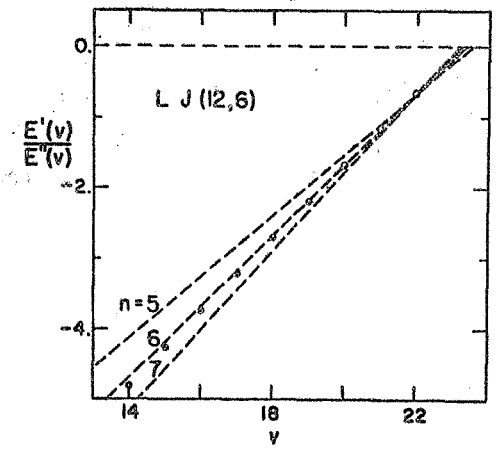

FIG. 2. $E'(v)/E''(v)$ vs v for the highest levels of the 24-level LJ (12,6) potential.[8] The broken lines have slopes corresponding to integer $n=5$, 6, and 7 [see Eq. (15)].

the left-hand side of Eq. (15). Figure 2 shows a plot of this derivative ratio vs v, compared with lines whose slopes correspond [via Eq. (15)] to integer $n=5$, 6, and 7.[32] A least-squares fit of these derivative ratios to Eq. (15) yielded $n=6.29$ and $v_D=23.27$ [32]; fixing n and v_D at these values, a subsequent fit of the eigenvalues to Eq. (16) yielded $D=1.0-1.31\times10^{-5}$ (the correct value is exactly 1.0) and $C_n=3.43$. These estimates of the parameters were then used as the initial trial values for a nonlinear fitting of the eleven energies to Eq. (6).[26,29] The parameters thus obtained were $D=1.0-1.29\times10^{-5}$, $n=6.30$, $C_n=3.46$, and $v_D=23.25$.

The above fitting procedure was then repeated several times while the deeper levels were successively omitted. Levels in the interval $v_L\leq v\leq v_H$ were included in a given fit; v_H was fixed at 23 (the highest level) while v_L was successively increased from 13 to 19.[33] In Fig. 3 the resulting parameter values (solid curves) are plotted against the energy of the lowest level included in a given fit, $E(v_L)$.

For a LJ (12,6) potential $\tilde{n}=6$, and the effective n at the outer turning point [from Eq. (14)] is always less than six. Thus the fact that four-parameter fits to Eq. (6)[29] always yield $n>6$ must be due to the first

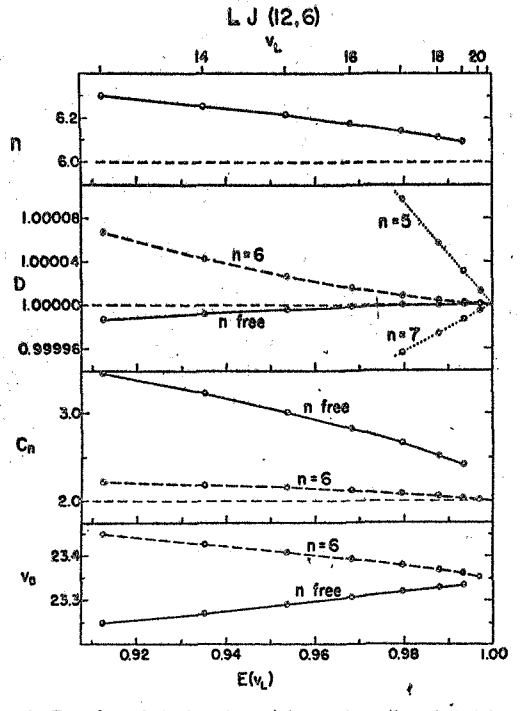

FIG. 3. Results of fitting Eq. (6) to the vibrational levels of the 24-level LJ (12,6) potential.[8,26,29] The points correspond to fits of levels v_L up to $v_H=23$. The broken horizontal lines denote the exact quantities $\tilde{n}=6$, $D=1.0$, and $C_6=2.0$. The "best" $n=6$ estimate of v_D is 23.353, in good agreement with the value 23.358 generated from the analytic expression of Stogryn and Hirschfelder.[35] Points joined by solid lines correspond to four-parameter fits with n being varied freely, while the others correspond to three-parameter fits with n held fixed at the indicated values. (*Note added in proof*: The extension of the dotted curves for D beyond $V_L=20$ was unintended.)

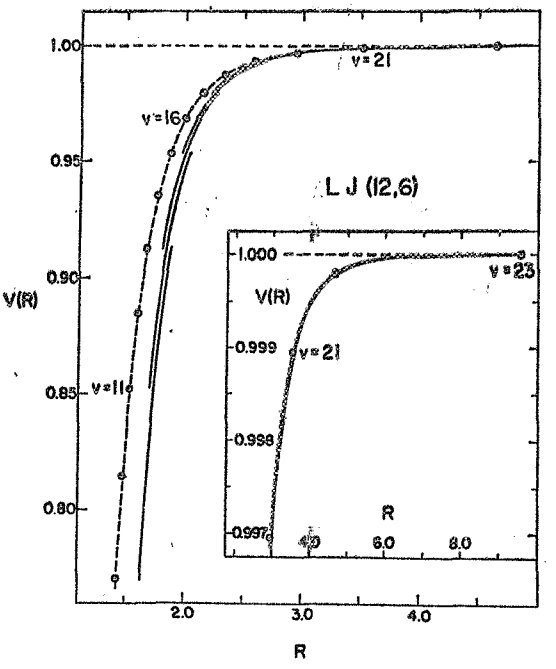

FIG. 4. Piecewise potentials constructed from three-parameter fits (D constrained at 1.0) of the LJ (12,6) vibrational energies[8] to Eq. (6).[26,29] ⊙, exact turning points for the specified levels; —, segments obtained from fits; - - -, exact asymptotic R^{-6} potential tail.

type of error discussed in Sec. II.C. To obtain more accurate estimates of D, C_n, and v_D, the above fitting procedure was repeated with n fixed at $\tilde{n}=6$. Levels v_L to $v_H=23$ were fitted while v_L was increased successively from 13 to 20,[29,33] yielding the parameter values joined by the dashed curves in Fig. 3. This procedure was repeated with n fixed in turn at 5 and 7, yielding the dotted curves in Fig. 3. Consideration of the different curves for D suggests that their comparative convergence (flattening) is a test of convergence to the true value of $\tilde{n}$.[34] In general, the three-parameter fits with n fixed at $\tilde{n}$ yield meaningful values of $C_n(n=\tilde{n})$ and v_D and give better estimates of D than do the four-parameter fits. "Best" values of all parameters are obtained from the right-hand ends of the dashed curves in Fig. 3: $D=1.0+0.13\times10^{-5}$, $C_6=2.01$, and $v_D=23.353$. This v_D value agrees well with the first order WKB value of 23.358.[35]

As pointed out above, the dominant error affecting these LJ (12,6) results arises from the effect of the singularity at $R_1(v)$. The values of n and C_n obtained from the four-parameter fits (and the C_6 values from the three-parameter fits) are somewhat large; as expected, the error diminishes as the deeper levels are successively dropped.

As discussed in Sec. II.C, the present method yields values of D, n, and C_n which provide "local" estimates of the potential over the range of energies being fitted. Hence, the outer tail of the potential may be approximated by the results of a series of piecewise fits. Further-

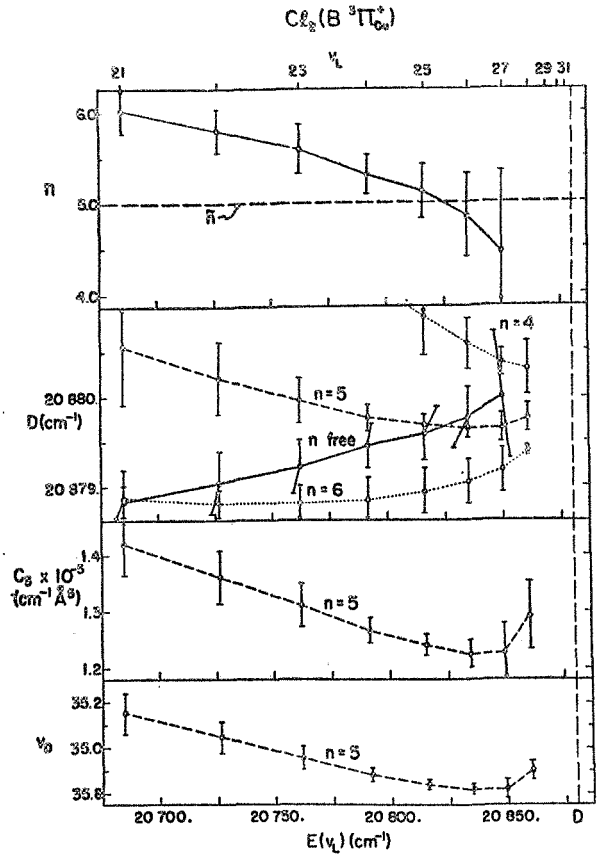

FIG. 5. Results of fitting Eq. (6)[26,29] to the experimental vibrational energies of Cl_2 ($B\ ^3\Pi_{0u}^+$).[36,37] The points correspond to fits of levels v_L up to $v_H=31$. The broken vertical line is the best estimate obtained for D. Points joined by solid curves correspond to four-parameter fits with n varied freely, while the others correspond to three-parameter fits with n held fixed at the indicated values.

more, since all of the pieces should correspond to the same value of D, holding D fixed at the "best" value obtained above should improve the accuracy of the derived potential, particularly for the deeper segments. To explore this point, levels v_L to v_H were fitted to Eq. (6),[29] with D held fixed at 1.0 and $v_H-v_L=4$, while v_H was successively decreased from 23 to 17. The resultant "local" curves are shown in Fig. 4 (only the segments corresponding to odd v_H have been included); the points are the exact turning points, and in this region are indistinguishable from the $-2/R^6$ asymptotic tail. As expected, the fitted segments are somewhat too deep. However the "nesting" of the successive segments shows the decreasing error in the fitted n and C_n as the dissociation limit is approached.[28]

B. Dissociation Limit and Potential Tail of $Cl_2(B\ ^3\Pi_{0u}^+)$

The method is now applied to experimental data for the $B\ ^3\Pi_{0u}^+$ state of Cl_2. Douglas, Møller, and Stoicheff[36] have reported accurate vibrational energies of levels $v=6$ to 31 of this state, the highest observed level lying only a few cm^{-1} below D. A B-S plot of their data shows positive curvature above $v=11$, and hence, these higher levels may be treated by the present method. In what follows, the zero of energy is conveniently set at the lowest vibrational-rotational level of the ground ($X\ ^1\Sigma_g^+$) electronic state; results are reported in the conventional spectroscopic energy and length units: cm^{-1} and angstroms.[37]

As in the LJ (12,6) case, the vibrational energies[36] were repeatedly fitted to Eq. (6) (with four free parameters)[26,29,33] while the deeper levels were successively omitted from consideration, yielding the values of n shown in Fig. 5. Theory indicates[38] that $\bar{n}=5$ for this state. The fact that the fitted n falls slightly below 5 (for $v_L=26$ and 27) is probably due to the second type of error discussed in Sec. II.C. Over the region where the fitted $n \lesssim 5$, the eigenvalue distribution is probably dominated by the R^{-5} term in the potential. In view of this, the data were refitted to Eq. (6) with n held fixed at 5,[26,29,33] to yield the estimates of D, C_n, and v_D joined by the dashed lines in Fig. 5. These ($n=5$) values of D are also compared to those obtained from analogous fits with n fixed, respectively, at 4 and 6 (dotted curves). A comparison of the limiting $[E(v_L)\rightarrow D]$ behavior of the three D curves for fixed n supports the conclusion that the highest five or six levels lie in the asymptotic $\bar{n}=5$ region. Furthermore, comparison of the $n=5$ and "n free" curves suggests that the former gives the more reliable estimate of D. This determination of $\bar{n}=5$ for this state (in agreement with theory) differs with the conclusion of Byrne, Richards, and Horsley[39]; the source of the error in the earlier work is discussed in Ref. 30.

The present analysis yields $D=20\,879.75(\pm 0.15)$ cm^{-1}, $C_5=1.29(\pm 0.06)\times 10^5$ cm^{-1} Å^5, and $v_D(n=5)=34.90(\pm 0.04)$.[40] This value of D is in agreement with, but is considerably more precise than the experimenters' best estimate[36] of $D=20\,880(\pm 2.0)$ cm^{-1}. The above C_5 compares well with the theoretical value[41] of $1.4_1\times 10^5$ cm^{-1} Å^5. Furthermore, the fitted value of v_D implies that there exist at least three unobserved bound levels above $v=31$. Table I lists the predicted level energies, obtained by substituting $n=5$ and the above values for the other three constants into Eq. (6).

It is interesting to explore the question of the accuracy of the D value which would have been obtained by the present method if the data for a few of the highest observed levels had not been available. In this case, the effective local potential for the highest remain-

TABLE I. Calculated energies (in cm^{-1}) for unobserved bound $Cl_2(B\ ^3\Pi_{0u}^+)$ levels.[37]

v	32	33	34
$E(v)$	20878.69	20879.49	20879.73

ing levels would not be dominated by the asymptotic R^{-6} term, so general four-parameter fits to Eq. (6) are necessary (cf. the three-parameter, n fixed at $\tilde{n}$ fits described above). Experimental energies were repeatedly fitted to Eq. (6), eight at a time, as the highest observed levels were successively dropped from consideration.[26,29,33] Figure 6 shows the values of D so obtained plotted vs the energy of the highest level included in a given fit $E(v_H)$.[42] It is noted that even if no levels had been observed above $v=20$ (which lies $\approx$244 cm^{-1} below D), the present method would have yielded an estimate of D within 5.5 cm^{-1} of the present "best" value! In contrast, a linear B–S extrapolation from $v=20$ yields an error in D of $\approx$69 cm^{-1}.

To obtain an estimate of the tail of the $Cl_2(B\,^3\Pi_{0u}^+)$ potential curve, the data were again fitted to Eq. (6)[29] eight levels at a time, except this time D was held fixed at the "best" value of 20 879.75 cm^{-1}.[43] In Fig. 7 the segmented potential so obtained is compared to the RKR turning points calculated by Todd, Richards, and Byrne.[44]

IV. CONCLUDING REMARKS

It has been shown that the distribution of vibrational levels near the dissociation limit of a diatomic molecule is governed mainly by the long-range attractive tail of the internuclear potential.[45] A simple approximate analytic expression has been derived for this distribution, in terms of the dissociation limit D, the power n and coefficient C_n of the effective local inverse-power potential, and an integration constant v_D (which has physical significance if $n=\tilde{n}$). These quantities may be determined via a least-squares fit of experimental vibrational energies to this equation.[26,29,33]

This approach yields the binding energy of the highest observed level with an error of at most a few percent, which is far superior to the error often resulting from use of the customary B–S extrapolation procedures.[3]

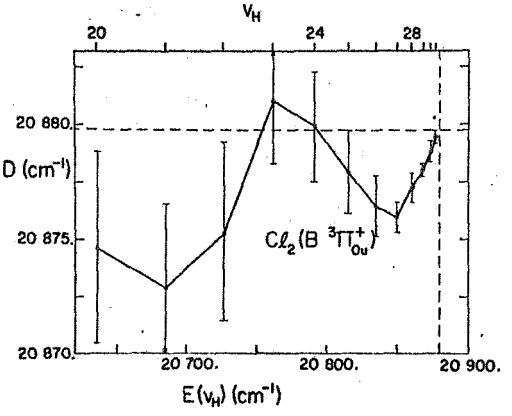

FIG. 6. D estimates obtained by fitting Eq. (6) to the energies of levels v_L to v_H,[26,29] where $v_H-v_L=7$ and v_H is varied. The vertical and horizontal broken lines denote the best present estimate of D.

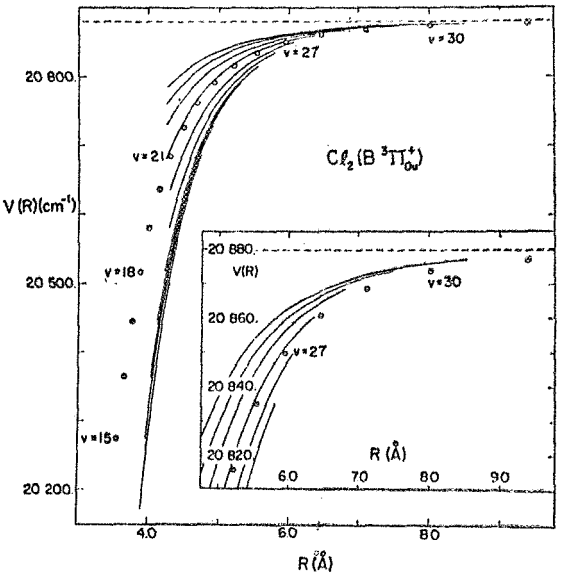

FIG. 7. Piecewise potentials constructed from three-parameter fits (with the constraint $D=20\,879.75$ cm^{-1}) of the experimental vibrational energies[36] of $Cl_2(B\,^3\Pi_{0u}^+)$ to Eq. (6).[26,29] ⊙, RKR turning points for the specified levels; —, segments obtained from fits.

It also leads to a determination of the power n and coefficient C_n of the asymptotically dominating lowest-power term in the inverse-power expansion for the potential; the results for $Cl_2(B\,^3\Pi_{0u}^+)$ accord well with theory.[46] In addition, one obtains an estimate of the outer branch of the potential over the range of the highest levels, albeit less accurate than that obtainable from an RKR potential.[7] However, the present method is much less restrictive in its data requirements and hence, may be applied in many situations where the RKR approach cannot. Here the only restrictions on the input data are that the levels must lie near the dissociation limit D, and that their B–S plot show positive curvature.[47]

A useful additional feature of the present method is its ability (when $n=\tilde{n}$) to predict the energies of all unobserved levels lying above the highest observed level.

The main alternative methods of obtaining estimates of D from spectroscopic data are through use of the less accurate B–S extrapolation (referred to earlier) or from the limiting curve of dissociation (LCD).[3,4] In the latter case, D is deduced by extrapolation to zero J of plots of the uppermost observed rotational levels vs $J(J+1)$. A large uncertainty in D is introduced by the problem of determining the breaking-off point J_{max} for each v; this is particularly important for the vibrational levels predissociating at small J, closest to the intercept of the LCD at D [e.g., see the case of $Br_2(B\,^3\Pi_{0u}^+)$ discussed in Ref. 30]. It appears that the LCD method is less reliable than the present one.

Alternative spectroscopic approaches to the deter-

mination of $\tilde{n}$ and $C_n(n=\tilde{n})$ are the standard RKR procedure and the predissociation method of Bernstein.[48] Difficulties in the use of the former are discussed in Ref. 30. The latter has been found to yield reasonable results for a number of systems[38,48,49]; however, it suffers from the above-mentioned problem of determining J_{max}. Furthermore, it presupposes an accurate value of D. In general, therefore, $\tilde{n}$ and $C_n(n=\tilde{n})$ values extracted from predissociation data are expected to be less reliable than those obtainable by the present method.

In addition to spectroscopic methods, atomic beam scattering measurements yield $\tilde{n}$ and $C_n(n=\tilde{n})$ values of roughly the same accuracy as those obtained from the present method.[50] These two techniques are essentially complementary. The present approach is best applied to electronic states of a strongly ("chemically") bound molecule with many vibrational levels, where the profusion of electronic states arising from the interaction of all but closed-shell atoms precludes the use of scattering measurements. On the other hand, the shallow van der Waals potential wells normally encountered with closed-shell atoms, ideal for study by the beam scattering technique, do not support enough bound states to be treated by the present method.

The new approach has been demonstrated by applying it to the exact computed eigenvalues of a model LJ (12,6) potential, and to the accurate experimental vibrational energies of $Cl_2(B\,^3\Pi_{0u}^+)$. In companion papers,[30] it is applied to the ground $(X\,^1\Sigma_g^+)$ state of Cl_2 and to the $B\,^3\Pi_{0u}^+$ states of Br_2 and I_2, and appears to be of quite general utility.[51] In addition, arguments based on it greatly facilitated the electronic reassignment of some levels of I_2 (see the reference cited in Ref. 21).

ACKNOWLEDGMENTS

The authors appreciate some relevant comments on interatomic forces by Professor J. O. Hirschfelder. They also acknowledge some early correspondence between R. B. B. and Dr. C. L. Beckel and discussions with Dr. H. Harrison, which helped pave the way for the present approach.

APPENDIX A: BIRGE-SPONER PLOTS FOR DIFFERENT POTENTIALS WITH IDENTICAL LONG-RANGE TAILS

The basis of the present method is the conclusion [Eq. (4)] that near the dissociation limit D, the density of vibrational levels $dv/dE(v)$ is determined almost solely by the nature of the outer (attractive) branch of the potential. Thus, B–S plots of the level spacings for different potentials with identical long-range tails and the same reduced mass (but with arbitrarily different short-range behavior) will be identical near the dissociation limit, provided their abscissa (v) scales are shifted appropriately relative to one another. This may be tested either by using exact (quantal) eigenvalues for suitably chosen potentials or, with little loss in accuracy, by the use of WKB-approximated eigenvalues. The latter procedure has been employed here. Reduced WKB integral tables are available for LJ (12,6) and exp(α, 6) ($\alpha=12.0$, 13.772, and 15.0) potentials.[6,52] The LJ (12,6) potential considered in these comparisons[8] is that utilized in Sec. III.A; throughout the present Appendix, all energies and lengths are scaled relative to its well depth and equilibrium distance, and the reduced mass μ is assumed to be the same.

For an exp(α, 6) potential with the same long-range R^{-6} tail as the model LJ (12,6),[8]

$$C_6=2=\frac{D_e R_e^6}{(1-6/\alpha)}. \tag{A1}$$

For any choice of D_e, Eq. (A1) defines the corresponding R_e; the appropriate B_z value[6] is then obtained by multiplying the $B_z(=10\,000.)$ for the model LJ (12,6) potential[8] by $D_eR_e^2$. The parameters of the chosen exp(α, 6) potentials are given in Table AI.

For LJ (12,6) and exp(α, 6) potentials with $\alpha=12.0$, 13.772, and 15.0, the WKB integral tables[6,52] [based on a reduced form of Eq. (1)] are presented as values of $\phi=(v+\frac{1}{2})/B_z^{1/2}$ vs $K\equiv-[D-E(v)]/D_e$ and $\theta\equiv(J+\frac{1}{2})^2/B_z$. Thus[5]

$$\Delta G(v)=(D_e/B_z^{1/2})\,dK/d\phi. \tag{A2}$$

Ignoring the Langer correction[16] for rotationless levels (i.e., using ϕ values for $\theta=0$, rather than for $J=0$),[53] one may obtain $dK/d\phi$ by direct numerical interpolation.[54] $\Delta G(v)$ values thus obtained, via Eq. (A2), yield curves B, C, D, and E in Fig. 8. The points on curve D are the exact quantal[8] vibrational spacings for this case,[5] $\Delta G_{v+1/2}$. Case A refers to a purely attractive potential $V(R)=D-2/R^6$, and Curve A was generated by substituting Eq. (6) into Eq. (4), with $n=6$ and $C_6=2$.[55] The abscissa scales have been shifted to make all v_D's coincide. The insert on Fig. 8 shows the five potentials of the same C_6.

The convergence of the different curves in Fig. 8 as the dissociation limit is approached is considered good evidence of the practical validity of the present method. Increases in reduced mass μ and/or the depth or breadth of the potentials (introducing more vibrational levels) would merely stretch the ordinate and abscissa scales and shift the lower curves up towards Curve A (which would remain unchanged).

TABLE AI. Parameters of exp(α, 6) potentials having same long-range tail as the model LJ (12,6).[8]

Case	E	C	B
α	12.0	13.772	15.0
D_e	1.0	1.5	2.0
R_e	1.0	0.953701	0.918386
B_z	10 000.0	13 643.20	16 868.65

APPENDIX B: ASYMPTOTIC INVERSE-POWER $\tilde{n}$ FOR ATOMIC INTERACTIONS

This section summarizes rules for determining the limiting asymptotic power $\tilde{n}$ in the internuclear interaction. It is based on the references cited in Refs. 20, 41, 56, and 57, and is limited to first- and second-order perturbation theory results. Magnetic (or relativistic) effects are ignored; this is reasonable for $R \lesssim 20$ a.u.,[58] and levels with outer turning points at larger distances would not be readily observed.

The $\tilde{n}$ of the lowest-order term in the inverse-power series expansion [Eq. (13)] for the long-range internuclear potential is determined by the nature of the two atoms to which the molecular state adiabatically dissociates. If the two atoms are charged, of course $\tilde{n}=1$; if one is charged and the other is in an electronic state with a permanent dipole moment,[59] $\tilde{n}=2$; if both atoms are uncharged and in electronic states with permanent dipole moments,[59] $\tilde{n}=3$. Another case in which $\tilde{n}=3$ occurs is in the interaction between two identical uncharged atoms in electronic states whose total angular momenta differ by one (i.e., $\Delta L=1$). This interaction is a first-order dipole resonance[56] and unlike the effects mentioned above, has no classical electrostatic analog. For interactions between a charged and a neutral atom, $\tilde{n}=4$ and $C_4=\frac{1}{2}(Z^2e^2\alpha)$, where Ze is the charge on the ion, and α the polarizability of the neutral. The case $\tilde{n}=4$ can also arise in the interaction of an atom with a permanent electric dipole moment,[59] and a non-S-state atom with a permanent quadrupole moment.

In general, pairs of (uncharged) non-S-state atoms have a first-order quadrupole–quadrupole interaction which corresponds to $\tilde{n}=5$, and theoretical C_5 values are available for a wide range of systems.[41] Occasionally the C_5 coefficient for a particular state is zero for reasons of symmetry [e.g., for the ground ($X\,^1\Sigma_g^+$) state of the halogens[38]], and in this case $\tilde{n}=6$. For states which do not fall into any of the above classifications, $\tilde{n}=6$ (since all interacting species are subject to the London induced dipole–induced dipole forces).

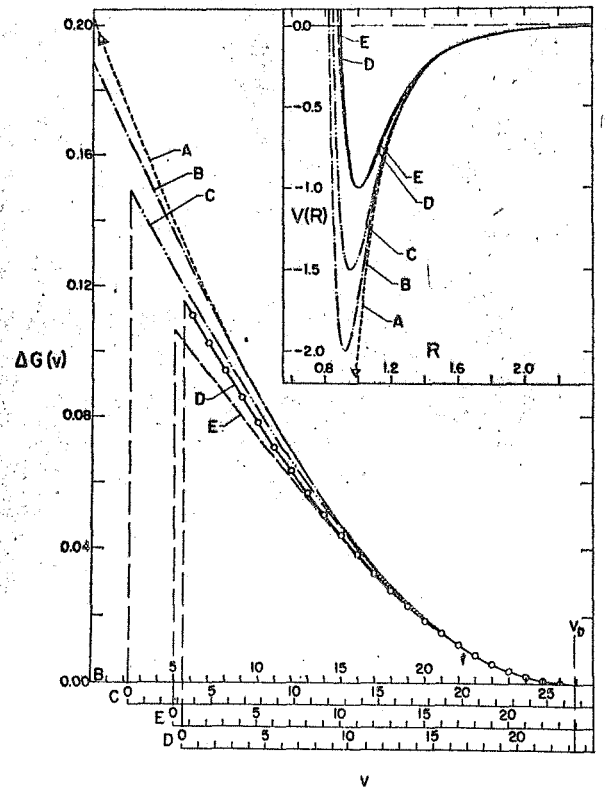

FIG. 8. Birge–Sponer plots for various potentials [LJ (12,6), exp(α, 6) and pure R^{-6}] with the same long-range tail; the insert shows the corresponding potential curves. A: pure R^{-6}, $V(R)=D-C_6/R^6$; B, C, and E: exp(α, 6), see Table AI; D: "model" LJ (12,6).[8] All B–S curves except A were generated from Eq. (A2) using WKB integral tables.[8,62] The points are exact quantal level spacings for the LJ (12,6) case,[8] and they confirm the accuracy of the WKB approximation. Curve A was obtained on substituting Eq. (6) into Eq. (4).[55]

* Work supported by National Science Foundation Grant GP-7409 and National Aeronautics and Space Administration Grant NGL 50-002-001. R. J. L. acknowledges with thanks the award of a National Research Council of Canada Postgraduate Scholarship.

[1] R. T. Birge and H. Sponer, Phys. Rev. 28, 259 (1926).

[2] R. T. Birge, Trans. Faraday Soc. 25, 707 (1929).

[3] For a recent review see A. G. Gaydon, *Dissociation Energies* (Chapman and Hall Ltd., London, 1968), 3rd. ed.

[4] G. Herzberg, *Molecular Structure and Molecular Spectra: I. Spectra of Diatomic Molecules* (D. Van Nostrand Co., Inc., Toronto, 1950), 2nd ed.

[5] Note that while $\Delta G(v)$ is Herzberg's ΔG_v, $\Delta G(v+\frac{1}{2}) \equiv dE(v+\frac{1}{2})/dv$ is not identical to the "observable" vibrational level spacing

$$\Delta G_{v+1/2}=\int_v^{v+1} \Delta G(v)\,dv$$

(see p. 98 in Ref. 4).

[6] (a) H. Harrison and R. B. Bernstein, J. Chem. Phys. 38, 2135 (1963); (b) Erratum 47, 1884 (1967).

[7] See the review by E. A. Mason and L. Monchick, Advan. Chem. Phys. 12, 329 (1967).

[8] The parameters of the LJ (12, 6) potential were chosen to allow for 24 bound states. In the notation of Ref. 6, this corresponds to $B_e=2\mu D_e R_e^2/\hbar^2=10\,000$, where D_e is the well depth, and R_e the position of the potential minimum. Eigenvalues were calculated numerically and are accurate to 10^{-7} D_e. This was done using a slightly modified form of the Cooley–Cashion program: J. W. Cooley, Math. Computation 15, 363 (1961); J. K. Cashion, J. Chem. Phys. 39, 1872 (1963).

[9] I. S. Gradshteyn and I. M. Ryzhik, *Table of Integrals, Series and Products* (Academic Press Inc., New York, 1965), Sec. 3.251, p. 295.

[10] M. Abramowitz and I. Stegun, Natl. Bur. Std. (U.S.), Appl. Math. Ser. 55 (1964); also *Handbook of Mathematical Functions* (Dover Publications, Inc., New York, 1965).

[11] This is because a direct fit of experimental data to Eq. (4) requires a prior numerical smoothing of the data to obtain accurate values of the derivatives $dE(v)/dv$.

[12] It is interesting to note that for $n=4$ (ion-induced dipole forces) Eq. (6) is simply a quartic in v, and for $n=6$ (induced dipole–induced dipole, London dispersion forces) it is cubic.

[13] By comparing Eq. (1) for $E(v)=D$ and $E(v)$ at a slightly smaller v, W. C. Stwalley (private communication, 1969) independently obtained a result for $n=6$ which, upon generalization for any $n>2$, may be cast into the useful form of Eq. (6). However, his factor equivalent to the present K_n is slightly less general, and his approach (unlike the present one) cannot be applied to cases with $n\leq 2$. While seeking a "natural" analytic expression to describe the vibrational spectrum of H_2, C. L. Beckel [J. Chem. Phys. 39, 90 (1963)] proposed empirical formulas somewhat similar in form to Eq. (6).

Chem. Phys. Lett. 6, 241 (1970).

[14] P. M. Morse and H. Feshbach, *Methods of Theoretical Physics* (McGraw-Hill Book Co., New York, 1953), Vol. 2, Sec. 12.3.

[15] For pure inverse-power potentials with $n>2$, there are a finite number of levels within any finite neighborhood of the dissociation limit, but there are an infinite number of discrete levels below it, extending down to infinite binding energy. For potentials with $n<2$, there exists a lowest level bound by a finite energy, while there are an infinite number of levels within any finite neighborhood of D. For $n=2$, the levels extend down to infinite binding energy, and there are an infinite number of levels in any finite neighborhood of D.

[16] R. E. Langer, Phys. Rev. **51**, 669 (1937). Using the Langer WKB modification [i.e., replacing $J(J+1)$ by $(J+\frac{1}{2})^2$] would require replacing Eq. (3a) by

$$V(R)=D-(C_n/R^n)+(\hbar^2/2\mu)\,(1/4R^2).$$

For $n=2$ this just means that C_2 in Eq. (7) becomes $[C_2-(\hbar^2/8\mu)]$, but for $n\neq 2$, the integral arising from Eq. (2) is no longer analytically soluble. However, for realistic systems the Langer correction is fortunately very small.

[17] Within the context of the present approach, potentials with exponential long-range tails (such as the Morse potential) correspond qualitatively to inverse-power potentials with very large n. The purely attractive exponential potential has both a discrete lowest level and a finite number of bound states within any finite neighborhood of D.

[18] A linear B–S plot for levels near the dissociation limit of a potential will be considered as an indication that the potential in the given region is effectively exponential in form.

[19] Care should be taken to avoid confusion between the well depth D_e and D, the position of the dissociation limit.

[20] See the discussion of intermolecular forces in (a) J. O. Hirschfelder, C. F. Curtiss, and R. B. Bird, *Molecular Theory of Gases and Liquids* (John Wiley & Sons, Inc., New York, 1964). (b) J. O. Hirschfelder and W. J. Meath, Advan. Chem. Phys. **12**, 3 (1967).

[21] Note that in the case where some of the dominant terms in Eq. (13) are repulsive (i.e., their $C_m<0$), some of these weighting factors will have differing signs, and the resulting value of n may then lie outside the range of the m's of the contributing terms. If the lowest inverse-power term is repulsive while the higher power terms are attractive, this gives rise to a potential maximum at large R. This appears to be the case for the $^3\Pi_{0g}^+$ state of I_2; R. J. LeRoy, J. Chem. Phys. **52**, 2678 (1970). Chapter 6.

[22] In this context a potential is "well behaved" if it has no potential maximum and no nonadiabatic perturbation.

[23] Of course, both errors approach zero for levels approaching D.

[24] (a) See, e.g., the discussion by J. K. Cashion, J. Chem. Phys. **48**, 94 (1968); see also Appendix A. (b) A. S. Dickinson (private communication, 1968).

[25] See Appendix B for a summary of the theoretical $\tilde{n}$ values for a wide variety of cases.

[26] Nonlinear least-squares regression computer programs for fitting arbitrary analytic functions are available at most computing centers. The present calculations used the University of Wisconsin Computing Center subroutine GASAUS for such fits.

[27] Primes denote differentiation with respect to v; e.g., $E'(v)=dE(v)/dv$.

[28] Parameter values obtained from Eqs. (15) and (16) should, in principle, be just as reliable as those obtained from Eq. (6). However, the former approach requires a prior smoothing of the data to obtain accurate values of the derivatives $E'(v)$ and $E''(v)$,[27] and in practice this introduces some error. Experience has shown that while trial parameter values from Eqs. (15) and (16) are satisfactory, they are measurably improved by four-parameter fittings to Eq. (6).[26]

[29] In all of the results presented, an initial fit of the data to Eqs. (15) and (16) yielded trial parameter values which were used to initiate the general nonlinear fit to Eq. (6).[26,30]

[30] R. J. LeRoy and R. B. Bernstein, (a) Wisc. Theoret. Chem. Inst. Tech. Rept. WIS-TCI-369, 1970. The report contains in an appendix FORTRAN listings of the programs used for carrying out fits to Eq. (6), (15), and (16). (b) See also, "Dissociation Energies of Diatomic Molecules from Vibrational Spacings of Higher Levels: Applications to the Halogens," Chem. Phys. Letters 5, 42 (1970), see Appendix A. Section 3.2

[31] This is mainly because of the problem of averaging the estimates of D and K_n obtained at different values of v, to yield a mutually consistent set of parameters. It is interesting that analogous to Eq. (17)

$$n=[4[E''(v)]^2/E'(v)\,E'''(v)]-2,$$

but because of the above problem, this expression is less reliable than is Eq. (15).

[32] Since the derivatives are obtained from the highest 11 energies only, they cannot be accurate at the end points, so only the 9 points shown on Fig. 2 are reliable.

[33] Since the input data (level energies) are never completely error free, a given fit should always utilize at least one level more than the number of free parameters being fitted. If there is significant experimental uncertainty in the energies (e.g., more than a few percent of the level spacings), a redundancy of more than one level may be required to yield meaningful values of the parameters.

[34] In the application of this method to the $B\,^3\Pi_{0u}^+$ state of I_2,[30] the experimental uncertainty introduces considerable imprecision into the four-parameter fits, so that n could not be directly determined within required accuracy of better than ± 1.

[35] D. E. Stogryn and J. O. Hirschfelder, J. Chem. Phys. **31**, 1531 (1959). These authors derived an analytic expression [their Eq. (89)] for the exact first-order WKB value of v_D (which omits the effect of the Langer correction[16]). A more exact value of the numerical constant in their Eq. (92) is 1.6826.

[36] A. E. Douglas, Chr. Kn. Møller, and B. P. Stoicheff, Can. J. Phys. **41**, 1174 (1963).

[37] The experimental data for this system are for the most common isotope $^{35,35}Cl_2$; all energies are expressed relative to the $v''=0$, $J''=0$ level of its ground electronic state.

[38] T. Y. Chang, Mol. Phys. **13**, 487 (1967); see also the discussion in Appendix B.

[39] M. A. Byrne, W. G. Richards, and J. A. Horsley, Mol. Phys. **12**, 273 (1967).

[40] In choosing these values it is assumed that the "hook" at the end of the $n=5$ curves in Fig. 5 is significant, illustrating the decrease of the error term for levels farther into the asymptotic ($n=\tilde{n}$) region. The indicated uncertainties (including the error bars in Figs. 5 and 6) correspond to a statistical confidence limit of 95%.

[41] It has been shown by J. K. Knipp [Phys. Rev. **53**, 734 (1938)] that C_6 coefficients may be expressed as a product of an angular factor and $[\langle r_A^2\rangle\langle r_B^2\rangle]$, the product of the expectation values for the square of the electron radii in the unfilled valence shells on interacting atoms A and B. Knipp presented values of the angular factors and approximate expectation values for a few systems, and T. Y. Chang [Rev. Mod. Phys. **39**, 911 (1967)] extended these results considerably. Recently C. F. Fischer [Can. J. Phys. **46**, 2336 (1968)] has reported Hartree–Fock values of $\langle r^2\rangle$ for all shells of atoms from He to Rn.

[42] The erratic nature of the curve in Fig. 6 is due to the influence of small errors in the experimental energies on the fitted values of the parameters; the corresponding values of n, C_n, and v_D show similar behavior. Including more levels in each fit dampens these oscillations.

[43] Holding D fixed dampens the "noise" due to experimental uncertainty,[42] yielding a more reliable segmented potential.

[44] J. A. C. Todd, W. G. Richards, and M. A. Byrne, Trans. Faraday Soc. **63**, 2081 (1967).

[45] For a related discussion of the quasibound states, see A. S. Dickinson and R. B. Bernstein, "Some Properties of Bound and Quasibound States for Various Interatomic Potential Functions," Mol. Phys. 18, 305 (1970)

[46] While the present method is expected to give values of C_n which are slightly small (see Sec. II.C), there is reason to suspect that the theoretical C_6 value used for comparison[41] may be somewhat too large. M. T. Marron (private communication, 1969) points out that Fischer's[41] values of $\langle r^2\rangle$ are based on Hartree–Fock wavefunctions which do not have correct asymptotic tails and that correcting for this may decrease $\langle r^2\rangle$, and hence the theoretical C_6.

[47] For a few systems, such as isotopic hydrogen and most hydrides, the inverse-power long-range forces are relatively weak, so that the B–S plot shows negative or zero curvature even for the very highest levels.

[48] R. B. Bernstein, Phys. Rev. Letters **16**, 385 (1966).

[49] J. A. Horsley and W. G. Richards. J. Chim. Phys. **66**, 41 (1969).

[50] See, for example, H. Pauly and J. P. Toennies, in *Atomic and Electron Physics: Atomic Interactions, Part A*, L. Marton, B.

Bederson, and W. L. Fite, Eds. (Academic Press Inc., New York, 1968), Vol. 7, Chap. 3.1, p. 227.

[51] Although all of the cases thus far considered correspond to $\tilde{n}=5$ or 6, the present method should be even more successful for systems with smaller $\tilde{n}$ (e.g., $\tilde{n}=4$, for molecules which dissociate to ion+neutral) because of the relatively higher density of levels near D.

[52] The present work utilized the corrected tables reported in Ref. 6b. These are available as Document No. 9499 in the ADI Auxiliary Publications Project, Photoduplication Service, Library of Congress, Washington, D.C. 20540.

[53] Comparison of the ϕ values[6,52] for $\theta=0$ and $\theta=10^{-4}$ shows that this introduces negligible error.

[54] This was done by piecewise fitting of third-order polynomials in ϕ. Despite the rather large gaps between the tabulated points for large ϕ, this is expected to be fairly accurate since the eigenvalue distribution for the highest levels of an R^{-6}-tailed potential is expected to be cubic in v (i.e., in ϕ).[12]

[55] Although the exact v_D is infinite for the pure R^{-6} attractive potential, there are a finite number of levels within any finite interval about D.[15] Hence the quantities (v_D-v) and Curve A in Fig. 8 are significant in the semiclassical (WKB) approximation.

[56] G. W. King and J. H. Van Vleck, Phys. Rev. 55, 1165 (1939).

[57] H. Margenau, Rev. Mod. Phys. 11, 1 (1939).

[58] This conclusion is partly based on Chang's conclusion[41] that for the 0_g^+ states of O_2 and Cu_2, these effects do not dominate the interaction until $R>60$ a.u.

[59] This case is, however, relatively uncommon; Hirschfelder and Meath[20b] point out that only an excited H atom can have a permanent dipole moment.

3.2 APPLICATION OF THE METHOD TO THE HALOGENS

The application of the method to $C\ell_2(B\ ^3\Pi^+_{0u})$, presented in Section 3.1, is reexamined here, and the analysis is extended to the analogous states of Br_2 and I_2 and to the ground electronic state of $C\ell_2$. In addition, a simple graphical means of utilizing the method is presented and verified. The work presented below will be published in the Journal of Molecular Spectroscopy, Volume 37 (Academic Press, New York, 1971). A preliminary account of these results, which was published in Chemical Physics Letters, Volume 5, pages 42-44 (North-Holland, Amsterdam, 1970), is reprinted in Appendix A.

Dissociation Energies and Long-Range Potentials of Diatomic Molecules From Vibrational Spacings: The Halogens[1]

ROBERT J. LE ROY[2] AND RICHARD B. BERNSTEIN

Theoretical Chemistry Institute and Chemistry Department, University of Wisconsin, Madison, Wisconsin 53706

A recently-developed method for obtaining dissociation limits and long-range internuclear potentials from the distribution of the uppermost vibrational levels of diatomic molecules is applied to existing data for the $B\ ^3\Pi_{0u}^+$ states of Cl_2, Br_2, and I_2, and the ground $X\ ^1\Sigma_g^+$ state of Cl_2. Values of the asymptotic long-range potential constants (C_n) are deduced from the data; they compare well with the best theoretical estimates. The analysis yields improved D_e values for the ground $X\ ^1\Sigma_g^+$ states of $^{35,35}Cl_2$, $^{79,79}Br_2$, $^{81,81}Br_2$, and $^{127,127}I_2$, respectively, as follows: 19 997.2$_5$ ($\pm$ 0.3), 15 894.5 ($\pm$ 0.4), 15 896.6 ($\pm$ 0.5), and 12 440.9($\pm$ 1.2) cm^{-1}. Presented also are: (i) a convenient graphical approximation procedure for utilizing the method, and (ii) a graphical means of making vibrational assignments for higher levels when gaps exist in the observed vibrational sequence. The latter approach suggests certain vibrational reassignments for ground-state $Cl_2(X\ ^1\Sigma_g^+)$ and for $Br_2(B\ ^3\Pi_{0u}^+)$.

I. INTRODUCTION

An expression has recently been derived which relates the distribution of vibrational levels near the dissociation limit D of a diatomic molecule to the attractive long-range part of its internuclear potential (*1*, *2*). For the common situation where the outer branch of the potential may be closely approximated by the attractive inverse-power functionality:

$$V(R) = D - C_n/R^n, \tag{1}$$

the distribution of vibrational eigenvalues $E(v)$ near D is closely approximated by

$$\frac{d}{dv}[E(v)] = K_n[D - E(v)]^{[(n+2)/2n]}. \tag{2}$$

Using physical constants from Ref. (*3*), the constant K_n is

$$K_n = \left[\frac{14.55487}{(\mu)^{1/2}(C_n)^{1/n}}\right]\left[\frac{n\Gamma(1 + (1/n))}{\Gamma(1/2 + (1/n))}\right] \tag{3}$$

for D and $E(v)$ in cm^{-1}, the reduced mass μ in amu, and C_n in cm^{-1} Å^n. As usual, $\Gamma(x)$ is the gamma function (*4*). A more useful expression is obtained by integrating Eq. (2):[3]

$$E(v) = D - [(v_D - v)H_n]^{[2n/(n-2)]}, \qquad n \neq 2, \tag{4}$$

where $H_n = [(n - 2)/2n]K_n$, and for $n > 2$ the integration constant v_D is the "effective" vibrational index at the dissociation limit: $E(v_D) = D$. Truncating

[1] Work supported by National Science Foundation Grant GB-16665 and National Aeronautics and Space Administration Grant NGL 50-002-001.

[2] National Research Council of Canada Postgraduate Scholar.

[3] Equation (4) is valid only for cases in which $n \neq 2$. However, analogous expressions for $n = 2$ and for the case of an attractive exponential long-range potential are given in Ref. (*2*).

v_D to an integer then yields the vibrational index of the highest bound rotationless level supported by the potential. Consideration of the third derivative of Eq. (4) shows that Birge-Sponer plots should show positive (upward) curvature for levels lying close to D where Eq. (1) is appropriate. The significance of the parameters and the types of errors inherent in Eqs. (1)–(4) are discussed in Ref. (*2*).

In general, values of the four unknowns D, n, C_n, and v_D may be obtained from a least-squares fit of experimental vibrational energies to Eq. (4). However, since it is nonlinear in the parameters, Eq. (4) requires good initial trial parameter values if the fit is to converge uniquely. All of the results presented below were obtained from general fits to Eq. (4), using initial trial values obtained by the method presented in Refs. (*2*, and *5*). Computer programs for these regression procedures are listed in Ref. (*5*).

The general smoothing and regression techniques discussed in Refs. (*2* and *5*) yield the best parameter values obtainable from Eqs. (2–4). However, results with almost the same accuracy may be obtained from a simple graphical treatment of the data, described below, if two extra conditions are satisfied. First, the value of $\tilde{n}$, the asymptotic value of the power in Eq. (1), must be known.[4] Second, the levels must be sufficiently "dense" to allow use of the approximation

$$\frac{dE(v)}{dv} \simeq \overline{\Delta G}_v \equiv \frac{1}{2}[\Delta G_{v-1/2} + \Delta G_{v+1/2}] = \frac{1}{2}[E(v+1) - E(v-1)]. \quad (5)$$

Then, with n held fixed at $\tilde{n}$,[4] Eq. (2) yields the approximate expression

$$(\overline{\Delta G}_v)^{[2n/(n+2)]} = [D - E(v)](K_n)^{[2n/(n+2)]}, \quad (6)$$

suggesting a plot of $(\overline{\Delta G}_v)^{[2n/(n+2)]}$ vs $E(v)$. For the highest levels this should be linear with intercept D, while for the relatively deeper levels it should show negative curvature. Hence, a linear extrapolation from such a plot should always give an upper bound to D. Once D has been determined in this manner, Eq. (4) may be rewritten as

$$[D - E(v)]^{[(n-2)/2n]} = (v_D - v)H_n\,. \quad (7)$$

With $n = \tilde{n}$, a plot of the left hand side vs v yields v_D as the intercept, and H_n (and hence C_n) from the slope. The usefulness of Eqs. (5–7) is demonstrated below.

In Sect. II, Eq. (4) is fitted to the experimental vibrational energies of the $B\,^3\Pi_{0u}^+$ states of Cl_2, Br_2, and I_2, yielding estimates of the asymptotic long-range potential constants, C_5, and improved values of the ground-state dissociation energies.[5] A further application of Eq. (4) is introduced in Sect. III, which suggests vibrational reasssignments for the highest observed levels of Br_2 ($B\,^3\Pi_{0u}^+$) and of ground state Cl_2 ($X\,^1\Sigma_g^+$). In the latter case, a fit to Eq. (4) then yields estimates of v_D and of the long-range C_6 constant.

II. GROUND-STATE DISSOCIATION ENERGIES AND B $^3\Pi_{0u}^+$ STATE POTENTIAL TAILS OF THE HALOGENS

A. Chlorine[6]

A detailed discussion of the fitting of the experimental data (*9*) for Cl_2 ($B\,^3\Pi_{0u}^+$)

[4] A summary of theoretical knowledge of the asymptotically dominating power $\tilde{n}$ is given in App. B of Ref. (*2*). For the $B\,^3\Pi_{0u}^+$ states of the halogens $\tilde{n} = 5$, while for their ground $X\,^1\Sigma_g^+$ states, $\tilde{n} = 6$ (*6*, *7*, *8*).

[5] Unless otherwise stated, throughout this paper all energies are expressed relative to the $v = 0$, $J = 0$ level of the ground electronic state of the designated isotopic molecular species.

[6] The present discussion of chlorine considers only the most common isotopic species, $^{35,35}Cl_2$.

to Eq. (4) has been presented (*2*). However, the reported (*1*, *2*) uncertainties in the parameters were incorrectly described as 95% statistical confidence intervals; they were actually two standard deviations, corresponding to the 95% confidence level only in the limit of many degrees of freedom. Parameter values obtained on fitting the experimental energies (*9*) to Eq. (4) with n free or fixed at $\tilde{n} = 5$ are given in Fig. 1, together with the proper 95% confidence intervals.[7]

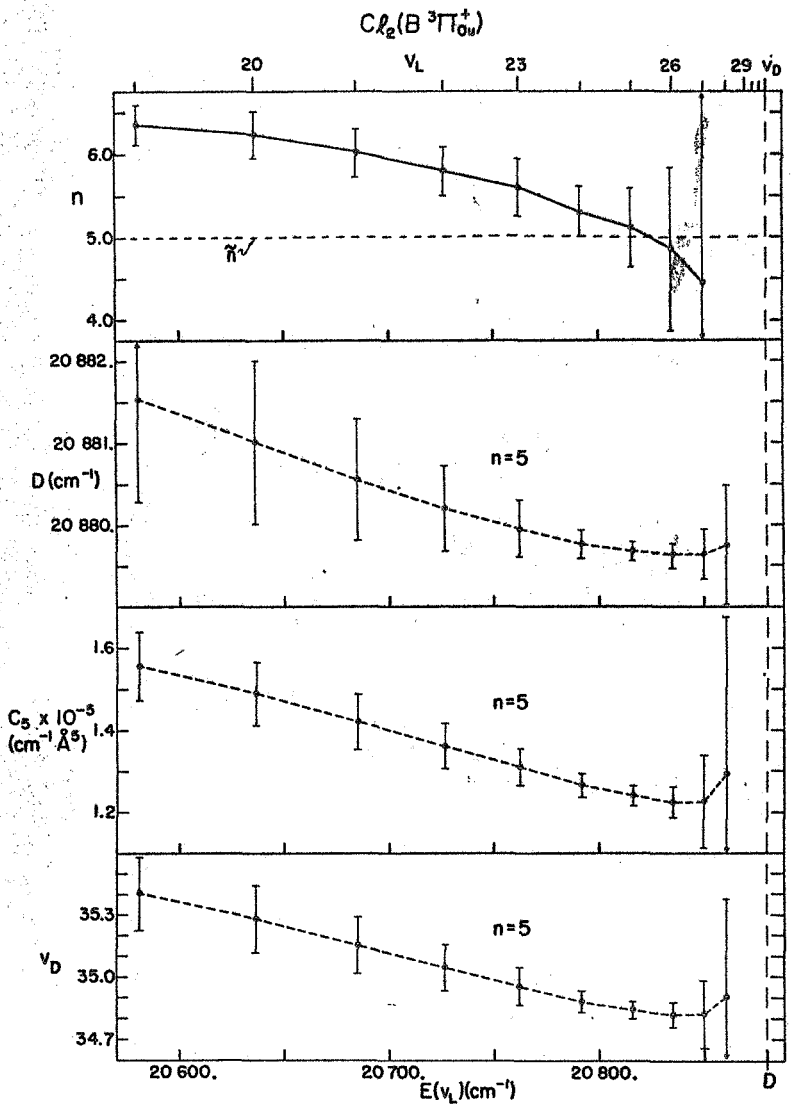

FIG. 1. Results of fitting experimental vibrational energies of $^{35,35}Cl_2$ ($B\ ^3\Pi_{0u}^+$) (*9*) to Eq. (4). The points correspond to fits of levels v_L up to $v_H = 31$. The vertical broken line is the best estimate obtained for D. Points joined by solid curves correspond to four-parameter fits with n varied freely, while the others correspond to three-parameter fits with n held fixed at $\tilde{n} = 5$. The error bars represent proper 95% confidence intervals.

[7] Unless otherwise stated, all uncertainties given in this paper correspond to 95% statistical confidence intervals.

It was concluded in Ref. (*2*) that the highest observed levels of Cl_2 ($B\,^3\Pi_{0u}^+$) depend mainly on the theoretical asymptotic $\tilde{n} = 5$ inverse-power term in the long-range potential.[4] The disagreement with the $\tilde{n} = 6$ suggestion of Byrne *et al.* (*10*) is discussed in Sect. IV. The values of D, C_5, and v_D reported in Ref. (*2*) (which also gave predicted energies of the unobserved highest bound levels of this state) are listed for the sake of completeness in Table I, together with the improved estimates of their uncertainties.[8] Similarly included are the results for the other halogen systems, to be discussed below.[9]

TABLE I

SUMMARY OF RESULTS FOR THE HALOGENS[a]

$B\,^3\Pi_{0u}^+$ states	D (cm^{-1})[b]	$n = \tilde{n}$	C_5 (cm^{-5}Å^n)	v_D
$^{35,35}Cl_2$	20879.7$_5$ (±0.3[c])	5	1.2$_9$ (±0.2[c]) × 10^5	34.9$_0$ (±0.2[c])
$^{79,79}Br_2$	19579.7$_1$ (±0.27)	5	1.7$_9$ (±0.2) × 10^6	60.5$_1$ (±0.3)
$^{81,81}Br_2$	19581.7$_7$ (±0.35)	5	1.7$_9$ (±0.2) × 10^6	61.2$_8$ (±0.3)
$^{127,127}I_2$	20044.0 (±1.2)	5	3.1$_1$ (±0.2) × 10^5	87.7 (±0.4)
$X\,^1\Sigma_g^+$ states	($D = D_e$)			
$^{35,35}Cl_2$	19997.2$_5$ (±0.3[c])	6	0.7$_4$ (±0.3[d]) × 10^5	61.0 (±1.2)[d]
$^{79,79}Br_2$	15894.5 (±0.4)	6	—	—
$^{81,81}Br_2$	15896.6 (±0.5)	6	—	—
$^{127,127}I_2$	12440.9 (±1.2)	6	—	—

[a] See footnote 7.
[b] See footnotes 5 and 9.
[c] See footnote 8.
[d] These uncertainties are only estimates.

While the parameters given in Table I are the best values obtainable from the available experimental data (*9*) using the present method, results of nearly the same quality are obtained on utilizing these data (*9*) directly in the simple graphical manner suggested by Eqs. (5–7). For this case the theoretical $\tilde{n} = 5$,[4] and Fig. 2 shows the plot suggested by Eq. (6); the intercept is indistinguishable from the value of D obtained from the fits to Eq. (4) (see Table I). Using this D and $n = \tilde{n} = 5$, Fig. 3 shows the plot suggested by Eq. (7); its slope and intercept are very close to the fitted values of H_n and v_D (from Table I).

Combining the fitted D value for Cl_2 ($B\,^3\Pi_{0u}^+$) with the $^2P_{1/2} - {}^2P_{3/2}$ atomic Cl spin–orbit splitting of 882.50 cm^{-1} (*12*, *13*) yields a ground-state dissociation energy of $D_e = 19\ 997.25$ (±0.3) cm^{-1}. This differs significantly from both the estimate of $D_e = 20\ 062$ (±40) cm^{-1} obtained by Rao and Venkateswarlu (*14*) from a Birge-Sponer extrapolation of their ground-state vibrational data, and from the $D_e = 20\ 040$ (±20) cm^{-1} which Clyne and Coxon (*15*) obtained on reinterpreting the data of Ref. (*14*). However, the discrepancy is removed by the vibrational reassignment of the highest observed ground-state level, discussed below in Sect. III.

B. Bromine

The present analysis of the $B\,^3\Pi_{0u}^+$ state of Br_2 makes use of concurrent fitting

[8] The final uncertainties in the best parameter values for Cl_2 ($B\,^3\Pi_{0u}^+$) differ from both the previously-reported values (*1*, *2*) and the true 95% statistical confidence intervals shown in Fig. 1. The values given are best estimates based on the 95% confidence intervals for the last few points to the right in Fig. 1.

[9] The uncertainties in these D values differ from those reported previously (*1*, *2*, *11*) because of the incorrect 95% confidence intervals in the earlier work.

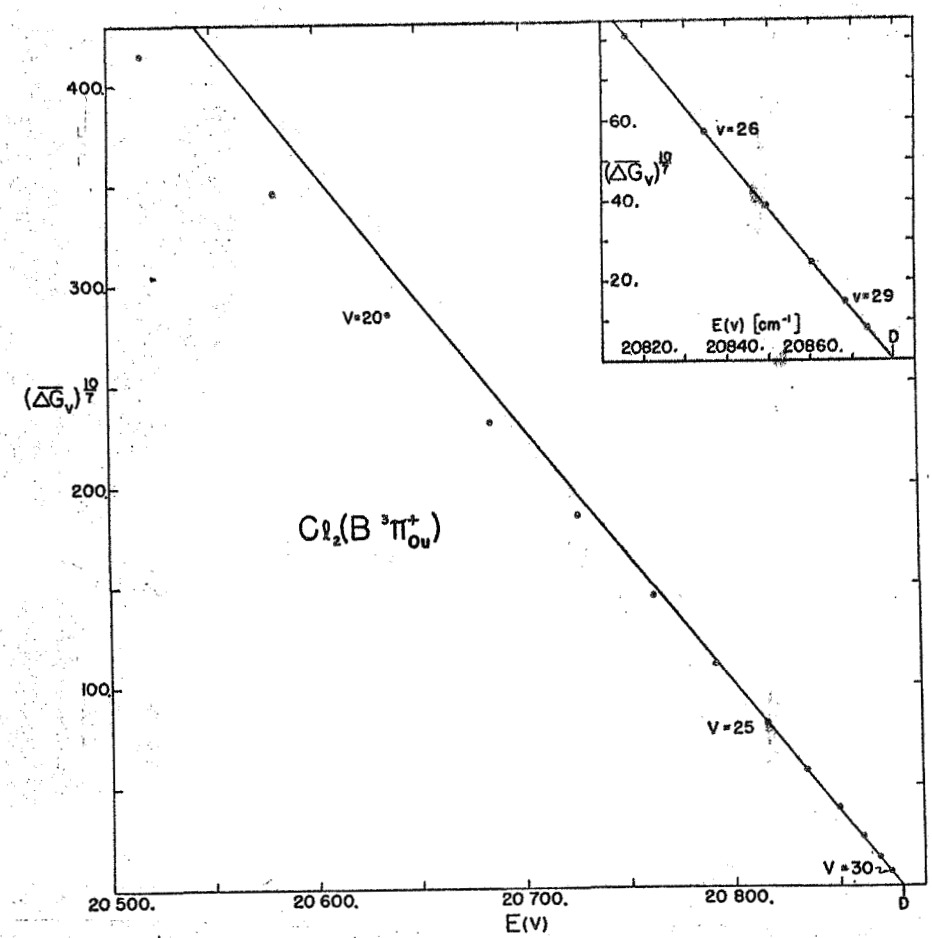

FIG. 2. Data for $^{35,35}Cl_2$ ($B\ ^3\Pi^+_{0u}$) (9) plotted according to Eqs. (5–6) with $n = \bar{n} = 5$ (see footnote 4). Energies are in cm^{-1}; the mark at D denotes the fitted value from Table I.

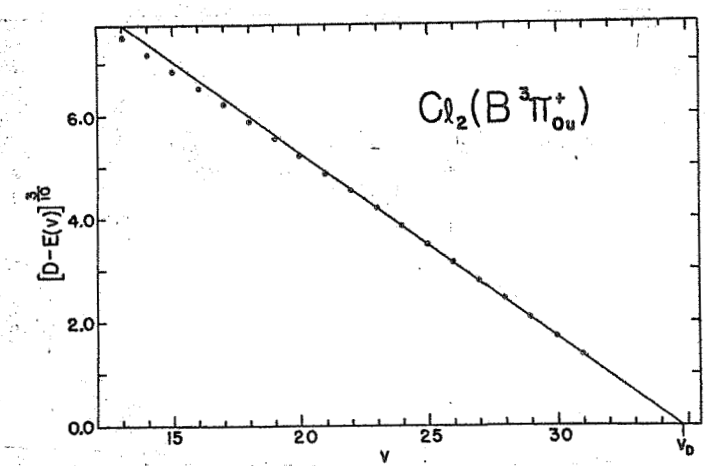

FIG. 3. Data for $^{35,35}Cl_2$ ($B\ ^3\Pi^+_{0u}$) (9) plotted according to Eq. (7) with $n = \bar{n} = 5$ (see footnote 4). Energies are in cm^{-1}; the mark at v_D denotes the fitted value from Table I.

to Eq. (4) of data for different isotopes in a given molecular electronic state. The only assumption required is that the long-range potential tails of the isotopic species be identical.[10] If the isotopic potentials are assumed to be identical everywhere, the number of free parameters in the problem is reduced further, since the ratio of v_D values for isotopic species i and j is then determined solely by the reduced mass ratio:

$$v_D(j)/v_D(i) = [\mu(j)/\mu(i)]^{1/2}. \tag{8}$$

To obtain trial parameter values for a multi-isotope case (*5*), Eq. (8) is assumed and the relative isotope shifts are estimated.[11] (Alternately, trial parameter values may be estimated separately by applying Eqs. (5–7) or the method of Ref. (*2*) to the data for the individual isotopic molecules.) However, in the final fits to Eq. (4), D, n, C_n, v_D for each isotope, and the relative energy shifts (ground-state zero-point energy shifts[5]) for the different species were the free parameters.

Horsley and Barrow (*18*) have measured vibrational energies of four adjacent vibrational levels, v = 50–53, near the dissociation limits of the $B\,^3\Pi_{0u}^+$ states of $^{79,79}Br_2$ and $^{81,81}Br_2$. (It is suggested in Sect. III that their vibrational assignment for these levels is one unit too small; the new numbering is used here.) Unfortunately, a fit of these eight observations to Eq. (4) with all six parameters free did not yield a reliable value of $\tilde{n}$. However, since all the levels considered lie within 20 cm^{-1} of the dissociation limit, it is probable that they depend primarily on the theoretical[4] asymptotic potential behavior ($V(R) \sim R^{-5}$). The plausibility of this assumption is strengthened by consideration of Fig. 2 which shows that for Cl_2 ($B\,^3\Pi_{0u}^+$), the levels within ca. 40 cm^{-1} of D accord with $\tilde{n} = 5$, while the theoretical C_5 for Cl_2 is considerably smaller than that for Br_2.[12]

Fixing $n = \tilde{n} = 5$,[4] the eight data were fitted to Eq. (4), yielding the parameters given in Table I, and an isotopic zero-point energy shift of 2.05 ($\pm$0.12) cm^{-1}.[7] The latter is in good agreement with the more precise value of 2.03 cm^{-1}, the difference between the ground-state isotopic zero-point energies calculated from the vibrational constants of Ref. (*18*).

The ratio of the Br_2 isotopic v_D's in Table I agrees well within the uncertainty of the fit with that predicted by Eq. (8), confirming its validity for this case. Hence, Eq. (8) may be applied for the mixed isotopic molecule $^{79,81}Br_2$, yielding v_D = 60.89. Furthermore, the (79,79)–(81,81) isotope shift suggests a value of D = 19 580.7$_4$ cm^{-1} for the mixed isotope (79,81). Using these interpolated parameters and the constants given in Table I, the energies of the highest vibrational levels of the $B\,^3\Pi_{0u}^+$ potential may be predicted from Eq. (4) for all three

---

[10] This is much less stringent than requiring precise potential invariance everywhere, including R values near the minima. Small differences between potential curves for different isotopic species in a given state arise from the coupling of nuclear and electronic motion. In their *a priori* calculations for the ground state of H_2, Kolos and Wolniewicz (*16*) showed that the effect of such coupling disappeared at long range. More generally, the effect of this coupling on an eigenvalue depends on the expectation value of the nuclear kinetic energy, and this goes to zero for levels approaching the dissociation limit [e.g., for ground state H_2, see Table III of Ref. (*17*)].

[11] These shifts were estimated in two ways: (a) by comparing vibrational zero-point energies, and (b) by separately smoothing the level energies for the different isotopic molecules as functions of a common abscissa χ (related to the vibrational quantum number by: $\chi = v(i)\,[\mu(1)/\mu(i)]^{1/2}$ and comparing the calculated ordinates at any chosen χ value.

[12] Values of long-range C_5 constants may be expressed as the product of a factor peculiar to the electronic state in question, and the expectation values of the square of the radii of the valence electrons $\langle r^2 \rangle$ on the interacting atoms (*6*). Knipp (*6*) and Chang (*7*) have presented tables of these numerical factors for a wide range of situations, and Fischer (*19*) has recently presented accurate Hartree-Fock values of $\langle r^2 \rangle$ for the shells of most atoms.

isotopic species. In Table II these are compared to the experimental energies of Ref. (*18*) for the pure (79,79) and (81,81) isotopes, and of Brown (*20*) for (79,81).[13]

As in the discussion of Cl_2, it is interesting to compare the best fitted parameter values with the estimates of them which would have been obtained from Eqs. (5–7), with $n = \bar{n} = 5$.[4] In this case the two isotopes must be considered separately; for each, the four observed energies yield only two $\overline{\Delta G}_v$ values, uniquely determining the intercepts D. These resultant D values for (79,79) and (81,81) are, respectively, only 0.05 and 0.15 cm^{-1} larger than the best fitted values (Table I). Using these (approximate) D's and fixing $n = 5$, Eq. (7) then yields Fig. 4. As before (for Cl_2, see Fig. 3), the slopes and intercepts lie within the statistical uncertainties in the fitted Table I parameter values.

Combining the fitted D values for the pure isotopes with the 3685.2 (±0.3) cm^{-1} spin–orbit splitting (*21*) yields ground-state dissociation energies of D_e (79,79) = 15 894.5 (±0.4) cm^{-1}, and D_e (81,81) = 15 896.6 (±0.5) cm^{-1}. The consistent estimated value for the mixed isotope is D_e (79,81) = 15 895.5 (±0.5) cm^{-1}.

TABLE II

CALCULATED ENERGIES (cm^{-1}) OF THE HIGHEST BOUND LEVELS OF ISOTOPIC $Br_2(B\ ^3\Pi_{0u}^+)$

Numbers in parentheses are experimental; for (79,79) and (81,81) these are from Ref. (*18*), while for (79,81) they are taken from Ref. (*20*)[a]

v	(79,79)		(79,81)		(81,81)	
41	19 453.44		19 448.89	(19 470.3)	19 444.00	
42	473.76		469.72	(486.2)	465.37	
43	491.66		488.13	(499.5)	484.31	
44	507.34		504.28	(512.5)	500.97	
45	520.94		518.36	(524.3)	515.53	
46	532.65		530.51	(531.5)	528.15	
47	542.62		540.90	(542.2)	538.98	
48	551.01		549.68	(551.4)	548.18	
49	557.97		557.01		555.90	
50	563.65	(19 563.65)	563.04		562.28	(19 562.28)
51	568.20	(568.20)	567.90		567.46	(567.45)
52	571.76	(571.77)	571.74		571.60	(571.61)
53	574.47	(574.47)	574.69		574.82	(574.81)
54	576.46		576.89		577.24	
55	577.84		578.46		579.00	
56	578.75		579.51		580.22	
57	579.2_9		580.1_7		581.00	
58	$579._{57}$		$580._{53}$		581.4_5	
59	$579._{69}$		$580._{69}$		$581._{68}$	
60	$579._{71}$		$580._{74}$		$581._{76}$	
61					$581._{77}$	

[a] See footnote 13.

[13] Brown (*20*) stated that: "In general the measurements are not accurate to better than 2 cm^{-1}, and in cases where the isotope effect has not been identified, the error is considerably greater." Furthermore, consideration of Table II suggests that some of his band heads might more properly be reassigned to the pure isotopes and/or to different vibrational levels. If this is done, for 6 of the 8 experimental (*79,81*) energies given in Table II the agreement is better than 2 cm^{-1}, while for the other two (v = 44 and 45) the disagreement is at worst 3.5 cm^{-1}. In any case, the calculated (Table II) energies for the deeper levels (e.g., $v \lesssim 43$) are likely to be increasingly in error.

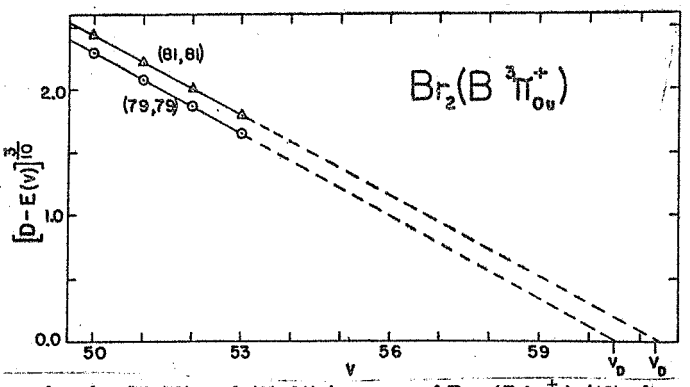

FIG. 4. Data for the (79,79) and (81,81) isotopes of Br_2 ($B\ ^3\Pi_{0u}^+$) (*18*) plotted according to Eq. (7) with $n = \tilde{n} = 5$ (see footnote 4); as in Fig. 3, the slopes of the lines differ by the amount predicted by the reduced mass factor in Eq. (3).

C. Iodine[14]

The only quantitative data for this state extending above $v = 58$ appear to be Brown's (*22*) band-head measurements for levels $v = 48$ to 72.[15] Since a Birge-Sponer plot of his vibrational spacings shows positive curvature everywhere, these data are suitable for treatment by the present method.

As for Cl_2 ($B\ ^3\Pi_{0u}^+$) (*2*), the vibrational energies were repeatedly fitted to Eq. (4) while the deeper levels were successively omitted from consideration. This was done in turn with all four parameters being varied freely, and with n fixed at $\tilde{n} = 5$. The resulting parameter values are shown in Fig. 5, plotted against the energy of the lowest level included in a given fit, $E(v_L)$.[7] Unfortunately, the scatter in the data is such that the four-parameter fits become unstable when fewer than 10 levels are considered at once, precluding a direct determination of $\tilde{n}$. Even when n is held fixed at $\tilde{n} = 5$, the three-parameter fits become erratic when fewer than 9 levels are considered at once.

While reliable "local values" of n cannot be determined directly, the flattening of the three broken line curves in Fig. 5 for $v_L \gtrsim 55$ strongly suggests that the highest ca. 18 observed levels lie in the asymptotic ($\tilde{n} = 5$) region. This is qualitatively confirmed by the fact that the fitted C_5 values are within 30% of the theoretical value[12] of $4.5_4 \times 10^5$ cm^{-1} Å^5. The present best estimates of D, C_5, and v_D, presented in Table I, were obtained by weighting the results for $v_L = 55$ to 64 by the squared inverse of their uncertainties.[9] The v_D value suggests that this state has 15 vibrational levels above the highest one observed by Brown (*22*); predicted values of their energies, generated from Eq. (4) and the parameters in Table I, are given in Table III.

As in the previous cases, the best fitted parameter values can be compared to estimates of them obtainable from Eqs. (5–7). Figure 6, based on Eqs. (5–6), yields an estimate of D indistinguishable from the value in Table I. Furthermore, the linearity of this plot for $v \gtrsim 55$ confirms the dominant $\tilde{n} = 5$ influence in this region. The ensuing plot based on Eq. 7 (Fig. 7) yields estimates of v_D and H_n lying well within the statistical uncertainties in the Table I values.

Combining the fitted value of D with the 7603.15 cm^{-1} atomic $^2P_{1/2} - {}^2P_{3/2}$ splitting (*12*, *25*) yields a ground-state dissociation energy of $D_o = 12\ 440.9$ (± 1.2) cm^{-1}.[9] The source of the disagreement between this result and Verma's (*26*) $D_o = 12\ 452.5$ (± 1.5) cm^{-1} is discussed elsewhere (*11*).

[14] The present discussion of iodine considers only the most common isotopic species $^{127,127}I_2$.

[15] The original vibrational numbering of these levels has since been revised (*23*, *24*); thus the numbering used by Brown (*22*) has been decreased by one unit.

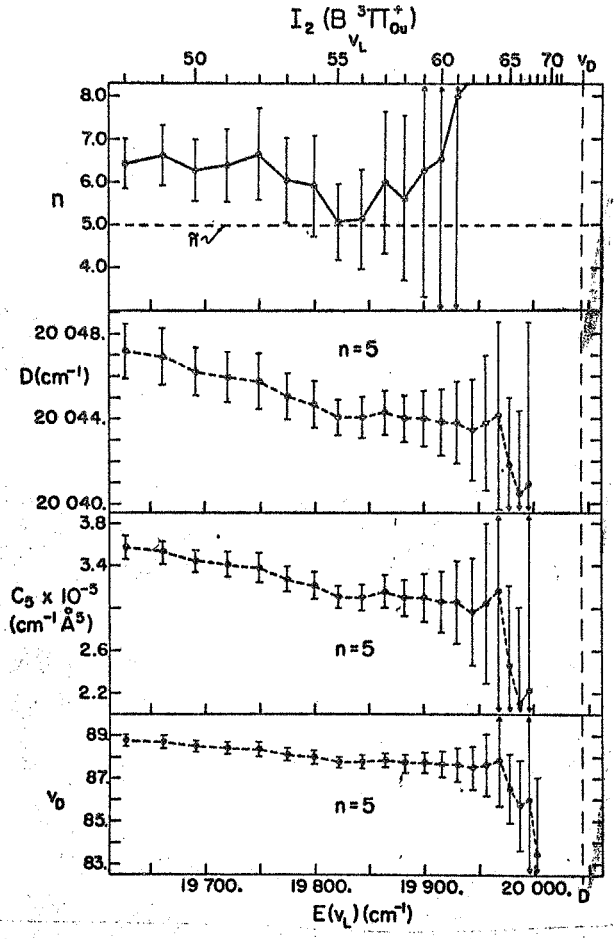

FIG. 5. Results of fitting experimental vibrational energies of $^{127,127}I_2$ ($B\ ^3\Pi_{0u}^+$) (*22*) to Eq. (4); as in Fig. 1.

TABLE III

CALCULATED ENERGIES (cm^{-1}) OF THE HIGHEST BOUND LEVELS OF $^{127,127}I_2$($B\ ^3\Pi_{0u}^+$)
Brown's (*22*) experimental energies for $v \leqq 72$ are given in parentheses.

v	$E(v)$	v	$E(v)$
66	19 987.2 (19 986.9)	77	20 038.6
67	19 995.5 (19 995.5)	78	040.1
68	20 002.8 (20 002.7)	79	041.3
69	009.4 (009.6)	80	042.2
70	015.2 (015.5)	81	042.9
71	020.2 (020.2)	82	043.3
72	024.7 (024.4)	83	043.6
73	028.5	84	043.86
74	031.7	85	043.94
75	034.4	86	043.99
76	036.7	87	044.00

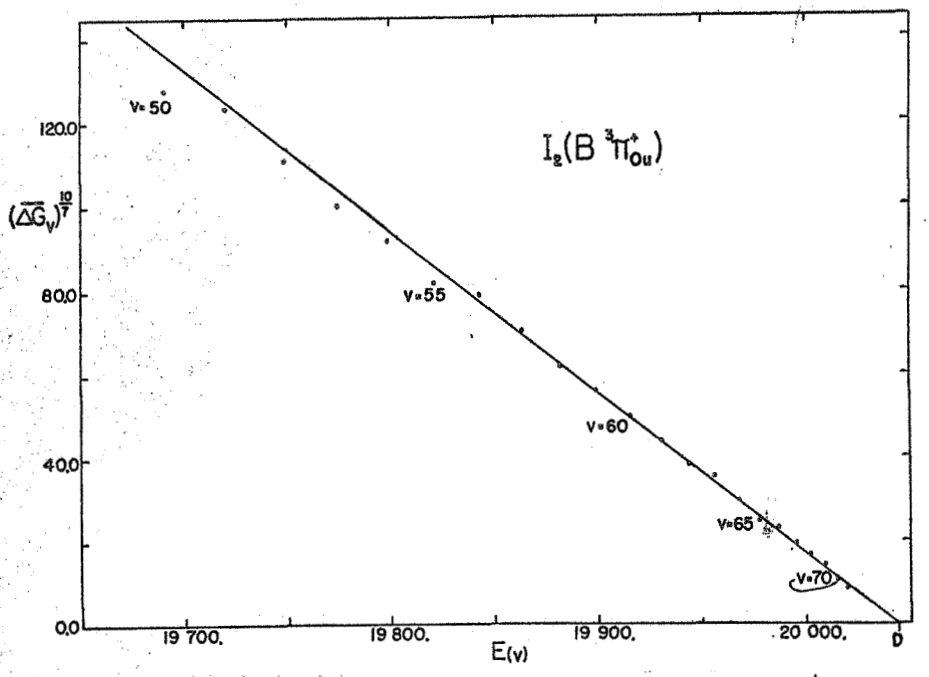

FIG. 6. Data for $^{127,127}I_2$ ($B\ ^3\Pi_{0u}^+$) (*22*) plotted according to Eqs. (5–6) with $n = \bar{n} = 5$ (see footnote 4); as in Fig. 2.

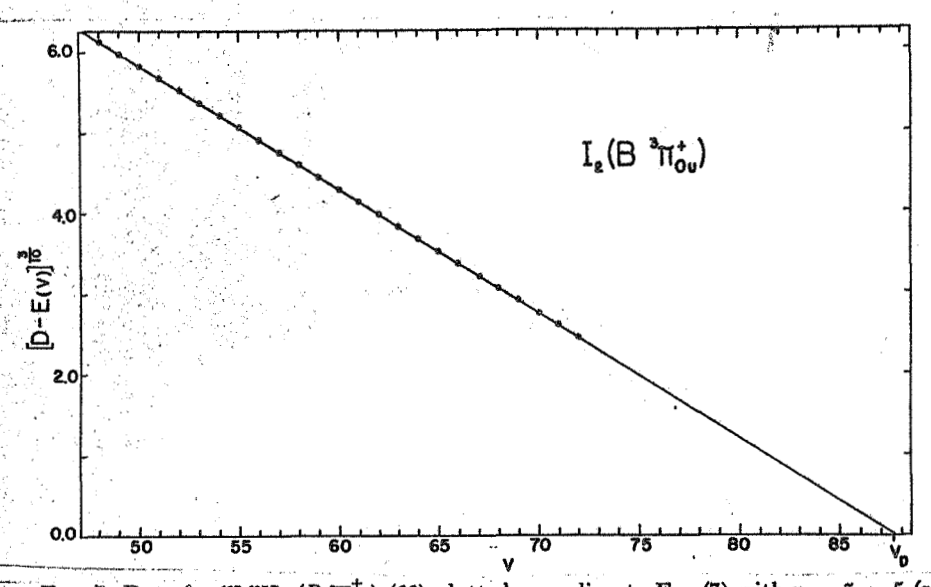

FIG. 7. Data for $^{127,127}I_2$ ($B\ ^3\Pi_{0u}^+$) (*22*) plotted according to Eq. (7) with $n = \bar{n} = 5$ (see footnote 4); as in Fig. 3.

III. PROPOSED VIBRATIONAL REASSIGNMENTS

A. General

Frequently the energies and indexing of the deeper vibrational levels of a given electronic state are accurately known, while near its dissociation limit D the data are often relatively sparse, with gaps of several vibrational quantum numbers between observed levels. In the absence of additional information, this may lead to errors in vibrational assignments.

One constraint which may be applied to the data is to require that the Birge-Sponer plot for the species in question should have positive curvature for levels

near D (*1*, *2*). The present approach implicitly includes this constraint while making more explicit use of Eq. (4). The necessary assumptions are a value for $\tilde{n}$, and a good estimate of D which is independent of the vibrational numbering under dispute. Then [according to Eq. (7)], for n fixed at $\tilde{n}$, a plot of $[D - E(v)]^{[(n-2)/2n]}$ vs v should be linear for levels very near D, while showing progressively stronger negative curvature for deeper levels (see discussion in Sect. I). Since the long-range interatomic interaction may be expressed (*27*, *28*) as a sum of inverse (integer)-power terms in R (of lowest order $\tilde{n}$), the effective "local" n at the outer turning points increases with the binding energy. However, consideration of Eq. (4) shows that in the limit of very large n, $[D - E(v)]$ varies directly as $(v_D - v)^2$. Thus, a plot of $[D - E(v)]^{1/2}$ vs v should have strong positive curvature near the dissociation limit (for $\tilde{n} > 4$ this curvature becomes infinite at D), while becoming increasingly linear for the deeper levels.

The present approach consists of requiring the vibrational assignment to be such that the two types of plot discussed above show the appropriate curved and linear regions. As a check, in Fig. 8 this approach was applied to the data of Douglas *et al.* (*9*) for Cl_2 ($B\,^3\Pi^+_{0u}$), for which $\tilde{n} = 5$.[4] Clearly, even had there been a gap of 10 unobserved levels somewhere in the range, Fig. 8 would have unambiguously fixed the vibrational assignments.

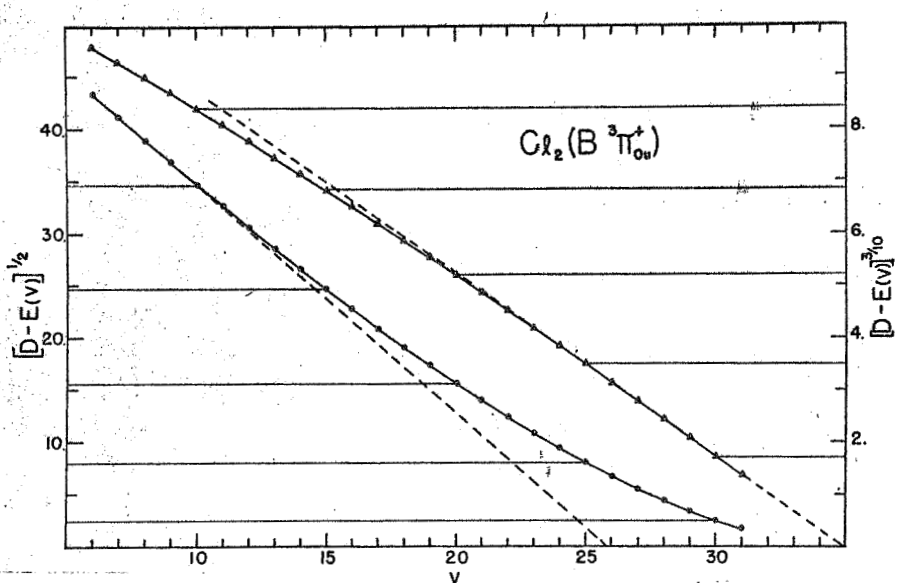

FIG. 8. $[D - E(v)]^{[(n-2)/2n]}$ vs v for observed levels of $^{35,35}Cl_2$ ($B\,^3\Pi^+_{0u}$) (*9*) with D from Table I, for both $n = \infty$ (●, left ordinate scale); and $n = \tilde{n} = 5$ (▲, right ordinates). All energies are in cm^{-1}. The broken lines are tangents to the two curves in their linear regions.

B. Vibrational Reassignment and Potential Tail of Ground-State Cl_2 ($X\,^1\Sigma_g^+$)

The only experimental data for highly excited vibrational levels of ground state Cl_2 are the UV resonance emission doublets reported by Rao and Venkateswarlu (*14*). The rotational assignment for these doublets has recently been revised (*15*) yielding slightly different energies, and these are used here. However, the validity of the present discussion does not hinge on this change.

In Ref. (*14*), the extrapolation of a Birge-Sponer plot gave a value for the ground-state dissociation energy 65 (± 10) cm^{-1} larger than that of Sect. IIA.[16]

[16] From the same data Clyne and Coxon (*15*) obtained a D_e value 43 cm^{-1} larger than the present estimate; however, this change does not affect the arguments presented here.

Furthermore, this plot showed growing *negative* curvature near the dissociation limit, which would be worsened if the extrapolation were constrained to yield the present D_o. This is the opposite of the expected behavior in this region, especially since the vibrational spacings for the analogous (but shallower) ground electronic state of I_2 (*29*) show positive curvature for levels lying within 1000 cm^{-1} of the dissociation limit. Although one expects the long-range inverse-power attractive potential tail to be somewhat weaker for Cl_2 than for I_2, its influence on the highest vibrational levels should not disappear altogether.

Ref. (*14*) reported observations of all adjacent or semiadjacent ground-state levels from $v = 9$ to 42. Above this point four other levels were observed, separated by gaps assigned, respectively, as two, three, two, and one unobserved levels. The anomalous increasingly negative Birge-Sponer curvature is explained if these gaps are too small. Using the theoretical $\tilde{n} = 6$ and the ground-state dissociation energy obtained in Sect. IIA, the observed level energies [reevaluated using the rotational reassignment of Ref. (*15*)] are presented in Fig. 9 in the form suggested by the preceding section. Above $v = 42$, each pair of adjacent points is joined by a straight line which is extrapolated to the tie-line corresponding to the next higher observed level. The possible vibrational assignments correspond to integer values of v on these tie-lines, and the three pairs of curves in Fig. 9, (A,A'), (B,B') and (C,C') correspond to the only plausible sets of assignments.

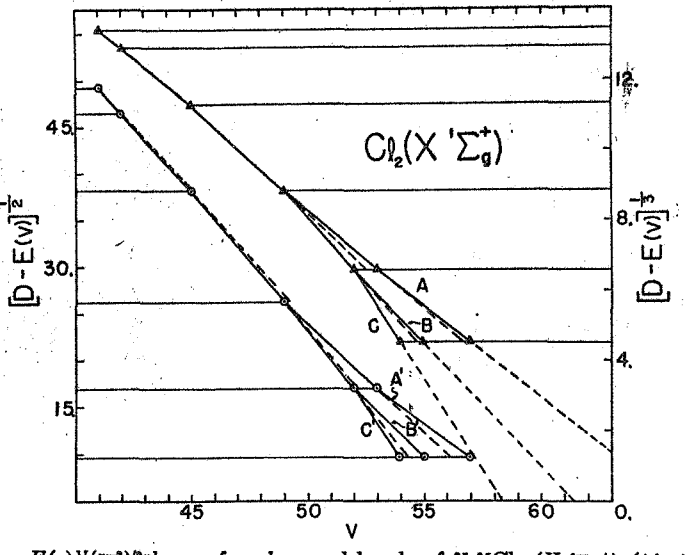

FIG. 9. $[D - E(v)]^{[(n-2)/2n]}$ vs v for observed levels of $^{35,35}Cl_2$ ($X\ ^1\Sigma_g^+$) (*14*, *15*) with D from Table I, for both $n = \infty$ (⊙, left ordinate scale); and $n = \tilde{n} = 6$ (△, right ordinate scale). All energies are in cm^{-1}. The possible vibrational assignments (points joined by solid lines) correspond to integer values of v on the tie-lines for the different levels near their intersections with the linear extrapolation from the two preceding levels (broken lines).

In Fig. 9, curves (C,C') correspond to the original assignment (*14*); as stated above and confirmed by the curvature shown, this is implausible. Curve A shows positive curvature for the higher levels which is too pronounced to be due to experimental error. However, the slight positive curvature in B at the highest observed level is within the uncertainty in the experimental energies.[17] Thus, it appears that the (B,B') reassignment of the original (*14*) $v = 54$ as $v = 55$ is correct.

[17] The scatter in the doublet splittings (*14*) which give the B_v values for the observed upper levels is large enough to yield possible errors of a few cm^{-1} in the level energies.

The main restriction on the use of this approach is the requirement for a good initial value of D. Applying the method to the same energies using trial D values in turn 50 cm^{-1} smaller and larger than the present value would have yielded (C,C') and (A,A'), respectively, as the most probable assignments. On the other hand, using D_o = 20 012 cm^{-1}, the best estimate available previous to Ref. (*14*), the present reassignment is obtained.

It is important to note that this reassignment negates the speculation concerning a possible barrier maximum (*9*, *15*). No such maximum is expected theoretically, since for the ground states of the halogens, at least the first two nonzero inverse-power potential terms are attractive [see the argument presented for I_2 in Ref. (*11*)], as well as the exchange forces which give rise to the chemical binding.

Using the known $\tilde{n}$ = 6 and D_o for the ground state, Eq. (4) was fitted to the three highest experimental energies (v = 49, 52, and 55) yielding the values of C_6 and v_D given in Table I. The C_6 obtained is in fortuitously good agreement with the theoretical $C_6 = 0.82 \times 10^5$ cm^{-1} Å^6, estimated by Caldow and Coulson (*30*). However, fitting the highest two levels using the (A,A') and (C,C') vibrational assignments would yield C_6 values respectively 7 times larger and ⅛ as large as the theoretical estimate. This lends credence to both the present vibrational reassignment and the significance of the fit itself. Table IV presents the energies predicted by the constants in Table I for the highest bound levels of Cl_2 ($X\ ^1\Sigma_g^+$).[17]

TABLE IV

CALCULATED ENERGIES (cm^{-1}) OF THE HIGHEST BOUND LEVELS OF GROUND-STATE $^{35,35}Cl_2(X^1\Sigma_g^+)$

The experimental level energies are given in parentheses.

v	$E(v)$	v	$E(v)$
48	19 119.	55	19 911. (19 905.[a])
49	306. (19 305.[a])	56	947.
50	465.	57	972.
51	597.	58	986.
52	706. (19 711.[a])	59	994.
53	792.	60	996.$_8$[b]
54	860.	61	997.$_{25}$[b]

[a] Calculated from the data in Table I of Ref. (*14*) using the rotational reassignment of Ref. (*15*) and the ground-state rotational constants of Ref. (*9*).

[b] Because of the uncertainty in v_D (see Table I), these levels may not exist.

C. *Vibrational Reassignment for* Br_2 ($B\ ^3\Pi_{0u}^+$)

The four vibrational levels observed near the dissociation limit of the $B\ ^3\Pi_{0u}^+$ state of each of $^{79,79}Br_2$ and $^{81,81}Br_2$ were originally assigned as v = 49–52 (*18*). The only other measurements of the upper vibrational levels of this state are Brown's (*20*) observation of levels up to v = 48 of $^{79,81}Br_2$. In order to compare these results, the (79,79) and (81,81) energies (*18*) were averaged to yield approximate (79,81) energies for the levels considered. For this species ($\tilde{n}$ = 5 and D was obtained in Sect. IIB), Fig. 10 is the plot suggested by Sect. IIIA. The solid points are from Ref. (*20*) and the open points are the interpolated energies mentioned above. It is apparent that the original (*18*) vibrational numbering of the latter four levels must be increased by one. This reassignment was used in Sect. IIB.

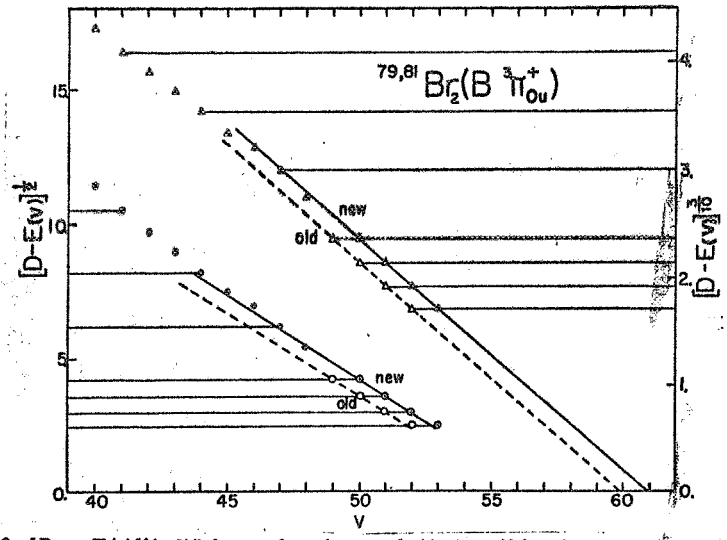

FIG. 10. $[D - E(v)]^{[(n-2)/2n]}$ vs v for observed ((20), solid points); and interpolated ((18), open points) levels of $^{79,81}Br_2$ ($B\ ^3\Pi_{0u}^+$) with D from Sect. IIB, for both $n = \infty$ (circles, left ordinate scale), and $n = \bar{n} = 5$ (triangles, right ordinates scale). All energies are in cm^{-1}; "old" and "new" refer to the vibrational assignments of the four highest levels.

IV. DISCUSSION

A. *Comparison of $B\ ^3\Pi_{0u}^+$ State D Values with Previous Results*

Most of the results in Table I differ somewhat from previous dissociation limits and conclusions about the nature of the long-range potentials, despite being based on the same data. For the D values, the appropriate quantity for comparison is $[D - E(v_H)]$, the binding energy of the highest observed level. Table V compares the present and best previous values of this quantity for the $B\ ^3\Pi_{0u}^+$ states of the halogens.

In the case of I_2, the discrepancy originates in the graphical extrapolation of Ref. (*22*) beyond the highest observed levels. This illustrates the errors which may arise from use of the Birge-Sponer (*31*) and Birge (*32*) extrapolation procedures.[18]

The previous best estimates of the dissociation limits of the (79,79) and (81,81) isotopes of Br_2 ($B^3\Pi_{0u}^+$) (*18*) were based on limiting curves of dissociation [e.g., see Chap. VI of Ref. (*33*)]. The discrepancy with the present results implies that the absorption series were incomplete; i.e., they did not extend to the predissociation limit. It has been shown (*34*) that for vibrational levels lying near

TABLE V

BINDING ENERGIES (cm^{-1}) OF HIGHEST OBSERVED LEVEL (v_H) OF THE $B\ ^3\Pi_{0u}^+$ STATES OF THE HALOGENS

Species	v_H	Present	Previous
$^{35,35}Cl_2$	31	2.8_5 (± 0.3)[a]	$3._1$ ($\pm 2.$)[b]
$^{79,79}Br_2$	53	5.2_4 ($\pm 0.2_7$)	2.7 (± 0.5)[c]
$^{81,81}Br_2$	53	6.9_6 ($\pm 0.3_5$)	4.1 (± 0.5)[c]
$^{127,127}I_2$	72	19.6 (± 1.2)	12.6[d]

[a] See footnote 8.
[b] From Ref. (*9*).
[c] From Ref. (*18*).
[d] From Ref. (*22*).

[18] For an excellent review of these methods, see Chap. V of the book by Gaydon (*33*).

the dissociation limit, the energies at which the rotational series for the different vibrational levels break off due to predissociation should vary as $[J_m(J_m + 1)]^{[n/(n-2)]}$, where $n = \tilde{n}$, and J_m is the rotational quantum number of the last unpredissociated level. For Br_2 ($B\,^3\Pi_{0u}^+$), (for which $\tilde{n} = 5$) the theoretical C_5 coefficient[12] yields a predicted slope of 2.0×10^{-5} [cm^{-1}] for plots of $E(J_m)$ vs $[J_m(J_m + 1)]^{5/2}$. Since the data (*18*) do not conform to this behavior, it is inferred that the experimenters did not observe the very highest nonpredissociating levels. This is consistent with their lack of observation of any broadened lines.

One further effect to be considered is the effect on the fitted D value of an error in the chosen value of $\tilde{n}$. Fitting the data to Eq. (4) in the manner described in Sect. II, but with n set equal to 6 instead of 5, one obtains D values for Cl_2, Br_2, and I_2, respectively, which are only 0.36, 0.50, and 2.7 cm^{-1} smaller than the best values (Table I).

B. The $B\,^3\Pi_{0u}^+$ State Potential Tails; Comparison with Previous Results and with Theory

Byrne *et al.* (*10*) concluded that the outer RKR turning points (*35*) for the $B\,^3\Pi_{0u}^+$ states of both Cl_2 and Br_2 followed an R^{-6} dependence, rather than the theoretical[4] asymptotic R^{-5} form. However, the validity of this conclusion is contingent on the accuracy of the RKR potential and of the value of D assumed.

For Cl_2 the reported turning points (*35*) are plotted against binding energy in Fig. 11, using both the present D and the experimenters' (*9*) D [presumably the value used in Ref. (*10*)].[19] The small difference between these D's has a negligible effect on this plot, and it appears that the previous $\tilde{n} = 6$ deduction is wrong since it requires ignoring the last few levels. [This also implies that the reported (*10*) "C_6" is spurious.] The difference between the intercepts of curves A and B in Fig. 11 indicates that either the present best C_5 is ca. 40% small, or that the RKR results are slightly in error. The latter is plausible since no experimental data were available for the lowest six levels of this state, spanning the lower 40% of the potential well.

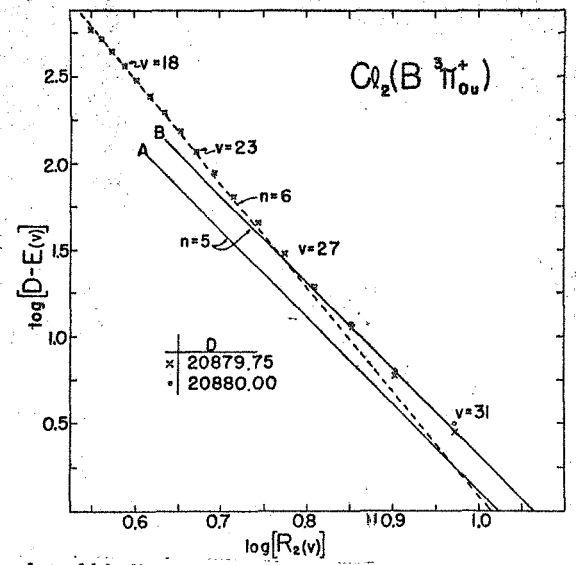

FIG. 11. Log–log plot of binding energies (cm^{-1}) vs calculated (*35*) RKR turning points (Å) for $^{35,35}Cl_2$ ($X\,^1\Sigma_g^+$) using both the present (×) and the previous (*9*) (●) estimates of D (see footnote 19). The straight lines have slope of $-n$; the intercept of A corresponds to the present (Table I) C_5, while line B is the best $n = 5$ fit to the points for the uppermost levels.

[19] The $v = 32$ turning point reported by Todd *et al.* (*35*) is ignored here as being spurious, since there is no reported observation of this level. This point would lie well above all the lines in Fig. 11, since their extrapolated $[E(32) - E(31)]$ is some 30% smaller than that predicted (*2*) on substituting the constants of Table I into Eq. (4).

The RKR potential for Br_2 ($B\,^3\Pi_{0u}^+$) from which Byrne *et al.* (*10*) concluded $\tilde{n} = 6$ appears to have been calculated (*35*) for the mixed isotope (79,81) from the averaged Ref. (*18*) data for (79,79) and (81,81). However, these results only span levels $9 \leqq v \leqq 19$ and those reassigned as $50 \leqq v \leqq 53$, and $v = 9$ lies ca. 37% of the well depth above the minimum. In addition to using the incorrect original (*18*) vibrational assignment for the four high levels, the interpolation over the large gaps in the spectrum is quite unreliable. For example, the interpolated $v = 30$ and 45 (79,81) energies are, respectively, 6 and 9 cm^{-1} higher than the values reported by Brown (*20*), while the extrapolated (*35*) $[E(9) - E(0)]$ is 8 cm^{-1} larger than the value obtained from the data of Darbyshire (*36*). Since the unreliability of the RKR potential (*35*) appears to be the source of the previous (*10*) anomalous $\tilde{n} = 6$ conclusion, log–log plots similar to Fig. 11 are not presented here. However, it is noted that increasing D by 2.4 cm^{-1} from the previous value (*18*) to the present one altered the binding energies for the highest levels sufficiently for the last two points on such a log–log plot to display the proper slope of -5.

Steinfeld *et al.* (*37*) calculated RKR turning points for levels $43 \leqq v \leqq 50$ of I_2 ($B\,^3\Pi_{0u}^+$), and on analyzing them, concluded that the potential was displaying its theoretical $\tilde{n} = 5$ behavior[4] in this region. On the other hand, the results presented in Figs. 5 and 6 suggest that the potential deviates significantly from this asymptotic behavior for $v \lesssim 55$; moreover their (*37*) apparent C_5 coefficient is more than 100% larger than the theoretical value.[12] Thus, their $\tilde{n} = 5$ conclusion appears fortuitous. Their turning points for $43 \leqq v \leqq 51$ were based on the measurement of two vibrational bands whose upper states they assigned as $v = 43$ and 49. However, their ensuing $v = 49$ energy is 11.4 cm^{-1} lower than the value observed by Brown (*22*), leading to a reassignment of their 49-1 band as 57-2 [see footnote 4, Ref. (*11*)]. This error in energy erroneously compressed the levels $43 < v < 49$, and this is the probable source of their apparent R^{-5} behavior.

In Table VI, the "experimental" C_5 values obtained by the present method are compared to the theoretical values.[12] Also given are the approximate binding energies beyond which deviations from simple R^{-5} behavior become apparent, as indicated by Table II and Figs. 2 and 6. These quantities will depend mainly on the relative strengths of the contributing R^{-5}, R^{-6}, and R^{-8} potential terms. It appears that for Br_2 this range is anomalously small in relation to the relative strengths of the C_5 coefficients. However, this may be spurious, due to errors in either the energies or the assignments of the (79,81) levels of Ref. (*20*).[13]

TABLE VI

COMPARISON OF PRESENT EXPERIMENTALLY DERIVED C_5 VALUES (cm^{-1} Å^5) WITH THEORETICAL ESTIMATES (SEE FOOTNOTE 12) FOR THE $B\,^3\Pi_{0u}^+$ STATES OF THE HALOGENS

E_b ($\tilde{n} = 5$) is the approximate binding energy beyond which deviations from R^{-5} behavior become apparent in Figs. 2 and 6 and Table II.

Species	Cl_2	Br_2	I_2
C_5, experimental	1.2_9 (± 0.2) $\times 10^5$	1.7_9 (± 0.2) $\times 10^5$	3.1_1 (± 0.2) $\times 10^5$
theoretical[a]	$1.4_4 \times 10^5$	$2.3_9 \times 10^5$	$4.5_4 \times 10^5$
E_b ($\tilde{n} = 5$) [cm^{-1}]	60	50[b]	200

[a] See footnote 12.

[b] As discussed in footnote 13, the isotopic assignments of Brown's (*20*) levels may be in error, in which case this 50 cm^{-1} is a lower bound to E_b ($\tilde{n} = 5$).

While the present "experimental" C_5 values are seen to be in reasonable agreement with theory, they are consistently small. Since there may be some residual bias inherent in the present method (*2*) it is difficult to make an appraisal of the theoretical values, although a potential weakness in them was mentioned in footnote 46 of Ref. (*2*). However, the qualitative agreement shown in Table VI does strongly confirm that the highest levels considered in the present analysis do depend mainly upon the asymptotically dominant R^{-5} potential tail.

V. CONCLUDING REMARKS

The main restriction on the use of the present method (fits to Eq. (4))[20] is that the levels considered must lie close enough to the dissociation limit that their Birge-Sponer plot shows positive curvature. It has also been found very advantageous to know the theoretical $\tilde{n}$ for the state under consideration.[4] If in addition the level density is great enough to satisfy the linear approximation of Eq. (5), then application of Eqs. (6, 7) may yield good approximations to the best parameter values (see Sect. II). Where appropriate, therefore, plots of the form of Eq. (6) should replace conventional Birge-Sponer extrapolations as a means of determining the dissociation limit D.

It is believed that the present methodology is now sufficiently well documented[20] to become another everyday tool in the spectroscopists' data analysis kit.

RECEIVED: June 26, 1970

REFERENCES

1. R. J. LEROY AND R. B. BERNSTEIN, *Chem. Phys. Lett.* **5**, 42 (1970); see Appendix A.
2. R. J. LEROY AND R. B. BERNSTEIN, *J. Chem. Phys.* **52**, 3869 (1970); see Section 3.1.
3. B. N. TAYLOR, W. H. PARKER, AND D. N. LANGENBERG, *Rev. Mod. Phys.* **41**, 375 (1969).
4. M. ABRAMOWITZ AND I. A. STEGUN, "Handbook of Mathematical Functions," Nat. Bur. Stand. (U.S.) Appl. Math. Ser. **55**, U. S. Dept. of Commerce, Washington, D. C. (1964); also available from Dover Publications Inc., New York (1965).
5. R. J. LEROY AND R. B. BERNSTEIN, Univ. Wis. *Theoret. Chem. Inst. Rep.* **WIS-TCI-369** (1970), Appendices.
6. J. K. KNIPP, *Phys. Rev.* **53**, 734 (1938).
7. T. Y. CHANG, *Rev. Mod. Phys.* **39**, 911 (1967).
8. T. Y. CHANG, *Mol. Phys.* **13**, 487 (1967).
9. A. E. DOUGLAS, C. K. MØLLER, AND B. P. STOICHEFF, *Can. J. Phys.* **41**, 1174 (1963).
10. M. A. BYRNE, W. G. RICHARDS, AND J. A. HORSLEY, *Mol. Phys.* **12**, 273 (1967).
11. R. J. LEROY, *J. Chem. Phys.* **52**, 2678 (1970); see Section 6.
12. C. E. MOORE, "Atomic Energy Levels," Vol. 3, *Nat. Bur. Stand. (U.S.) Circ.* **467** (1958).
13. S. AVELLÉN, *Ark. Fys.* **8**, 211 (1954).
14. Y. V. RAO AND P. VENKATESWARLU, *J. Mol. Spectrosc.* **9**, 173 (1962).
15. M. A. A. CLYNE AND J. A. COXON, *J. Mol. Spectrosc.* **33**, 381 (1970).
16. W. KOLOS AND L. WOLNIEWICZ, *J. Chem. Phys.* **41**, 3663 (1964).
17. R. J. LEROY AND R. B. BERNSTEIN, *J. Chem. Phys.* **49**, 4312 (1968); see Section 5.
18. J. A. HORSLEY AND R. F. BARROW, *Trans. Faraday Soc.* **63**, 32 (1967).
19. C. F. FISCHER, *Can. J. Phys.* **46**, 2336 (1968), and the report mentioned therein.
20. W. G. BROWN, *Phys. Rev.* **38**, 1179 (1931).
21. J. L. TECH, *J. Res. Nat. Bur. Stand., Sect. A* **67**, 505 (1963).
22. W. G. BROWN, *Phys. Rev.* **38**, 709 (1931).

[20] Recently Stwalley (*38*) presented an alternate derivation of Eq. (4) which he then applied to data for the $B\ ^1\Sigma_u^+$ state of H_2 (for which $\tilde{n} = 3$) by performing fits to Eq. (7) while varying the value of D to minimize deviations. In his more approximate derivation, a numerical factor of $\pi/2$ occurs in the place of the ratio of gamma functions in Eq. (3) (*38*). For a given fitted value of H_n, use of his numerical factor would give values of C_n for $n = 3$ and 6 which are too large by factors of 1.41 and 4.68, respectively. However, Stwalley (*38*) verified the present Eqs. (3–4) for the exact calculated eigenvalues of an LJ (12, 3) potential (i.e., a well with an R^{-3} potential tail), obtaining the same good agreement as had previously been found for a model R^{-6}-tailed potential (*2*).

23. J. I. Steinfeld, R. N. Zare, L. Jones, M. Lesk, and W. Klemperer, *J. Chem. Phys.* **42**, 25 (1965).
24. R. L. Brown and T. C. James, *J. Chem. Phys.* **42**, 33 (1965).
25. C. C. Kiess and C. H. Corliss, *J. Res. Nat. Bur. Stand., Ser. A* **63**, 1 (1959).
26. R. D. Verma, *J. Chem. Phys.* **32**, 738 (1960).
27. J. O. Hirschfelder, C. F. Curtiss, and R. B. Bird, "Molecular Theory of Gases and Liquids," Wiley, New York, 1964.
28. J. O. Hirschfelder and W. J. Meath, *Advan. Chem. Phys.* **12**, 3 (1967).
29. R. J. LeRoy, *J. Chem. Phys.* **52**, 2683 (1970).
30. G. L. Caldow and C. A. Coulson, *Trans. Faraday Soc.* **58**, 633 (1962).
31. R. T. Birge and H. Sponer, *Phys. Rev.* **28**, 259 (1926).
32. R. T. Birge, *Trans. Faraday Soc.* **25**, 707 (1929).
33. A. G. Gaydon, "Dissociation Energies," 3rd ed. Chapman and Hall, London, 1968.
34. R. B. Bernstein, *Phys. Rev. Lett.* **16**, 385 (1966).
35. J. A. C. Todd, W. G. Richards, and M. A. Byrne, *Trans. Faraday Soc.* **63**, 2081 (1967).
36. O. Darbyshire, *Proc. Roy. Soc., Ser. A* **159**, 93 (1937).
37. J. I. Steinfeld, J. D. Campbell, and N. A. Weiss, *J. Mol. Spectrosc.* **29**, 204 (1969).
38. W. C. Stwalley, *Chem. Phys. Lett.* **6**, 241 (1970).

3.3 FURTHER DISCUSSION OF THE METHOD

Approximate Graphical Procedure for Determining the Power n

In the two preceding sections,[1,2] values of the potential parameters D, n and C_n, and of the limiting vibrational index v_D, were obtained from (non-linear) least-squares fits of sets of experimental vibrational energies to the expression:

$$E(v) = D - [(v_D - v)H_n]^{[2n/(n-2)]} , \qquad (1)$$

where H_n is a known function of n and C_n.[3] On the other hand, in part I of Ref. (2), simple graphical procedures (utilizing an assumed known value of n) were presented for determining D, C_n and v_D from such data. The latter are slightly less accurate than fits to Eq.(1), insofar as they assume that the first derivative of the vibrational energy with respect to v, E'(v), may be accurately obtained from the difference formula:

$$E'(v) \simeq \overline{\Delta G}_v \equiv \tfrac{1}{2}[\Delta G_{v-\frac{1}{2}} + \Delta G_{v+\frac{1}{2}}] = \tfrac{1}{2}[E(v+1) - E(v-1)] . \qquad (2)$$

However, this does not appear to introduce serious errors, since in the cases considered, the graphically-obtained parameter values are virtually indistinguishable from the results of general least-squares fits with the same assumed n.[2] It will now be shown that a similar approximate graphical procedure may sometimes be used to determine n.

The second derivative E''(v) may be reasonably approximated by an expression analogous to Eq.(2) :

$$E''(v) \simeq \Delta^2 G_v \equiv [\Delta G_{v+\frac{1}{2}} - \Delta G_{v-\frac{1}{2}}] = [E(v+1) - 2E(v) + E(v-1)] . \qquad (3)$$

Replacing the derivatives in Eq. (15) of Ref. (1), by Eqs. (2-3), one obtains[4]

$$\overline{\Delta G}_v \Big/ \Delta^2 G_v = - \left(\frac{n-2}{n+2}\right) (v_D - v) \qquad (4)$$

Fig. 1 shows the plot suggested by Eq. (4) for the highest observed vibrational levels[5] of $C\ell_2(B\ ^3\Pi^+_{0u})$; the three lines have slopes corresponding to n = 4, 5 and 6. It is evident that the five highest points (based on the seven highest observed levels) correspond most closely to n = 5. The negative curvature of the remaining points reflects the growing influence of other contributions to the potential.

The results in Fig. 1 are in accord with the previous conclusion[6] that the distribution of the highest observed vibrational levels of B-state $C\ell_2$ depends mainly on the theoretically asymptotically-dominant R^{-5} potential term. This demonstrates the validity of Eqs. (2-3) for this system.[7] Thus, it appears that whenever the approximations of Eqs. (2-3) are fairly accurate, Eq. (4) can fulfil the same useful role as Eqs. (6-7) of Ref. (2). Unfortunately, it may not be applied to the analogous states of Br_2 and I_2, because of the paucity of the data for the former, and the scatter in the data for the latter.

Validity of Approximating the Potential by a Single Inverse-Power Term

Over a sufficiently narrow interval, any monotonic attractive potential with negative curvature may be accurately represented by the three-parameter expression:

$$V(R) = D - C_n/R^n \qquad (5)$$

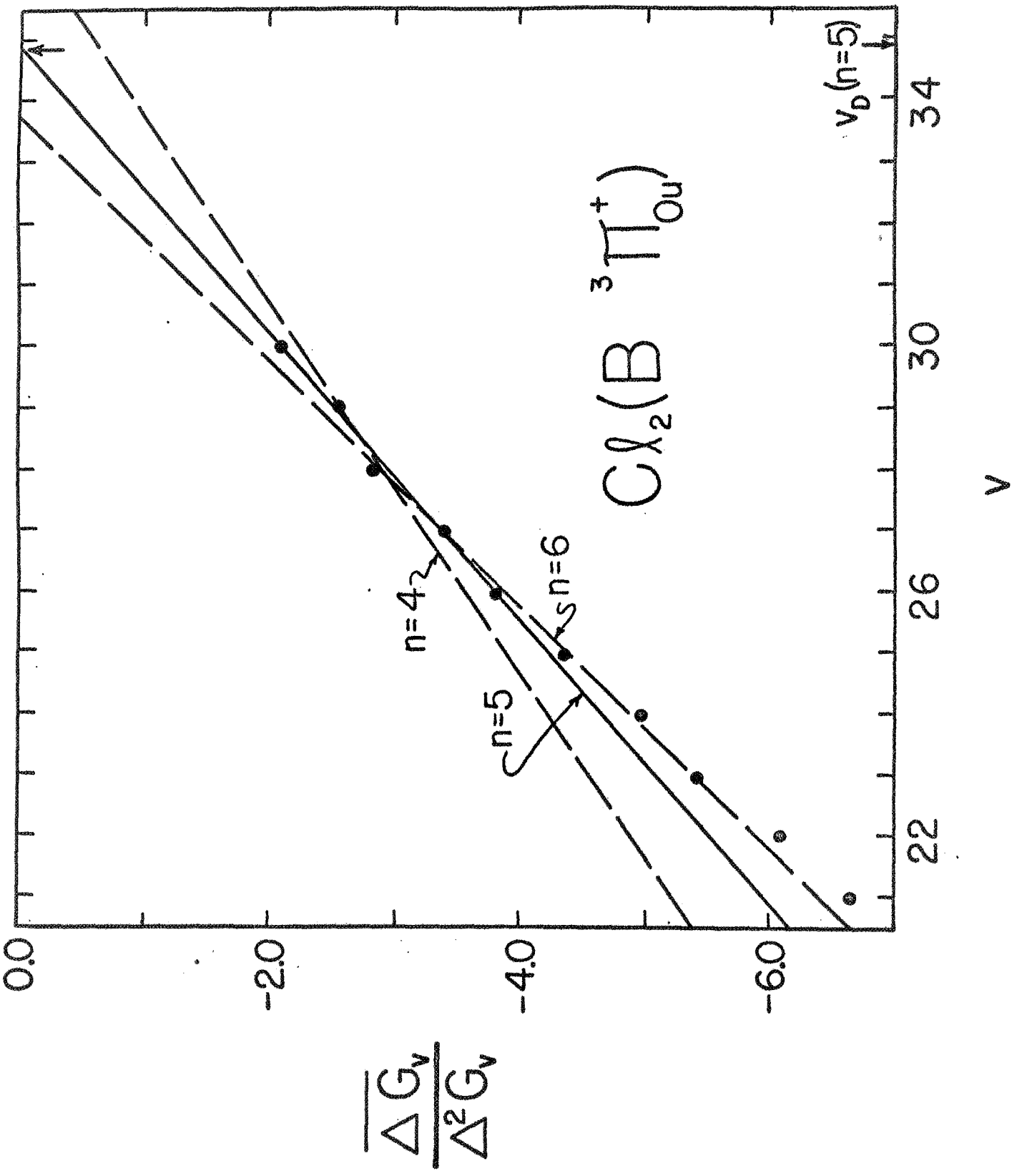

Figure 1: Experimental data for $Cl_2(B\ ^3\Pi^+_{0u})$ [5] plotted according to Eq. (4).

In view of the inverse-power form of the perturbation-theory expansion for long-range interatomic potentials,[8]

$$V(R) = D - \sum_{n=\tilde{n}} C_n/R^n \quad , \tag{6}$$

Eq.(5) is particularly appropriate at the outer turning points of vibrational levels lying near D. However, since Eq.(5) (on which Eq.(1) is based) is only a local approximation to Eq.(6), the parameters n, C_n and v_D in Eq.(1) have no theoretical significance unless they describe levels sufficiently near D to depend on the limiting power $\tilde{n}$. Consequently, applications of Eq.(1)[1,2,9] have placed most emphasis on fitting it to the very highest observed levels, while fixing n equal to the theoretically known $\tilde{n}$.[8] While this was shown to be a very good assumption in Ref.(9), it is somewhat less accurate for the systems discussed above.[1,2]

For the $B(^3\Pi^+_{0u})$-state halogens discussed in the present work,[1,2] Eq.(6) becomes (see Section 2.3):

$$V(R) = D - C_5/R^5 - C_6/R^6 - C_8/R^8 \ldots \quad , \tag{7}$$

so that the levels nearest D correspond (via Eq.(1)) to $n=\tilde{n}=5$. The only direct evidence of this was obtained for Cl_2 (see Fig.5 in Ref.(1), Fig.1 in Ref.(2), and Fig.1 here), the data for Br_2 and I_2 being respectively too few and too uncertain to allow definitive conclusions.[2] However, the agreement of the derived "experimental" C_5 values with theory (see Table VI in Ref.(2)) apparently attests to the validity of this assumption for the highest observed vibrational levels of all three species. On the other hand, the relative

magnitude of the second inverse-power term in Eq.(7) decreases slowly with increasing R, so that it may still contribute significantly in the region of interest. In view of the results of Section 2.3, the effect of such terms should be considered.

The analyses in Section 2.3 of the four outermost RKR turning points for the B-states of Cl_2 and Br_2 suggested that in this region, the R^{-5} term in Eq.(7) is responsible for only ca. 65-75% of the total potential. Thus, although it still preponderates, use of a single-term R^{-5} approximation for the potential is somewhat in error. Qualitative consideration of the origin of Eq.(1) shows[1] that this causes the apparent C_5 constants obtained from fits to Eq.(1) to be somewhat small, as was found.[1,2] However, these errors will probably not significantly affect the reported[2] D and v_D values.[10]

It appears that the non-negligible influence of potential contributions other than the asymptotically-dominant $R^{-\tilde{n}}$ term most seriously affects the coefficients $C_{\tilde{n}}$ yielded by the fits to Eq.(1). However, this deficiency is at least partially removed by an expansion of Eq.(1) which takes account of other contributions to the potential, work which will be reported elsewhere.[11]

FOOTNOTES

1. Section 3.1; also, published in J. Chem. Phys. 52, 3869 (1970), by R. J. Le Roy and R. B. Bernstein.
2. Section 3.2; also, to be published in J. Mol. Spectry. 37 (1971), by R. J. Le Roy and R. B. Bernstein.
3. See Eqs.(3-4) in Ref.(2).
4. Eq.(4), with the differences replaced by the corresponding derivatives, was previously applied to the exact computed eigenvalues of a model Lennard-Jones (12,6) potential.[1] The slope of the ensuing plot had the expected n=6 value of 1/2, and was distinctly different from the n=5 and 7 slopes of 3/7 and 5/9, respectively. However, in this model system the approximations of Eqs.(2-3) are quite poor for the highest levels, so that Eq.(4) may not be used.
5. A. E. Douglas, Chr. Kn. Møller, and B. P. Stoicheff, Can. J. Phys. 41, 1174 (1963).
6. This prior conclusion was obtained by the more complicated procedure of performing least-squares fits to Eq.(1).[1]
7. For B-state Cl_2, replacing the differences in Eq.(4) by the corresponding derivatives mainly smoothes the points in Fig.1, and does not significantly affect the present conclusions. Note, however, footnote 4.
8. Here, $\tilde{n}$ is the power of the lowest-order term contributing to Eq.(6). A summary of the rules determining $\tilde{n}$ is given in Appendix B of Ref.(1).
9. W. C. Stwalley, Chem. Phys. Lett. 6, 241 (1970).

10. This is concluded on the basis of the observation that fixing n=6 in fits of Eq.(1) to the highest observed B-state levels of Cl_2, Br_2 and I_2, had only a small effect on the D values obtained.[2]

11. R. J. Le Roy (to be published).

4. OTHER METHODS OF OBTAINING INTERATOMIC POTENTIALS

The present discussion is mainly concerned with the empirical determination of interatomic potentials. Hence, no examination of ab initio calculations is attempted here, and the reader is referred to reviews and texts on this subject.[1-7] The following is a very brief summary of a number of techniques, presented mainly to put the methods of the preceding chapters into some kind of perspective.

4.1 UTILIZING SPECTROSCOPIC DATA

In addition to the approaches utilized in the preceding chapters, there are two other, somewhat older procedures for determining diatomic potential wells from experimental vibrational-rotational energy levels. The first of these is due to Dunham,[8] who used the WKB approximation to relate the constants Y_{nm} in the expression for the energy levels,

$$E(v,J) = \sum_{n,m} (v+\tfrac{1}{2})^n [J(J+1)]^m Y_{nm} \quad ,$$

to the coefficients of a polynomial expansion of the potential about its equilibrium internuclear distance. Sandeman[9] then inverted Dunham's relations, expressing turning points at a given energy E in terms of the Y_{nm}. Two decades later, Jarmain[10] cast the RKR[11] expressions into Sandeman's[9] form and found that the Dunham[8] and RKR[11] methods are formally equivalent. Finally, Davies and Vanderslice[12] proved that for all energies up to the dissociation limit, this equivalence holds, and the Jarmain-Sandeman series[9,10] is convergent. However, despite the equivalence of the two procedures, the Jarmain-Sandeman series[9,10] has

been virtually ignored, while the RKR approach[11] is very popular.

In the second general method, Dunham's[8] polynomial in the internuclear distance R is replaced by a simple parameterized analytic potential function. The most familiar expression of this kind is the Morse potential, for which the simple exact relation between the parameters and the vibrational eigenvalues is well known.[13,14] However, in most other cases exact expressions for the eigenvalues in terms of the potential parameters are not known, and this approach becomes an approximate form of the Dunham[8] procedure. The chosen (usually 3- or 5-parameter) algebraic function is expanded about its minimum as a power series in R , and the characteristic parameters extracted from the experimental Y_{nm} values using Dunham's[8] relations for the power series coefficients. For a wide variety of such functions, comparisons have been made of both their ability to reproduce experimental eigenvalues, and their agreement with the more general RKR potential curves.[15,16] No strong predilliction for any particular analytic form was shown, other than the expected conclusion that the 5-parameter potentials are better than the 3-parameter ones.[15,16] In any case, this approach is only suitable when the limited flexibility of the parameterized potential can accurately account for all the experimental data; in practice, this means when there are very few data.

A rather different means of utilizing experimental vibrational-rotational energies to determine interatomic potentials has been proposed by Bernstein.[17] He derived an expression relating the nature of the long-range potential tail to the observed breaking-off of rotational series due to predissociation through the centrifugal potential barrier.

This is discussed further in part V of Chapter 7.

All of the methods discussed up to this point use vibrational-rotational eigenvalue data to determine attractive potential wells. On the other hand, the frequency and temperature dependance of the intensity of absorption or emission into the continuum region above the molecular dissociation limit can in principle yield purely repulsive potential functions, or the short-range repulsive part of attractive potentials. This approach is discussed in part IIIC of the review by Mason and Monchick,[18] and examples of more recent work are the present Refs.(19-24). While it shows promise, very few potentials have as yet been obtained in this manner, and conclusions regarding their uniqueness and accuracy should await further investigations.

A more efficient utilization of continuum absorption/emission intensities is in conjunction with the results of a velocity analysis of the photodissociation products. The latter have recently become obtainable by the techniques developed by Wilson and co-workers.[25] While too new to have become a widely used tool, this development[25] is very propitious.

4.2 UTILIZING NON-SPECTROSCOPIC DATA

The spectroscopic methods considered above are essentially complementary to most other procedures for determining potentials. This is because the selection rules for optical transitions allow the study of individual potential curves among the profusion of molecular states which arise from the interaction of atoms with unfilled valence shells.

In most other methods, all energetically accessible states contribute concurrently to the experimental observables. Thus, the non-spectroscopic methods may only be effectively applied to the study of interactions in which at least one of the atoms is a closed-shell (inert-gas) species, as only then do the particles have just a single possible potential curve. However, this is the type of system for which the attractive potential well will be relatively shallow, supporting few vibrational levels, and is thus least appropriate for study by the WKB-based methods of Chapters 2 and 3.

Molecular Beam Techniques

The determination of interatomic potentials from molecular beam scattering measurements has lately received considerable attention.[18,26-36] The measurements are of two distinct kinds. Using a simple classical analysis, high energy (collision energies E of ca. 1-100 eV) elastic scattering yields information on the short-range repulsive forces in a region inaccessible to spectroscopic measurements. Accurate work of this type has been done since 1940 and is well reviewed elsewhere.[26,32]

Scattering data obtained at thermal energies ($E \lesssim 0.1$ eV) may be used to determine both the long-range attractive potential tail, and the general features of a potential well. The former may be extracted from the absolute values of the total elastic cross section, in the form of the coefficient $C_{\tilde{n}}$ of the asymptotically-dominant inverse-power potential term (in cases where only one potential is involved, $\tilde{n}=6$). In this way C_6 constants have been obtained for a wide variety of

systems.[29,33] The characteristics of attractive potential wells may be obtained from an analysis of the quantal features of the angle and energy dependence of the cross section.[29,34] This is usually done by assuming a plausible two- or three-parameter model potential and varying the parameters until the experimental results are reproduced. In this way, approximate values of the well depth and minimum position have been obtained for a number of systems.[29,33] In principle, however, an exact inversion of the experimental data to yield accurately the whole of the potential well is also possible.[30,35] However, in practice this type of approach has very stringent data requirements, and currently has been successfully applied to very few systems.[36]

Bulk Properties

There exists a very extensive literature, accessible through Refs.(1, 18, and 37-39), which contemplates the extraction of intermolecular potentials from virial coefficients and transport properties of gases. In this work, one usually assumes a model potential function, calculates the desired properties from statistical mechanics,[1] and then varies the potential parameters and repeats the calculation until the best possible agreement with experiment is obtained. However, significant ambiguities can occur; for example, it is well known that the second virial coefficients of a number of simple molecules are fairly well reproduced by a number of potentials with quite different shapes, having in common only the area of their potential wells.[1,18] It is only relatively recently that quantitative studies of these ambiguities have

been made.[38,39] It is apparent that this uniqueness problem should be carefully considered whenever a high degree of accuracy is expected. Despite these difficulties, the analysis of bulk properties is a very important source of information on intermolecular forces. However, only in a few cases where the data are particularly extensive do the potentials obtained approach "spectroscopic" accuracy.[40]

Another macroscopic property which can yield approximate potential wells is the equilibrium constant between the molecular state and the dissociated atoms. For an assumed parameterized potential form, the unknowns may be determined from its absolute value and temperature dependence. This type of procedure may sometimes be applied to equilibrium constants extracted from chemical rate measurements, and while the potential obtained is quite crude, better estimates may not be available from other sources. An example of this type of problem is the determination of the I-Ar potential from atomic iodine recombination measurements, presented in Appendix B.

Addenda

In addition to the features discussed above, information on interatomic potentials may be extracted from a number of other physical properties, including thermal diffusion in gases and the properties of condensed phases.[18,38,41] However, these are currently less widely used than the techniques already mentioned, and their omission does not detract from the present purpose of putting the spectroscopic methods of Chapters 2 and 3 into perspective.

FOOTNOTES

1. J. O. Hirschfelder, C. F. Curtiss, and R. B. Bird, Molecular Theory of Gases and Liquids (John Wiley and Sons, Inc., New York, 1964).
2. F. Prosser and H. Shull, Ann. Rev. Phys. Chem. 17, 37 (1966).
3. A Dalgarno and W. D. Davison, Adv. At. Mol. Phys. 2, 1 (1966).
4. A. Golebiewski and H. S. Taylor, Ann. Rev. Phys. Chem. 18, 353 (1967).
5. J. O. Hirschfelder (editor), Adv. Chem. Phys. 12 (Intermolecular Forces, 1967).
6. H. Margenau and N. R. Kestner, Theory of Intermolecular Forces (Pergamon Press Ltd., Oxford, 1969).
7. A. D. Buckingham and B. D. Utting, Ann. Rev. Phys. Chem. 21, 287 (1970).
8. J. L. Dunham, Phys. Rev. 41, 713 and 721 (1932).
9. I. Sandeman, Proc. Roy. Soc. (Edinburgh) 60, 210 (1940).
10. W. R. Jarmain, Can. J. Phys. 38, 217 (1960).
11. The Rydberg-Klein-Rees (RKR) method is discussed with appropriate references in Chapter 2.
12. R. H. Davies and J. T. Vanderslice, Can. J. Phys. 44, 219 (1966).
13. a) P. M. Morse, Phys. Rev. 34, 57 (1929); b) D. Ter Haar, Phys. Rev. 70, 222 (1946).
14. G. Herzberg, Spectra of Diatomic Molecules (D. Van Nostrand Company, Inc., Toronto, 1950).
15. Y. P. Varshni, Rev. Mod. Phys. 29, 664 (1957).
16. D. Steele, E. R. Lippincott, and J. T. Vanderslice, Rev. Mod. Phys. 34, 239 (1962).
17. R. B. Bernstein, Phys. Rev. Lett. 16, 385 (1966).

18. E. A. Mason and L. Monchick, Adv. Chem. Phys. 12 (Intermolecular Forces, J. O. Hirschfelder editor), 329 (1967).

19. R. J. Le Roy, M.Sc. thesis, University of Toronto (1967).

20. G. H. Dunn, Phys. Rev. 172, 1 (1968).

21. R. O. Doyle, J. Quant. Spectry. Radiat. Transf. 8, 1555 (1968).

22. A. L. Smith, J. Chem. Phys. 49, 4813 and 4817 (1968).

23. M. Bixon, B. Raz, and J. Jortner, Mol. Phys. 17, 593 (1969).

24. A. Dalgarno, K. M. Sando, and A. C. Allison, Air Force Cambridge Research Laboratories report AFCRL-70-0249 (1970).

25. a) G. E. Busch, R. T. Mahoney, R. I. Morse, and K. R. Wilson, J. Chem. Phys. 51, 449 and 837 (1969); b) G. E. Busch, J. F. Cornelius, R. T. Mahoney, R. I. Morse, D. W. Schlosser, and K. R. Wilson, Rev. Sci. Instr. 41, 1066 (1970); c) R. J. Oldman, R. K. Sander, and K. R. Wilson, "Reinterpretation of the I_2 Main Visible Continuum", J. Chem. Phys. (to be published).

26. E. A. Mason and J. T. Vanderslice, in Atomic and Molecular Processes, D. R. Bates, editor (Academic Press, New York, 1962), Chapter 17.

27. H. Pauly and J. P. Toennies, Adv. At. Mol. Phys. 1, 195 (1965).

28. J. Ross (editor) Adv. Chem. Phys. 10, (Molecular Beams, 1966).

29. R. B. Bernstein, and J. T. Muckerman, Adv. Chem. Phys. 12 (Intermolecular Forces, J. O. Hirschfelder editor), 389 (1967).

30. T. J. P. O'Brien, "Aspects of the Inversion Problem of Scattering Theory", PhD thesis, University of Wisconsin, 1968; also, J. Chem. Phys. 51, 5112 (1969).

31. Chr. Schlier, Ann. Rev. Phys. Chem. 20, 191 (1969).

32. I. Amdur and J. E. Jordan, Adv. Chem. Phys. 10 (Molecular Beams, J. Ross editor), 29 (1966).

33. R. B. Bernstein, "Recent Advances in Elastic Scattering", University of Wisconsin Theoretical Chemistry Institute report WIS-TCI-397G (1970).

34. See, e.g., R. B. Bernstein, Adv. Chem. Phys. 10 (Molecular Beams, J. Ross editor), 75 (1966).

35. R. G. Newton, Scattering Theory of Waves and Particles (McGraw-Hill Book Company, Toronto, 1966).

36. a) R. E. Olson and C. R. Mueller, J. Chem. Phys. 45, 2519 (1966); b) R. E. Olson, J. Chem. Phys. 49, 4499 (1968); c) U. Buck and H. Pauly, J. Chem. Phys. 51, 1662 (1969).

37. D. D. Fitts, Ann. Rev. Phys. Chem. 17, 59 (1966).

38. H. J. M. Hanley, editor, Transport Phenomena in Fluids (Marcel Dekker, Inc. New York, 1969), especially Chapter 9.

39. a) H. J. M. Hanley and M. Klein, Natl. Bur. Std. (U.S.) Tech. Note No. 360 (1967); b) M. Klein and H. J. M. Hanley, Trans. Faraday Soc. 64, 2927 (1968); c) H.-M. Lin and R. L. Robinson, Jr., J. Chem. Phys. 52, 3727 (1970).

40. Two molecules for which the accuracy appears particularly good are Ar_2 and He_2. The empirical potentials for the former are critically discussed by L. W. Bruch and I. J. McGee, J. Chem. Phys. 53, 4711 (1970), and those for the latter are compared to their new ab initio results by H. F. Schaefer, III, D. R. McLaughlin, E. E. Harris and B. J. Alder, Phys. Rev. Lett. 25, 988 (1970), and by P. Bertoncini and A. C. Wahl, Phys. Rev. Lett. 25, 991 (1970).

41. E. A. Mason, R. J. Munn, and F. J. Smith, Adv. At. Mol. Phys. 2, 33 (1966).

5. TESTING AND CORRECTING A GIVEN POTENTIAL: GROUND-STATE ($X\ ^1\Sigma_g^+$) H_2

The accuracy of most empirical or ab initio potentials in the region $V(R) < 0$ may be tested by calculating their vibrational eigenvalues and comparing them to experiment. Discrepancies may then be accounted for in terms of errors in the potential, and a suitable correction function derived. When this was done (below) for the theoretical ground-state H_2 potential of Kołos and Wolniewicz,[1] two possible corrections Δ' and Δ'' were derived, corresponding respectively to assuming the existence of error in either the experimental,[2] or the theoretical dissociation energy. Herzberg's new measurements[3] have since resolved this choice in favor of the latter, so the correction function Δ' and its implications should now be ignored. The accuracy of the proper correction function, Δ'', is discussed further in part IV of Chapter 7.

The work presented below is reprinted from the Journal of Chemical Physics, Volume 49, pp. 4312-4321 (American Institute of Physics, New York, 1968).

REFERENCES

1. W. Kołos and L. Wolniewicz, J. Chem. Phys. 41, 3663 (1964); ibid 43, 2429 (1965); ibid 49, 404 (1968).
2. G. Herzberg and A. Monfils, J. Mol. Spectry. 5, 482 (1960).
3. G. Herzberg, J. Mol. Spectry. 33, 147 (1970); see also W. C. Stwalley, Chem. Phys. Lett. 6, 241 (1970).

Reprinted from THE JOURNAL OF CHEMICAL PHYSICS, Vol. 49, No. 10, 4312–4321, 15 November 1968
Printed in U. S. A.

Dissociation Energy and Vibrational Terms of Ground-State ($X\,^1\Sigma_g^+$) Hydrogen*

ROBERT J. LEROY AND RICHARD B. BERNSTEIN

Theoretical Chemistry Institute and Department of Chemistry, University of Wisconsin, Madison, Wisconsin 53706

(Received 20 May 1968)

In an attempt to elucidate the discrepancy between the theoretical and experimental dissociation energies of H_2, accurate binding energies and term differences have been computed for the 15 vibrational levels using the Kołos and Wolniewicz clamped-nuclei potential with its various corrections. The results suggest possible interpretations of the discrepancy. In one of these an extrapolation method is introduced which combines experimental term differences with computed binding energies for the uppermost levels to yield the dissociation energy; this result is in accord with the experimental value of Herzberg and Monfils. The effect of uncertainties in the values of the natural constants is considered. Apparent inconsistencies between previously computed vibrational energies are explained.

I. INTRODUCTION

Considerable attention has been devoted to the problem of accurate *ab initio* computation of the dissociation energy and vibrational terms of the various isotopic forms of hydrogen. For the best studied case of ground-state H_2, a discrepancy of some 4 cm^{-1} exists between Herzberg and Monfils' possible experimental value of the dissociation energy,[1] 36 113.6($\pm$0.3) cm^{-1}, and the "fully corrected" theoretical value of Kołos and Wolniewicz (KW),[2] 36 117.4 cm^{-1}. This discrepancy is especially serious since the theoretical value is a variational result (except for -0.2 cm^{-1} due to the radiative correction) and is thus expected to be a lower bound. A serious but less publicized discrepancy exists between the observed[3] and computed[2,4–9] vibrational term differences; the experimental $\Delta G_{v+1/2}$ values (accurate to $\pm$0.05 cm^{-1}) differ with the calculated ones by an accumulated total of $\sim$4 cm^{-1} over the 15 vibrational levels. It is not clear whether or not these two discrepancies are related.

In the present study, the computed vibrational spectrum is used as a measure of the local accuracy of the theoretical potential. Corresponding to two of the possible interpretations of the source of the disagreement between theory and experiment, two empirical "correction functions" to the KW potential are presented for consideration.

II. METHOD

A. Vibrational Eigenvalues as a Local Test of the Accuracy of a Potential

For any given diatomic internuclear potential, exact bound-state eigenfunctions and eigenvalues may be efficiently computed.[8–12] In addition, it may be shown (see Appendix A) that a given eigenvalue is especially sensitive to small changes in the potential in the immediate neighborhood of its two turning points $R_1(v)$ and $R_2(v)$. For the higher levels, this dependence is increasingly weighted towards the outer turning point $R_2(v)$. The inverse problem of deriving a potential "correction function" which would remove the difference between computed and observed energies may also be solved uniquely, provided that the maximum error in the original theoretical potential is everywhere reasonably small. The results in Appendix A indicate that this inversion is possible for H_2 if the KW potential[2,13,14] is accurate to better than about 10 cm^{-1} over the range of the turning points of the 15 vibrational levels. That this is the case is shown by the approximate ($\pm$5 cm^{-1}) agreement between its computed eigenvalue spectrum and experiment.

B. Method of Comparing Computed and Observed Eigenvalues

The customary comparison of computed and observed vibrational–rotational energies via the quantity $T_0(v, J)=[T(v, J)-T(0, 0)]$ (e.g., Ref. 7) is undesirable here, since it assumes that the absolute value of the energy computed for the ground ($v=0$, $J=0$) state agrees with experiment. A better approach would be to compare the binding energies[15] $E_b(v)$. However, the $\pm$0.3 cm^{-1} uncertainty in the experimental D_0

* Research supported by National Science Foundation Grant GP-7409 and National Aeronautics and Space Administration Grant NsG-275-62.

[1] G. Herzberg and A. Monfils, J. Mol. Spectry. 5, 482 (1960). The value given corresponds to the $B'(^1\Sigma_u^+)$ assignment of the upper state of the observed transition. Their alternate assignment, the $C(^1\Pi_u)$ state corresponding to $D_0=36\,113.0(\pm 0.3\ cm^{-1})$, is made very unlikely by *ab initio* computations of the potential for this state which show it to possess a barrier with a maximum of $\sim$100 cm^{-1}.

[2] (a) W. Kołos and L. Wolniewicz, Phys. Rev. Letters 20, 243 (1968); (b) J. Chem. Phys. 49, 404 (1968).

[3] G. Herzberg and L. L. Howe, Can. J. Phys. 37, 636 (1959).

[4] J. K. Cashion, J. Chem. Phys. 45, 1037 (1966).

[5] L. Wolniewicz, J. Chem. Phys. 45, 515 (1966).

[6] J. D. Poll and G. Karl, Can. J. Phys. 44, 1467 (1966).

[7] T. G. Waech and R. B. Bernstein, J. Chem. Phys. 46, 4905 (1967).

[8] D. F. Zetik and F. A. Matsen, J. Mol. Spectry. 24, 122 (1967).

[9] F. M. Greenawalt and A. S. Dickinson, J. Mol. Spectry. (unpublished).

[10] J. W. Cooley, Math. Computation 15, 363 (1961).

[11] J. K. Cashion, J. Chem. Phys. 39, 1872 (1963).

[12] H. Harrison and R. B. Bernstein, J. Chem. Phys. 38, 2135 (1963); 47, 1884 (1967), Erratum.

[13] W. Kołos and L. Wolniewicz, J. Chem. Phys. 41, 3663 (1964).

[14] W. Kołos and L. Wolniewicz, J. Chem. Phys. 43, 2429 (1965).

[15] Throughout, the "binding energy" of a given level is the energy difference between that level and the asymptote of the potential, while "dissociation energy" refers to the binding energy of the $v=0$, $J=0$ level.

would yield experimental binding energies with uncertainties too great for the current analysis.

The present approach combines the accurate *observed* vibrational spacings (reported to 0.01 cm^{-1}) with the precise binding energies *computed* from the best available potential. As is illustrated in Fig. 1, the experimental and computed levels for a given v are matched, and the computed binding energy is added to the experimental vibrational energy to yield an "apparent" ground-state dissociation energy, defined $D_0(v)=[E_b(v)+T_0(v,\,0)]$. If the theoretical potential were exact, the curve of $D_0(v)$ vs v would be horizontal at the true dissociation energy since the difference between each $D_0(v)$ and the true D_0 is merely the error in the computed $E_b(v)$. Otherwise, $[D_0(v+1)-D_0(v)]$ is the negative of the error in the computed $\Delta G_{v+1/2}$ so that a $D_0(v)$ curve is effectively a second-order Birge–Sponer plot with unknown ordinate zero. It will be seen (in Sec. IV.B) that under certain conditions this type of plot may be used in an extrapolation procedure to yield the "true" D_0.

III. CALCULATIONS

A. Computation of Vibrational Energies

Vibrational eigenvalues were obtained by solving the radial Schrödinger equation numerically using a modified version of the Cooley–Cashion program.[10,11] (See Appendix B for a comparison of this with the Harrison and Bernstein[12] and Zetik and Matsen[8,9] methods.)

The integration is performed on the equation expressed in the reduced form

$$(d^2Y/dz^2)+B_z[E^*-V^*(z)]Y=0, \qquad (1)$$

where $z=R/R_m$, $V(z)=z\chi(R)$, $E^*=E/\epsilon$, $V^*(z)=V(R)/\epsilon$, and $B_z=2\mu\epsilon R_m^2/\hbar^2$; the parameters R_m and ϵ are arbitrary scaling factors (usually chosen close to R_e and D_e). The reduced mass used for most of the computations was that for two protons. Despite the contrary arguments of Cashion,[4] this appears to be the correct choice of mass since Eq. (1) describes the motion of the nuclei in an effective potential arising from the field of the electrons. The total potential $V(R)$ includes the usual clamped-nuclei and centrifugal potentials, and for most of the calculations it contained the relativistic and nuclear motion (adiabatic) corrections as well. The integration was carried out over the interval $0.4\leq R\leq 10$ a.u., and the increment used (the "mesh size") was 0.007 a.u. Expanding the interval or decreasing the mesh size affected the eigenvalues negligibly (i.e., by <0.01 cm^{-1}).

The required physical constants are all collected in the factor $B_z=3.64566\times10^3\mu\epsilon R_m^2(\pm0.5\times10^{-3}\,\%)$,[16] where μ is the reduced mass in "unified" atomic mass units ($^{12}C=12$), and ϵ and R_m are both expressed in atomic units. The effect on the eigenvalues of error in the physical constants is tempered by the radial kinetic-energy factor $T_K=[E-V(z)]$ with which B_z is combined in Eq. (1). To a first approximation, a given error in B_z, say ΔB_z, introduces an error

$$\Delta E_v=-(\Delta B_z/B_z)\langle v\,|\,T_K\,|\,v\rangle \qquad (2)$$

to the computed energy for level v. The kinetic energies $\langle v\,|\,T_K\,|\,v\rangle$ (e.g. those later presented in Table III) cause the effect of error in the physical constants to diminish for levels approaching either the top or the bottom of the well, while reaching a maximum about $\frac{3}{4}$ of the way up. An adjustment of the electron mass[16,17] changing B_z by one standard error ($\pm0.5\times10^{-3}\,\%$) affects the H_2 vibrational energies for levels 6–11 (where $\langle v\,|\,T_K\,|\,v\rangle$ is greatest) by $\sim\mp0.06$ cm^{-1}, while affecting the $v=0$ energy by less than ∓0.01 cm^{-1}.

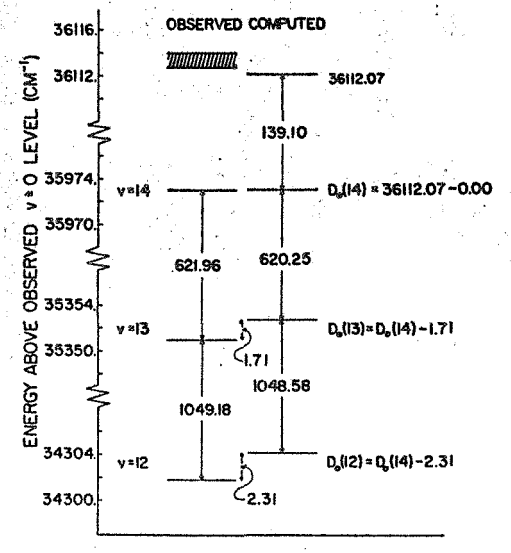

FIG. 1. Derivation of $D_0(v)$ values by matching computed and observed levels at $v=14$. The number 36 112.07 [i.e., $D_0(14)$] would equal the dissociation energy if the computed value of $E_b(14)$ were exactly correct. Here the $E_b(v)$ were obtained for the relativistic, adiabatic KW potential (using nuclear reduced mass).

B. Effect of Interpolation on Eigenvalue Precision

The KW clamped-nuclei potential for H_2 was reported at 87 points in the interval $0.4<R<10$ a.u., while $\sim$1500 points are needed in the numerical integration. The interpolation between the given points is therefore very critical, and indeed appears to be the major source of eigenvalue imprecision.

[16] With μ, ϵ, and R_m expressed in unified atomic mass units ($^{12}C=12$) and atomic units, the numerical part of B_z is just $2/m_e$ where m_e is the electron mass in atomic mass units. The uncertainty is the standard error in the best known value of m_e.[17] The uncertainties in the nuclear and atomic reduced mass of H_2 ($\mu=0.50363831$ and 0.50391261 amu, respectively[17]), contribute negligible error to B_z.

[17] E. R. Cohen and J. W. DuMond, Rev. Mod. Phys. 37, 537 (1965).

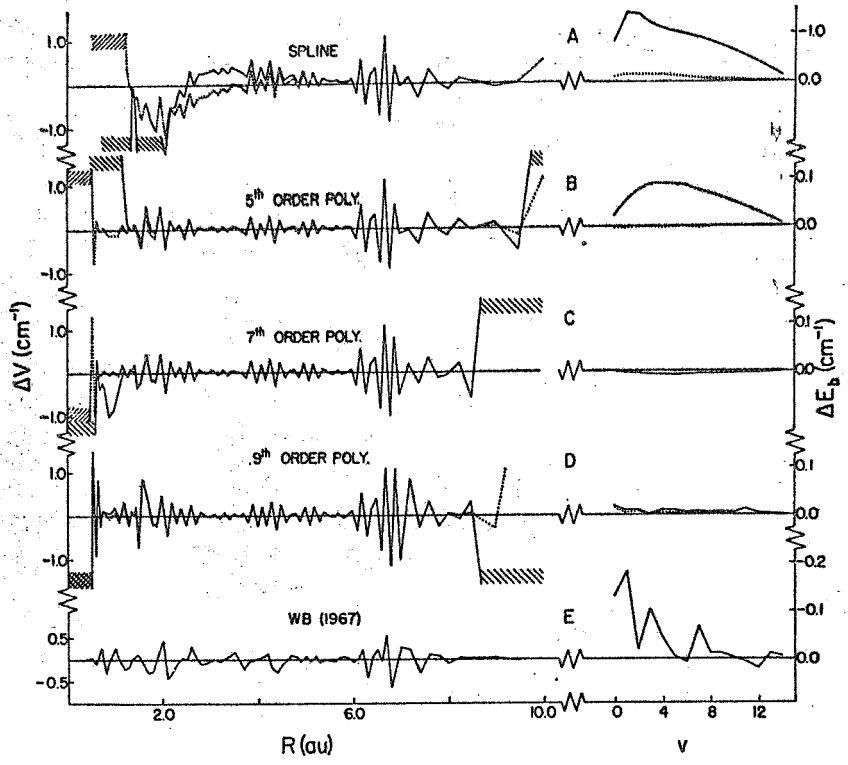

FIG. 2. Comparison of effects of divers interpolation schemes on the potential and its eigenvalues. $\Delta V=\{V_{KW}-V_{int}\}$; $\Delta E_b=\{E_b$[seventh-order polynomial over (R^2V)]$-E_b$(other)$\}$. ···· Interpolation over $\{R_i^2V_{KW}(R_i)\}$; —— Interpolation over $\{V_{KW}(R_i)\}$. Note the several different scales on the right ordinate. Case A uses eight point third-order spline fits; Case B uses fifth-order polynomials; Case C uses seventh-order polynomials; Case D uses ninth-order polynomials; and Case E uses the analytic formula of Ref. 7.

The accuracies of several interpolation schemes were tested by omitting in turn each of the computed KW clamped-nuclei points, and comparing the ith omitted value $V_{KW}(R_i)$ to that obtained by interpolation over the remaining data, $V_{int}(R_i)$. All of the methods used were piecewise fits which selected an equal number of the given points from either side of the desired value. It is clear that interpolating over $\{R_i^2V_{KW}(R_i)\}$ (as suggested by Poll and Karl[6]) rather than over $\{V_{KW}(R_i)\}$ significantly improves the results. The interpolations giving rise to the differences $\Delta V_i=[V_{KW}(R_i)-V_{int}(R_i)]$ in Fig. 2 used 85 of the KW[14] points, the entries at $R=1.400$ and 1.401 a.u. being omitted.[18] Figure 2 also shows the effect on the computed eigenvalues of using different interpolation schemes, the binding energies obtained via the piecewise seventh-degree polynomial interpolation over $\{R_i^2V_{KW}(R_i)\}$ being used as a reference. The precision of the best results is $\sim\pm0.02$ cm^{-1}. Combining this interpolation imprecision with the uncertainty in B_e shows that the accuracy with which our computed eigenvalues "reflect" the KW potential lies within the limits ±0.03 cm^{-1} (for $v=0$) and ±0.08 cm^{-1} (for $v=6$–11).

The differences ΔV_i in Parts A–D of Fig. 2 are, however, considerably larger than the actual error in $V(R)$ carried into the eigenvalue calculation, since the interpolated potential actually used is constrained to pass through all the KW points. In Part E, on the other hand, the differences ΔV_i are the actual errors in the analytical potential[20] of Ref. 7.

C. The Total Potential $V(R)$

In the present work a smooth clamped-nuclei potential was obtained in the interval $0.45\leq R<9.0$ a.u. using a series of seventh-order-polynomial fits[19] over $\{R_i^2V_{KW}(R_i)\}$ to 85 of the 87[18] KW (1965) points. At the ends of this range where the numerical interpolation becomes least accurate (see Fig. 2) the potential was extrapolated analytically. For $R<0.45$ a.u. it was approximated by a function of the form $V(R)=A/R^B+C$, where the three constants were determined by fitting the function to the three KW points at smallest R. For $R\geq9.0$ a.u. the potential was represented by a theoretical five-term analytical expression derived from perturbation theory. The C_6, C_8, C_{10}, and

[18] The KW points at 1.400 and 1.401 a.u. were omitted from the interpolations since their inclusion yielded an anomalously high density of data in this region, producing erroneously large errors (large ΔV_i) at adjacent points interpolated using the higher-order (seventh- and ninth-order) polynomials.[19] The removal of these two values changed the potential yielded by the piecewise seventh-order-polynomial interpolation enough to increase the binding energy of the $v=0$ level by 0.035 cm^{-1}, though it affected higher levels by less than 0.01 cm^{-1}.

[19] The Lagrangian interpolation subroutine of R. N. Zare [University of California Radiation Laboratory Report, UCRL-10925, 1963, (unpublished)] was used for all of our piecewise polynomial interpolations.

[20] The analytic fit of Ref. 7 [using the method of G. E. Forsythe, J. Soc. Ind. Appl. Math. 5, 74 (1957)] of the whole potential to a single polynomial expression of 32nd degree is of course not constrained to give precise agreement with all 87 reported KW[14] values.

TABLE I. Difference between KW clamped-nuclei-potential[a] and perturbation-theory results.[b]

R(a.u.)	7.0	7.2	7.6	7.8	8.0	8.25	8.5	9.0	9.5	10.0
$E_{\text{Pt bn}}-E_{\text{KW}}$(cm^{-1})	2.26	1.27	0.72	0.53	0.24	0.11	0.13	−0.15	−0.11	0.11
$-E_{\text{KW}}$(cm^{-1})	41.56	31.47	19.05	14.97	11.74[c]	8.87	6.89	4.06	2.66	2.00

[a] Reference 14. [b] Reference 21. [c] Reference 22.

C_{11} inverse-power potential constants and the exponential expression for the exchange contribution were taken from Hirschfelder and Meath.[21] Table I shows the agreement between the KW potential and the above extrapolation over the range $R=7$–10 a.u.[22] Since these long-range (for $9\leq R\leq 10$ a.u.) and short-range (for $0.40\leq R<0.45$ a.u.) extrapolations are applied to R values outside the range of the classical turning points of the highest vibrational level [$(R_1(14)\cong 0.78$ a.u. and $R_2(14)\cong 6.2$ a.u.], any errors they introduce are expected to produce a negligible effect on the eigenvalues.

Series of third-order polynomials were used to interpolate between the KW values of the relativistic and nuclear motion (adiabatic) corrections. Beyond the range of their computations, the relativistic correction at large R and the adiabatic correction at small R were extrapolated using analytic functions,[23] errors in which would at worst introduce errors of $\sim$0.03 cm^{-1} in the computed eigenvalues for levels above $v=11$. In addition, the adiabatic correction at large R was approximated by an exponential fitted to pass through the last two values at finite R and decaying to the asymptote. Although other workers[2,5,6] have used significantly different extrapolations, the exponential tail seems most reasonable in view of its excellent qualitative agreement (see Fig. 3) with the correction computed from the expressions derived by Van Vleck.[24] Inaccuracy in this extrapolation could at worst introduce errors of $\sim$0.5 cm^{-1} in the eigenvalues computed for levels above $v=10$.

D. The Nonadiabatic Correction

The nonadiabatic correction to the eigenvalues arising from the coupling of the ground state to excited electronic states was approximated by a formula derived by Van Vleck[24] (and recently used by Poll and Karl[6]). This treatment starts with a second-order perturbation energy, and by using an Unsöld approximation and summing over complete sets of vibrational and electronic states yields the following expression:

$$\Delta E(v)=-\frac{4}{\nu_0}\langle v\,|\,T_K\,|\,v\rangle \times\left\langle \Phi_e(r_e,R)\left|-\frac{\hbar^2}{2\mu}\frac{\partial^2}{\partial R^2}\right|\Phi_e(r_e,R)\right\rangle^{R_v}, \quad (3)$$

where ν_0 is the Unsöld energy, T_K is the radial kinetic energy, and the third factor is an expectation value over the electronic coordinates of the ground state, evaluated with the nuclei separated by $R_v=\langle v\,|\,R\,|\,v\rangle$. This factor is one of those contributing to the adiabatic correction, for which Van Vleck had derived an analytic expression. The value initially chosen for the Unsöld energy, $\nu_0=1.35\times10^5$ cm^{-1}, was derived[25] from consideration of sums of a different type of matrix element and may be somewhat inaccurate. It may be more correct, too, to replace ν_0 by $\nu_v=[\nu_0-T_0(v,0)]$. The expectation values $\langle v\,|\,T_K\,|\,v\rangle$ are readily evaluated from the radial wavefunctions which are obtained from the eigenvalue calculation.

IV. RESULTS

A. Sources of Disagreement of Previous Computed Eigenvalues

Several calculated sets of vibrational eigenvalues for the KW potential have already been published.[4–8] Waech and Bernstein[7] compared those results supposedly based on the clamped-nuclei potential and found discrepancies of up to 12 cm^{-1}. Upon further study it appears that these differences result from the use of slightly different potentials and physical constants. The most prominent single effect is due to the

[21] J. O. Hirschfelder and W. J. Meath, Advan. Chem. Phys. 12, 3 (1967).

[22] It has been pointed out by P. R. Certain, J. O. Hirschfelder, W. Kołos, and L. Wolniewicz [J. Chem. Phys. 49, 24 (1968)] that a calculation using an improved basis set of electronic wavefunctions lowers the KW[14] clamped-nuclei energy at 8.0 a.u. by 0.15 cm^{-1} to −11.74 cm^{-1}. This improved value was used in Table I. It should be remembered that the estimated rounding errors in the single-precision KW clamped-nuclei results were stated to be ±0.1 cm^{-1}.

[23] The relativistic correction at large R was approximated by an exponential fitted to the last two KW points at finite R and decaying to the asymptote, a distance of 0.42 cm^{-1}. The adiabatic correction for $R<0.6$ a.u. was extrapolated by an exponential fitted to pass through the two KW points at smallest R (absolute values were used in this fit; cf. values expressed relative to the asymptote). Since the latter extrapolation begins at 0.6 a.u.$<R_1(14)\cong 0.78$ a.u., it could introduce only negligible errors to the computed eigenvalues.

[24] J. H. Van Vleck, J. Chem. Phys. 4, 327 (1936). Although the Wang electronic wavefunction used by Van Vleck is relatively inappropriate at small R, it becomes increasingly suitable as R increases through the region in question and is almost exact at the asymptote. Values of the Wang function's variational exponential parameter were derived by extrapolating over the values reported by J. O. Hirschfelder and J. W. Linnett [J. Chem. Phys. 18, 130 (1950)]. Equation (51) in this paper by Van Vleck contains an extraneous factor of b^2.

[25] J. H. Van Vleck and A. Frank, Proc. Natl. Acad. Sci. (U.S.) 15, 539 (1929).

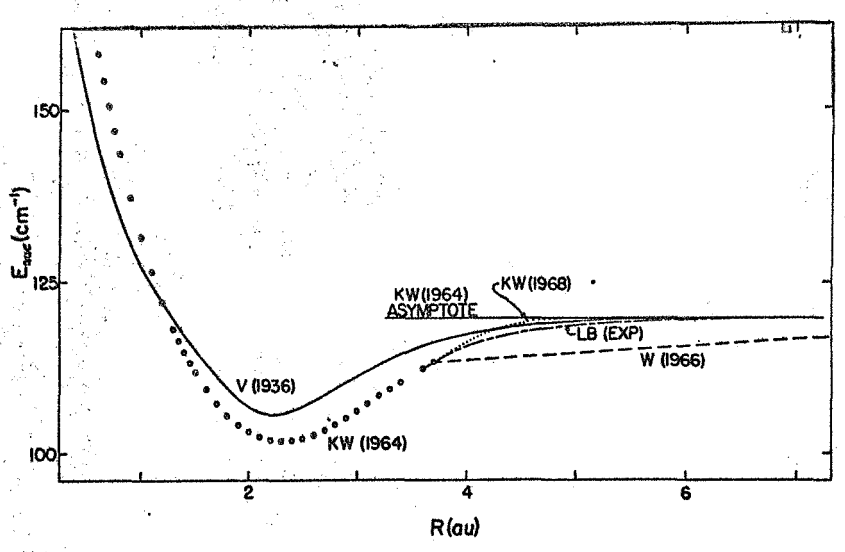

FIG. 3. Nuclear motion correction. O are the 1964 KW points; V(1936) comes from the Van Vleck formulation[24]; KW(1968), 1968 KW[3] graphical extrapolation; LB(EXP), present authors' exponential extrapolation; and W(1966), Wolniewicz'[18] linear extrapolation.

TABLE II. $D_0^{(i)}(v)$ results.[a]

	$i=1$	2		3		4			5		
v	$D_0(v)$	$D_0(v)$	$\Delta_{W(3)}$	$D_0(v)$	$\Delta_{PK(3)}$	$D_0(v)$	Δ_C	Δ_{WB}	$D_0(v)$	$\Delta_{W(5)}$	$\Delta_{PK(5)}$
0	36 118.0	36 117.9	0.0	36 117.4	0.0	36 112.8	0.0	0.2	36 112.2	0.0	−1.0
1	18.1	17.0	0.1	16.4	0.1	11.5	0.0	0.4	09.8	0.0	−1.1
2	18.2	16.2	0.1	15.6	0.1	10.5	−0.1	0.4	07.9	0.0	−1.1
3	17.7	14.9	0.1	14.3	0.1	09.1	−0.5	0.6	05.7	0.1	−1.0
4	17.6	14.0	0.1	13.4	0.1	08.3	−0.9	0.6	04.2	0.1	−1.3
5	17.3	13.3	0.2	12.7	0.2	07.7	−1.6	0.6	03.0	0.1	−1.9
6	17.0	12.4	0.2	11.8	0.2	07.2	−2.8	0.7	02.0	0.1	−3.0
7	16.6	11.7	0.2	11.2	0.2	07.0	−4.5	0.7	01.5	0.1	−4.6
8	16.2	11.2	0.2	10.6	0.3	07.0	−7.5	0.6	01.4	0.1	−7.6
9	15.8	10.7	0.2	10.2	0.3	07.3	−11.9	0.6	01.7	0.1	
10	15.3	10.3	0.3	09.9	0.3	07.7		0.6	02.3	0.1	
11	14.7	10.1	0.8	09.7	0.2	08.3		0.5	03.4	0.2	
12	13.9	10.1	1.8	09.7	−0.2	08.9		0.4	04.7	0.2	
13	13.4	10.6		10.3	−0.6	10.0		0.3	06.9		
14	13.6	12.2		12.1	−0.4	12.0		0.2	10.5		

[a] Δ is the amount (in cm^{-1}) by which the previously reported $E_b(v)$ [and hence $D_0(v)$] exceeds that computed here for the same case. Δ_W compares present results to those of Wolniewicz[3]; Δ_{PK} compares with Poll and Karl[4]; Δ_C compares with Cashion[4]; and Δ_{WB} compares with Waech and Bernstein.[7] The parameter i denotes a particular choice of potential and reduced mass: $i=1$: relativistic, adiabatic, μ atomic; 2: nonrelativistic, adiabatic, μ nuclear; 3: relativistic, adiabatic, μ nuclear; 4: clamped nuclei, μ atomic; and 5: clamped nuclei, μ nuclear.

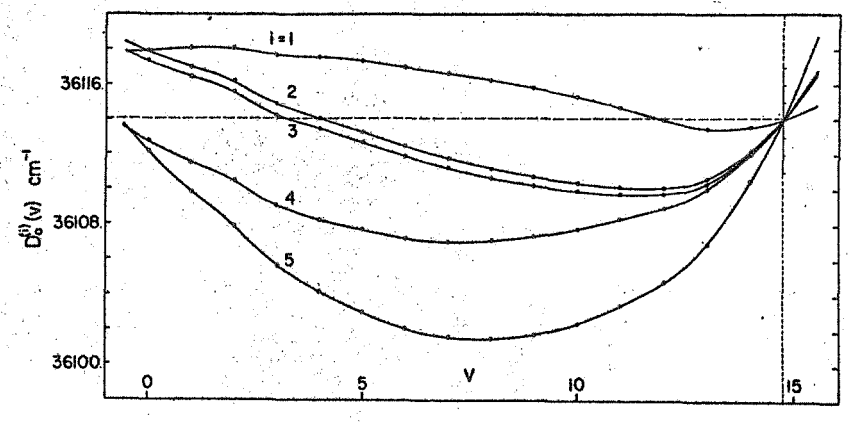

FIG. 4. $D_0^{(i)}(v)$ curves plotted from the results in Table II. The curves were derived by piecewise interpolation with series of second-order polynomials. The "bumps" at $v=2$ are explained in Sec. IV.A.

use of different values for the reduced mass; in some of the studies[4,7] the atomic rather than the nuclear masses were used.[26] The various possible cases have now been analyzed and sets of apparent dissociation energies $D_0^{(i)}(v)$ have been computed for five of them ($i=1, \cdots, 5$). These are plotted in Fig. 4 and are compared to the previously published results in Table II. The causes of the remaining differences Δ between the present results and those reported previously for the same case, are given below.

The largest differences, Δ_C and $\Delta_{PK(i=5)}$, both arise from their use of the earlier (1964), less-accurate versions[13] of the clamped nuclei potential.[27] In $\Delta_{W(2)}$ and $\Delta_{PK(3)}$ the escalating deviance above $v=0$ corresponds to the use of extrapolations of the nuclear motion correction differing markedly from that used here. The linear extrapolation of Wolniewicz[5] ($\Delta_{W(2)}$) is shown by Fig. 3 to be much too coarse.

The remainder of $\Delta_{W(2)}$ and $\Delta_{PK(3)}$ as well as $\Delta_{W(5)}$ and much of Δ_{WB} may be quantitatively explained in terms of the effect of error in the physical constants, discussed in Sec. III.A. Wolniewicz,[5] Poll and Karl,[6] and Waech and Bernstein[7] used values of B_e which were all too large[28] by, respectively, 1.3×10^{-3} %, 1.2×10^{-3} %, and 8.7×10^{-3} %. Upon substituting these differences into Eq. (2) along with the kinetic energies from Table III, most of the given Δ's are explained, except that portion of Δ_{WB} which Fig. 2 shows to be due to the Waech and Bernstein interpolation procedure. Some small errors in the earlier work are also due to the use by Waech and Bernstein[7] and Poll and Karl[6] of integration meshes two and three times larger than used here.

The differences between results calculated using the same potential but slightly different reduced masses (e.g., compare cases $i=1$ and 4, respectively, to $i=3$ and 5) are also quantitatively explained in terms of the effect of the difference in reduced mass on the B_e factor. Changing from nuclear to atomic reduced mass increases B_e by 0.0545%, which when substituted in Eq. (2) yields the observed differences.

Since none of the curves in Fig. 4 are flat, none of the sets $i=1, \cdots, 5$ yield vibrational spectra in agreement with experiment; also, the relativistic adiabatic μ-nuclear ($i=3$) curve which should be best appears worse than the corresponding μ-atomic case ($i=1$).

TABLE III. Results from the 1968 relativistic adiabatic KW potential.[a]

v	$E_b(v)$[b]	$D_0(v)$	$\langle v \mid T_K \mid v \rangle$	$\Delta E(v)$	$\Delta E'(v)$
0	36 117.54	36 117.5	1 079.	−0.65	−0.65
1	31 955.44	16.6	3 040.	−1.83	−1.89
2	28 028.78	15.8	4 770.	−2.89	−3.07
3	24 332.61	15.0	6 275.	−3.82	−4.19
4	20 863.88	14.2	7 555.	−4.59	−5.17
5	17 621.61	13.5	8 609.	−5.15	−5.97
6	14 607.10	12.8	9 427.	−5.67	−6.74
7	11 824.31	12.1	9 996.	−6.03	−7.35
8	9 280.42	11.4	10 292.	−6.27	−7.82
9	6 986.80	10.7	10 278.	−6.33	−8.07
10	4 960.09	10.3	9 904.	−6.16	−8.01
11	3 223.20	10.1	9 098.	−5.69	−7.53
12	1 808.15	10.0	7 754.	−4.84	−6.49
13	759.48	10.5	5 713.	−3.51	−4.76
14	139.16	12.1	2 755.	−1.65	−2.24

[a] All energies are in cm^{-1}. The kinetic energies are approximately the same as for cases $i=1, \cdots, 5$ in Table II. $\Delta E(v)$, the nonadiabatic correction to the energy, is the negative of the correction to the binding energy and to $D_0(v)$. The unprimed nonadiabatic correction was evaluated using ν_0 and corresponds to Curve B in Fig. 5, while $\Delta E'(v)$ was evaluated using the adjusted Unsöld energies ν_v and yielded Curve C.

[b] As indicated in Secs. III.A and III.B, these eigenvalues reflect the KW potential with accuracies ranging from ±0.03 cm^{-1} to ±0.08 cm^{-1}. They may not be directly compared to the most recent KW results[2] since the latter did not include the relativistic correction in the effective potential.

The addition of the nonadiabatic correction improves the situation, but it will be shown that results for the theoretically best case still do not yield the observed vibrational ladder.

All of the curves in Fig. 4 exhibit an anomalous "bump" at $v=2$ which is due to small errors in the Herzberg and Howe[3] energies for $v=1$ and 2.[29] These have been remeasured[30–32] and the most recent data[32] give $T_0(1, 0)=4161.181$ cm^{-1} and $T_0(2, 0)=8087.01$ cm^{-1}. Substituting these values for those of Herzberg and Howe increases all $D_0(1)$ values in Table II and Fig. 4 by 0.04 cm^{-1}, and decreases all $D_0(2)$ values by 0.10 cm^{-1}, completely removing the apparent anomaly.

B. The Dissociation Energy and the Vibrational Spectrum

In the following work the Herzberg and Howe[3] vibrational ladder is used with the addition of the corrected experimental values of $T_0(1, 0)$ and $T_0(2, 0)$ given above. The eigenvalues reported below were computed (using the nuclear reduced mass) from the relativistic adiabatic potential described in Sec. III.C, with

[26] We are indebted to Dr. T. G. Waech for bringing this to our attention.

[27] Poll and Karl[6] ($\Delta_{PK(5)}$) used the energies computed with 54-term electronic wavefunctions over the whole of the interval $0.4\leq R\leq3.7$ a.u., and Cashion[4] (Δ_C) added to these the more accurate potential energies reported in the more restricted interval about the minimum $0.55\leq R\leq2.0$ a.u.

[28] With the Cohen and DuMond[17] constants as a reference, Wolniewicz[5] used a reduced mass which is $\sim1.3\times10^{-3}$ % too large, Poll and Karl[6] used a value of the Bohr radius 0.6×10^{-3} % too large, and Waech and Bernstein[7] used values of Planck's constant and the Bohr radius which were, respectively, $6.\times10^{-3}$ % too small and $1.\times10^{-3}$ % too large.

[29] The Herzberg–Howe results[3] are a composite of three sets of nonoverlapping experimental data: their own Lyman-band measurements which place the levels $v=3$ to 14 relatively, B. P. Stoicheff's [Can. J. Phys. 35, 730 (1957)] Raman data for the $v=0$–1 transition, and G. Herzberg's [Can. J. Res. A28, 144, (1950)] pioneering quadrupole absorption measurements of the $v=0$–2 and 0–3 transitions (as reinterpreted by Stoicheff).

[30] C. H. Church, Ph.D. thesis, University of Michigan, Ann Arbor, Mich., Rept. UMRI-2609-3-T, 1959 (unpublished).

[31] U. Fink, T. A. Wiggins, and D. H. Rank, J. Mol. Spectry. 18, 384 (1965).

[32] J. V. Foltz, D. H. Rank, and T. A. Wiggins, J. Mol. Spectry. 21, 203 (1966).

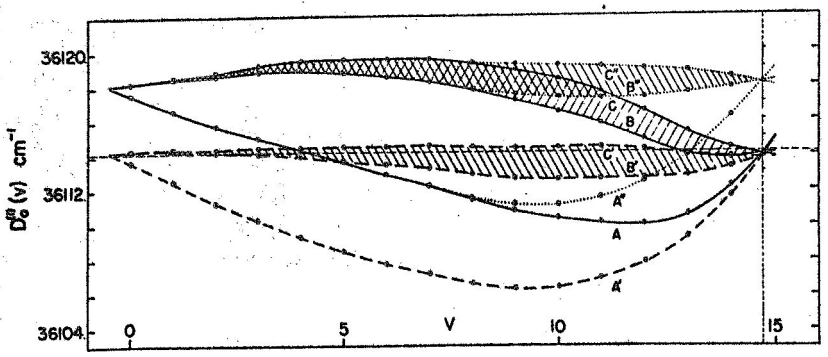

FIG. 5. $D_0(v)$ curves from best KW-(1968) potential. Curve A corresponds to Column 3 in Table III; B and C include the nonadiabatic corrections from Columns 5 and 6, respectively; the shaded area is a measure of the uncertainty in the nonadiabatic correction. A′, B′, and C′, and A″, B″, and C″, respectively, illustrate the effect on Curves A, B and C of adding corrections Δ' and Δ'' in Fig. 6 to the effective potential.

one modification; KW's 1965 clamped-nuclei results in the interval $1.0 \leq R \leq 3.2$ a.u. have been replaced by their more recent[2] double-precision results.[33]

In Appendix A it is shown that eigenvalues computed for the highest vibrational levels are most sensitive to the accuracy of the potential just inside their respective outer turning points. This is confirmed by the convergence of the several curves in Fig. 4 at $v = 14.71(\pm 0.02)$.[35] This occurs because the relativistic and adiabatic corrections monotonically approach their asymptotes over the range of the $R_2(v)$ for the highest levels, thus causing the difference between the several effective potentials to approach zero in this region. It occurs despite the fact that these effective potentials differ significantly (by between $+20$ and -17 cm^{-1} relative to the asymptote) over the region between the turning points.

By definition, $D_0(v)$ is equal to the true dissociation energy if the computed binding energy for level v is correct. For the highest levels this is equivalent to requiring that the potential be accurate in the neighborhood of $R_2(v)$. Since the computed potential is exact at $R = \infty$, $D_0(14.71)$ must equal the true dissociation energy, though the question may be raised whether the "true" value of $D_0(14.71)$ may be derived from a simple extrapolation on a graph such as Fig. 4. This is the case if the clamped-nuclei potential exhibits its true asymptotic behavior in the interval spanned by the $R_2(v)$'s for the highest levels, or more precisely, if the error in the clamped-nuclei potential monotonically approaches zero in this interval. With this assumption, the present results yield $D_0(14.71) = D_0 = 36114.1(\pm 0.2)$[35] cm^{-1}. This value agrees within the mutual uncertainties with the experimental value,[1] $D_0 = 36113.6(\pm 0.3)$ cm^{-1}.

We have recomputed eigenvalues from the relativistic adiabatic potential (including the improved 1968 clamped-nuclei results) and added in the nonadiabatic correction, evaluating the latter using both Van Vleck and Frank's[25] Unsöld energy ν_0, and the present "adjusted" values ν_v (Sec. III.D). These results, given in Table III, yield the three solid curves (A, B, and C) in Fig. 5. Since the nonadiabatic correction is the same for the several cases in Table II as it is here, Fig. 5 shows that its addition does not affect the values of the intersection point. The distance between Curves B and C is a measure of the uncertainty in the nonadiabatic correction, though it does not represent a bound. The radiative correction to the energies is not discussed here since Wolniewicz[5] has derived a bound on its magnitude which is smaller than the uncertainty n the nonadiabatic correction.

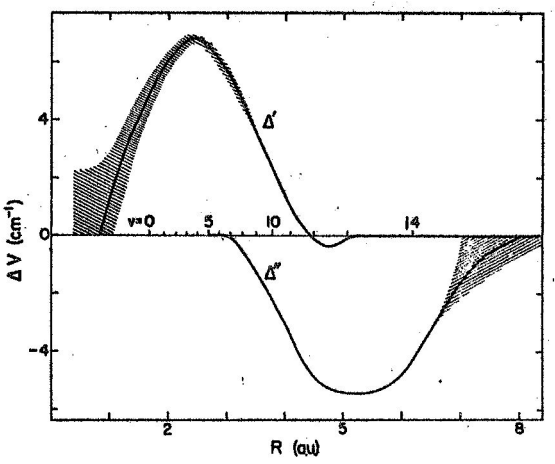

FIG. 6. Empirical "correction functions" for the KW potential. Addition of either of these functions, Δ' or Δ'', to $V(R)$ induced a flattening of the initially computed nonadiabatic $D_0(v)$ curves (B and C) in Fig. 5, corresponding to better agreement between computed and observed vibrational spacings. The shaded regions are an estimate of the nonuniqueness of the inversion of the primed and double-primed results in Fig. 5 which yielded Δ' and Δ'', respectively. The v designations on the abscissae denote the outer turning points $R_2(v)$.

[33] Unfortunately the new values are reported only at 17 of the 29 original points on this interval. In order to minimize the interpolation error, the difference between the old and new results was assumed to vary continuously (except for the expected discontinuities[34] at 1.6 and 2.0 a.u.) and improved values were obtained at all 29 original points. Omitting the thus improved points affected the eigenvalues by as much as 0.05 cm^{-1}.

[34] An error in the 1965 KW point at $R = 1.6$ a.u. has been pointed out by C. L. Beckel and J. P. Sattler [J. Mol. Spectry. 20, 153 (1966)], while the discontinuity at $R = 2.0$ a.u. is expected since this is the point at which the 1965 KW results switched from an 80-term to a 54-term electronic wavefunction. The discontinuities at these points are also evidenced by the relatively large amplitude, in their neighborhoods, of the interpolation error functions in Fig. 2.

[35] This uncertainty in the point of intersection is the average deviation of the results of several different numerical extrapolation schemes.

Since neither the adiabatic nor the nonadiabatic results reproduce the observed vibrational term differences within reasonable limits, we have derived two possible "correction functions" for the potential, curves Δ' and Δ'' in Fig. 6. The addition of these functions to the effective potential causes the eigenvalue calculation to yield the $D_0(v)$ curves A′, B′, and C′ (corresponding to Δ'), and A″, B″, and C″ (corresponding to Δ'') in Fig. 5. Δ' and Δ'' are uniquely determined by their respective $D_0(v)$ curves to within the indicated uncertainties. The nonuniqueness of Δ' at small R arises since a given change in one of the lowest vibrational eigenvalues could be induced by changes in the potential at either or both turning points (see Appendix A). The uncertainty in the tail of Δ'' [for $R>R_2(14)\cong 6.2$ a.u.] arises since the eigenvalues are only slightly affected by small changes in the potential beyond the outer turning point; however, it seems likely that it should quickly approach zero for $R>8$ a.u. where the KW potential agrees with perturbation theory results (see Table I).

V. DISCUSSION

Although the addition of the nonadiabatic correction yields better agreement with experiment (compare B and C in Fig. 5, with A), the computed vibrational ladder is still elongated relative to the experimental one by an accumulated total of 4 cm^{-1} (two orders of magnitude greater than the uncertainty in the experimental data). This implies that the theoretical potential for $R\leq R_2(14)$ is stretched relative to the exact curve by about 4 cm^{-1}, approximately the disagreement between the experimental and computed dissociation energies; of course the two disagreements may not be related.

If the two effects mentioned above are related, any questioning of the accuracy of the experimental dissociation energy is equally a questioning of the experimental term differences involving an accumulated total of 4-cm^{-1} error. Alternately, if the experimental dissociation energy is assumed to be correct [agreeing with $D_0(14.71)$], the clamped-nuclei potential must be too deep by $\sim$4 cm^{-1}. In this case the relative flatness of Curves B and C in Fig. 5 over the range $v=0$–8 merely indicates that the bowl of the KW[2,13,14] potential has essentially the correct shape. The correction to the potential suggested by this interpretation is curve Δ' in Fig. 6, and its "beneficial" effect on the eigenvalues is shown by Curves A′, B′, and C′ in Fig. 5. These nonadiabatic results (Curves B′ and C′) yield reasonable agreement with both the observed vibrational spectrum and dissociation energy. However, this interpretation requires a reasonable accuracy ($\sim\pm 0.5$ cm^{-1}) for the KW potential at large R ($R\cong 6$ a.u.), and KW point out[2] that this part of the adiabatic potential is expected to be less accurate than that in the vicinity of equilibrium. On the other hand, the good agreement with perturbation-theory results (see Table I) for $R>8$ a.u. implies that the KW potential is indeed quite accurate (e.g., ± 0.5 cm^{-1}) in this region,[36] which makes it seem unlikely that it be 4 cm^{-1} too shallow at $R=6$ a.u.

Another interpretation, believed by the present authors to be less likely, would treat the disagreements of the dissociation energy and of the vibrational levels as unrelated. The former would be due to some as yet undiscovered error in the experimental work or its interpretation,[1] the latter to error in the clamped-nuclei potential at large R. This error (curve Δ'' in Fig. 6) would not exhibit its asymptotic behavior (i.e., would not monotonically approach zero) over the range of $R_2(v)$'s for the highest levels, thus invalidating the extrapolation method suggested in Sec. IV.B.

In a recent paper which also discusses the present problem,[2] KW arrived at a "final" theoretical value for $D_0(0)=E_b(0)$, of 36117.4 cm^{-1}. We see here that the inclusion of the nonadiabatic correction which is necessary for reducing the disagreement with the experimental vibrational term differences increases this to 36 118.0 cm^{-1} [our nonadiabatic $D_0(0)$ evaluated from Table III, plus the radiative correction[37]] which increases the disagreement with the experimental value to 4.4 cm^{-1}. The variational contribution to this theoretical dissociation energy is 36 117.54 cm^{-1}. This is a rigorous upper bound[38] to the exact ground-state energy of a fictitious system described by the KW adiabatic Hamiltonian plus the Breit–Pauli approximation to the relativistic correction. However, since this simplified total Hamiltonian cannot be expected to accurately describe H_2, the above quantity *need not* be an upper bound to the experimental dissociation energy. Thus the correction function Δ' in Fig. 6 does not violate the variational principle if, for example, it is interpreted as an improvement in the relativistic correction. In this case, the total relativistic correction to the ground-state energy would be 6 cm^{-1}.

It should be emphasized that the present paper does not resolve the question of the discrepancy between the experimental dissociation energy of H_2 and $E_b(0)=D_0(0)$. On the basis of the evidence at hand it cannot be decided which of the values $D_0(0)=36\,118.0$ cm^{-1} or $D_0(14.71)=36\,114.1$ cm^{-1} best represents the "theoretical" dissociation energy. While the former is the quantity customarily considered, the latter has the advantage of being determined mainly by the potential at large R where the relativistic and adiabatic corrections, whatever their accuracy elsewhere, are approaching their asymptotic values.

[36] This is further suggested by the results in Footnote 22 which show that the use of an improved electronic-wavefunction basis set only affected the clamped-nuclei potential at 8.0 a.u. by 0.15 cm^{-1}.

[37] J. D. Garcia, Phys. Rev. 147, 66 (1966).

[38] This assumes that replacing the 54-term electronic wavefunction with which the adiabatic and Breit–Pauli relativistic corrections were calculated,[18] by the 100-term wavefunction used in the most recent clamped-nuclei calculations,[2] would not significantly change the corrections.

Although an accurate relativistic treatment of this problem is beyond the scope of present methods, the results presented here suggest two feasible calculations which would shed some light on the question of the H_2 dissociation energy. The first is a more accurate recalculation of the clamped-nuclei potential in the interval ($3 \lesssim R \lesssim 7$ a.u.), where Δ'' (see Fig. 6) is nonzero; the second, a more accurate treatment of the nonadiabatic correction, such as that suggested by modern variational techniques.

ACKNOWLEDGMENT

The authors gratefully acknowledge a number of illuminating discussions with Professor S. T. Epstein.

APPENDIX A: LOCALIZATION OF THE "POTENTIAL DEPENDENCE" OF A VIBRATIONAL EIGENVALUE

The high sensitivity of an eigenvalue E_v to the potential near its turning points may be qualitatively explained by considering the effect on the semiclassical JWKB phase integral

$$I_v = 2\frac{\mu}{\hbar^2}\int_{R_1(v)}^{R_2(v)} [E_v - V(R)]^{1/2} dR = (v+\tfrac{1}{2})\pi$$

of a small shift in the potential (ΔV) over a narrow interval ($\Delta E'$) about a given value of $E_v' = [E_v - V(R)]$. To a first approximation, the change is

$$\Delta I_v = -\frac{\mu}{\hbar^2}\frac{\Delta V}{(E_v')^{1/2}}\frac{\Delta E_v'}{|\,dV/dR\,|}$$

for $E_v'/|\,\Delta V\,| > 1$; it reaches a maximum of

$$(\mu/\hbar^2)\,|\,\Delta V\,|^{1/2}(\Delta E_v'\,|\,dV/dR\,|^{-1})$$

(for $\Delta V < 0$) at the classical turning point, where $\Delta E_v'/(-\Delta V) \to 0$. An analogous result for $E_v' \to 0$ can be evaluated for the somewhat more complicated case $\Delta V > 0$. Since $I_v = (v+\frac{1}{2})\pi$, ΔV must induce a change in E_v which varies as $[(E_v')^{1/2}\,|\,dV/dR\,|\,]^{-1}$, but approaches a finite limit at the turning points where $E_v' = 0$. For the higher levels, the $|\,dV/dR\,|$ factor shifts this sensitivity almost exclusively to the outer turning point $R_2(v)$.

The potential dependence of the eigenvalues as described above is modulated somewhat by the oscillating nature of the exact radial wavefunction. This effect may be seen by considering the perturbation theory expression for the eigenvalue change due to the given potential shift, $|\,Y_v\,|^2 \Delta V(\Delta E_v'\,|\,dV/dR\,|^{-1})$. The term involving the wavefunction $|\,Y_v\,|^2$ shifts the potential dependence inward from the turning point to the region where it has its outermost maximum.

These considerations were illustrated by direct computations, by observing the effect on the H_2 vibrational eigenvalues of localized shifts in the relativistic, adiabatic KW potential.[13,14] The results, given in Table IV, indicate that error in an eigenvalue indeed reflects error in the potential in the neighborhood of its turning points, especially the outer one; this is of course contingent on the assumption that the maximum absolute error in the potential is everywhere relatively small. If this condition is not satisfied, the effect on the eigenvalues of inaccuracy in $V(R)$ midway between the turning points will no longer be distinguishable from that of error in their immediate proximity.

APPENDIX B: COMPARISON OF BOUND-STATE EIGENVALUE PROGRAMS

The Cooley–Cashion[10,11] (C–C) method was quantitatively compared to that of Harrison and Bernstein[12] (HB) and found to be faster by a factor of ~ 5. One large difference between the two lies in their respective methods of estimating the improvement in the trial eigenvalue while iteratively converging on the exact result. In the HB program the increment of improvement decreases by a factor of $\frac{1}{2}$ in successive steps, while with the predictor–corrector formula of C–C the necessary improvement decreases by about two orders of magnitude with each iteration. The other major difference between these methods is that the Runge–Kutta integration of HB requires three to four times as much computation as the Numerov method of C–C to span a given interval for the same increment.

Both of the above methods proceed by direct numerical integration of the radial Schrödinger equation. Zetik and Matsen,[8] on the other hand, expand the

TABLE IV. Effect on H_2 vibrational eigenvalues of changing the potential over a given interval.[a]

v	E_b	A	B	C
0	36 118.	0.0	0.0	0.0
2	28 029.	0.0	0.0	0.0
4	20 864.	0.0	0.0	0.2
6	14 607.	0.0	0.0	0.3
7	11 824.	−0.1	0.0	0.3
8	9 280.	−0.6	0.2	0.4
9	6 987.	−1.0	0.7	0.4
10	4 960.	−0.1	1.7	0.3
11	3 223.	−0.4	2.2	0.3
12	1 808.	−0.1	2.6	0.1
13	759.	−0.1	3.1	0.1
14	139.	−0.1	3.6	0.0

[a] E_b (cm^{-1}) are the binding energies for the unperturbed potential. Δ (cm^{-1}) is the amount by which the vibrational levels are lowered. Case A (localized perturbation): $\Delta V = 5.5$ cm^{-1} at $R = 3.25$ a.u. $\cong R_2(8)$, 0.01 cm$^{-1} > \Delta V \to 0$ for $R \lesssim R_2(7) \cong 3.07$ a.u., and $R \gtrsim R_2(9) \cong 3.48$ a.u.; Case B: $\Delta V = -4$ cm^{-1} for $R \gtrsim R_2(8)$, $\Delta V = 0$ for $R < R_2(8)$; Case C $\Delta V = -4$ cm^{-1} for $0 < R \lesssim 0.9$ a.u. $\cong R_1(4)$.

radial wavefunctions in a truncated harmonic-oscillator basis set and determine the coefficients variationally. Their results with basis sets of up to 100 terms were somewhat less accurate than the numerical (C–C) results [$T_0(v, 0)$ in error by up to $\sim$6 cm^{-1}], as well as being significantly slower. Greenawalt and Dickinson[9] have extended their method using Morse-potential eigenfunctions as a basis set and achieved considerably greater success in terms of eigenvalue accuracy, with computation times comparable to the C–C method.

PART II

THE UTILIZATION OF POTENTIAL CURVES

6. SPECTROSCOPIC REASSIGNMENT AND GROUND-STATE DISSOCIATION ENERGY OF I_2

Quantitative and qualitative utilizations of the method of Chapter 3 point out the need for the reassignment discussed here. Mulliken[1] recently pointed out that the 0_g^+ state to which the levels in question are reassigned may in fact be $^3\Sigma_g^-(0^+)$, rather than $^3\Pi_{0g}^+$; however, he notes[1] that there are no good grounds for deciding between these two possibilities. Fortunately, this identification question does not affect the arguments presented below. This work is reprinted from the Journal of Chemical Physics, Volume 52, pp. 2678-82 (American Institute of Physics, New York, 1970).

FOOTNOTE

1. R. S. Mulliken, "Iodine Revisited", (1971, to be published). The author is very grateful to Professor Mulliken for making this manuscript available in advance of publication.

Reprinted from THE JOURNAL OF CHEMICAL PHYSICS, Vol. 52, No. 5, 2678–2682, 1 March 1970
Printed in U. S. A.

Spectroscopic Reassignment and Ground-State Dissociation Energy of Molecular Iodine*

ROBERT J. LEROY
Theoretical Chemistry Institute and Department of Chemistry, University of Wisconsin, Madison, Wisconsin 53706

(Received 3 September 1969)

Reanalyzing some early bandhead data for $I_2[B\ 0_u^+(^3\Pi)]$, an improved value of the ground-state dissociation energy is found to be $D_0 = 12\,440.9 \pm 1.1$ cm^{-1}, differing significantly from the previously accepted value of Verma, $12\,452.5 \pm 1.5$ cm^{-1}. This result implies that the final state of one of the uv resonance series reported by Verma must have a rotationless potential maximum some 13.1 ± 1.4 cm^{-1} high. It is further shown that the original electronic assignment of this state as ground-state $X\ 0_g^+(^1\Sigma)$ is implausible. A reassignment as $0_g^+(^3\Pi)$ is proposed, and the nature of the $0_g^+(^3\Pi)$ potential is considered.

I. INTRODUCTION

Verma observed[1] six series of uv resonance emission doublets which were excited by absorption of the 1830.4-Å iodine atomic line by molecules in five rotational levels of the $v'' = 0$ level[2] of the ground electronic state of I_2. This absorption corresponded to transitions into five resonant vibrational–rotational levels of an excited 0_u^+ electronic state, and the subsequent emission from these levels yielded the observed series. Verma concluded[1] that this emission always produced molecules in the ground electronic state. This is unquestionably true for those final levels to which he assigned vibrational quantum numbers $v'' \leq 84$. However, the separate set of levels at the convergence limit of the emission spectrum (Verma's $v'' = 98$–115) causes a strange flattening of the Birge–Sponer plot for the ground state. Furthermore, their sharp convergence-limit cutoff lies above a value of the ground-state dissociation energy obtained from other data, which implies that the state to which they belong has a potential maximum. This suggests that the present best value of the dissociation energy,[1] which is based on the position of this cutoff, is too large by an amount equal to the height of the barrier. The present paper presents a new value of the ground-state dissociation energy and proposes that the levels in question be reassigned to the $0_g^+(^3\Pi)$ state.

II. DISSOCIATION ENERGY OF GROUND STATE $I_2[X\ 0_g^+(^1\Sigma)]$

Two main approaches to the determination of the dissociation energy are considered. In the first, an

estimate for D_0 is obtained by subtracting the $^2P_{3/2}$–$^2P_{1/2}$ spin–orbit splitting of iodine atoms from the convergence limit of the $B\ 0_u^+(^3\Pi)$–$X\ 0_g^+(^1\Sigma)$ band spectrum.[3,4]

Brown[5] has reported bandhead measurements for levels $v'=48$–72 of the $B\ 0_u^+(^3\Pi)$ state. Careful extrapolation from these data places the B-state dissociation limit $20\,044.0\pm1.1$ cm^{-1} above the $v''=0$, $j''=0$ level of the ground state.[7,8] Subtracting from this the 7603.15-cm^{-1} $^2P_{1/2}$–$^2P_{3/2}$ spin–orbit splitting energy[9] yields $D_0=12\,440.9\pm1.1$ cm^{-1}.[10] This result corresponds to the $B=1$ state having 89 ± 1 vibrational levels.[8]

A second approach to D_0, that used by Verma,[1] is based on the sharp low-energy cutoff of the uv resonance series at the convergence limit. The electronic assignment of the lower state of this series is immaterial since it could only dissociate to yield two ground-state $^2P_{3/2}$ atoms. Furthermore, the original rotational assignment of this resonance series ($J_r=25$) is based on the rotational constants for the emitting levels and hence is valid independent of the electronic assignment of the final state. Utilizing the data in essentially the same manner as Verma[1] yields a D_0 estimate of $12\,452.4\pm1.8$ cm^{-1}.[11]

In general, the final electronic states of the two transitions considered above may have repulsive potential barriers as well as attractive wells. Therefore, the two estimates of D_0 are both upper bounds, being equal to the true D_0 plus the height of the appropriate barrier. Since the first value obtained is 11.5 ± 3 cm^{-1} smaller than the second, the state giving rise to the latter must have a rotationless ($J=0$) potential barrier at least 11.5 ± 3 cm^{-1} high.

The moderately long-range interaction of two ^2P ($^2P_{3/2}$ or $^2P_{1/2}$) iodine atoms may be expressed as[13]

$$V(R)=\frac{C_5}{R^5}+\frac{C_6}{R^6}+\frac{C_8}{R^8}+\frac{C_{10}}{R^{10}}+\cdots, \qquad (1)$$

where the first term arises from the first-order perturbation energy, and the next three terms from the second order. It may readily be shown that C_6, C_8, and C_{10} are negative (attractive) for all molecular states formed from two ground-state ($^2P_{3/2}$) atoms.[14] Furthermore, theoretical values of C_5 have been calculated for all the states formed on combining $^2P_{3/2}+{}^2P_{3/2}$ or $^2P_{3/2}+{}^2P_{1/2}$ atoms.[13,15] These values show which states are attractive and which are repulsive at the large distances at which the R^{-5} term dominates the interaction.

The theoretical C_5 for the $B\ 0_u^+(^3\Pi)$ state, which dissociates to $^2P_{3/2}+{}^2P_{1/2}$, is negative (attractive).[13,15] Furthermore, in Ref. 8 it is shown that the potential at the outer turning points of the highest observed B-state levels is dominated by this R^{-5} term. Therefore, the $B\ 0_u^+(^3\Pi)$ potential cannot have a barrier maximum, $D_0=12\,440.9\pm1.1$ cm^{-1} for the ground electronic state, and the state giving rise to the uv convergence-limit resonance series must have a potential barrier $\approx11.5\pm3$ cm^{-1} high.

III. Reassignment of the uv Resonance Series at the Convergence Limit

A. The Need for a Reassignment

The data considered for reassignment are the lines in the convergence limit portion of Verma's resonance series IVb, presented in his Table V.[1] He concluded that the lower state of this series was the ground electronic state. While this is unquestionably the case for the other five uv resonance series observed, it is shown below that this assignment is quite implausible for the series in question.

The theoretical C_5 for the ground $X\ 0_g^+(^1\Sigma)$ state of I_2 is zero[13,15]; hence, the moderately long-range forces are dominated by the attractive second-order perturbation terms (C_6, C_8, and C_{10}). Since the exchange forces are also attractive (as is evidenced by the deep potential well), this state cannot have a potential maximum. Therefore, the final state of the uv convergence-limit resonance series cannot be the ground state.

A more qualitative objection to the original assignment is based on the Franck–Condon accessibility of the final levels. Verma's Fig. 1(g)[1] shows that the emission into the 18 adjacent levels at the dissociation limit has roughly constant intensity. Therefore, it seems strange that none of the 13 levels immediately below his $v''=98$ would be sufficiently accessible from the upper state to allow measurable emission. The observed behavior suggests that Verma's $v''=98$ is actually the lowest vibrational level of some excited electronic state.

A final argument against the $X\ 0_g^+(^1\Sigma)$ assignment is based on the expected behavior of a Birge–Sponer plot for vibrational levels lying near the dissociation limit. It has been shown that when the outer branch of the potential in this region is a short sum of attractive inverse-power terms, the plot should have positive (upward) curvature.[8,16] For the ground state of I_2 this positive curvature is observed above $v''=73$ and increases from there up to $v''=82$ (the highest well-known level below the convergence-limit resonance series), where it equals 0.060 cm^{-1}.[12] For this state, the theory suggests[8] that above the point of inflection at $v''=73$ the curvature $[d^3G(v)/dv^3]$ should increase, perhaps pass through a slight maximum, and asymptotically approach a constant value of $94/(C_6)^{1/2}$ cm^{-1} (where C_6 is in cm^{-1} Å^6).[17] For a reasonable C_6 of $3.0\times10^{+6}$ cm^{-1} Å^6, this asymptotic curvature would be 0.054 cm^{-1}. On the other hand, the level spacings in the convergence limit resonance series show negligible curvature ($\lesssim0.001$ cm^{-1}; see

TABLE I. $I_2[0_g^+(^3\Pi)]$ vibrational energies (in cm^{-1}) expressed relative to the $v''=0, J''=0$ level of the ground state.

v'	E	v'	E	v'	E
0	12 362.4	6	12 413.6	12	12 444.0
1	12 372.5	7	12 420.1	13	12 447.2
2	12 381.9	8	12 426.0	14	12 449.7
3	12 390.5	9	12 431.4	15	12 451.5
4	12 399.0	10	12 436.1	16	12 452.9
5	12 406.6	11	12 440.4	17	12 453.7

Fig. 2).[18] This strengthens the argument that these levels cannot belong to the ground state.

Theory shows[8] that vibrational levels lying near the dissociation limit, which yield a linear Birge–Sponer plot, correspond to a long-range potential which is either exponential or is dominated by an effective inverse-power term R^{-n} with n being large ($n \gg 10$).[19] This high effective power is qualitatively the type of behavior one would expect on the inner side of a potential barrier arising from a sum of attractive and repulsive inverse power terms.

B. The Reassignment

The final state to which the levels in question belong must have a potential barrier of height $\approx 11.5 \pm 3$ cm^{-1} as well as an attractive well, and must correlate with two ground-state $^2P_{3/2}$ atoms. Nine states in addition to the ground state correlate with two ground-state atoms; of these, three are nondegenerate and six are doubly Ω degenerate.[20] The nature of the emission and absorption spectrum of Verma's upper state clearly indicates that it is 0_u^+.[21] Therefore, the $\Delta\Omega = 0, \pm 1$ electronic selection rule immediately removes two possible assignments. In addition, the gerade–ungerade symmetry selection rules for electric dipole[23] transitions ($g \leftrightarrow u$, $g \leftrightarrow g$, $u \leftrightarrow u$)[24] leave the $0_g^+(^3\Pi)$ and $1g(^3\Pi)$ states as the only electronically allowed assignments.

The rotational selection rules for transitions from a 0_u^+ state into singly degenerate 0_g^+ or doubly

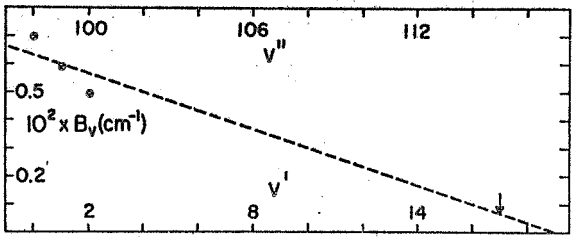

FIG. 1. Rotational constants for final state of convergence-limit resonance series. The v'' numbering corresponds to Verma's $X\ 0_g^+(^1\Sigma)$ assignment[1] and v' numbering to the present $0_g^+(^3\Pi)$ assignment. ◎ are Verma's experimental values, and the arrow denotes the highest observed level.

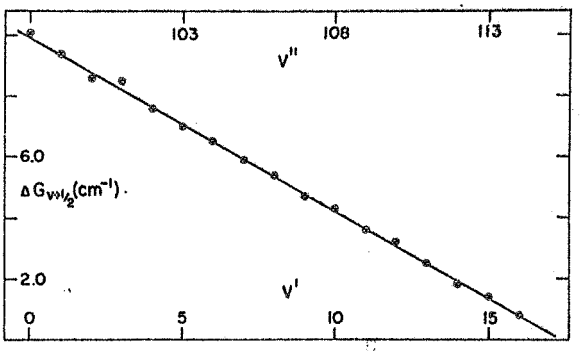

FIG. 2. Vibrational spacings of levels in convergence-limit resonance series. v'' represents the old $X\ 0_g^+(^1\Sigma)$ vibrational numbering[1] and v' the proposed $0_g^+(^3\Pi)$ numbering. The curve is generated from expression (2).

Ω-degenerate $1g$ states allow $\Delta J = \pm 1$ and $\Delta J = 0, \pm 1$ transitions, respectively. The first gives rise to doublet and the second to triplet structure. While transitions into the separate branches of the Ω doublet ($1g$) would correspond to $\Delta J = \pm 1$ and $\Delta J = 0$, respectively, the intensity of the Q branch ($\Delta J = 0$) is theoretically twice that of the P or R branches, so this spectrum would be observed as either the full triplet or as a singlet.[24] Verma was able to resolve the structure of the emission into the three lowest levels of the convergence-limit series, and it is clearly doublet in nature. Therefore, the only completely allowed reas-

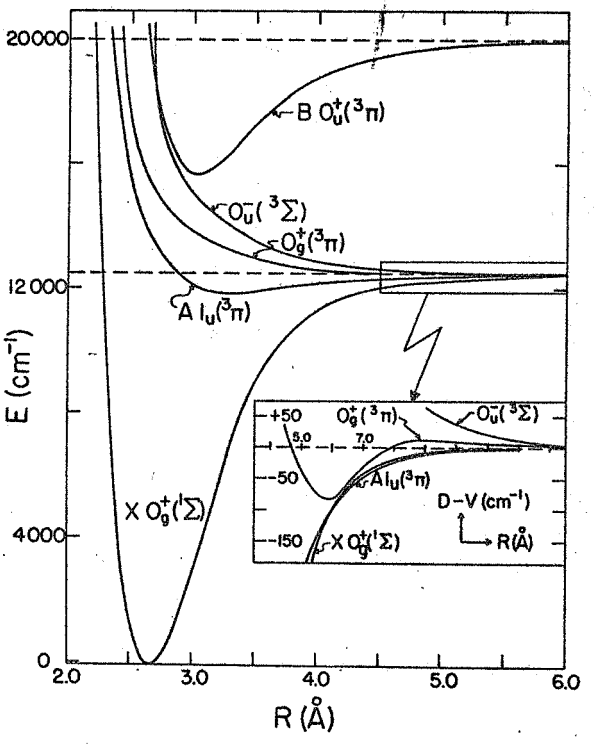

FIG. 3. Schematic potential curves for $0_g^+(^3\Pi)$ and some neighboring states. The zero of energy is the $v''=0$, $J''=0$ level of the ground electronic state.

signment of the levels in question is to the $0_g^+(^3\Pi)$ state.

The theoretical long-range R^{-5} term for the $0_g^+(^3\Pi)$ state is repulsive,[13,15] while its R^{-6}, R^{-8}, and R^{-10} terms are attractive[14]; thus it seems plausible that it will have an attractive well bounded by a potential maximum. On the other hand, the theoretical C_5 for this state (2.3×10^5 cm^{-1} Å^5)[13,15] is too small to yield a 11.5 ± 3 cm^{-1} barrier at large R, either alone or when the competing attractive R^{-6} term is taken into account.[25]

Although the origin of the potential barrier is somewhat uncertain, the reassignment of the uv convergence-limit resonance series to the $0_g^+(^3\Pi)$ state still seems much more likely than its original assignment as $X\ 0_g^+(^1\Sigma)$. The validity of this reassignment will now be assumed and the concomitant properties of the $0_g^+(^3\Pi)$ state will be considered.

IV. THE $0_g^+(^3\Pi)$ STATE

This state was previously observed by Venkateswarlu[22] in diffuse bands arising as emission from discrete levels of the previously mentioned highly excited 0_u^+ state. Venkateswarlu concluded that its potential was repulsive in the neighborhood of the minimum of the ground-state potential, and that it lay below and to the left of the $B\ 0_u^+(^3\Pi)$ curve.[22] This same conclusion was also inferred from considerations involving the quenching of B-state fluorescence.[26]

Due to this intermediate-range repulsiveness of the $0_g^+(^3\Pi)$ curve, its potential minimum must lie at reasonably large R, and the well is unlikely to be very deep. The noncrossing rule which forbids it from crossing the ground-state $X\ 0_g^+(^1\Sigma)$ curve also implies that the well must be quite shallow. In view of this and of the roughly constant intensity of the emission into the observed levels, it seems probable that the lowest observed level is $v'=0$. If this numbering is incorrect, it seems unlikely that it would be more than one or two units too small.

The energies and assumed vibrational assignments of the convergence limit levels are given in Table I. The small rotational energy contributions to the observed lines were removed after extrapolating beyond the three experimental $B_{v'}$ values in the manner shown in Fig. 1. Utilizing Fig. 1 to obtain $B_{v'}$ values, rather than the approach of Ref. 1, places the convergence limit of this series at $12\,454.0\pm0.3$ cm^{-1} (1.6 cm^{-1} higher than the previous estimate). This yields 13.1 ± 1.4 cm^{-1} as a better estimate of the height of the potential maximum. Six of the 18 observed levels are metastable (for $J'=0$), being bound only by this potential barrier.

Using the above vibrational assignment, the vibrational energies may be represented within a standard error of ±0.08 cm^{-1} by

$$E(v')=12\,357.3+10.522(v'+\tfrac{1}{2})-0.2866(v'+\tfrac{1}{2})^2, \quad (2)$$

where the energy zero is the $v''=0$, $J''=0$ level of the ground state. This shows that this state has a potential well at least 83.6 ± 1.1 cm^{-1} deep (relative to the dissociation limit, not the potential maximum). Furthermore, the observed rotational splittings would place the potential minimum at 6.0 ± 0.6 Å. The experimental vibrational spacings are compared with those calculated from expression (2) in Fig. 2. The curve suggests that there may exist one more, as yet unobserved, quasibound state.

The potential curve for $0_g^+(^3\Pi)$ is shown schematically in Fig. 3, together with curves for a number of neighboring states. The ground-state potential up to 11 933 cm^{-1} and the $B\ 0_u^+(^3\Pi)$-state potential up to 19 705 cm^{-1} are RKR potentials (taken from Ref. 12, and Refs. 4 and 6, respectively). The $0_u^-(^3\Sigma)$ curve was taken from Ref. 27 and the $A\ 1u(^3\Pi)$ curve is based on the conclusions of Brown.[28] At large distances the $A\ 1u(^3\Pi)$ and $X\ 0_g^+(^1\Sigma)$ curves must cross, since the latter dies off as R^{-6} and the former as R^{-5}. Furthermore, the $A\ 1u(^3\Pi)$ curve may also cut across the $0_g^+(^3\Pi)$ well. The theoretical C_5 for $0_u^-(^3\Sigma)$ is a third larger than that for $0_g^+(^3\Pi)$,[13,15] so these curves should not cross at long range.

V. CONCLUSIONS

It has been shown that, contrary to the original assignment, a portion of the uv resonance spectrum of I_2 does not correspond to emission into the ground electronic state. The most probable reassignment for the levels in question was found to be $0_g^+(^3\Pi)$. This state appears to be an example of a van der Waals[29] molecule (bound only by the moderately long-range dispersion forces[30]) which has a potential barrier. An improved estimate of the ground-state dissociation energy is $D_0=12\,440.9\pm1.1$ cm^{-1}.

If the present reassignment is correct, Verma's uv spectrum[1] is the first observation of the discrete levels of the $0_g^+(^3\Pi)$ state. These levels clearly cannot be observed in absorption from the ground state because of the $g\nleftrightarrow g$ symmetry selection rule. However, they may be observable in near ir fluorescence (at around 1.4 μ) from some of the higher levels of the $B\ 0_u^+(^3\Pi)$ state. One restriction to this type of measurement is that the fluorescing state cannot have a very high rotational quantum number, as in this case the centrifugal potential would bury the shallow $0_g^+(^3\Pi)$ well. However, if appropriate $B\ 0_u^+(^3\Pi)$ levels can be excited, these $0_g^+(^3\Pi)$ levels may be observed together with neighboring $X\ 0_g^+(^1\Sigma)$ levels, giving direct confirmation of the proposed reassignment.

ACKNOWLEDGMENTS

I am pleased to acknowledge pertinent discussions with Dr. A. S. Dickinson; the comments, encouragement, and support of Professor R. B. Bernstein; and

helpful correspondence with Professor J. I. Steinfeld. I am also deeply indebted to Professor R. D. Verma for some very telling criticisms of an early version of this paper.

* Research supported by National Science Foundation Grant GP-7409 and National Aeronautics and Space Administration Grant NGL-50-002-001.

[1] R. D. Verma, J. Chem. Phys. **32**, 738 (1960).

[2] Throughout, double primed quantities will refer to the ground electronic state and single primed quantities to an excited electronic state.

[3] This step is necessary because $B\ 0_u^+(^3\Pi)$ dissociates to $^2P_{3/2}+^2P_{1/2}$, while the ground X state dissociates to $^2P_{3/2}+^2P_{3/2}$.

[4] In their recent measurements of the $B\ 0_u^+(^3\Pi)\leftarrow X\ ^1\Sigma_g^+$ absorption spectrum, J. I. Steinfield, J. D. Campbell, and N. A. Weiss [J. Mol. Spectry. **29**, 204 (1969)] reported long P and R branches for the 43–0 and 49–1 bands. However, the energy thus obtained for level $v'=49$ is 11 cm^{-1} smaller than that reported by Brown,[5] and 8.5 cm^{-1} smaller than the earlier value of R. Mecke [Ann. Phys. **71**, 104 (1923)]. It appears [J. I. Steinfeld concurs in this conclusion (private communication, 1969)] that Steinfeld *et al.*'s 49–1 band should be reassigned as 57–2 ,since this assumption yields a $v'=57$ energy which is only 2.6 cm^{-1} smaller than Brown's[5] value and 0.4 cm^{-1} larger than Mecke's.

[5] W. G. Brown, Phys. Rev. **38**, 709 (1931). The accepted vibrational numbering for the B state has recently been revised,[6] so the numbering used by Brown should be decreased by one.

[6] J. I. Steinfeld, R. N. Zare, L. Jones, M. Lesk, and W. Klemperer, J. Chem. Phys. **42**, 25 (1965); R. L. Brown and T. C. James, *ibid.* 42, 33 (1965).

[7] The extrapolation procedure is based on a new method for determining long-range forces from vibrational spacings, which is reported elsewhere.[8]

[8] R. J. LeRoy and R. B. Bernstein, Wisc. Theoret. Chem. Inst. Tech. Rept. WIS-TCI-362 (1969)+J. Chem. Phys. 52,3869 (1970). The extrapolation to the dissociation limit of the B state is discussed in more detail by the same authors in Chem. Phys. Letters 5, 42 (1970), and in Wisc. Theoret. Chem. Inst. Tech. Rept. WIS-TCI-369 (1970), J. Mol. Spectry. 37 (1971).

Section 3.1

Appendix A.

[9] C. Moore, Natl. Bur. Std. (U.S.), Circ. **467**, Vol. 3, 105 (1958). The results quoted are based on the data of C. C. Kiess and C. H. Corliss [J. Res. Natl. Bur. Std. **63A**, 1 (1959)].

[10] This value agrees fairly well with Brown's[5] 12439±8 cm^{-1}, because although his extrapolation to the dissociation limit is ≈7 cm^{-1} too short, his value of the spin–orbit splitting (7598 cm^{-1}) was 5 cm^{-1} too small.

[11] The slight difference with Verma's[1] 12 452.5±1.5 cm^{-1} arises from the use of a slightly different frequency for the line exciting the resonance series (see Ref. 12), and the use of the $J=26$ rotational energy rather than $J=24$.

[12] R. J. LeRoy, J. Chem. Phys. **52**, 2683 (1970), following paper; see Section 2.2.

[13] T. Y. Chang, Rev. Mod. Phys. **39**, 911 (1967).

[14] J. O. Hirschfelder, C. F. Curtiss, and R. B. Bird, *Molecular Theory of Gases and Liquids* (John Wiley & Sons, Inc., New York, 1954). The expression for the second-order perturbation energy derived in Sec. 13.3b is negative for all states formed from two ground-state atoms.

[15] J. K. Knipp, Phys. Rev. **53**, 734 (1938).

[16] This was noted previously by H. Harrison and R. B. Bernstein [J. Chem. Phys. **38**, 2135 (1963)] for the cases of Lennard-Jones (12,6) and exp(α,6) potentials, both of which have R^{-6} tails.

[17] This is true because the long-range potential for the ground state is described by expression (1) with $C_5=0.0$[13,15] and C_6, C_8, and C_{10} all attractive (negative).[14]

[18] A third-order least-squares fit to these energies (see Table I) had the same standard error as a second-order fit (0.08 cm^{-1}) and yielded a curvature of only 0.0012 cm^{-1}. A curvature rate of 0.054 cm^{-1} over the 18 observed levels would add 7.8 cm^{-1} to $dG/dv[\Delta G(v)]$ for the highest observed level over the value obtained by linearly extrapolating from the lowest dG/dv values. For a curvature of 0.0012 cm^{-1}, this effect is reduced to 0.17 cm^{-1}.

[19] The potential is assumed to be fitted to an expression of the form A/R^n+B.

[20] R. S. Mulliken, Phys. Rev. **36**, 699 (1930). Case c coupling is assumed.

[21] This upper state has been previously observed in absorption by H. Cordes [Z. Physik **97**, 603 (1935)], and in emission by P. Venkateswarlu.[22] This electronic assignment was not questioned in the later analyses by L. Mathieson and A. L. G. Rees [J. Chem. Phys. **25**, 753 (1956)] and by A. Nobs and K. Wieland [Helv. Phys. Acta **39**, 564 (1966)].

[22] P. Venkateswarlu, Proc. Indian Acad. Sci. **24A**, 480 (1946). The author would like to thank R. D. Verma for bringing this reference to his attention.

[23] The intensity of the observed emission indicates that the transitions could only be electric dipole.

[24] G. Herzberg, *Spectra of Diatomic Molecules* (D. Van Nostrand Co., Inc., Toronto, Canada, 1950), 2nd ed.

[25] F. E. Cummings has developed a new method of calculating R^{-6} terms, and applied it to the different states of I_2 correlating with two ground-state atoms. This work was presented at the 24th Symposium on Molecular Structure and Spectroscopy, Ohio State University, Columbus, Ohio, September 1969; the present author is grateful to Dr. Cummings for making his results available in advance.

[26] J. E. Selwyn and J. I. Steinfeld, Chem. Phys. Letters **4**, 217 (1969).

[27] E. O. Degenkolb, J. I. Steinfeld, E. Wasserman, and W. Klemperer, J. Chem. Phys. **51**, 615 (1969).

[28] W. G. Brown, Phys. Rev. **38**, 1187 (1931).

[29] See Ref. 24, p. 377.

[30] This seems rather likely since the $0_g^+(^3\Pi)$ potential well is quite shallow, and its $R_{EQ}\approx 6$ Å is considerably larger than the 2.66 Å for the ground $X\ 0_g^+(^1\Sigma)$ state,[12] 3.03 Å for the $B\ 0_u^+(^3\Pi)$ state,[4] and ≈3.2 Å for the $A\ 1u(^3\Pi)$ state.[28]

see Section 3.2.

7. SHAPE RESONANCES AND ROTATIONALLY PREDISSOCIATING LEVELS: THE ATOMIC COLLISION TIME-DELAY FUNCTIONS AND QUASIBOUND LEVEL PROPERTIES OF H_2 ($X\ ^1\Sigma_g^+$)

This chapter is reprinted from University of Wisconsin Theoretical Chemistry Institute Report WIS-TCI-427 (1971), which will be submitted for publication.

SHAPE RESONANCES AND ROTATIONALLY PREDISSOCIATING LEVELS: THE ATOMIC COLLISION TIME-DELAY FUNCTIONS AND QUASIBOUND LEVEL PROPERTIES OF $H_2(X\ ^1\Sigma_g^+)$*

by

Robert J. Le Roy† and Richard B. Bernstein

Theoretical Chemistry Institute and Department of Chemistry

University of Wisconsin, Madison, Wisconsin 53706

ABSTRACT

The energy dependence of the collisional time-delay function has been computed for H(1S) atoms interacting via the ab initio $H_2(X\ ^1\Sigma_g^+)$ potential. Peaks in this function determine the scattering resonance energies E_r and widths Γ, and the lifetimes for each of the corresponding quasibound vibrational-rotational levels. Small differences are found between these E_r and Γ, and the values obtained by a "maximum internal amplitude" approach (intended to characterize the spectroscopically observable predissociating levels). Approximate procedures for rapid, accurate numerical evaluation of E_r are appraised; a new outer-boundary-condition criterion for resonances leads to the best agreement with the

- - - - - - - - - - - - - - - - - - -

*Work supported by National Science Foundation Grant GB-16665 and National Aeronautics and Space Administration Grant NGL 50-002-001.

†National Research Council of Canada Postgraduate Scholarship holder, 1969-71. Present address: Department of Physics, University of Toronto, Toronto 181, Ontario, Canada.

exact results. Also, a primitive WKB procedure yields Γ's of usable accuracy. For ground-state H_2, HD and D_2, the onset of line broadening due to centrifugal barrier penetration is found to occur at energies some hundreds of cm^{-1} below the locus of barrier maxima. The predissociation method of estimating long-range interatomic forces therefore cannot be expected to yield valid results for hydridic diatomics.

I. INTRODUCTION

The influence of long-lived quasibound states, or orbiting resonances, on virial and transport properties of gases and on chemical reaction rates is now widely recognized.[1-10] While any pair of colliding atoms may be considered to be temporarily bound with some sort of characteristic lifetime,[11,12] what is considered here is the purely quantal phenomenon of the metastable levels arising from the existence of both a minimum and a maximum in the effective interaction potential. These levels qualitatively correspond to discrete vibrational-rotational diatomic levels which would be truly bound by the barrier if it were impenetrable.

Although orbiting (or "shape") resonances are, in principle, observable in molecular beam scattering experiments,[13-17] the beam technology has not quite reached the point at which the required resolution is obtainable.[18] On the other hand, under the pseudonym of "rotationally-predissociating levels", spectroscopists have been studying them for more than 40 years.[19,20] The structure seen in these experiments is a manifestation of the "pseudo-quantization" of the continuum wave functions by the potential barrier. In the present paper the properties characterizing the observables in the two types of experiments are examined and small systematic differences are noted. The relation between the limiting curve of dissociation (LCD), corresponding to the breaking-off of rotational series due to rotational predissociation, and the locus of the centrifugal barrier maxima (LBM) is also examined.

A number of different procedures for determining the resonance energies and widths for a given potential are examined; rapid and accurate approximate algorithms are presented. All results are illustrated with calculations for the ground ($X\ ^1\Sigma_g^+$) state of H_2 and its isotopes, using the ab initio relativistic-adiabatic potential of Kołos and Wolniewicz.[21,22] The influence of small potential corrections is also considered.

II. RESONANCE ENERGIES AND WIDTHS VIA SCATTERING THEORY: THE TIME-DELAY FUNCTION

A. General

The manifestation of a resonance in the energy dependence of an atomic scattering cross section arises from a rapid growth (essentially by π) of the phase shift $\delta_J(E)$ for a partial wave with angular momentum quantum number J, with increasing collision energy E.[7-9,13,23,24] However, it is well known[13] that this structure can exhibit a variety of shapes, depending on the so-called background phase shift. Thus, it may be difficult to characterize this observable cross-section structure by a precise resonance energy E_r and width Γ. On the other hand, a resonance can always be characterized by the functionality of the appropriate partial-wave phase shifts. Within the Breit-Wigner parameterization,[25] in the neighborhood of an isolated resonance:

$$\delta_J(E) = \beta_J(E) + \arctan\left(\frac{\Gamma/2}{E_r - E}\right) \quad , \tag{1}$$

where $\beta_J(E)$ is the background phase shift. If $\beta_J(E) = 0$, the resonance width Γ is the full width at half maximum (FWHM) of the resonance peak in the cross section. For energies well below the maximum in the effective potential, the energy dependence of the background phase is negligible,[7-9] and the phase shift derivative

$$\frac{d}{dE}\left[\delta_J(E)\right] = \frac{\Gamma/2}{(E_r - E)^2 + (\Gamma/2)^2} \tag{2}$$

attains its maximum (namely $2/\Gamma$) at $E = E_r$. However, for the broad resonances lying near (above or below) the barrier maximum, $\beta_J(E)$ has distinct negative curvature[7-9] which will tend to shift the maxima of $d\delta_J(E)/dE$ to energies somewhat lower than E_r. On the other hand, the division of the total phase shift into a resonant and a background contribution (i.e., fitting to Eq. (1)), does not appear to be particularly fruitful.[26] In the present work, the more conventional[8,16,30] scattering-theory definitions will be used, that is, taking the resonance positions as the points of inflection of $\delta_J(E)$ (i.e., the maxima of $d\delta_J(E)/dE$), and the widths as

$$\Gamma = 2/[d\delta_J(E)/dE]_{max} \tag{3}$$

B. The Collisional Time-Delay Function

In 1960 Smith[12] elaborated on the original Eisenbud-Wigner[11] concept by defining the collisional time-delay function $\tau_d(E,J)$ [in Smith's[1,4,12] notation $Q_{\ell\ell}(E)$ or $Q(E,L)$] in terms of an integral of the time-independent wave function. He then related it to the phase shift derivatives by proving the identity

$$\tau_d(E,J) = 2\hbar \frac{d\delta_J(E)}{dE} \tag{4}$$

Scattering-theory resonance energies for the J-th partial wave therefore correspond to the energies at which maxima occur in $\tau_d(E,J)$, while the widths [from Eq. (3)] are

$$\Gamma = 4\,\hbar/[\tau_d(E,J)]_{max} \quad . \tag{5}$$

It should be noted that Eqs. (4-5) are identities; also $[\tau_d(E,J)]_{max}$ is not the predissociation lifetime τ of the quasibound state. The latter may be shown[31] to be

$$\tau = \frac{1}{4}\,[\tau_d(E,J)]_{max} = \hbar/\Gamma \quad .$$

The method used here for computing $\tau_d(E,J)$ from Smith's[12] formal expression is described in Appendix A.

The nature of the time-delay function is illustrated in Figs. 1 and 2 for several partial waves for H + H and D + D collisions governed by the $(X\ ^1\Sigma_g^+)$ ground-state molecular potential. Contrary to the suggestion of Fig. 5 in Ref. (4), $\tau_d(E,J)$ shows no structure at energies significantly above the potential maximum (this was found to be the case for H + H, H + D and D + D, for all J). As is inferred from the phase shift curves in Refs. (7-9), at sufficiently high energies $\tau_d(E,J)$ eventually becomes negative as the influence of the repulsive core of the potential becomes dominant; it then passes through a very broad minimum and asymptotically approaches zero from below. This behavior is seen in Fig.3 (solid curves) for several low partial waves of H + H. There is apparently no localized structure in $\tau_d(E,J)$ associated with the barrier maximum; the only noticeable effect is the change in the sign of the slope of the non-resonant background time-delay (see Figs. 1 and 2). However, for low J this occurs at energies

below the barrier maximum (see the J = 4 curve in Fig. 3), and in any case it is usually obscured by the structure due to the highest resonance.

It is desirable to examine the appropriateness of the Breit-Wigner parametrization, implicit to Eqs. (1)-(3) and (5), for broad resonances near the barrier maximum where the curvature of the background phase is not negligible.[32] It implies that the full width at half maximum (FWHM) of a resonance peak in $\tau_d(E,J)$ is equal to the Γ defined by Eq. (5). This question is examined in Table I for broad H + H resonances lying close to the barrier maxima for the indicated J's; the penultimate column tabulates the FWHM of the $\tau_d(E,J)$ peaks, while the preceding one lists the widths given by Eq. (5). The agreement is good, especially for the narrower resonances, which indicates that the simple parametrization of Eq. (1), with $\beta_J(E) \equiv 0$, is at least adequate for resonances narrower than ca. 100 cm^{-1}.

III. SPECTROSCOPIC RESONANCE POSITIONS AND WIDTHS: THE INTERNAL-AMPLITUDE FUNCTION

A. Qualitative Discussion

A quasibound level may be observed spectroscopically as a peak in the continuum absorption or emission for transitions between it and a discrete bound state. The transition probability varies as

$$\rho(\nu,E)\left|\int_0^\infty \Psi_d(R)\, M_e(R)\, \Psi_{E,J}(R)\, dR\right|^2 . \qquad (6)$$

Here ν is the frequency of the emitted/absorbed light, $\Psi_d(R)$ the radial wave function of the discrete state, $M_e(R)$ the electronic transition moment function, and $\Psi_{E,J}(R)$ the continuum quasibound-level wave function with total orbital angular momentum quantum number J, at an energy E above the diatomic dissociation limit. The function $\rho(\nu,E)$ factors into the density of continuum levels at energy E, times unity for absorption or ν^3 for emission. For $h\nu >> \Gamma$ (the usual situation) this frequency factor does not affect the intensity distribution near a resonance, and hence can be ignored. Also, the asymptotic wave function normalization will be chosen such that the density of states is constant,[33] completely removing the $\rho(\nu,E)$ term from the problem. This normalization is

$$\Psi_{E,J}(R) \sim A\, k^{-\frac{1}{2}} \left\{\sin(kR + \delta_J(E) - J\pi/2)\right\} \quad , \qquad (7)$$

where A is a constant and $k = \sqrt{2\mu E/\hbar^2}$. Observable spectroscopic structure arises because the amplitude of $\Psi_{E,J}(R)$ behind (at smaller R than) the potential barrier, peaks sharply in the neighborhood of a resonance. At the same time, despite the drastic change in the internal amplitude, the radial positions of the wave function nodes lying behind the barrier change only very slightly across the width of the resonance.[34] This suggests that the continuum wave function behind the barrier and near a resonance may be factored into a nearly energy-independent radial function, and an energy-dependent amplitude:

$$\Psi_{E,J}(R) = IA(E,J) \times \phi_J(R) \quad , \tag{8}$$

Resonance structure in the absorption/emission intensity thus depends only on IA(E,J); this "internal amplitude" function is examined below and its behavior compared to that of $\tau_d(E,J)$.

B. Semiclassical Treatment of Orbiting Resonances

Before proceeding with the fully quantal computational investigation, it is instructive to examine the implications of a semiclassical analysis. The best semiclassical treatments of orbiting resonances start by approximating the potential barrier by a simple model function (e.g., an inverted parabola) for which the exact wave functions are known.[35-37] They next define the semiclassical wave function over the potential well behind the barrier:

$$\Psi_{E,J}(R) = \left(\frac{IA(E,J)}{P_J(R)}\right)^{\frac{1}{2}} \cos\left(\int_{R_1(E)}^{R} P_J(y)\, dy - \frac{\pi}{4}\right) \quad , \tag{9}$$

where

$$P_J(R) = \left\{\frac{2\mu}{\hbar^2}\left[E - V(R) - \frac{(J+\frac{1}{2})^2}{R^2}\right]\right\}^{\frac{1}{2}} \quad ,$$

and $R_1(E)$ is the innermost classical turning point at the energy E. Then the exact solutions for the model barrier are used to connect Eq. (9) to the solution outside the barrier at asymptotically large R:

$$\Psi_{E,J}(R) \sim \left(\frac{IA(E,J)}{P_J(\infty)}\right)^{\frac{1}{2}} \left\{ f(E) \sin\left(P_J(\infty)R - [J+\tfrac{1}{2}]\,\frac{\pi}{2}\right) + g(E) \cos\left(P_J(\infty)R - [J+\tfrac{1}{2}]\,\frac{\pi}{2}\right) \right\} , \tag{10}$$

where f(E) and g(E) are complicated functions of the energy and the properties of the model barrier. Casting Eq. (10) into the semiclassical form equivalent to Eq. (7) yields

$$IA(E,J) = [f^2(E) + g^2(E)]^{-1} , \tag{11}$$

and

$$\delta_J(E) = \arctan [g(E)/f(E)] \tag{12}$$

Substituting Eq. (12) into Eq. (4) yields

$$\tau_d(E,J) = 2\hbar\, [f(E)\, g'(E) - g(E)\, f'(E)]\, [f^2(E) + g^2(E)]^{-1} , \tag{13}$$

where primes denote differentiation with respect to E. Comparison of Eqs. (11) and (13) suggests the origin of the coincidence previously noticed between the scattering-theory resonance positions and the structure in the internal amplitude function (and thus in the optical transition probability).[7,27,30] However, the residual energy dependence of the middle term in Eq. (13) will cause a "skewing" of the resonance peaks of $\tau_d(E,J)$ relative to those of the IA(E,J) function, which may be sufficient to cause a significant difference between their respective maxima. This question is examined below using exact numerically calculated wave functions for ground-state H_2.

C. Resonance Behavior of the Internal-Amplitude Function

Buckingham and Fox[7] noted that the internal amplitude passes through a maximum at resonance, and both Allison[27] and Jackson and Wyatt[30] suggested quantitative criteria for locating resonances, based on this effect. In Ref. (27) the resonance energy was taken as that corresponding to the minimum in the asymptotic normalization of the wave functions obtained on numerically integrating from "constant initial conditions" at the inner boundary (where $R \to 0$). Because of the uncertainty inherent in the definition of this constant initial condition, in Ref. (30) the resonance energy was located at the maximum in the "ratio of the maximum amplitude inside the centrifugal barrier over the amplitude at large internuclear distances". However, both these approaches neglect the additional $E^{-\frac{1}{4}}$ energy dependence of the asymptotic normalization (see Eq. (7)), which can be fairly important for broad low-lying resonances.[38]

In the present work, exact numerical continuum wave functions were calculated and given the asymptotic normalization appropriate to a constant density of states (see Eq. (7)). Then quadratures were carried out from the origin to $R^{(n)}(E)$, the n^{th} node of $\Psi_{E,J}(R)$ lying inside the potential barrier, and a conveniently scaled amplitude function defined as

$$IA^{(n)}(E,J) = \int_0^{R^{(n)}(E)} |\Psi_{E,J}(R)|^2 \, dR \Big/ [R^{(n)}(E) - R_1(E)], \qquad (14)$$

where (as in Eq. (9)) $R_1(E)$ is the innermost classical turning point. In Figs. 3 and 4 the internal amplitude functions (right ordinate scale) defined by Eq. (14) for n = 1 (upper dashed curves) and n = 4 (lower dashed curves) are compared to the $\tau_d(E,J)$ functions (solid curves, left ordinate scale) for several J values for ground-state H_2. The IA(E,J) values in Figs. 3 and 4 have units [cm] and correspond to the constant A in Eq. (7) being $A = (4 \mu c a_o/\hbar)^{\frac{1}{2}}$, where a_o is the Bohr radius. While the absolute value of $IA^{(n)}(E,J)$ depends on n, the functional dependence on E is virtually independent of n for $R^{(n)}(E) < R_{max}(J)$, where $R_{max}(J)$ is the position of the potential barrier maximum.[39]

For the broad H_2 resonances closest to the barrier maxima the resonance positions defined by the maxima in $\tau_d(E,J)$ and IA(E,J) are compared in Table I (columns 3 and 4). The FWHM of the IA(E,J) peaks (last column) are also compared there to FWHM(τ_d), and to the widths predicted by Eq. (5). It is evident that the IA(max) criterion always places the resonances at slightly higher energies than does τ_d(max), the differences being about 5% of the widths Γ.[40] Also, though the IA(E,J) peaks are skewed to higher energy relative to the more symmetrical $\tau_d(E,J)$ maxima, the FWHM of the two functions are still in good accord with each other, and with the widths yielded by Eq. (5). Only for the very broad resonances lying well above the barrier or at low J and E does the relative magnitude of the non-resonance background significantly alter this conclusion. Examples of this are the v = 14,

J = 6 and 7 resonances in Fig. 3, and the v = 7, J = 25 resonances in Fig. 4. However, these cases are relatively unimportant, as the structure is too diffuse to be spectroscopically observable and the collision delay time too small to be of physical interest.

The fact that the internal-amplitude criterion places resonances at energies higher than those of the maxima in $\tau_d(E,J)$ was previously noted in Ref. (27) for one particular quasibound level of H_2 (v = 14, J = 5). It is seen here that this is probably true for all resonances, and that the magnitude of the displacement is proportional to the resonance width. Thus, spectroscopic measurements should place quasibound levels at slightly higher energies than yielded by the time-delay (or phase shift) analysis. However, due to the complicating effect of the background phase[13] the differences would probably be unobservable in a comparison with possible molecular beam cross-section measurements.

An effect which may distort the spectroscopic implications of the IA(E,J) analysis arises from the fact that the separation of variables in Eq. (8) is only approximate, particularly for broad low-energy resonances. This means that the residual dependence on E of the nodal structure of the continuum wave function (i.e., of $\phi_J(R)$ in Eq. (8)) will tend to skew the transition probability of expression (6) relative to the IA(E,J) peak. Of course the direction and magnitude will depend on the particular discrete state ($\Psi_d(R)$ in expression (6)) connected to the resonance by the transition. However, if this

skewing is steep enough there may be a significant shift of the transition probability peak away from IA(max). Furthermore, if this displacement is a significant fraction of Γ, it could also result in a considerable narrowing of the spectral line relative to the FWHM(IA).[41]

IV. ACCURACY OF PRESENT RESONANCE ENERGIES AND WIDTHS FOR GROUND-STATE MOLECULAR HYDROGEN

The Kołos-Wolniewicz (KW) potential[21,22] for ground-state H_2 was the first ab initio potential to achieve "spectroscopic accuracy", yielding a better dissociation energy than the experimental value then available.[42,43] However, analysis of the vibrational level spectrum indicated that even after non-adiabatic effects were taken into account, this potential still required small corrections at moderately long range.[44] One indication of this is the fact that the $v = 14$, $J = 4$ H_2 resonance predicted from the KW potential lies $3.8\ cm^{-1}$ above the

dissociation limit, while experiment shows it to be bound by 0.8 (± 0.5) cm^{-1}.[45] This particular error is significant, since it implies that this quasibound level should not have been utilized in the calculation of the termolecular recombination rate for atomic hydrogen (see Ref. (2)).[46] Apart from this, errors introduced by ignoring non-adiabatic effects and omitting the empirical potential improvement[44] will be small. Correcting for them would shift the predicted resonances some 0 - 6 cm^{-1} to lower energy, while not significantly affecting the widths, as is shown below.

The influence of the empirical potential correction[44] Δ" on the resonances considered in Table I is shown in Table II; clearly the effects on both the energies and widths is quite small. The continued neglect of nonadiabatic effects is quite unimportant for these cases, since their magnitude depends on the expectation value of the kinetic energy[44,47] which becomes very small for levels near the top of the centrifugal barrier.[48] Since the correction Δ" was defined so as to bring the experimental and calculated J = 0 vibrational energies (including the nonadiabatic correction[47]) into agreement,[44] the results in Table II are essentially correct and unlikely to be significantly altered by further improvements in the potential. Indeed, when the nonadiabatic correction (following Ref. (44)) was added in, the v = 14, J = 4 level in Table II becomes barely bound with an eigenvalue of - 0.08 (± 0.15) cm^{-1}, almost (within mutual uncertainties) the experimental value of - 0.8 (± 0.5) cm^{-1}. However, the Ref. (44)

estimates of the nonadiabatic corrections are believed to be slightly large, so that further small corrections to the potential may be needed (i.e., increasing Δ'' slightly, particularly at long range). In any case, none of the resonance energies of Table II is likely to change by more than 1.5 - 2.0 cm^{-1}.

A further demonstration of the insensitivity of the resonance widths to moderate changes in the potential will be discussed in Section VI.

A compilation of the energies of all quasibound levels of ground-state H_2, HD, and D_2 with widths of less than 100 cm^{-1}, and the widths for those which are broader than 0.05 cm^{-1} is available in Ref. (48). The locus of the centrifugal barrier maximum as a function of J is also given there. Annotated FORTRAN listings of the computer programs used in the present calculations are also available.[49]

V. ROTATIONAL PREDISSOCIATION BROADENING AND THE LIMITING CURVE OF DISSOCIATION (LCD)

The onset of line broadening, followed by the "breaking-off" of a rotational series is often related to the height of the maximum in the effective potential U(R) arising from the centrifugal potential for a given J value.[19,20] The locus of the energy of this onset as a function of J(J+1) is known as the limiting curve of dissociation (LCD), and its extrapolation to zero J has long been used as a means of obtaining diatomic dissociation limits.[19] This relation has been

further exploited by Bernstein[14] who related the shape of the LCD to the nature of the long-range interatomic potential tail. His treatment involved two assumptions: (i) the long-range potential may be accurately approximated by a single inverse-power term for R values near the centrifugal barrier maxima for the J values considered, and (ii) the experimental LCD is identical to the locus of (centrifugal) barrier maxima (hereafter designated LBM). The second of these assumptions is critically examined below.

In Fig. 5 (lower half) is plotted the LBM for the ground ($X\ ^1\Sigma_g^+$) states of H_2, HD and D_2; the three isotopes are combined by use of the indicated reduced abscissa scale. The dashed curves represent the predicted experimental LCD's (i.e., the onset of observable predissociation broadening), defined as the loci of the energies of quasibound levels having widths

$$0.05 < \Gamma < 0.25\ \text{cm}^{-1}.$$

Also shown are the "error terms" ΔE, i.e., the differences between the LBM and the predicted LCD curves, which range from 10 to 40% of the LBM energy with the greatest relative error at small J. Thus, it is clear that the predissociation analysis of Ref. (14) should not be applied to diatomic hydrides or deuterides, and should probably be used cautiously for other light diatomics.[50]

VI. RAPID AND ACCURATE DETERMINATION OF RESONANCE ENERGIES, AND THE WKB APPROXIMATION FOR THEIR WIDTHS

A. Determination of Resonance Energies

Most of the procedures suggested for locating quasibound states either utilize an asymptotic property of the wave function, or treat the resonances as bound levels with a discrete outer boundary condition. The first type includes the approaches discussed in the preceding sections, defining the resonance energy as a maximum of the $\tau_d(E,J)$ or $IA(E,J)$ function. These require considerable computational effort; the wave function must be numerically integrated out to the asymptotic region where the non-centrifugal part of the potential is negligible, and there is no efficient algorithm for converging on a resonance.[53] In addition, these methods do not readily yield reasonable estimates of the widths of very sharp resonances unless the entire calculation is performed in multiple precision arithmetic capable of resolving Γ.

In the boundary condition (BC) method one tries to select a discrete criterion for the wave function at some arbitrary outer boundary (such as the barrier maximum) which corresponds to the maximum of $\tau_d(E,J)$ or $IA(E,J)$. Combining this with the usual inner boundary condition yields a simple one-dimensional eigenvalue problem with no necessity of numerically integrating past the chosen outer boundary.

This also allows utilization of the eigenvalue predictor-corrector formula which automatically converges very rapidly to the eigenvalue nearest to the arbitrary initial trial energy.[54]

Other approximate methods of locating resonances fall into neither of the categories described above, in particular, the method of Ref. (28) and the bound-state approach of Ref. (16). While these approaches avoid the necessity of integrating beyond the potential barrier, they do not include a means of rapidly converging on the resonance energy, as is introduced by the use of a discrete outer boundary condition.[54] Hence, they will not be considered further.

Several different outer BC's were tested here. These required, respectively, that the wave function: (i) have zero slope at the barrier maximum, $R_{max}(J)$,[55,56] (ii) have zero slope at the outermost classical turning point, $R_3(E)$,[56] (iii) behave as an Airy function of the second kind at $R_3(E)$,[57] (iv) behave as the first-order WKB solution with negative exponent (exponentially increasing inwards) at $R_{max}(J)$,[59] (v) have a node at $R_3(E)$, and (vi) have a node at $R_{max}(J)$. In Table III the energies of the broad quasibound levels of H_2 calculated using the first five of these criteria are compared to those defined by the maxima in IA(E,J). Considering these shifts in units of the respective widths Γ (from Table I) shows that: BC(i) yields eigenvalues too low by some 250% of Γ;[60] BC(ii) results are too low by ca. 75% of Γ;[60] BC(iii) is the best criterion considered, yielding eigenvalues in error by only ca. $\pm$ 4% of Γ; BC(iv) results are either too high or too low, with average errors of ca. $\pm$ 25%

of Γ; BC(v) predicts resonance positions which are too high by ca. 100% of Γ.[61] In addition, the fact that wave function nodes move inward with increasing energy discredits BC(vi), since necessarily

$$\mathrm{BC(i)} \lesssim \mathrm{BC(ii)} < \left\{ \begin{matrix} \mathrm{BC(iii)} \\ \mathrm{BC(iv)} \end{matrix} \right\} < \mathrm{BC(v)} \lesssim \mathrm{BC(vi)} \quad ,$$

where the equalities hold only at the energies of the barrier maxima where $R_{max}(J) = R_2(E) = R_3(E)$. The magnitudes of the shifts described above should be considered in light of the fact that the average difference between $\tau_d(\mathrm{max})$ and IA(max) is 5% of Γ.[61]

Since the Airy-function boundary condition [BC(iii)] yields the best results, the resonance positions it predicts are listed in Table I (column 5). Of the other criteria, BC(i) and (ii) may also be of some practical use for detecting resonances which lie slightly above the barrier maximum, where they cannot be located by BC(iii).[62] However, in most cases the Airy-function approach, in addition to being most accurate, successfully detects all important resonances. For H_2, except for (v,J) = (9,19), (12,12), (13,9) and (14,5) [see Tables I and III], the only resonances undetectable by this approach lay significantly above the centrifugal barrier, with widths $\gtrsim$ 100 cm^{-1}.

B. WKB APPROXIMATION FOR RESONANCE WIDTHS

The predissociation lifetime τ of a quasibound state may be obtained semiclassically[24] as the product of ω, the probability per collision of tunneling through the barrier, times t_{vib}, the period of

oscillation in the potential well. The latter is simply the quadrature over the potential minimum

$$t_{vib} = \sqrt{\frac{\mu}{2}} \int_{R_1(E)}^{R_2(E)} [E - U(R)]^{-\frac{1}{2}} \, dR \quad , \tag{15}$$

where $R_1(E)$ and $R_2(E)$ are the first two classical turning points, at which the effective potential

$$U(R) \equiv V(R) + \frac{J(J+1)}{R^2} \frac{\hbar^2}{2\mu} = E$$

Similarly, the former involves a quadrature "through the barrier", yielding

$$\omega = \exp \left\{ - \frac{\sqrt{8\mu}}{\hbar} \int_{R_2(E)}^{R_3(E)} [U(R) - E]^{\frac{1}{2}} \, dR \right\} \quad , \tag{16}$$

where $R_3(E)$ is the third (outermost) classical turning point. Thus, by the uncertainty principle, the level width is

$$\Gamma(WKB) = \hbar/\tau = \hbar/(\omega \, t_{vib}) \quad . \tag{17}$$

Resonance widths for H_2 calculated from Eqs. (15-17) at the energies corresponding to the Airy-function boundary condition are presented in column 6 ("WKB") of Table I; they are within ca. 12% of the more accurate estimates of columns 7-9. It should be noted that Eqs. (15-17) provide estimates of widths (or quasibound-level predissociation lifetimes) for resonances which are far too narrow for convenient evaluation by the methods of sections II and III.

It is interesting to consider the dependence of these WKB widths on the estimate of the resonance energy. This is conveniently done by evaluating Eqs. (15-17) at the resonance energies predicted by five of the boundary conditions discussed above. The results are presented in the second half of Table III. The energy dependence of the widths is small enough that no significant errors are introduced into the WKB widths in Table I by the displacements of the Airy-function eigenvalues from the exact resonance energies. This small energy dependence also confirms the conclusion (see Section IV) that any future corrections required by the ab initio ground-state H_2 potential would not significantly affect the resonance widths given in Table II.

An entirely different procedure (the "stabilization method") for determining resonance energies and widths has been described by Hazi and Taylor.[63] However, it would appear to be most useful as generalized to the multi-channel case (compound-state resonances);[64] it seems unnecessarily complicated for the practical description of single-channel (shape) resonances.

APPENDIX A: Calculation of $\tau_d(E,J)$ and Verification of Eq. (4)

Smith's[12] collision delay time $\tau_d(E,J)$ (his Q(E) or $Q_{\ell\ell}(E)$) is the difference between the time two particles spend together during an actual collision with energy E, and the transit time for the same initial conditions in the absence of an interaction potential. Here the orbital angular momentum quantum number J (Smith's ℓ) merely specifies the magnitude of the centrifugal contribution to the effective potential. Smith showed that this "delay time" was

$$\tau_d(E,J) = \int_0^\infty (\Psi^* \Psi - \Psi_\infty^* \Psi_\infty)\, dR + \left(\frac{\mu}{\hbar k^2}\right) \left\{\sin(2\delta_J(E) - J\pi)\right\}, \quad (A1)$$

where the exact radial wave function is asymptotically normalized as

$$\Psi \sim \Psi_\infty = \left(\frac{4\mu}{\hbar k}\right)^{\frac{1}{2}} \left\{\sin\left(kR + \delta_J(E) - \frac{J\pi}{2}\right)\right\}, \quad (A2)$$

with notation as in Sections II and III. For most cases of interest (i.e., those considered here) the non-centrifugal part of the interaction potential is effectively negligible at some finite internuclear distance R_+. Thus, for all $R \gtrsim R_+$ the exact solution is indistinguishable from

$$\Psi = \left(\frac{4\mu}{\hbar k}\right)^{\frac{1}{2}} kR \left\{\cos[\delta_J(E)]\, j_J(kR) - \sin[\delta_J(E)]\, y_J(kR)\right\}, \quad (A3)$$

where $j_J(z)$ and $y_J(z)$ are the spherical Bessel functions of the first and second kind.[65] In the present approach, as in the standard phase shift calculation, exact numerical integration of the radial wave equation is performed out to the smallest such R_+. There the solution

is decomposed into the form of Eq. (A3) to yield $\delta_J(E)$, and given the desired asymptotic normalization. Then, defining $Z_+ \equiv kR_+$, Eq. (A1) becomes

$$\tau_d(E,J) = \int_0^{R_+} \Psi^* \Psi \, dR - \frac{\mu}{\hbar k^2} [2Z_+ - \sin(2Z_+ + 2\delta_J(E) - J\pi)] + \frac{\Delta(Z_+,J)}{k} \quad . \tag{A4}$$

Here the integral may be readily computed from the exact numerical wave function, and the residual asymptotic contribution

$$\Delta(Z_+,J) \equiv \int_{Z_+}^{\infty} (\Psi^* \Psi - \Psi_\infty^* \Psi_\infty) \, dz \quad , \tag{A5}$$

where $z \equiv kR$, and Ψ and Ψ_∞ are given by Eqs. (A3) and (A2) respectively, may be computed essentially analytically.

For $J = 0$, $\Delta(Z_+,J)$ is identically zero, while its evaluation for $J > 0$ is described below. The magnitude of this term clearly depends on the criterion used for selecting Z_+ (i.e., for selecting R_+). In the present calculation this was done by constraining $Z_+ > J$ and requiring differences of $\leq 10^{-4}$ radians between the values of $\delta_J(E)$ evaluated at three consecutive wave function nodes.[23b] The relative contribution of $\Delta(Z_+,J)$ to the sum in Eq. (A4) varied from being a negligible fraction (at a very sharp resonance), to becoming the dominant term both at broad resonances and away from resonance.

Using the Rayleigh expansion for the Bessel functions in Eq. (A3)[65] one obtains:

$$\left.\begin{aligned} z\, j_J(z) &= (-1)^J \sum_{m=0}^{J} N_J^m\, z^{-m} \sin\left[z + (J-m)\tfrac{\pi}{2}\right] \\ z\, y_J(z) &= (-1)^{J+1} \sum_{m=0}^{J} N_J^m\, z^{-m} \cos\left[z + (J-m)\tfrac{\pi}{2}\right] \end{aligned}\right\} \quad \text{(A6)}$$

where for the coefficients N_J^m :

$$\left.\begin{aligned} N_J^0 &= 1 && \text{for all } J \\ N_J^m &= 0 && \text{for all } m > J \\ N_J^m &= N_{J-1}^m - (J+m-1)N_{J-1}^{m-1} && \text{for all } m \leq J \ . \end{aligned}\right\} \quad \text{(A7)}$$

A simple corollary to Eqs. (A7) is

$$N_J^J = -\, N_J^{J-1} = -\,(2J-1)N_{J-1}^{J-1}$$

Substituting Eqs. (A6) into Eq. (A3), and the latter and Eq. (A2) into Eq. (A5) yields:

$$\Delta(Z_+,J) = \left(\frac{4\mu}{\hbar k}\right) \sum_{m=1}^{J} \left\{A_J^m\ S(2m-1) - B_J^m\, C(2m) + C_J^m/(Z_+)^{2m-1}\right\} \quad , \qquad \text{(A8)}$$

where A_J^m , B_J^m and C_J^m are simple functions of the known N_J^m coefficients:

$$\left.\begin{aligned} A_J^m &= (-1)^{J-m} \sum_{n=0}^{\min[m-1,J-m]} N_J^{m+n} \; N_J^{m-n-1} \\ B_J^m &= (-1)^{J-m} \left\{ \frac{\left(N_J^m\right)^2}{2} + \sum_{n=1}^{\min[m,J-m]} N_J^{m+n} \; N_J^{m-n} \right\} \\ C_J^m &= \frac{1}{(2m-1)} \left\{ \frac{\left(N_J^m\right)^2}{2} + \sum_{n=1}^{\min[m,J-m]} (-1)^n \, N_J^{m+n} \; N_J^{m-n} \right\} . \end{aligned}\right\} \quad \text{(A9)}$$

The remaining factors in Eq. (A8) are the quadratures

$$S(2m-1) = \int_{Z_+}^{\infty} \frac{\sin(2z + 2\delta_J)}{z^{2m-1}} \, dz$$

$$C(2m-2) = \int_{Z_+}^{\infty} \frac{\cos(2z + 2\delta_J)}{z^{2m-2}} \, dz \quad ,$$

which are related through the recursion relations

$$\left.\begin{aligned} S(2m-1) &= \frac{\cos(2Z_+ + 2\delta_J)}{2(Z_+)^{2m-1}} - (m - \tfrac{1}{2}) \; C(2m) \\ C(2m-2) &= \frac{\sin(2Z_+ + 2\delta_J)}{2(Z_+)^{2m-2}} + (m - 1) \; S(2m-1) \end{aligned}\right\} \quad \text{(A10)}$$

These relations are used to generate the terms in the sum in Eq. (A8) as m decreases from J to 1;[66] thus one needs C(2J) as a starting value. Making use of the fact that $Z_+ > J$, C(2J) may be expanded by repeated applications of Eqs. (A10). After n iterations it becomes

$$C(2J) = \frac{1}{2(Z_+)^{2J}} \left\{ -\sin(2Z_+ + 2\delta_J) \left[1 + \sum_{\ell=1}^{n-1} (-1)^\ell \prod_{k=0}^{(2\ell-1)} \left(\frac{J+k/2}{Z_+} \right) \right] \right.$$

$$\left. + \left(\frac{J}{Z_+} \right) \cos(2Z_+ + 2\delta_J) \left[1 + \sum_{\ell=1}^{n-1} (-1)^\ell \prod_{k=1}^{2\ell} \left(\frac{J+k/2}{Z_+} \right) \right] \right\} + R(n) \quad , \quad \text{(A11)}$$

where

$$R(n) = (-1)^n \, C(2J + 2n) \prod_{k=0}^{2n-1} (J + k/2) \quad . \quad \text{(A12)}$$

It is readily seen that

$$|R(n)| < \frac{1}{2(Z_+)^{2J}} \prod_{k=0}^{2n-2} \left(\frac{J + k/2}{Z_+} \right) \quad , \quad \text{(A13)}$$

and hence the series in Eq. (A11) converges for $n < n_{max}$, where n_{max} is the largest integer $< (Z_+ + 1 - J)$. If the bound given by Eq. (A13) is not negligible for $n = n_{max}$, the remainder $R(n_{max})$ may be evaluated using a numerical quadrature for $C(2J + 2n_{max})$. Because of the large power of z in the denominator, this requires very few mesh points.

The evaluation of $\Delta(Z_+,J)$ via Eqs. (A7) - (A13) was tested for a number of cases by comparing the results to a numerical quadrature of Eq. (A5) with expressions (A2) and (A3) substituted for Ψ and Ψ_∞. For $1 \leq J \leq 30$ and $Z_+ = 2J$ the numerical quadratures (which required orders of magnitude more computation time) were in excellent agreement with the "analytic" results from Eqs. (A7) - (A13).[67] In the present

calculations on ground-state H_2, HD, and D_2 the total time delay computation, including the calculation of the phase shift, took on the average less than 0.2 sec for a given J and E,[68] compared to 0.15 sec for the evaluation of the phase shift alone.[17]

For the time delay defined by Eq. (A1), Smith[12] proved the identity of Eq. (4); this is used here as a check on the present method of calculating $\tau_d(E,J)$. The potential used was that employed by Waech and Bernstein[16] in their phase shift calculations for H_2. For the resonance energies listed in their Table V,[16] whose widths range from 3 to 150 cm^{-1}, the present approach (i.e., use of Eqs. (A4) and (A7-A13)) yielded widths differing with theirs on the average by $\pm$ 5%.[69] These differences reflect both the lower accuracy of the computations of Ref. (16) and error introduced through the finite difference approximation they used for the derivative in Eqs. (4). This latter effect is a difficulty inherent in any calculation of delay times using Eq. (4). This problem is illustrated here for H_2 for J = 8 at E = 89.95 cm^{-1}, which is very near the center of the v = 13, J = 8 resonance (for which E_r = 89.93 cm^{-1} and Γ = 1.90 cm^{-1}). Using the first difference formula (energies in cm^{-1})

$$\bar{\tau}_d(89.95,8) = \frac{1}{\pi c}\frac{\Delta\delta_J}{\Delta E} \qquad \text{(A14)}$$

with the differences centered at 89.95 cm^{-1}, time delays for different ΔE values are given in Table IV; the "correct" value, obtained from Eq. (A4), is 1.119×10^{-11} sec. The uncertainties in Table IV cor-

respond to estimated absolute phase shift accuracies of $\pm$ 0.0005 radians. As expected, use of a small ΔE mesh yields a loss of precision in the phase shift differences, while for a large mesh the first difference approximation for the derivative is no longer accurate.

Annotated FORTRAN listings of the computer program used in the present $\delta_J(E)$ and $\tau_d(E,J)$ calculations are available in Ref. (49).

TABLE I

H_2 resonance energies and widths via different criteria.

v	J	$E_r[cm^{-1}]$ τ_d(max)	IA(max)	BC(Airy)	$\Gamma[cm^{-1}]$ WKB	$\left(\frac{2/\pi c}{\tau_d(max)}\right)^a$	FWHM(τ_d)	FWHM(IA)
0	38	7510.0	7514.0	7508.7	87.0	80.0	92.4	98.1
0	37	6513.3	6513.5	6513.3	5.60	5.84	5.89	5.98
1	35	5549.8	5550.0	5549.7	14.9	14.1	14.4	14.3
2	33	4688.4	4689.0	4688.2	22.5	20.4	21.0	20.8
3	31	3925.0	3925.4	3924.9	26.7	23.6	24.4	25.1
4	29	3254.7	3255.4	3254.8	28.4	24.7	25.4	25.4
5	27	2673.0	2673.8	2673.4	29.3	25.1	26.0	25.8
6	25	2175.0	2176.0	2175.7	31.4	26.5	27.6	27.4
7	23	1755.3	1756.7	1756.4	36.9	30.4	31.8	31.7
8	21	1407.0	1409.4	1409.4	48.3	39.4	41.6	42.1
9	19	1121.6	1127.2	b	b	57.9	62.0	66.2
9	18	725.9	725.9	726.0	0.55	0.52	0.53	0.53
10	16	586.0	586.0	586.1	3.22	2.92	2.92	2.93
11	14	480.1	481.0	481.7	22.3	17.9	18.1	18.5
11	13	199.4	199.4	199.4	0.0053	0.0053	0.005	0.005
12	12	385.0	398.6	b	b	74.5	70.3	116.[c]
12	11	215.5	215.5	215.6	3.09	2.63	2.62	2.62
13	9	195.0	205.6	b	b	56.6	48.3	89.6[c]
13	8	89.9	90.0	90.1	2.38	1.90	1.88	1.89
14	6	81.9	121.0	b	b	115.	91.	79.[d]
14	5	45.7	49.2	b	b	20.5	16.2	26.4
14	4	3.76	3.76	3.76	0.0085	0.0060	0.007	0.007

a) This is identically $2/(d\delta_J/dE)_{max}$; see Eq. (5).

b) The boundary condition places this level above the barrier maximum so that it cannot be detected by this approach.

c) This value is much larger than the other estimates of this width because of the pronounced asymmetry of the IA(E,J) curves for the highest resonances at low J, shown in Fig. 3. A more appropriate estimate is obtained by taking twice the (low E) half-width at half-maximum; this yields a value ca.20% smaller than the τ_d(max) estimate (column 7).

d) This is actually twice the half-width at half-maximum of the IA(E,J) curve, since as is suggested by Fig. 3, the FWHM(IA)$\gg$900 cm^{-1}. Similarly, twice the half-width at half-maximum of τ_d(E) for this level is 123. cm^{-1}.

TABLE II. Best estimates of resonance energies and widths for ground-state H_2, calculated from the "corrected" potential, i.e., including the empirical correction[44] Δ''_{21} (cf. Table I which corresponds to the ab initio potential[21] alone).

v	J	$E_r[cm^{-1}]$		$\Gamma[cm^{-1}]$
		$\tau_d(max)$[a]	IA(max)[b]	$\left(\frac{2/\pi c}{\tau_d(max)}\right)$[c]
0	38	7509.2	7513.5	80.9
0	37	6513.0	6513.0	5.97
1	35	5549.1	5549.2	14.4
2	33	4687.0	4687.3	20.8
3	31	3923.0	3923.5	24.1
4	29	3252.3	3253.0	25.2
5	27	2670.2	2671.0	25.7
6	25	2172.0	2172.8	27.1
7	23	1751.8	1753.0	31.0
8	21	1402.9	1405.4	40.0
9	19	1117.0	1123.1	58.3
9	18	722.4	722.4	0.51
10	16	582.0	582.0	2.84
11	14	475.7	476.5	17.3
11	13	195.5	195.5	0.004
12	12	380.3	393.1	71.3
12	11	211.4	211.4	2.32
13	9	191.4	200.8	52.3
13	8	86.3	86.3	1.48
14	6	81.5	114.8	104.
14	5	44.1	46.8	17.4
14	4	1.0	1.0	0.0005[d]

a) "Scattering theory" resonance energy.

b) "Spectroscopic" quasibound level energy.

c) This is identically $2/(d\delta_J/dE)_{max}$.

d) This resonance was too sharp to resolve $\tau_d(max)$ conveniently, so this width was obtained using the semiclassical method discussed in Section VI. As discussed in text, Herzberg and Howe's observations show this level to be truly bound.[41]

TABLE III

Comparative test of different outer boundary conditions, and comparison of WKB widths calculated at their respective energies.

		E_r[BC] − E_r[IA(max)] [cm^{-1}]					Γ[cm^{-1}]				
v	J	Slope(R_{max})[a]	Slope(R_3)[b]	Airy(R_3)[c]	WKB(R_{max})[d]	Node(R_3)[e]	WKB(i)[a]	WKB(ii)[b]	WKB(iii)[c]	WKB(iv)[d]	WKB(v)[e]
0	38	− 76.8	− 63.6	− 5.3	− 26.9	f	56.7	62.2	87.0	78.4	f
0	37	− 30.3	− 5.6	− 0.2	1.9	4.9	4.35	5.36	5.60	5.70	5.85
1	35	− 41.7	− 12.9	− 0.3	2.6	12.7	10.7	13.5	14.9	15.3	16.5
2	33	− 45.7	− 18.3	− 0.8	1.9	19.2	15.5	19.5	22.5	23.0	26.4
3	31	− 46.3	− 20.3	− 0.6	1.7	23.6	17.9	22.5	26.7	27.2	32.7
4	29	− 44.7	− 20.7	− 0.5	1.3	25.7	18.8	23.5	28.4	28.9	35.9
5	27	− 42.4	− 20.5	− 0.4	1.0	27.4	19.1	24.0	29.3	29.7	38.5
6	25	− 40.4	− 20.9	− 0.3	0.3	31.4	20.1	25.1	31.4	31.7	43.7
7	23	− 39.3	− 22.8	− 0.2	− 1.0	48.0	23.0	28.2	36.9	36.5	59.3
8	21	− 38.3	− 27.2	0.0	− 5.6	f	30.3	35.0	48.3	45.4	f
9	19	− 38.3	− 34.4	f	f	f	44.7	46.7	f	f	f
9	18	− 14.9	− 0.4	0.1	0.8	0.5	0.38	0.54	0.55	0.56	0.55
10	16	− 18.9	− 2.3	0.1	1.8	2.6	1.98	3.04	3.22	3.37	3.44
11	14	− 23.1	− 11.7	1.7	0.9	f	12.6	16.7	22.3	22.4	f
12	11	− 14.8	− 1.9	0.1	1.7	2.5	1.53	2.83	3.09	3.32	3.45
13	8	− 10.9	− 1.3	0.1	1.5	1.9	0.93	2.13	2.38	2.65	2.75
14	5	− 6.3	− 6.2	f	f	f	11.4	10.9	f	f	f

a) BC(i): Zero slope at $R_{max}(J)$.
b) BC(ii): Zero slope at $R_3(E)$.
c) BC(iii): Airy function at $R_3(E)$.
d) BC(iv): WKB-exponential at $R_{max}(J)$.
e) BC(v): Node at $R_3(E)$.
f) This boundary condition places this level above the barrier maximum so that it cannot be detected by this approach. The resonances (v,J) = (13,9) and (12,12) listed in Tables I-II are detected by none of these criteria.

TABLE IV

H_2 delay time for J = 8 at E = 89.95 cm^{-1} calculated by finite differences from Eq. (A14) with several different mesh sizes. The corresponding value obtained from Eq. (A4) is $\tau_d(89.95,8) = 1.119 \times 10^{-11}$ sec.

$\Delta E[cm^{-1}]$	0.02	0.04	0.06	0.08	0.10	0.30	0.50	0.70
$\Delta\delta_J$(radians)	0.0208	0.0427	0.0627	0.0830	0.1052	0.3152	0.5208	0.7130
$10^{11}\ \tau_d[sec]^a$	1.10(±.05)	1.14(±.03)	1.11(±.02)	1.10(±.01)	1.12(±.01)	1.116(±.004)	1.106(±.002)	1.081(±.002)

a) The uncertainties correspond to the ± 0.0005 radian uncertainty in the absolute phase shift.

FOOTNOTES

1. a) F. T. Smith, J. Chem. Phys. 36, 248 (1962); b) ibid, 38, 1304 (1963).

2. a) R. E. Roberts, R. B. Bernstein, and C. F. Curtiss, Chem. Phys. Lett. 2, 366 (1968); b) ibid, J. Chem. Phys. 50, 5163 (1969); c) R. E. Roberts and R. B. Bernstein, Chem. Phys. Lett. 6, 282 (1970).

3. F. H. Mies, J. Chem. Phys. 51, 787 and 798 (1969).

4. F. T. Smith, Chapter 9 in Kinetic Processes in Gases and Plasmas, A. R. Hochstim, editor (Academic Press, New York, 1969).

5. R. D. Levine, Accts. Chem. Res. 3, 273 (1970).

6. J. L. Jackson and R. E. Wyatt, "Quantum Effects in Transient Pair Formation in Gases: The Equilibrium Constant For $O + H \rightleftharpoons OH(X^2\Pi_i)$," J. Chem. Phys. (1971, to be published).

7. R. A. Buckingham and J. W. Fox, Proc. Roy. Soc. A267, 102 (1962).

8. R. A. Buckingham, J. W. Fox, and E. Gal, Proc. Roy. Soc. A284, 237 (1965).

9. R. A. Buckingham and E. Gal, Adv. At. Molec. Phys. 4, 37 (1968).

10. S. Imam-Rahajoe, C. F. Curtiss, and R. B. Bernstein, J. Chem. Phys. 42, 530 (1965).

11. a) L. Eisenbud, dissertation, Princeton University, June 1948 (unpublished); b) E. P. Wigner, Phys. Rev. 98, 145 (1955).

12. F. T. Smith, Phys. Rev. 118, 349 (1960); erratum, ibid, 119, 2089 (1960).

13. R. B. Bernstein, C. F. Curtiss, S. Imam-Rahajoe, and H. Wood, J. Chem. Phys. 44, 4072 (1966).

14. R. B. Bernstein, Phys. Rev. Lett. 16, 385 (1966).

15. J. W. Fox and E. Gal, Proc. Phys. Soc. 90, 55 (1967).

16. T. G. Waech and R. B. Bernstein, J. Chem. Phys. 46, 4905 (1967).

17. M. E. Gersh and R. B. Bernstein, Chem. Phys. Lett. 4, 221 (1969).

18. a) W. C. Stwalley, A. Niehaus, and D. R. Herschbach, Proc. 5th Int. Conf. Physics of Electron and Atom Collisions, 639 (1967); b) W. C. Stwalley, Ph.D. thesis, Harvard University (1968).

19. See the references mentioned in the discussions of rotational predissociation by: a) G. Herzberg, Spectra of Diatomic Molecules, 2nd edition (D. Van Nostrand Co., Toronto, 1950); b) A. G. Gaydon, Dissociation Energies and Spectra of Diatomic Molecules, 3rd edition (Chapman and Hall Ltd., London, 1968).

20. Particularly illuminating examples of this are found in the work, three decades apart, of L. Farkas and S. Levy (Z. Physik 84, 195 (1933)) on AlH, and of T. L. Porter (J. Opt. Soc. Am. 52, 1201 (1962)) on HgH. In both cases, rotational progressions are followed from a sharp line, to a measurably broad one, and on to a barely discernable (very broad) one.

21. a) W. Kołos and L. Wolniewicz, J. Chem. Phys. 41, 3663 (1964); b) ibid, 43, 2429 (1965); c) ibid, 49, 404 (1968).

22. Note that since the adiabatic correction to the clamped-nuclei (Born-Oppenheimer) potential is weighted by the inverse of the nuclear reduced mass,[21] the potentials for the isotopically different hydrogens are not quite identical.

23. a) R. A. Buckingham and A. Dalgarno, Proc. Roy. Soc. A213, 506 (1952); b) R. B. Bernstein, J. Chem. Phys. 33, 795 (1960).

24. K. W. Ford, D. L. Hill, M. Wakano, and J. A. Wheeler, Ann. Phys. (N. Y.) 7, 239 (1959).

25. See, e.g., E. Merzbacher, Quantum Mechanics (John Wiley and Sons, Inc., New York, 1961), § 12.6.

26. This separation was considered in Refs. (27) and (28), and an illustration of the difficulty of properly effecting it is the conclusion in the latter that the E_r lay below, rather than above the inflection point of $\delta_J(E)$. The difficulty lies in the transition of $\beta_J(E)$ from having well-defined positive curvature at very high energies, through an interval of negative curvature about the barrier maximum, to a constant multiple of π at energies below the peak.[7-9] This situation contrasts with that for compound-state resonances where a background phase may often be quite clearly defined in the neighborhood of broad resonances.[29]

27. A. C. Allison, Chem. Phys. Lett. 3, 371 (1969).

28. B. R. Johnson, G. G. Balint-Kurti, and R. D. Levine, Chem. Phys. Lett. 7, 268 (1970).

29. a) R. D. Levine, B. R. Johnson, J. T. Muckerman, and R. B. Bernstein, J. Chem. Phys. 49, 56 (1968); b) J. T. Muckerman and R. B. Bernstein, J. Chem. Phys. 52, 606 (1970).

30. J. L. Jackson and R. E. Wyatt, Chem. Phys. Lett. 4, 643 (1970).

31. T. -Y. Wu and T. Ohmura, Quantum Theory of Scattering (Prentice-Hall Inc., Englewood Cliffs, N. J., 1962), §A7.

32. The magnitude of this curvature is indicated by the change in slope of the "background" functionality under the broad, highest resonances in Figs. 1 and 2.

33. An elegant relation between the density of states and the asymptotic normalization of the continuum wave function is given by: A. Messiah, Quantum Mechanics (North-Holland Publishing Co., Amsterdam, 1962), Volume II, § 17.4.

34. These effects are clearly illustrated by the numerically calculated wave functions presented in Fig. 2 of Ref. (7) and Fig. 1 of Ref. (30).

35. The clearest treatments are those of Connor,[36] who used an inverted parabolic barrier, and Dickinson,[37] who used an inverted Morse potential. These authors refer to and discuss the prior literature. Note, however, that the presently derived qualitative results relating IA(E,J) and $\tau_d(E,J)$ are also obtained from the most primitive approach to the barrier penetration problem (see, e.g., Ref. (24)).

36. a) J. N. L. Connor, Mol. Phys. 15, 621 (1968); b) ibid, 16, 525 (1969).

37. A. S. Dickinson, Mol. Phys. 18, 441 (1970).

38. This neglect may explain why Ref. (27) and the present work agree upon the (14,4) and (14,5) H_2 resonance energies suggested by the scattering theory criterion (maximum of $\tau_d(E,J)$), but the former places the IA(E,J) maximum for the 20 cm^{-1} broad (14,5) resonance at E = 50.8 cm^{-1}, compared to the present 49.2 cm^{-1} (see Table I).

39. This was verified for all partial waves (J values) for ground-state H_2, where resonances occur with 0-14 nodes inside the barrier maximum. In any case where the peak positions did vary with n, the shifts were always much smaller than the difference between the positions of the respective IA(E,J) and $\tau_d(E,J)$ maxima, which difference was itself much smaller than Γ (e.g., see the v = 7 resonance for J = 25 in Fig. 4). Occasionally the residual background in $IA^{(n)}(E,J)$ also shows an extremely broad but insignificant maximum at an energy far above the barrier. An example of this is found in the $IA^{(n)}(E,4)$ curves at E $\simeq$ 400-500 cm^{-1} (depending on n, cf. Fig. 3). However, this type of structure cannot be associated with a resonance since there is no corresponding structure in $\tau_d(E,J)$, and because the node count behind the potential barrier is more than one greater than its value at the nearest lower-energy resonance for the given J.

40. This was the case for all the resonances of ground-state H_2, HD and D_2. One might speculate that the energy of the internal amplitude maximum is the Breit-Wigner resonance position, E_r in Eq. (1), since its shift relative to $\tau_d(max)$ is in the correct direction, and it depends only on the wave function in the region $R \leq R_{max}(J)$.

41. This may explain the discrepancy previously pointed out between G. Herzberg and L. L. Howe's (Can. J. Phys. 37, 636 (1959)) two determinations of the energy of the v = 14, J = 5 quasibound level of H_2 , and their disagreement with the calculated peak position.[27] The two experimental values were respectively 0.5 Γ below and 0.9 Γ above the calculated value, where Γ = 20 cm^{-1} .[27] If a skewing of the IA(E,5) peak were responsible for these apparently discordant observations, it would also explain why the observed lines "are still quite sharp", while the calculated (see Table I here, and Refs.(16) and (27)) width is ca. 20 cm^{-1} .

42. G. Herzberg and A. Monfils, J. Mol. Spectry. 5, 482 (1960).

43. A new experimental dissociation energy, considered to be better than the theoretical one, was recently reported by G. Herzberg, J. Mol. Spectry. 33, 147 (1970). A slight improvement over this result was obtained from the reanalysis of his data by W. C. Stwalley, Chem. Phys. Lett. 6, 241 (1970).

44. R. J. Le Roy and R. B. Bernstein, J. Chem. Phys. 49, 4312 (1968). The improved experimental dissociation energy[43] has since shown that Δ'' is the better of the two possible empirical potential corrections suggested.

45. The theoretical result is given in Table I and Fig. 3 (and in Refs. (16) and (27)), while the experimental energy is obtained by combining the level energy reported by Herzberg and Howe[41] with the dissociation energy of Refs.(43).

46. R. E. Roberts (private communication, 1970) reports that removing this contribution will lower all the theoretical[2b] H + H recombination rate constants k(T) by some 10-20%, while not significantly affecting the position of the predicted k(T) maximum.

47. a) J. H. Van Vleck, J. Chem. Phys. 4, 327 (1936); b) J. D. Poll and G. Karl, Can. J. Phys. 44, 1467 (1966).

48. R. J. Le Roy, "Eigenvalues and Certain Expectation Values for All Bound and Quasibound Levels of Ground-State ($X\ ^1\Sigma_g^+$) H_2, HD and D_2", University of Wisconsin Theoretical Chemistry Institute Report WIS-TCI-387 (1971).

49. R. J. Le Roy, University of Wisconsin Theoretical Chemistry Institute Report WIS-TCI-429G (1971).

50. This casts considerable doubt on the long-range potential constants obtained from applications of this method to HgH and HgD,[14] to HF and DF,[51] and to OH.[52]

51. M. A. Byrne, W. G. Richards, and J. A. Horsley, Mol. Phys. 12, 273 (1967).

52. J. A. Horsley and W. G. Richards, J. Chim. Phys. 66, 41 (1969).

53. Ref. (30) also suggested that if the energy grid used in a resonance search was broader than, say $\Gamma/2$, the resonance might be overlooked. However, this difficulty is removed from both the $\tau_d(E,J)$ and IA(E,J) approaches by simply counting the wave function nodes inside the barrier, or by evaluating the absolute phase shift.

54. J. W. Cooley, Math. Computation 15, 363 (1961); b) J. K. Cashion, J. Chem. Phys. 39, 1872 (1963).

55. It may be shown analytically that BC(i) would give the maximum possible amplitude growth across a rectangular barrier.

56. BC(i) and (ii) were examined in Ref. (30); there appears to be a misprint there as they discuss having a node and zero slope at $R_{max}(J)$ or $R_3(E)$, which would yield the trivial solution $\Psi_{E,J}(R) \equiv 0$ everywhere.

57. This refers to the function Bi discussed in §10.4 of Ref. (58). One needs only initial values of this function very near the turning point (where its argument is quite small), and they are readily obtained by summing the first few terms in the ascending power series expansion for Bi (Eq. (10.4.3) in Ref. (58)). This criterion was chosen because it gives the maximum possible amplitude growth across a right triangular barrier.

58. M. Abramowitz and I. A. Stegun, Handbook of Mathematical Functions, Natl. Bur. Std. (U.S.) Appl. Math. Ser. 55 (U.S. Dept. of Commerce, 1964; also Dover Publications Inc., New York, 1965).

59. Within the first-order WKB approximation this should correspond exactly to BC(iii).

60. This relative ordering of the results for BC(i) and (ii) was found in Ref. (30) for the two broad resonances considered there; however it is interesting here to note its generality and the relation between the shift and the resonance width.

61. The analyses of these relative shifts omitted the sharp resonances since the effects there are obscured by the limited precision of the calculation.

62. See, e.g., (v,J) = (9,19) and (14,5) in Tables I and III.

63. A. U. Hazi and H. S. Taylor, Phys. Rev. A1, 1109 (1970).

64. a) W. H. Miller, Chem. Phys. Lett. 4, 627 (1970); b) M. F. Fels and A. U. Hazi, "Calculation of Energies and Widths of Compound-State Resonances in Elastic Scattering: Stabilization Method" (to be published); c) A. U. Hazi and M. F. Fels, "Computation of Resonance Parameters For Elastic Scattering" (to be published).

65. See §10.1 of Ref. (58).

66. The alternate approach would invert Eqs. (A10) and evaluate the sum in Eq. (A8) starting at m = 1. However, since $Z_+ > J$ (and often $Z_+ >> J$), this causes a serious loss of precision when using these recursion relations, yielding completely spurious values of C(2m) and S(2m-1) for m as low as 5.

67. The residual differences ranged from < 0.004% of $\Delta(Z_+,J)$ for $J \leq 10$, to 1.2% for $J = 30$, probably reflecting accumulated errors in the numerical quadratures.

68. This program[49] was coded in Fortran V and run on a Univac 1108 computer.

69. The only serious exception is the $v = 10$, $J = 17$ resonance, for which an apparently erroneous width of 376 cm^{-1} was reported previously[16] (*cf.* Eq. (5) yielded 92.9 cm^{-1}). The worst disagreement for all the other widths reported was 12%, and the differences were usually within the uncertainties reported in Ref. (16).

FIGURE LEGENDS

Fig. 1 Collisional time delays $\tau_d(E,J)$ [sec] for atomic H + H collisions governed by the singlet ground-state H_2 potential curve. The vertical dashed lines denote the energies of the barrier maxima for the different J. The v labeling of the peaks indicates the number of nodes in the radial wave function for internuclear separations smaller than that corresponding to the potential maximum.

Fig. 2 Collisional time delays $\tau_d(E,J)$ [sec] for D + D collisions; as in Fig. 1.

Fig. 3 Comparison of $\tau_d(E,J)$ functions (solid curves, left ordinate scale) with the $IA^{(n)}(E,J)$ functions (right ordinate scale) for n = 1 (upper dashed curves) and n = 4 (lower dashed curves), for H + H collisions. The vertical arrows indicate the precise location of the respective maxima; as in Fig. 1.

Fig. 4 Comparison of $\tau_d(E,J)$ and IA(E,J) functions for H + H collisions; as in Fig. 3.

Fig. 5 Lower: comparison of the LBM (solid curve; with this abscissa it is the same for the different isotopes) with the predicted LCD's (dashed curves) for ground-state H_2, HD and D_2. Upper: the error term $\Delta E \equiv [E(LBM,J) - E(LCD,J)]$ vs $J(J+1)$.

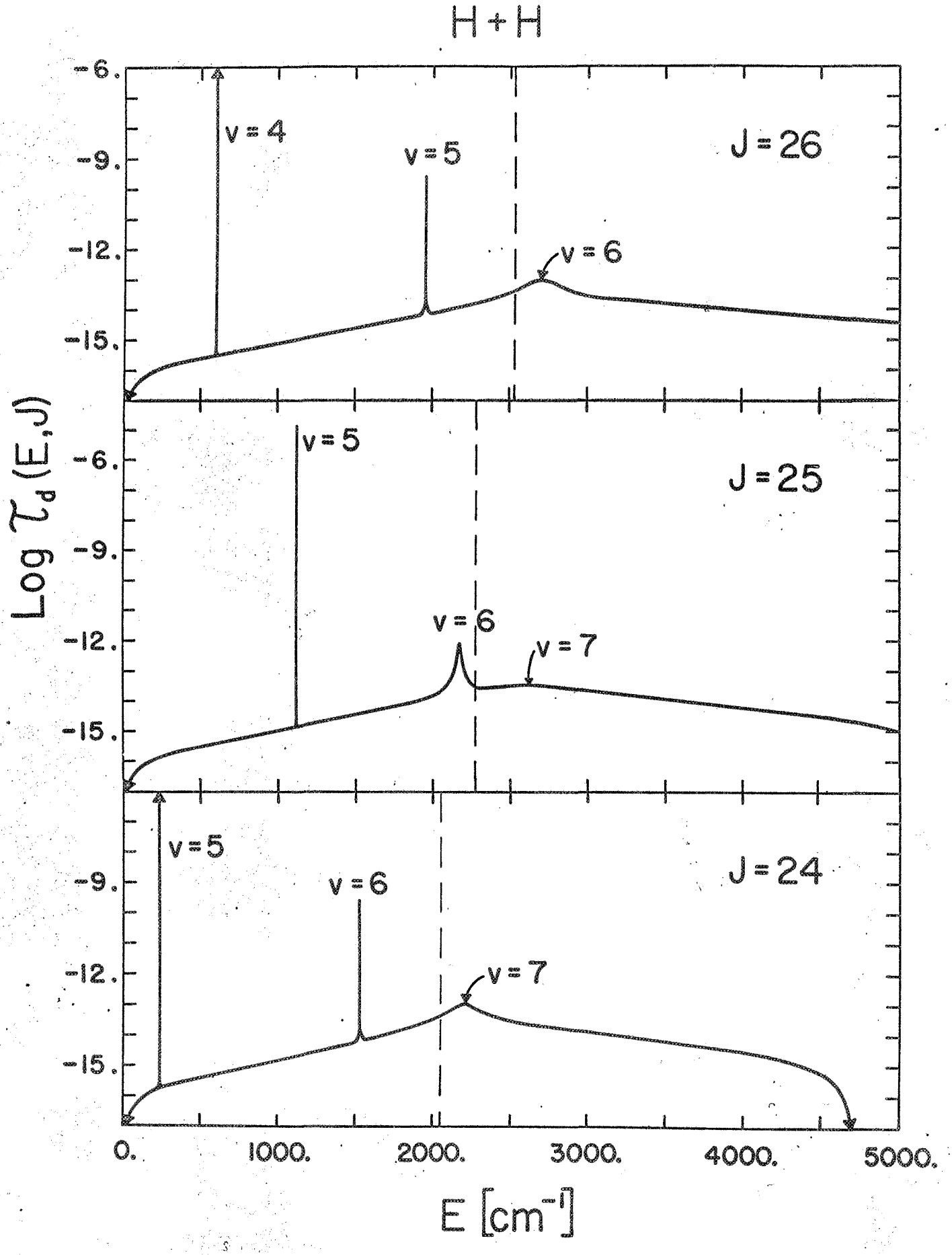
H + H
J = 26
v = 4
v = 5
v = 6
J = 25
v = 5
v = 6
v = 7
J = 24
v = 5
v = 6
v = 7
-6.
-9.
-12.
-15.
Log $\tau_d(E,J)$
0.
1000.
2000.
3000.
4000.
5000.
E [cm^{-1}]

Figure 1.

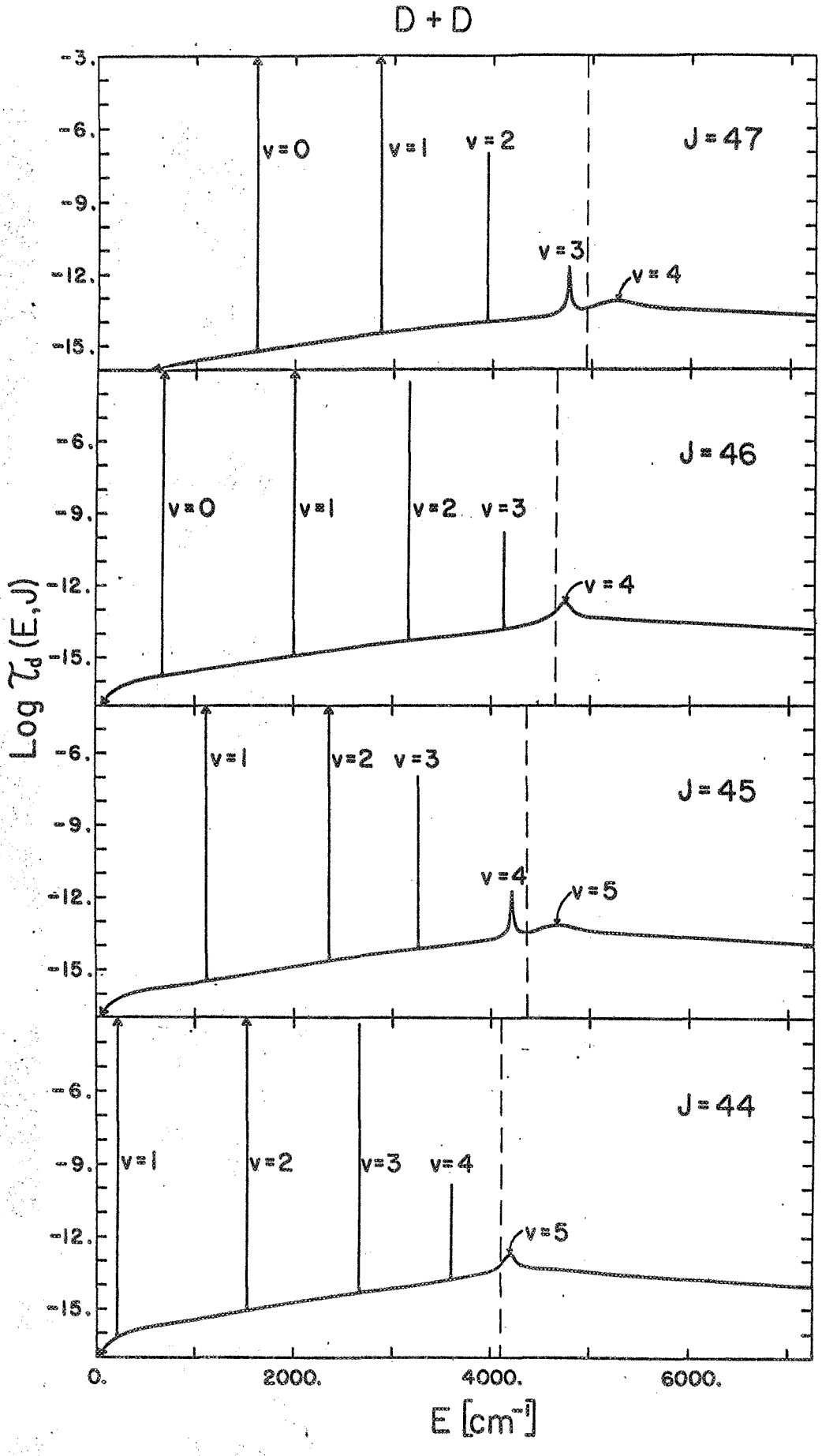
D + D
J = 47
v = 0
v = 1
v = 2
v = 3
v = 4
J = 46
v = 0
v = 1
v = 2
v = 3
v = 4
J = 45
v = 1
v = 2
v = 3
v = 4
v = 5
J = 44
v = 1
v = 2
v = 3
v = 4
v = 5
-3.
-6.
-9.
-12.
-15.
Log τ_d(E,J)
0.
2000.
4000.
6000.
E [cm^{-1}]

Figure 2.

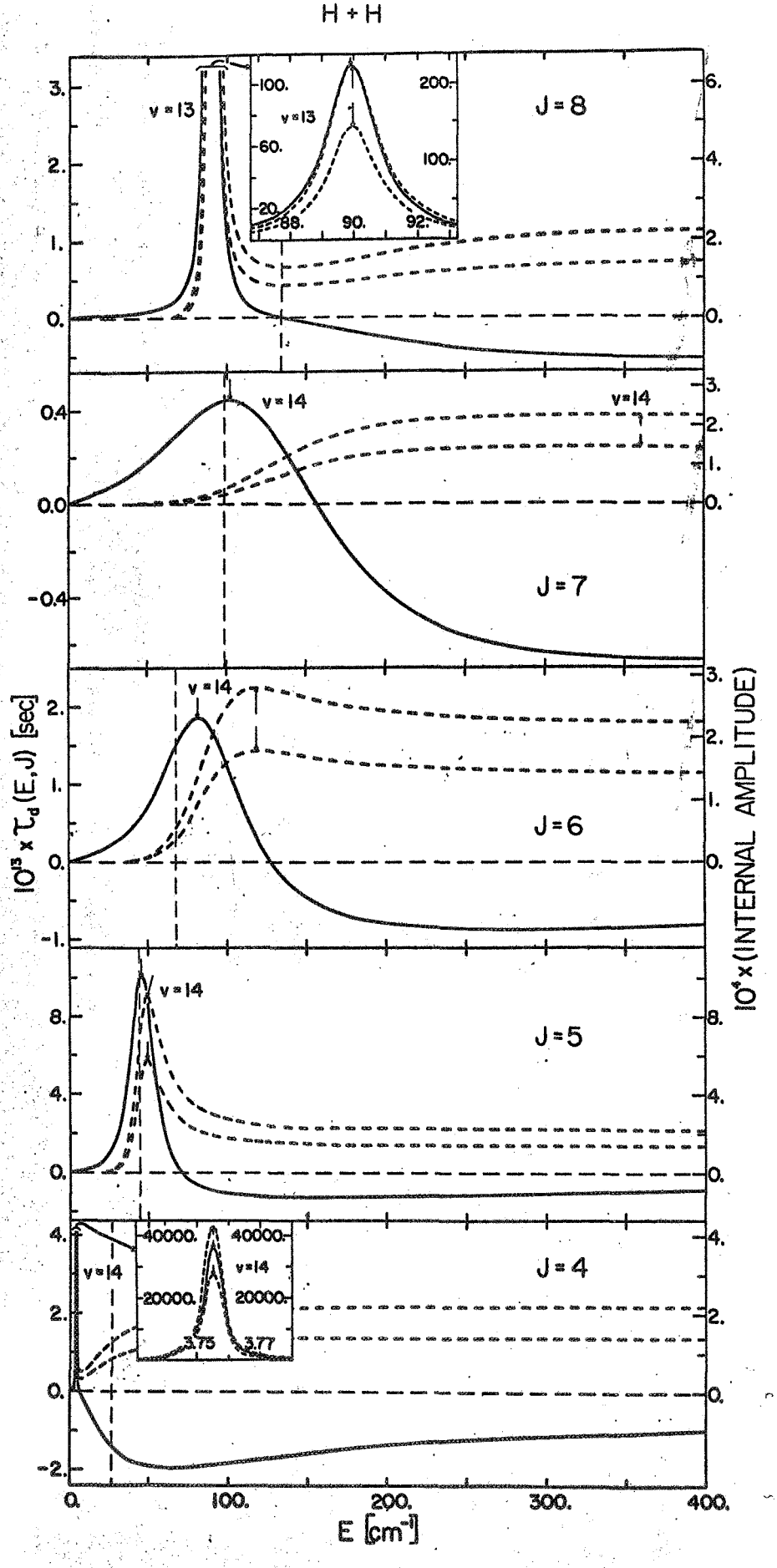
H + H
J = 8
v = 13
J = 7
v = 14
J = 6
J = 5
J = 4
$10^{13} \times \tau_d(E,J)$ [sec]
$10^4 \times$ (INTERNAL AMPLITUDE)
E [cm^{-1}]

Figure 3

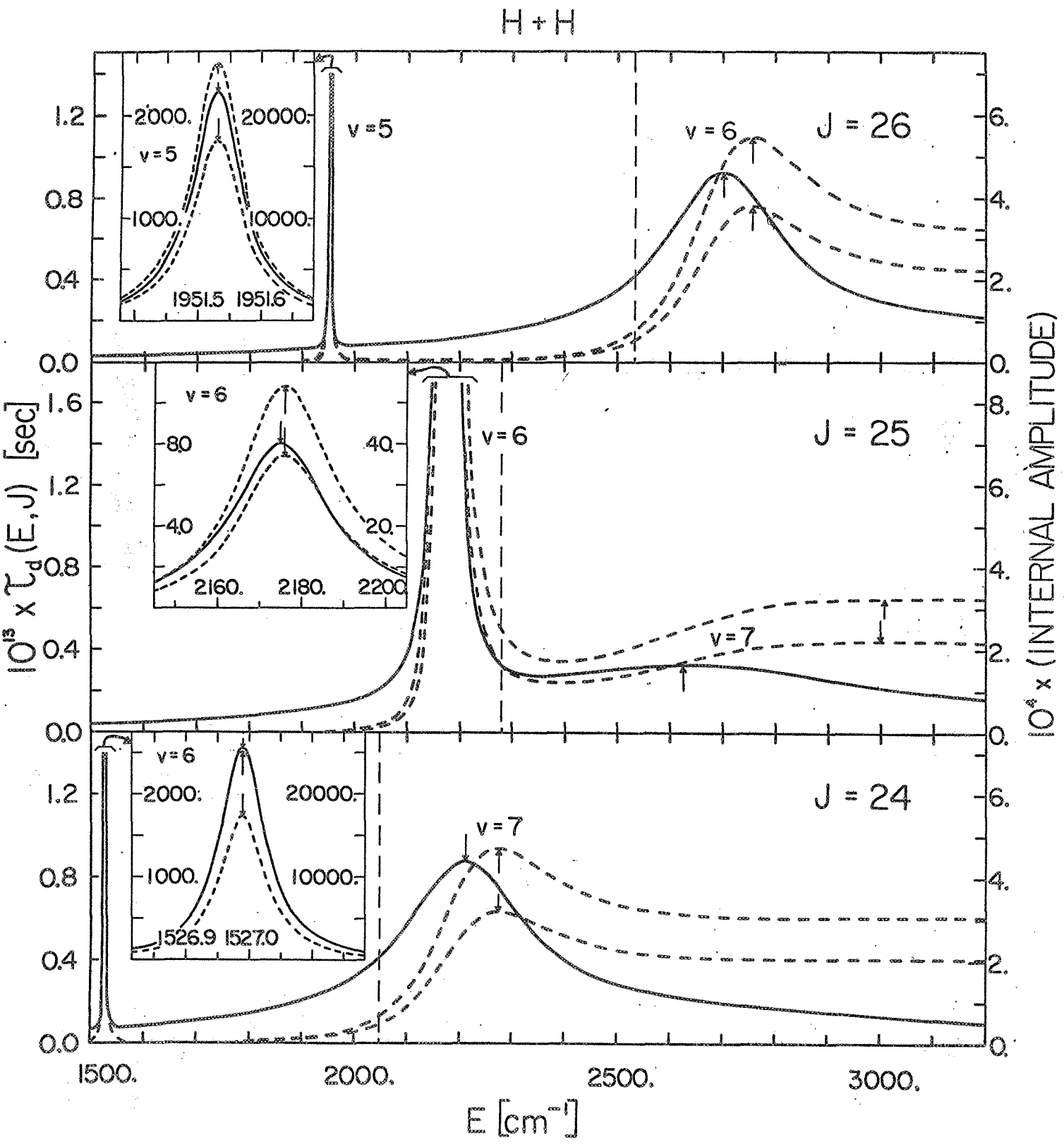
H + H
J = 26
J = 25
J = 24
v = 5
v = 6
v = 7
2000.
20000.
1000.
10000.
1951.5
1951.6
80.
40.
4.0
20.
2160.
2180.
2200.
1526.9
1527.0
1.2
0.8
0.4
0.0
1.6
6.
4.
2.
8.
1500.
2000.
2500.
3000.
E [cm⁻¹]
10¹³ x τd(E,J) [sec]
10⁴ x (INTERNAL AMPLITUDE)

Figure 4.

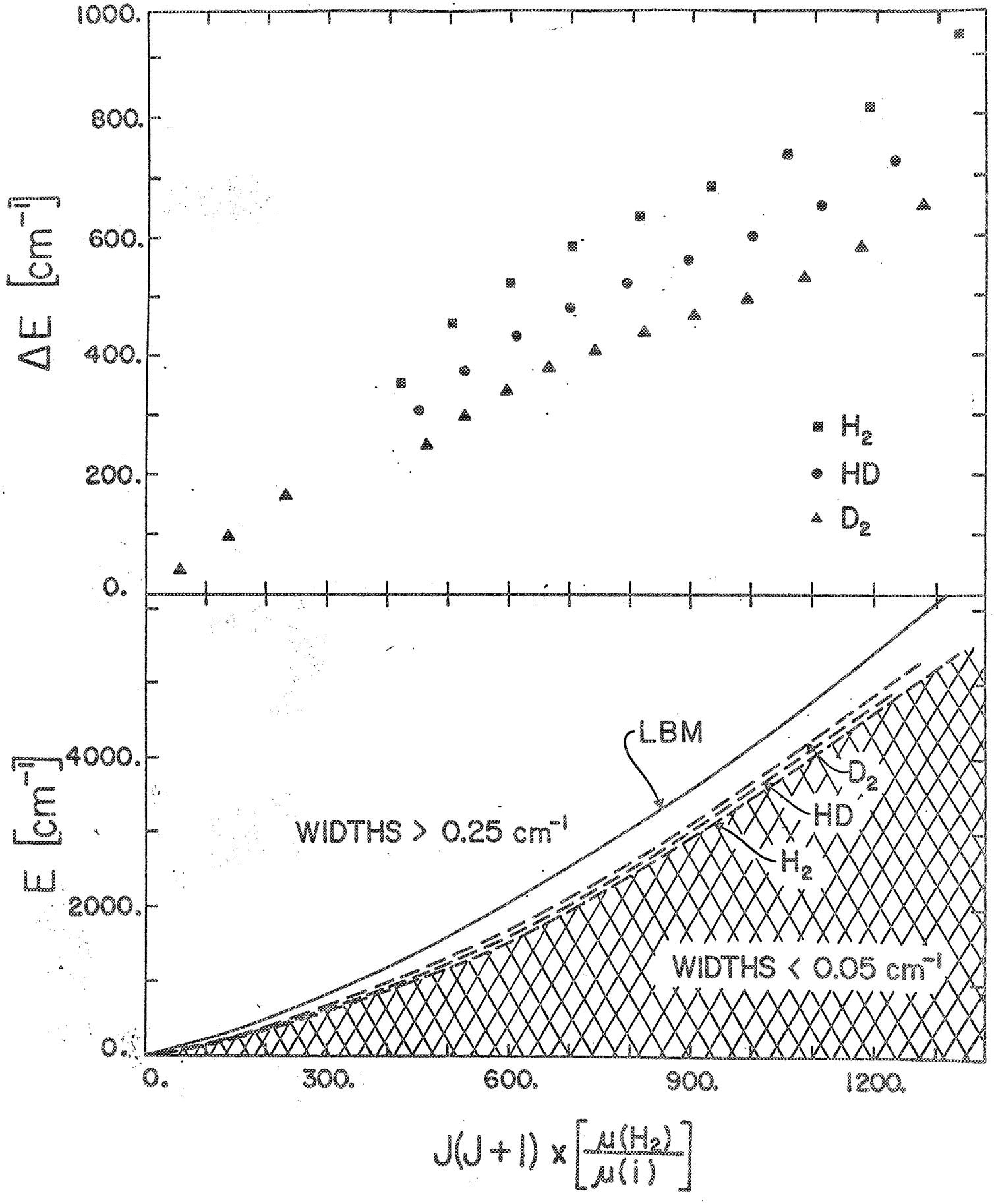
1000.
800.
600.
400.
200.
0.
ΔE [cm⁻¹]
H₂
HD
D₂
4000.
2000.
0.
E [cm⁻¹]
LBM
D₂
HD
H₂
WIDTHS > 0.25 cm⁻¹
WIDTHS < 0.05 cm⁻¹
0.
300.
600.
900.
1200.
J(J+1) x [μ(H₂)/μ(i)]

Figure 5.

8. EIGENVALUES AND CERTAIN EXPECTATION VALUES FOR ALL BOUND AND QUASI-BOUND LEVELS OF GROUND-STATE ($X\ ^1\Sigma_g^+$) H_2, HD AND D_2

This chapter is reprinted from University of Wisconsin Theoretical Chemistry Institute Report WIS-TCI-387 (1971).

EIGENVALUES AND CERTAIN EXPECTATION VALUES FOR ALL BOUND AND QUASIBOUND LEVELS OF GROUND-STATE ($X\ ^1\Sigma_g^+$) H_2, HD and D_2*

Robert J. Le Roy†

Theoretical Chemistry Institute and Department of Chemistry
University of Wisconsin, Madison, Wisconsin 53706

ABSTRACT

The eigenvalues, and the expectation values of R, R^2, R^{-2} and kinetic energy have been calculated for all vibrational-rotational levels of ground-state ($X\ ^1\Sigma_g^+$) H_2, HD and D_2, from the relativistic, adiabatic potential of Kołos and Wolniewicz. The widths Γ are also given for all quasibound levels for which $0.05 < \Gamma \lesssim 100$ cm^{-1}.

- - - - - - - - - - -

*Work supported by National Science Foundation Grant GB-16665 and National Aeronautics and Space Administration Grant NGL 50-002-001.

†National Research Council of Canada Scholarship holder, 1969-71; present address: Department of Physics, University of Toronto, Toronto 181, Ontario, Canada.

I. INTRODUCTION

A detailed knowledge of the properties of the vibrational-rotational level spectra of diatomic molecules is required for a proper understanding of many simple chemical processes. For example, the computed eigenvalues of the bound levels of ground-state H_2 were used by McElwain and Pritchard in theoretical studies of the dissociation of a diatomic gas.[1] Another case is the orbiting resonance theory of atomic recombination, which requires a knowledge of the energy, width, and average internuclear distance of each of the quasibound levels contributing to the recombination.[2] This information is also of predictive interest in relation to possible spectroscopic and atomic scattering experiments.[3]

The Kołos and Wolniewicz (KW) calculation[4] of the internuclear potential for ground-state molecular hydrogen aroused considerable interest, as it yielded the first ab initio potential to achieve "spectroscopic" accuracy. Their work was shortly followed by a number of independent computations of the potential's vibrational eigenvalue spectrum,[5-9] which showed that the fully-corrected relativistic, adiabatic potential[4] had a dissociation energy some 4 cm^{-1} greater than the best existing experimental value.[10] This result was rather unsettling, as it appeared to contradict the variational principle's assertion that a calculation such as that of KW[4] must give a lower bound to the ground-state dissociation energy. However, this discrepancy has since been resolved by improved measurements, and the present best experimental dissociation

energy, obtained from Stwalley's[11] reanalysis of Herzberg's[12] new data, is 0.7 ($\pm$ 0.5) cm^{-1} greater than the theoretical value.[12]

Waech and Bernstein[8] previously calculated the energies of all the vibrational-rotational levels of ground-state H_2 from the KW potential.[4] However, they only used the clamped nuclei (Born-Oppenheimer) potential, and omitted both the diagonal correction for nuclear motion (adiabatic correction) and the relativistic correction. In addition, they (incorrectly) used the reduced mass of the atoms rather than that of the nuclei.[9] Because of the great deal of interest in this system,[13] it seems timely to conduct a more thorough study of the properties of the bound and quasibound levels of the hydrogen isotopes, using the fully corrected KW potential and the correct (nuclear) reduced mass. The eigenvalues, and the expectation values of R, R^2, R^{-2} and kinetic energy for all the bound and quasibound levels of ground-state H_2, HD and D_2 are presented below. These results should be considered in conjunction with a recent study of properties of the quasibound levels.[3]

II. METHODS OF CALCULATION

The interpolation and extrapolation over the computed[4] values of the clamped nuclei potential and its relativistic and adiabatic corrections to obtain the smoothed potential used in the present calculations, is described in sections IIIB and C of Ref. (9). One additional point to be noted is that the adiabatic correction is scaled by the inverse of the nuclear reduced mass, so that the total non-centrifugal potential

is slightly different for different isotopes. The radial Schrödinger equation for the bound states was solved in the manner described in section IIIA of Ref. (9); the only difference is that the present calculations consider $J \neq 0$ levels, so a term $J(J+1)/z^2$ is added to the scaled effective potential.[9] Up to 4000 mesh points were used in the numerical integration, starting at an inner boundary of 0.3 au and using increments of 0.0070, 0.0056 and 0.0048 au for H_2, HD and D_2 respectively.

The only physical constants required for the eigenvalue[9] and expectation value computations are the masses of the atomic nuclei and of the electron, all in amu(^{12}C=12), and the energy conversion factor 1 au = 219474.62 cm^{-1}. The masses used, taken from Cohen and DuMond,[14] are given in Table I. The effect of small errors in these masses on the computed level energies would vary as the expectation value of the kinetic energy, as is shown by Eq. (2) of Ref. (9).[15]

Quasibound levels with very small widths, i.e., $\Gamma < 0.05$ cm^{-1}, were located using the Airy-function boundary condition method described in Ref. (3). For the broad quasibounds lying near the centrifugal barrier maxima, the level energies were placed at the peaks of the internal amplitude function (see Ref. (3)), and hence should correspond to the spectroscopically observed level positions. The quasibound widths Γ, on the other hand, were calculated from the height of the

TABLE I: Electron, proton, and deuteron masses in amu(^{12}C=12).[14]

m_e	M_p	M_d
5.48597×10^{-4}	1.00727663	2.0135560

resonance peaks in the collisional time-delay functions, $\tau_d(E,J)$:[3,17]

$$\Gamma = 2 \,/\, [\pi \, c \, \tau_d(\max)] \quad .$$

The expectation value $\langle f \rangle$ of a quantity $f(R)$, is

$$\langle f \rangle = \int_0^{R_+} |\Psi_{v,J}(R)|^2 \, f(R) \, dR \Big/ \int_0^{R_+} |\Psi_{v,J}(R)|^2 \, dR \quad ,$$

where $\Psi_{v,J}(R)$ is the computed exact radial eigenfunction. For the truly bound levels lying below the dissociation limit, $R_+ = \infty$,[18] while for the quasibound levels lying behind the centrifugal barrier, $R_+ = R_{max}(J)$, the position of the barrier maximum for the given J. The expectation values for the quasibound levels were evaluated at the level energies yielded by the Airy-function boundary condition method.[3] This means that they are not reported for levels lying above the centrifugal barrier maxima. More seriously, it implies that the expectation values for the broad levels may not precisely correspond to the reported eigenvalues, since the latter were defined by the maxima in the internal amplitude function. However, relative to the width of these levels, such inconsistencies are of negligible importance.[3]

Annotated FORTRAN listings of the computer programs used in the present calculations are available in Ref.(19). The bound-state eigenvalue program incorporates a number of improvements over the Cooley-Cashion program on which it is based,[20] and is quite efficient.

For example, the calculation of the eigenvalues and expectation values for the 348 levels of H_2 required slightly less than 2 minutes on a Univac 1108 computer.

III. RESULTS AND DISCUSSION

Tables II-XVI give the eigenvalues, and the expectation values of kinetic energy, R, R^2 and R^{-2} for all the bound and quasibound levels of the ground $(X\ ^1\Sigma_g^+)$ states of H_2, HD and D_2, calculated from the relativistic-adiabatic Kołos and Wolniewiz[4] potential. Energies are given in cm^{-1} and lengths in au (1 au = 0.52917715 Å [16]); the expectation values of R^2 and R^{-2} are given as $\langle R^2\rangle^{\frac{1}{2}}$ and $\langle R^{-2}\rangle^{-\frac{1}{2}}$ to simplify comparisons. In the eigenvalue tables, the widths of all quasibound levels for which $0.05 < \Gamma \lesssim 100\ cm^{-1}$ are given in parentheses; levels for which $\Gamma \gtrsim 100\ cm^{-1}$ are omitted. The heights and positions of the centrifugal barrier maxima corresponding to the different J values are listed under U(max) (in the eigenvalue tables) and R(max) (in the $\langle R\rangle$, $\langle R^2\rangle^{\frac{1}{2}}$ and $\langle R^{-2}\rangle^{-\frac{1}{2}}$ tables), respectively. The solid line across each of the expectation-value tables separates the results for bound levels from those for the quasibound; the functional dependence of these quantities on v and J is clearly continuous across these artificial boundaries.

The results presented in Tables II-XVI were obtained from the ab initio potential alone, without any empirical corrections.

However, in Ref. (9) it was shown that even after taking the theoretical non-adiabatic corrections into account, the KW potential still required small adjustments in order to bring the calculated vibrational eigenvalues into agreement with experiment. The recent improved measurements of the molecular dissociation energy have since shown that the better of the two possible derived corrections[9] is that labeled Δ''. Although Δ'' is not the final word (see, e.g., the discussion in section IV of Ref. (3)), it is a fair measure of the direction and magnitude of the small errors in the ab initio potential.[4] The effect on the eigenvalues of Table II of adding Δ'' to the KW potential is seen in Table XVII; clearly the deeper eigenvalues are unperturbed, while the higher ones are shifted deeper by as much as a few cm^{-1}. However, the derivation of Δ'' depends on an assumed knowledge of the non-adiabatic effects,[21] and the latter may not readily be incorporated into the expectation values. Therefore, the effects of small residual errors in the ab initio potential are not considered further.

Acknowledgements

The author gratefully acknowledges discussions with Professor R. B. Bernstein which helped shape the course of this work.

v \ J	0	1	2	3	4	5	6	7	8	9	10	11	12	13	14	U(MAX)
0	-36117.5	-31955.4	-28028.8	-24332.6	-20863.9	-17621.6	-14607.1	-11824.3	-9280.4	-6986.8	-4960.1	-3223.2	-1808.1	-759.5	-139.2	0.0
1	-35999.0	-31842.9	-27922.0	-24231.5	-20768.4	-17531.8	-14523.0	-11746.1	-9208.4	-6921.3	-4901.6	-3172.6	-1766.5	-728.6	-122.1	1.1
2	-35763.1	-31618.7	-27709.4	-24030.3	-20578.5	-17353.2	-14355.8	-11590.7	-9065.2	-6791.1	-4785.5	-3072.2	-1684.1	-667.9	-89.6	5.3
3	-35412.0	-31285.2	-27393.0	-23730.9	-20295.9	-17087.5	-14107.3	-11359.7	-8852.5	-6597.9	-4613.6	-2923.8	-1563.0	-579.8	-45.4	13.5
4	-34948.6	-30845.1	-26975.8	-23336.1	-19923.5	-16737.4	-13779.9	-11055.7	-8573.0	-6344.4	-4388.3	-2730.2	-1406.1	-467.6	3.8	26.2
5	-34377.2	-30302.5	-26461.5	-22849.6	-19464.7	-16306.4	-13377.2	-10682.0	-8229.7	-6033.6	-4113.0	-2494.8	-1217.2	-336.4	49. (20.)	44.4
6	-33702.4	-29662.0	-25854.5	-22275.7	-18923.7	-15798.6	-12903.0	-10242.5	-7826.6	-5669.5	-3791.7	-2221.8	-1001.2	-192.6		68.0
7	-32929.8	-28928.8	-25159.9	-21619.3	-18305.3	-15218.4	-12361.8	-9741.6	-7368.1	-5256.6	-3429.0	-1916.4	-764.0	-45.1		98.4
8	-32065.2	-28108.7	-24383.3	-20885.8	-17614.7	-14571.1	-11758.7	-9184.3	-6859.2	-4799.9	-3030.2	-1584.1	-512.8	90.0(1.9)		134.5
9	-31115.1	-27207.8	-23530.7	-20080.9	-16857.5	-13862.1	-11098.9	-8575.8	-6305.0	-4304.8	-2601.0	-1231.8	-256.4	206. (57.)		178.8
10	-30086.0	-26232.4	-22608.0	-19210.5	-16039.4	-13096.9	-10388.1	-7921.6	-5711.3	-3777.1	-2147.9	-866.9	-6.7			230.2
11	-28984.8	-25189.0	-21621.7	-18280.7	-15166.3	-12281.4	-9631.8	-7227.5	-5083.8	-3223.1	-1677.8	-498.5	215.5(2.6)			289.1
12	-27818.1	-24084.3	-20577.9	-17297.6	-14244.2	-11421.3	-8835.9	-6499.3	-4428.7	-2649.3	-1198.5	-137.7	399. (74.)			357.1
13	-26592.8	-22924.6	-19483.1	-16267.3	-13279.0	-10522.7	-8006.4	-5743.1	-3752.4	-2062.9	-719.0	199.4				434.7
14	-25315.4	-21716.4	-18343.3	-15195.9	-12276.7	-9591.3	-7149.1	-4965.1	-3061.5	-1471.8	-250.0	481. (18.)				520.8
15	-23992.5	-20465.9	-17164.6	-14089.2	-11243.1	-8633.0	-6270.0	-4171.4	-2363.0	-884.6	193.8					617.9
16	-22630.2	-19179.1	-15952.9	-12953.0	-10183.9	-7653.6	-5375.1	-3368.7	-1664.7	-312.0	586.0(2.9)					725.3
17	-21234.5	-17861.8	-14713.8	-11792.8	-9104.5	-6658.7	-4470.5	-2563.8	-975.0	232.4	903. (94.)					844.1
18	-19811.1	-16519.6	-13452.7	-10614.1	-8010.7	-5654.0	-3562.4	-1764.0	-304.0	725.9(0.5)						974.8
19	-18365.4	-15157.6	-12174.9	-9422.1	-6907.6	-4645.4	-2657.3	-977.5	335.0	1127. (58.)						1118.2
20	-16902.6	-13781.1	-10885.4	-8221.8	-5800.7	-3638.7	-1762.3	-214.2	921.0(0.2)							1274.7
21	-15427.5	-12394.7	-9589.1	-7018.4	-4695.3	-2640.1	-885.1	513.4	1409. (39.)							1445.2
22	-13944.7	-11003.1	-8290.6	-5816.7	-3597.0	-1656.1	-35.2	1185.3(0.1)								1630.3
23	-12458.6	-9610.7	-6994.4	-4621.7	-2511.3	-694.3	775.2	1757. (30.)								1830.6
24	-10973.3	-8221.7	-5705.2	-3438.3	-1444.5	236.6	1527.0(0.1)									2047.4
25	-9492.7	-6840.2	-4427.2	-2271.9	-403.6	1124.8	2176. (27.)									2281.1
26	-8020.7	-5470.2	-3165.2	-1128.0	603.2	1951.5(0.1)										2533.1
27	-6560.7	-4115.7	-1923.7	-13.1	1564.5	2674. (25.)										2804.2
28	-5116.3	-2780.7	-708.0	1064.9	2462.5(0.1)											3095.5
29	-3691.1	-1469.5	476.2	2095.8	3255. (25.)											3408.4
30	-2288.5	-186.6	1621.8	3062.4(0.2)												3744.4
31	-912.2	1063.0	2719.3	3925. (24.)												4104.9
32	434.1	2273.1	3753.4(0.2)													4491.8
33	1746.0	3435.6	4689. (20.)													4906.8
34	3018.4	4537.4(0.1)														5353.4
35	4245.1	5550. (14.)														5834.6
36	5416.3(0.1)															6354.8
37	6513.6(5.8)															6919.5
38	7514. (80.)															7539.2
39	8456.(165.)															8230.5

H_2

$E(v, J)$

TABLE II

v	0	1	2	3	4	5	6	7	8	9	10	11	12	13	14
0	1078.6	3040.0	4770.2	6274.8	7555.3	8608.9	9427.5	9996.4	10291.7	10277.8	9903.7	9097.9	7753.6	5712.7	2754.7
1	1077.0	3035.6	4763.1	6264.9	7542.6	8593.2	9408.6	9973.9	10264.9	10245.8	9864.9	9050.0	7692.8	5631.9	2635.2
2	1074.0	3026.8	4748.7	6245.1	7517.2	8562.0	9371.0	9929.0	10211.5	10181.6	9787.2	8953.9	7570.5	5468.7	2387.9
3	1069.5	3013.7	4727.3	6215.5	7479.3	8515.3	9314.7	9861.8	10131.3	10085.4	9670.3	8809.0	7385.3	5219.4	1988.0
4	1063.5	2996.4	4699.0	6176.3	7429.0	8453.3	9239.9	9772.5	10024.5	9956.9	9514.0	8614.4	7134.9	4877.7	1491.5
5	1056.1	2974.9	4663.9	6127.6	7366.6	8376.3	9146.9	9661.2	9891.3	9796.1	9317.6	8368.6	6815.8	4432.1	
6	1047.3	2949.4	4622.2	6069.8	7292.3	8284.6	9036.0	9528.1	9731.6	9602.8	9080.3	8069.5	6422.1	3860.9	
7	1037.2	2920.0	4574.1	6003.2	7206.5	8178.5	8907.4	9373.5	9545.4	9376.5	8800.8	7714.0	5945.6	3114.1	
8	1025.8	2886.9	4519.9	5927.9	7109.5	8058.3	8761.4	9197.4	9332.5	9116.4	8477.1	7297.4	5371.8	2175.6	
9	1013.2	2850.2	4459.8	5844.3	7001.7	7924.4	8598.4	9000.0	9092.6	8821.6	8106.5	6812.5	4675.5		
10	999.5	2810.2	4394.1	5752.8	6883.3	7777.1	8418.4	8781.1	8825.1	8490.4	7684.9	6248.0	3797.8		
11	984.6	2766.9	4323.0	5653.7	6754.8	7616.7	8221.6	8540.5	8529.0	8120.4	7206.4	5584.8	2681.6		
12	968.7	2720.7	4246.9	5547.2	6616.5	7443.4	8007.9	8277.8	8203.0	7707.9	6661.6	4786.1			
13	951.9	2671.6	4165.9	5433.7	6468.5	7257.2	7777.2	7992.0	7844.9	7247.5	6035.2	3786.2			
14	934.2	2619.8	4080.3	5313.4	6311.1	7058.2	7529.0	7681.8	7451.7	6731.3	5299.0	2527.1			
15	915.7	2565.5	3990.3	5186.4	6144.3	6846.3	7262.6	7345.5	7018.7	6146.2	4398.7				
16	896.4	2508.9	3896.1	5053.0	5968.2	6621.0	6976.9	6980.1	6538.9	5469.6	3198.0				
17	876.4	2449.9	3797.8	4913.2	5782.6	6381.7	6670.2	6581.7	6000.9	4656.7					
18	855.8	2388.8	3695.5	4767.0	5587.2	6127.5	6340.0	6144.3	5385.1	3601.6					
19	834.5	2325.7	3589.2	4614.3	5381.5	5856.8	5982.8	5658.1	4654.1						
20	812.6	2260.5	3478.9	4454.8	5164.6	5567.7	5593.3	5106.2	3721.3						
21	790.1	2193.2	3364.5	4288.0	4935.4	5257.0	5163.0	4456.3	2530.2						
22	767.0	2123.9	3245.9	4113.4	4692.1	4920.1	4677.8	3635.0							
23	743.4	2052.5	3122.6	3930.0	4432.2	4550.0	4110.1	2538.3							
24	719.2	1978.8	2994.3	3736.5	4152.0	4134.6	3397.6								
25	694.4	1902.7	2860.2	3530.8	3845.5	3650.7	2425.4								
26	668.9	1823.9	2719.5	3310.2	3502.9	3046.2									
27	642.7	1741.9	2570.7	3070.1	3105.2	2218.1									
28	615.6	1656.2	2411.9	2802.7	2610.7										
29	587.6	1566.1	2239.9	2493.8	1935.4										
30	558.5	1470.4	2049.4	2111.1											
31	527.9	1367.3	1830.5	1592.8											
32	495.6	1253.8	1561.7												
33	460.9	1124.5	1199.8												
34	423.0	968.2													
35	380.1	761.8													
36	329.3														
37	264.5														
38	210.4														

H_2

$\langle E(v,J)-U(R)\rangle$

TABLE III

J \ V	0	1	2	3	4	5	6	7	8	9	10	11	12	13	14	R(MAX)
0	1.4487	1.5454	1.6461	1.7518	1.8635	1.9828	2.1119	2.2537	2.4127	2.5961	2.8153	3.0908	3.4636	4.0366	5.2238	∞
1	1.4509	1.5476	1.6485	1.7543	1.8662	1.9857	2.1150	2.2572	2.4167	2.6008	2.8212	3.0984	3.4748	4.0567	5.2886	12.193
2	1.4553	1.5522	1.6532	1.7593	1.8715	1.9914	2.1213	2.2641	2.4247	2.6102	2.8328	3.1139	3.4978	4.0982	5.4340	9.916
3	1.4618	1.5589	1.6603	1.7668	1.8795	2.0000	2.1307	2.2746	2.4367	2.6245	2.8505	3.1376	3.5331	4.1638	5.7127	8.900
4	1.4704	1.5679	1.6697	1.7767	1.8901	2.0115	2.1432	2.2886	2.4527	2.6436	2.8744	3.1698	3.5821	4.2588	6.0465	8.382
5	1.4810	1.5791	1.6814	1.7891	1.9032	2.0257	2.1588	2.3061	2.4729	2.6677	2.9049	3.2114	3.6467	4.3927		8.011
6	1.4937	1.5923	1.6953	1.8038	1.9190	2.0427	2.1775	2.3271	2.4972	2.6971	2.9423	3.2633	3.7303	4.5849		7.492
7	1.5084	1.6076	1.7114	1.8208	1.9372	2.0625	2.1993	2.3517	2.5259	2.7320	2.9873	3.3271	3.8377	4.8856		7.366
8	1.5250	1.6250	1.7297	1.8402	1.9580	2.0850	2.2243	2.3801	2.5592	2.7728	3.0409	3.4052	3.9779	5.3187		7.163
9	1.5435	1.6443	1.7500	1.8618	1.9812	2.1103	2.2525	2.4122	2.5972	2.8201	3.1042	3.5010	4.1679			6.855
10	1.5637	1.6655	1.7724	1.8856	2.0068	2.1384	2.2839	2.4484	2.6404	2.8746	3.1791	3.6202	4.4502			6.806
11	1.5857	1.6885	1.7967	1.9116	2.0350	2.1694	2.3187	2.4887	2.6893	2.9375	3.2683	3.7730	4.8715			6.582
12	1.6094	1.7134	1.8231	1.9398	2.0656	2.2032	2.3570	2.5336	2.7445	3.0102	3.3761	3.9802				6.385
13	1.6348	1.7401	1.8514	1.9702	2.0987	2.2400	2.3991	2.5835	2.8070	3.0951	3.5097	4.2835				6.301
14	1.6618	1.7685	1.8817	2.0028	2.1344	2.2800	2.4452	2.6391	2.8781	3.1956	3.6830	4.7369				6.133
15	1.6903	1.7987	1.9139	2.0377	2.1728	2.3234	2.4958	2.7011	2.9598	3.3174	3.9248					6.028
16	1.7204	1.8306	1.9480	2.0748	2.2141	2.3704	2.5515	2.7709	3.0550	3.4711	4.3088					5.916
17	1.7521	1.8643	1.9842	2.1144	2.2583	2.4214	2.6130	2.8500	3.1686	3.6784						5.797
18	1.7853	1.8997	2.0225	2.1566	2.3059	2.4770	2.6814	2.9412	3.3093	3.9928						5.685
19	1.8201	1.9369	2.0630	2.2014	2.3571	2.5379	2.7583	3.0486	3.4945							5.580
20	1.8564	1.9760	2.1057	2.2493	2.4124	2.6050	2.8460	3.1797	3.7668							5.482
21	1.8944	2.0170	2.1509	2.3004	2.4724	2.6797	2.9483	3.3494	4.1692							5.384
22	1.9340	2.0601	2.1988	2.3552	2.5381	2.7643	3.0718	3.5934								5.293
23	1.9754	2.1053	2.2496	2.4143	2.6108	2.8621	3.2295	3.9691								5.194
24	2.0185	2.1530	2.3037	2.4785	2.6923	2.9789	3.4524									5.103
25	2.0636	2.2033	2.3617	2.5490	2.7857	3.1265	3.8007									5.019
26	2.1108	2.2565	2.4242	2.6273	2.8963	3.3323										4.928
27	2.1604	2.3131	2.4922	2.7163	3.0345	3.6521										4.844
28	2.2124	2.3737	2.5672	2.8206	3.2247											4.753
29	2.2674	2.4390	2.6515	2.9493	3.5160											4.669
30	2.3257	2.5103	2.7490	3.1238												4.585
31	2.3879	2.5894	2.8675	3.3857												4.494
32	2.4550	2.6795	3.0246													4.410
33	2.5283	2.7864	3.2556													4.319
34	2.6099	2.9233														4.221
35	2.7037	3.1166														4.123
36	2.8175															4.018
37	2.9667															3.898
38	3.1173															3.765

H_2

$\langle R \rangle$

TABLE IV

J \ V	0	1	2	3	4	5	6	7	8	9	10	11	12	13	14	R(MAX)
0	1.4584	1.5729	1.6903	1.8115	1.9381	2.0715	2.2140	2.3688	2.5404	2.7357	2.9660	3.2513	3.6316	4.2071	5.3909	∞
1	1.4606	1.5752	1.6926	1.8141	1.9407	2.0744	2.2172	2.3723	2.5444	2.7404	2.9719	3.2590	3.6428	4.2270	5.4559	12.193
2	1.4650	1.5797	1.6974	1.8191	1.9461	2.0802	2.2235	2.3794	2.5524	2.7499	2.9837	3.2746	3.6657	4.2681	5.6028	9.916
3	1.4715	1.5865	1.7045	1.8266	1.9541	2.0888	2.2330	2.3900	2.5646	2.7643	3.0015	3.2983	3.7009	4.3331	5.8882	8.900
4	1.4801	1.5955	1.7139	1.8366	1.9648	2.1003	2.2456	2.4041	2.5808	2.7836	3.0256	3.3307	3.7498	4.4272	6.1972	8.382
5	1.4907	1.6066	1.7256	1.8489	1.9780	2.1147	2.2614	2.4218	2.6012	2.8081	3.0563	3.3724	3.8142	4.5598		8.011
6	1.5034	1.6199	1.7396	1.8637	1.9938	2.1318	2.2803	2.4431	2.6259	2.8378	3.0941	3.4245	3.8973	4.7505		7.492
7	1.5181	1.6352	1.7557	1.8809	2.0122	2.1518	2.3024	2.4681	2.6550	2.8731	3.1395	3.4884	4.0041	5.0509		7.366
8	1.5347	1.6526	1.7740	1.9003	2.0331	2.1746	2.3277	2.4968	2.6887	2.9144	3.1935	3.5666	4.1432	5.4657		7.163
9	1.5532	1.6719	1.7944	1.9220	2.0565	2.2002	2.3562	2.5294	2.7272	2.9622	3.2572	3.6624	4.3317			6.855
10	1.5734	1.6931	1.8168	1.9460	2.0824	2.2286	2.3880	2.5660	2.7710	3.0174	3.3326	3.7814	4.6124			6.806
11	1.5954	1.7162	1.8413	1.9722	2.1108	2.2599	2.4233	2.6070	2.8206	3.0810	3.4223	3.9336	5.0189			6.582
12	1.6192	1.7412	1.8678	2.0006	2.1417	2.2941	2.4622	2.6526	2.8766	3.1545	3.5305	4.1397				6.385
13	1.6445	1.7679	1.8963	2.0312	2.1752	2.3315	2.5049	2.7033	2.9400	3.2402	3.6643	4.4386				6.301
14	1.6715	1.7965	1.9267	2.0641	2.2114	2.3721	2.5518	2.7598	3.0121	3.3415	3.8374	4.8755				6.133
15	1.7001	1.8267	1.9591	2.0993	2.2503	2.4161	2.6033	2.8228	3.0948	3.4641	4.0778					6.028
16	1.7303	1.8588	1.9935	2.1369	2.2921	2.4638	2.6599	2.8937	3.1912	3.6184	4.4536					5.916
17	1.7620	1.8926	2.0300	2.1770	2.3370	2.5157	2.7225	2.9741	3.3061	3.8257						5.797
18	1.7953	1.9282	2.0686	2.2196	2.3853	2.5723	2.7921	3.0667	3.4480	4.1365						5.685
19	1.8301	1.9656	2.1095	2.2651	2.4373	2.6343	2.8704	3.1756	3.6342							5.580
20	1.8665	2.0049	2.1526	2.3136	2.4936	2.7026	2.9597	3.3084	3.9054							5.482
21	1.9046	2.0462	2.1983	2.3654	2.5547	2.7789	3.0638	3.4798	4.2981							5.384
22	1.9443	2.0895	2.2467	2.4211	2.6217	2.8651	3.1893	3.7245								5.293
23	1.9857	2.1352	2.2982	2.4813	2.6958	2.9648	3.3492	4.0931								5.194
24	2.0290	2.1832	2.3531	2.5466	2.7789	3.0839	3.5739									5.103
25	2.0743	2.2339	2.4119	2.6184	2.8743	3.2341	3.9181									5.019
26	2.1217	2.2877	2.4754	2.6984	2.9873	3.4426										4.928
27	2.1714	2.3449	2.5446	2.7893	3.1285	3.7608										4.844
28	2.2236	2.4062	2.6210	2.8959	3.3220											4.753
29	2.2789	2.4724	2.7070	3.0277	3.6137											4.669
30	2.3375	2.5447	2.8067	3.2060												4.585
31	2.4001	2.6251	2.9280	3.4700												4.494
32	2.4677	2.7169	3.0890													4.410
33	2.5416	2.8262	3.3234													4.319
34	2.6241	2.9664														4.221
35	2.7191	3.1635														4.123
36	2.8348															4.018
37	2.9865															3.898
38	3.1405															3.765

H_2

$\langle R^2 \rangle^{1/2}$

TABLE V

J \ V	0	1	2	3	4	5	6	7	8	9	10	11	12	13	14	R(MAX)
0	1.4193	1.4561	1.4949	1.5364	1.5813	1.6303	1.6850	1.7472	1.8199	1.9079	2.0193	2.1693	2.3906	2.7727	3.7144	∞
1	1.4215	1.4583	1.4973	1.5390	1.5839	1.6332	1.6880	1.7505	1.8236	1.9121	2.0244	2.1758	2.4000	2.7897	3.7738	12.193
2	1.4258	1.4629	1.5021	1.5440	1.5892	1.6388	1.6941	1.7571	1.8310	1.9206	2.0346	2.1889	2.4191	2.8249	3.9075	9.916
3	1.4323	1.4697	1.5092	1.5514	1.5971	1.6472	1.7032	1.7670	1.8421	1.9334	2.0500	2.2089	2.4484	2.8809	4.1621	8.900
4	1.4409	1.4787	1.5186	1.5613	1.6076	1.6584	1.7152	1.7803	1.8568	1.9505	2.0707	2.2361	2.4892	2.9623	4.5588	8.382
5	1.4516	1.4898	1.5303	1.5736	1.6206	1.6723	1.7302	1.7967	1.8753	1.9720	2.0970	2.2709	2.5430	3.0781		8.011
6	1.4644	1.5031	1.5442	1.5883	1.6361	1.6889	1.7482	1.8164	1.8976	1.9980	2.1291	2.3144	2.6125	3.2465		7.492
7	1.4790	1.5184	1.5603	1.6052	1.6540	1.7081	1.7690	1.8394	1.9236	2.0287	2.1675	2.3675	2.7024	3.5139		7.366
8	1.4956	1.5358	1.5784	1.6243	1.6743	1.7298	1.7926	1.8657	1.9535	2.0643	2.2128	2.4324	2.8203	3.9663		7.163
9	1.5141	1.5550	1.5986	1.6456	1.6970	1.7542	1.8192	1.8952	1.9876	2.1053	2.2661	2.5118	2.9820			6.855
10	1.5343	1.5762	1.6208	1.6690	1.7219	1.7810	1.8486	1.9282	2.0259	2.1522	2.3288	2.6107	3.2265			6.806
11	1.5563	1.5991	1.6449	1.6945	1.7492	1.8105	1.8810	1.9648	2.0689	2.2058	2.4031	2.7381	3.6405			6.582
12	1.5800	1.6239	1.6709	1.7221	1.7786	1.8425	1.9164	2.0052	2.1170	2.2673	2.4925	2.9125				6.385
13	1.6053	1.6503	1.6988	1.7517	1.8104	1.8771	1.9550	2.0497	2.1710	2.3386	2.6032	3.1784				6.301
14	1.6322	1.6785	1.7285	1.7833	1.8445	1.9145	1.9970	2.0988	2.2319	2.4224	2.7473	3.6407				6.133
15	1.6607	1.7084	1.7601	1.8170	1.8809	1.9547	2.0428	2.1531	2.3012	2.5236	2.9520					6.028
16	1.6907	1.7399	1.7935	1.8528	1.9199	1.9980	2.0926	2.2136	2.3814	2.6511	3.3014					5.916
17	1.7222	1.7731	1.8287	1.8907	1.9614	2.0447	2.1472	2.2816	2.4764	2.8243						5.797
18	1.7553	1.8080	1.8659	1.9309	2.0057	2.0951	2.2073	2.3593	2.5935	3.0977						5.685
19	1.7899	1.8446	1.9051	1.9735	2.0532	2.1498	2.2743	2.4499	2.7478							5.580
20	1.8261	1.8830	1.9463	2.0187	2.1041	2.2097	2.3499	2.5598	2.9799							5.482
21	1.8638	1.9232	1.9898	2.0667	2.1589	2.2757	2.4373	2.7015	3.3766							5.384
22	1.9031	1.9653	2.0356	2.1179	2.2184	2.3497	2.5418	2.9080								5.293
23	1.9442	2.0094	2.0841	2.1728	2.2836	2.4344	2.6743	3.2637								5.194
24	1.9870	2.0558	2.1355	2.2319	2.3561	2.5345	2.8628									5.103
25	2.0317	2.1045	2.1903	2.2963	2.4383	2.6597	3.1850									5.019
26	2.0784	2.1560	2.2490	2.3673	2.5345	2.8345										4.928
27	2.1273	2.2106	2.3124	2.4470	2.6533	3.1270										4.844
28	2.1787	2.2687	2.3818	2.5394	2.8161											4.753
29	2.2329	2.3311	2.4591	2.6521	3.0814											4.669
30	2.2903	2.3988	2.5476	2.8033												4.585
31	2.3514	2.4734	2.6536	3.0420												4.494
32	2.4171	2.5575	2.7924													4.410
33	2.4887	2.6561	3.0036													4.319
34	2.5679	2.7807														4.221
35	2.6582	2.9596														4.123
36	2.7666															4.018
37	2.9093															3.898
38	3.0785															3.765

H_2

$\langle R^{-2} \rangle^{-1/2}$

TABLE VI

v / J	0	1	2	3	4	5	6	7	8	9	10	11	12	13	14	15	16	17	U(MAX)
0	-36405.4	-32772.5	-29317.2	-26035.8	-22926.0	-19986.2	-17216.5	-14617.9	-12193.0	-9946.5	-7885.0	-6018.1	-4358.6	-2923.3	-1734.9	-823.6	-229.2	-2.5	0.0
1	-36316.1	-32687.1	-29235.5	-25957.9	-22851.8	-19915.7	-17149.7	-14554.8	-12133.8	-9891.2	-7833.8	-5971.3	-4316.5	-2886.5	-1704.1	-799.7	-213.9	0.4(0.4)	0.7
2	-36138.3	-32516.9	-29072.9	-25802.7	-22703.9	-19775.2	-17016.5	-14429.1	-12015.7	-9781.0	-7731.8	-5878.1	-4232.9	-2813.4	-1642.9	-752.5	-184.1	7.0(11.)	3.5
3	-35873.0	-32263.2	-28830.4	-25571.3	-22483.5	-19565.8	-16818.1	-14241.8	-11839.8	-9616.9	-7580.2	-5739.6	-4108.7	-2705.1	-1552.5	-683.4	-141.5	32. (50.)	9.2
4	-35522.1	-31927.5	-28509.7	-25265.3	-22192.1	-19288.9	-16555.9	-13994.4	-11607.6	-9400.4	-7380.2	-5557.2	-3945.4	-2563.0	-1434.6	-594.2	-88.8		18.1
5	-35087.9	-31512.3	-28113.0	-24886.9	-21831.8	-18946.7	-16231.8	-13688.8	-11320.9	-9133.3	-7133.7	-5332.8	-3744.9	-2389.2	-1291.4	-487.5	-30.2		30.7
6	-34573.2	-31020.1	-27642.9	-24438.6	-21405.1	-18541.6	-15848.4	-13327.4	-10982.0	-8817.9	-6843.0	-5068.6	-3509.6	-2186.1	-1125.6	-366.8	26.8(0.8)		47.3
7	-33981.2	-30454.1	-27102.5	-23923.3	-20914.8	-18076.2	-15408.2	-12912.7	-10593.6	-8456.8	-6510.7	-4767.2	-3242.1	-1956.7	-940.5	-236.2	78. (27.)		68.0
8	-33315.4	-29817.8	-26495.0	-23344.4	-20364.2	-17553.8	-14914.3	-12447.9	-10158.6	-8052.8	-6139.7	-4431.7	-2945.6	-1704.3	-740.0	-101.4			94.1
9	-32579.9	-29114.9	-25824.2	-22705.3	-19756.5	-16977.7	-14370.0	-11935.9	-9680.1	-7609.2	-5733.1	-4065.3	-2623.5	-1432.8	-528.9	29.6			124.2
10	-31778.6	-28349.4	-25093.9	-22009.7	-19095.5	-16351.4	-13778.7	-11380.4	-9161.5	-7129.3	-5294.5	-3671.5	-2279.7	-1146.5	-312.7	141.7(8.9)			159.8
11	-30915.7	-27525.4	-24308.1	-21261.6	-18385.0	-15678.5	-13144.0	-10784.7	-8606.3	-6616.7	-4827.5	-3254.2	-1918.2	-850.2	-98.4	248. (79.)			201.9
12	-29995.8	-26647.1	-23470.8	-20464.9	-17628.7	-14963.0	-12469.7	-10152.7	-8018.2	-6075.1	-4335.8	-2817.4	-1543.8	-549.9	103.8				248.3
13	-29023.1	-25718.9	-22586.2	-19623.6	-16830.7	-14208.5	-11759.5	-9488.1	-7401.1	-5508.3	-3823.5	-2365.5	-1161.3	-252.2	274. (11.)				301.7
14	-28002.2	-24744.9	-21658.5	-18741.9	-15994.9	-13419.0	-11017.2	-8794.5	-6758.6	-4920.2	-3294.8	-1903.2	-776.7	33.9					361.7
15	-26937.4	-23729.4	-20691.8	-17823.5	-15125.1	-12598.3	-10246.7	-8076.0	-6094.7	-4315.1	-2754.0	-1435.6	-396.5	294.2(0.3)					428.8
16	-25833.0	-22676.6	-19690.0	-16872.7	-14225.3	-11750.3	-9451.8	-7336.3	-5413.4	-3697.0	-2206.0	-968.4	-29.2	505. (35.)					502.0
17	-24693.2	-21590.6	-18657.3	-15893.1	-13299.3	-10878.7	-8636.2	-6579.3	-4718.8	-3070.3	-1655.6	-508.1	313.1						583.7
18	-23522.2	-20475.4	-17597.5	-14888.7	-12350.7	-9987.2	-7803.7	-5808.8	-4014.9	-2439.6	-1108.6	-62.7	606.2(9.0)						673.0
19	-22323.8	-19334.8	-16514.3	-13863.0	-11383.4	-9079.5	-6958.1	-5028.8	-3306.0	-1810.0	-571.3	356.6							770.4
20	-21102.0	-18172.5	-15411.3	-12819.8	-10400.8	-8159.3	-6103.1	-4243.4	-2596.6	-1186.6	-51.4	729.5(2.0)							876.6
21	-19860.3	-16992.1	-14292.2	-11762.4	-9406.4	-7230.1	-5242.4	-3456.5	-1891.4	-575.9	440.5	1032. (70.)							991.9
22	-18602.2	-15797.0	-13160.2	-10694.2	-8403.7	-6295.4	-4379.9	-2672.4	-1195.7	14.7	886.5(0.6)								1116.7
23	-17331.2	-14590.5	-12018.5	-9618.6	-7396.0	-5358.8	-3519.4	-1895.8	-515.4	575.1	1253. (47.)								1251.3
24	-16050.3	-13375.7	-10870.5	-8538.6	-6386.6	-4423.9	-2665.1	-1131.7	142.1	1088.6(0.2)									1396.3
25	-14762.6	-12155.7	-9719.0	-7457.5	-5378.8	-3494.3	-1821.2	-385.8	767.1	1520. (34.)									1552.2
26	-13470.9	-10933.3	-8567.1	-6378.3	-4376.1	-2573.9	-992.5	334.9	1343.7(0.1)										1719.2
27	-12178.1	-9711.3	-7417.5	-5304.1	-3381.7	-1666.7	-184.6	1021.0	1836. (27.)										1898.2
28	-10886.7	-8492.4	-6273.2	-4237.9	-2399.3	-777.3	595.8	1656.8(0.1)											2089.6
29	-9599.3	-7279.2	-5137.0	-3182.9	-1432.6	89.1	1339.5	2207. (24.)											2293.8
30	-8318.3	-6074.3	-4011.5	-2142.4	-486.0	926.0	2031.5(0.1)												2511.8
31	-7045.9	-4880.1	-2899.8	-1119.8	435.7	1724.6	2637. (22.)												2744.1
32	-5784.6	-3699.3	-1804.7	-119.2	1326.3	2470.3(0.1)													2991.3
33	-4536.6	-2534.4	-729.5	854.9	2177.4	3129. (21.)													3254.4
34	-3304.0	-1388.1	322.2	1796.9	2975.0(0.2)														3534.2
35	-2089.2	-263.2	1346.3	2698.8	3687. (21.)														3831.7
36	-894.5	837.1	2337.7	3547.5(0.2)															4148.0
37	277.6	1909.2	3289.2	4313. (19.)															4484.3
38	1424.5	2948.6	4189.1(0.2)																4841.5
39	2543.0	3949.2	5011. (15.)																5222.0
40	3629.0	4901.4(0.1)																	5627.9
41	4679.4	5784.2(9.3)																	6061.4
42	5685.5																		6525.8
43	6634.6(3.4)																		7025.5
44	7507. (52.)																		7568.2
45	8327.(190.)																		8165.0

HD

E(v,J)

TABLE VII

J \ v	0	1	2	3	4	5	6	7	8	9	10	11	12	13	14	15	16	17
0	936.9	2663.3	4215.1	5596.6	6809.8	7854.6	8728.1	9424.1	9933.1	10239.9	10323.3	10153.4	9692.0	8883.5	7654.1	5892.6	3460.9	316.0
1	935.9	2660.4	4210.4	5590.1	6801.6	7844.5	8716.0	9409.9	9916.7	10220.7	10300.9	10127.1	9660.9	8846.0	7607.7	5833.5	3380.1	247.8
2	933.9	2654.7	4201.0	5577.1	6785.0	7824.3	8692.0	9381.7	9883.8	10182.5	10256.2	10074.7	9598.6	8770.7	7514.6	5714.4	3215.8	
3	931.0	2646.1	4187.0	5557.8	6760.3	7794.1	8656.0	9339.4	9834.5	10125.2	10189.3	9995.9	9504.9	8657.4	7374.0	5533.6	2961.2	
4	927.1	2634.7	4168.5	5532.1	6727.6	7754.0	8608.2	9283.3	9769.0	10048.8	10100.0	9890.7	9379.7	8505.4	7184.4	5287.9	2602.3	
5	922.2	2620.6	4145.4	5500.2	6686.8	7704.1	8548.7	9213.3	9687.3	9953.6	9988.3	9759.0	9222.3	8313.9	6944.1	4972.7	2106.4	
6	916.5	2603.9	4117.9	5462.2	6638.2	7644.7	8477.7	9129.8	9589.6	9839.5	9854.4	9600.6	9032.4	8081.6	6650.1	4579.9	1500.9	
7	909.8	2584.5	4086.2	5418.3	6582.1	7575.8	8395.4	9032.9	9476.0	9706.6	9698.0	9415.1	8808.9	7806.8	6298.3	4096.1		
8	902.3	2562.5	4050.3	5368.6	6518.4	7497.7	8302.0	8922.7	9346.7	9554.9	9519.0	9202.0	8550.8	7486.8	5882.9	3494.8		
9	893.9	2538.2	4010.4	5313.3	6447.5	7410.7	8197.7	8799.5	9201.8	9384.4	9317.1	8960.6	8256.5	7118.0	5394.7	2743.2		
10	884.8	2511.5	3966.6	5252.6	6369.6	7315.0	8082.8	8663.4	9041.4	9194.9	9092.0	8689.9	7923.8	6695.2	4817.9	1890.1		
11	874.8	2482.5	3919.1	5186.7	6284.9	7210.7	7957.4	8514.5	8865.4	8986.3	8842.9	8388.4	7549.7	6210.6	4122.3			
12	864.2	2451.4	3868.0	5115.7	6193.7	7098.1	7821.7	8353.0	8673.9	8758.2	8569.0	8054.1	7130.0	5652.2	3252.3			
13	852.9	2418.3	3813.6	5039.9	6096.0	6977.4	7676.0	8178.9	8466.6	8510.0	8269.1	7684.2	6657.9	4999.6	2173.8			
14	840.9	2383.2	3755.8	4959.5	5992.2	6848.8	7520.2	7992.2	8243.1	8241.0	7941.5	7274.9	6123.3	4216.4				
15	828.3	2346.3	3695.0	4874.6	5882.4	6712.4	7354.5	7792.6	8003.1	7950.1	7583.5	6820.5	5509.4	3214.0				
16	815.1	2307.7	3631.2	4785.4	5766.7	6568.3	7178.8	7580.1	7745.6	7635.6	7191.7	6312.9	4785.2					
17	801.4	2267.4	3564.6	4692.0	5645.3	6416.6	6992.9	7354.1	7469.8	7295.5	6761.1	5738.0	3893.8					
18	787.2	2225.6	3495.3	4594.6	5518.3	6257.2	6796.7	7114.0	7174.3	6926.5	6284.1	5070.9	2709.8					
19	772.5	2182.2	3423.4	4493.2	5385.6	6090.0	6589.8	6858.7	6857.0	6524.2	5749.0	4263.0						
20	757.3	2137.5	3348.9	4387.9	5247.3	5914.9	6371.5	6587.1	6515.4	6082.0	5135.3	3195.2						
21	741.7	2091.4	3271.9	4278.7	5103.2	5731.5	6141.1	6297.3	6145.5	5589.3	4402.4							
22	725.7	2044.0	3192.5	4165.6	4953.2	5539.2	5897.5	5987.0	5741.2	5028.4	3451.9							
23	709.4	1995.3	3110.6	4048.4	4797.1	5337.4	5639.1	5652.6	5293.4	4364.7								
24	692.6	1945.3	3026.3	3927.2	4634.3	5125.2	5363.6	5289.2	4786.4	3517.3								
25	675.5	1894.1	2939.4	3801.5	4464.3	4901.2	5068.1	4888.6	4190.3	2435.8								
26	658.1	1841.6	2849.8	3671.2	4286.4	4663.5	4748.2	4437.2	3435.9									
27	640.2	1787.7	2757.5	3535.7	4099.4	4409.6	4396.8	3908.6	2433.6									
28	622.0	1732.4	2662.1	3394.5	3901.9	4135.6	4002.4	3243.9										
29	603.4	1675.6	2563.3	3246.7	3691.6	3835.7	3542.4	2341.0										
30	584.4	1617.1	2460.7	3091.2	3465.5	3499.9	2965.9											
31	564.9	2353.8	2926.2	1556.8	3218.9	3109.6	2181.1											
32	544.9	1494.4	2241.7	2749.6	2943.6	2622.3												
33	524.3	1429.6	2123.3	2557.5	2624.4	1956.4												
34	503.1	1361.9	1996.9	2343.8	2227.6													
35	481.1	1290.6	1860.1	2097.1	1687.6													
36	458.3	1214.9	1708.6	1792.3														
37	434.2	1133.3	1534.8	1379.3														
38	408.8	1043.5	1321.8															
39	381.5	941.4	1036.2															
40	351.6	818.4																
41	318.0	656.6																
42	278.2																	
43	227.8																	
44	181.4																	

HD

$\langle E - U(R) \rangle$

TABLE VIII

J\V	0	1	2	3	4	5	6	7	8	9	10	11	12	13	14	15	16	17	R(MAX)
0	1.4422	1.5255	1.6117	1.7014	1.7952	1.8939	1.9988	2.1111	2.2329	2.3672	2.5179	2.6913	2.8972	3.1526	3.4891	3.9799	4.8536	9.6164	∞
1	1.4439	1.5272	1.6134	1.7032	1.7971	1.8960	2.0009	2.1135	2.2355	2.3700	2.5211	2.6952	2.9020	3.1587	3.4978	3.9941	4.8869	9.2974	12.988
2	1.4471	1.5305	1.6170	1.7069	1.8010	1.9001	2.0053	2.1182	2.2407	2.3758	2.5277	2.7029	2.9115	3.1711	3.5154	4.0231	4.9571		10.404
3	1.4520	1.5356	1.6222	1.7124	1.8067	1.9062	2.0118	2.1252	2.2484	2.3844	2.5376	2.7146	2.9258	3.1899	3.5423	4.0682	5.0734		9.323
4	1.4584	1.5423	1.6292	1.7196	1.8144	1.9143	2.0205	2.1346	2.2587	2.3959	2.5508	2.7303	2.9452	3.2154	3.5792	4.1318	5.2568		8.807
5	1.4665	1.5506	1.6378	1.7287	1.8239	1.9244	2.0313	2.1463	2.2716	2.4104	2.5675	2.7501	2.9699	3.2480	3.6273	4.2175	5.5635		8.163
6	1.4760	1.5605	1.6481	1.7395	1.8353	1.9364	2.0442	2.1603	2.2871	2.4278	2.5876	2.7741	3.0000	3.2885	3.6881	4.3315	5.9597		8.000
7	1.4871	1.5720	1.6601	1.7520	1.8485	1.9505	2.0593	2.1767	2.3052	2.4482	2.6113	2.8026	3.0361	3.3376	3.7640	4.4854			7.501
8	1.4997	1.5850	1.6737	1.7662	1.8635	1.9664	2.0764	2.1954	2.3259	2.4717	2.6387	2.8359	3.0787	3.3967	3.8587	4.7032			7.389
9	1.5137	1.5996	1.6888	1.7821	1.8803	1.9843	2.0957	2.2165	2.3493	2.4984	2.6701	2.8742	3.1285	3.4675	3.9780	5.0209			7.254
10	1.5291	1.6156	1.7055	1.7997	1.8988	2.0041	2.1171	2.2399	2.3755	2.5284	2.7056	2.9182	3.1865	3.5526	4.1322	5.4283			6.930
11	1.5458	1.6330	1.7237	1.8188	1.9191	2.0258	2.1406	2.2657	2.4045	2.5619	2.7456	2.9683	3.2542	3.6560	4.3426				6.829
12	1.5639	1.6518	1.7434	1.8395	1.9411	2.0494	2.1662	2.2940	2.4365	2.5991	2.7905	3.0256	3.3336	3.7843	4.6518				6.801
13	1.5833	1.6720	1.7645	1.8618	1.9648	2.0749	2.1940	2.3249	2.4716	2.6403	2.8409	3.0912	3.4277	3.9491	5.1051				6.565
14	1.6039	1.6935	1.7871	1.8856	1.9902	2.1023	2.2241	2.3585	2.5100	2.6859	2.8975	3.1667	3.5413	4.1734					6.369
15	1.6258	1.7163	1.8111	1.9110	2.0174	2.1317	2.2565	2.3949	2.5521	2.7364	2.9615	3.2548	3.6827	4.5133					6.302
16	1.6489	1.7405	1.8365	1.9380	2.0463	2.1632	2.2913	2.4343	2.5982	2.7925	3.0342	3.3591	3.8682						6.173
17	1.6732	1.7659	1.8633	1.9665	2.0770	2.1967	2.3286	2.4770	2.6487	2.8551	3.1178	3.4860	4.1307						6.067
18	1.6986	1.7926	1.8915	1.9967	2.1096	2.2325	2.3687	2.5233	2.7042	2.9256	3.2156	3.6475	4.5442						5.966
19	1.7252	1.8205	1.9212	2.0284	2.1440	2.2706	2.4118	2.5736	2.7657	3.0058	3.3327	3.8685							5.865
20	1.7530	1.8498	1.9522	2.0618	2.1805	2.3112	2.4583	2.6286	2.8343	3.0985	3.4788	4.2108							5.764
21	1.7819	1.8803	1.9848	2.0970	2.2192	2.3546	2.5084	2.6890	2.9117	3.2084	3.6732								5.669
22	1.8120	1.9122	2.0189	2.1340	2.2601	2.4009	2.5627	2.7560	3.0004	3.3434	3.9648								5.585
23	1.8432	1.9453	2.0546	2.1730	2.3035	2.4507	2.6221	2.8309	3.1045	3.5198									5.495
24	1.8756	1.9799	2.0920	2.2141	2.3497	2.5044	2.6873	2.9161	3.2309	3.7772									5.411
25	1.9093	2.0159	2.1311	2.2574	2.3990	2.5626	2.7600	3.0153	3.3940	4.1546									5.327
26	1.9442	2.0535	2.1722	2.3033	2.4519	2.6263	2.8421	3.1348	3.6274										5.248
27	1.9804	2.0926	2.2153	2.3520	2.5089	2.6967	2.9370	3.2872	3.9823										5.164
28	2.0179	2.1335	2.2607	2.4040	2.5709	2.7758	3.0503	3.5021											5.086
29	2.0569	2.1763	2.3087	2.4598	2.6391	2.8665	3.1936	3.8343											5.007
30	2.0975	2.2211	2.3596	2.5200	2.7152	2.9742	3.3933												4.935
31	2.1397	2.4140	2.5858	2.2682	2.8018	3.1090	3.7001												4.856
32	2.1838	2.3179	2.4723	2.6587	2.9038	3.2950													4.783
33	2.2298	2.3706	2.5356	2.7411	3.0304	3.5795													4.710
34	2.2781	2.4269	2.6051	2.8372	3.2027														4.632
35	2.3290	2.4874	2.6829	2.9550	3.4629														4.559
36	2.3829	2.5532	2.7725	3.1128															4.481
37	2.4403	2.6260	2.8807	3.3476															4.408
38	2.5020	2.7085	3.0225																4.335
39	2.5692	2.8058	3.2286																4.251
40	2.6437	2.9290																	4.167
41	2.7289	3.1010																	4.077
42	2.8312																		3.982
43	2.9636																		3.875
44	3.1085																		3.752

HD

⟨R⟩

TABLE IX

J \ V	0	1	2	3	4	5	6	7	8	9	10	11	12	13	14	15	16	17	R(MAX)
0	1.4506	1.5495	1.6504	1.7539	1.8609	1.9722	2.0891	2.2131	2.3462	2.4913	2.6525	2.8359	3.0511	3.3145	3.6570	4.1495	5.0176	10.1738	∞
1	1.4523	1.5512	1.6521	1.7557	1.8628	1.9743	2.0913	2.2155	2.3488	2.4942	2.6558	2.8398	3.0559	3.3206	3.6656	4.1635	5.0505	9.5347	12.988
2	1.4555	1.5546	1.6556	1.7594	1.8666	1.9783	2.0957	2.2202	2.3540	2.5000	2.6625	2.8476	3.0654	3.3330	3.6831	4.1923	5.1201		10.404
3	1.4604	1.5596	1.6609	1.7649	1.8724	1.9845	2.1023	2.2273	2.3618	2.5088	2.6725	2.8594	3.0799	3.3519	3.7099	4.2369	5.2357		9.323
4	1.4668	1.5663	1.6678	1.7722	1.8801	1.9926	2.1110	2.2368	2.3723	2.5204	2.6859	2.8753	3.0994	3.3774	3.7467	4.2997	5.4187		8.807
5	1.4749	1.5746	1.6765	1.7813	1.8897	2.0028	2.1219	2.2486	2.3853	2.5351	2.7027	2.8953	3.1242	3.4101	3.7945	4.3844	5.7288		8.163
6	1.4844	1.5845	1.6868	1.7921	1.9011	2.0150	2.1349	2.2628	2.4009	2.5527	2.7230	2.9196	3.1546	3.4507	3.8550	4.4971	6.1026		8.000
7	1.4955	1.5960	1.6988	1.8047	1.9144	2.0291	2.1501	2.2794	2.4193	2.5734	2.7470	2.9484	3.1909	3.4999	3.9304	4.6491			7.501
8	1.5081	1.6091	1.7124	1.8189	1.9295	2.0452	2.1675	2.2983	2.4403	2.5972	2.7748	2.9820	3.2337	3.5590	4.0243	4.8647			7.389
9	1.5221	1.6236	1.7276	1.8349	1.9463	2.0632	2.1869	2.3196	2.4640	2.6242	2.8065	3.0207	3.2838	3.6297	4.1425	5.1755			7.254
10	1.5375	1.6396	1.7443	1.8525	1.9650	2.0831	2.2085	2.3433	2.4905	2.6546	2.8425	3.0651	3.3422	3.7146	4.2951	5.5622			6.930
11	1.5542	1.6570	1.7626	1.8717	1.9854	2.1050	2.2323	2.3695	2.5199	2.6886	2.8830	3.1157	3.4101	3.8176	4.5033				6.829
12	1.5723	1.6759	1.7823	1.8925	2.0076	2.1289	2.2582	2.3982	2.5524	2.7263	2.9285	3.1735	3.4897	3.9450	4.8068				6.801
13	1.5917	1.6961	1.8035	1.9149	2.0315	2.1546	2.2864	2.4295	2.5880	2.7681	2.9795	3.2396	3.5839	4.1086	5.2415				6.565
14	1.6124	1.7177	1.8262	1.9389	2.0571	2.1824	2.3168	2.4636	2.6270	2.8143	3.0368	3.3157	3.6974	4.3301					6.369
15	1.6343	1.7406	1.8503	1.9645	2.0846	2.2121	2.3497	2.5005	2.6698	2.8656	3.1015	3.4042	3.8383	4.6627					6.302
16	1.6574	1.7648	1.8758	1.9917	2.1138	2.2440	2.3850	2.5405	2.7166	2.9225	3.1750	3.5089	4.0228						6.173
17	1.6817	1.7902	1.9028	2.0204	2.1448	2.2780	2.4229	2.5839	2.7679	2.9860	3.2594	3.6360	4.2818						6.067
18	1.7071	1.8170	1.9311	2.0508	2.1777	2.3142	2.4636	2.6310	2.8243	3.0575	3.3579	3.7974	4.6823						5.966
19	1.7338	1.8451	1.9610	2.0829	2.2126	2.3529	2.5075	2.6822	2.8868	3.1387	3.4757	4.0169							5.865
20	1.7616	1.8744	1.9923	2.1166	2.2496	2.3941	2.5547	2.7382	2.9565	3.2325	3.6223	4.3521							5.764
21	1.7905	1.9051	2.0251	2.1522	2.2888	2.4382	2.6057	2.7997	3.0351	3.3434	3.8165								5.669
22	1.8206	1.9371	2.0594	2.1896	2.3303	2.4853	2.6610	2.8678	3.1251	3.4794	4.1046								5.585
23	1.8519	1.9704	2.0954	2.2290	2.3744	2.5360	2.7215	2.9440	3.2305	3.6565									5.495
24	1.8844	2.0052	2.1331	2.2706	2.4213	2.5906	2.7880	3.0307	3.3584	3.9124									5.411
25	1.9181	2.0414	2.1727	2.3146	2.4714	2.6500	2.8620	3.1315	3.5228	4.2800									5.327
26	1.9531	2.0792	2.2141	2.3611	2.5252	2.7149	2.9457	3.2527	3.7562										5.248
27	1.9893	2.1186	2.2578	2.4106	2.5833	2.7867	3.0423	3.4069	4.1037										5.164
28	2.0270	2.1598	2.3037	2.4634	2.6465	2.8674	3.1577	3.6229											5.086
29	2.0661	2.2029	2.3523	2.5201	2.7161	2.9600	3.3031	3.9502											5.007
30	2.1068	2.2481	2.4040	2.5814	2.7937	3.0698	3.5048												4.935
31	2.1492	2.4591	2.6485	2.2956	2.8822	3.2072	3.8087												4.856
32	2.1934	2.3458	2.5183	2.7229	2.9864	3.3958													4.783
33	2.2396	2.3991	2.5827	2.8071	3.1157	3.6794													4.710
34	2.2881	2.4560	2.6535	2.9053	3.2912														4.632
35	2.3393	2.5173	2.7329	3.0259	3.5522														4.559
36	2.3934	2.5841	2.8244	3.1871															4.481
37	2.4512	2.6580	2.9352	3.4242															4.408
38	2.5133	2.7420	3.0804																4.335
39	2.5811	2.8414	3.2897																4.251
40	2.6563	2.9675																	4.167
41	2.7425	3.1428																	4.077
42	2.8464																		3.982
43	2.9810																		3.875
44	3.1278																		3.752

HD

$\langle R^2 \rangle^{1/2}$

TABLE X

J \ V	0	1	2	3	4	5	6	7	8	9	10	11	12	13	14	15	16	17	R(MAX)
0	1.4168	1.4484	1.4815	1.5165	1.5537	1.5936	1.6369	1.6846	1.7379	1.7987	1.8698	1.9555	2.0629	2.2048	2.4071	2.7339	3.4074	7.3859	∞
1	1.4184	1.4501	1.4833	1.5184	1.5556	1.5956	1.6391	1.6869	1.7404	1.8014	1.8728	1.9590	2.0670	2.2100	2.4143	2.7460	3.4377	7.7005	12.988
2	1.4217	1.4535	1.4868	1.5220	1.5595	1.5997	1.6434	1.6915	1.7453	1.8068	1.8788	1.9658	2.0752	2.2204	2.4289	2.7706	3.5020		10.404
3	1.4265	1.4585	1.4921	1.5275	1.5652	1.6057	1.6497	1.6983	1.7526	1.8148	1.8878	1.9762	2.0876	2.2363	2.4514	2.8090	3.6092		9.323
4	1.4330	1.4653	1.4991	1.5348	1.5728	1.6137	1.6582	1.7073	1.7624	1.8256	1.8998	1.9900	2.1043	2.2577	2.4821	2.8633	3.7796		8.807
5	1.4410	1.4736	1.5077	1.5438	1.5823	1.6237	1.6688	1.7186	1.7746	1.8390	1.9149	2.0075	2.1254	2.2851	2.5222	2.9369	4.0656		8.163
6	1.4506	1.4835	1.5181	1.5546	1.5936	1.6356	1.6814	1.7321	1.7893	1.8551	1.9330	2.0286	2.1511	2.3190	2.5730	3.0359	4.5247		8.000
7	1.4617	1.4950	1.5300	1.5671	1.6067	1.6494	1.6960	1.7478	1.8063	1.8738	1.9543	2.0534	2.1818	2.3600	2.6365	3.1711			7.501
8	1.4743	1.5081	1.5436	1.5812	1.6215	1.6650	1.7127	1.7656	1.8257	1.8953	1.9787	2.0823	2.2178	2.4092	2.7160	3.3656			7.389
9	1.4883	1.5226	1.5587	1.5970	1.6380	1.6825	1.7312	1.7856	1.8475	1.9196	2.0065	2.1154	2.2598	2.4680	2.8169	3.6676			7.254
10	1.5037	1.5386	1.5753	1.6144	1.6563	1.7017	1.7518	1.8077	1.8717	1.9467	2.0378	2.1530	2.3084	2.5387	2.9487	4.1363			6.930
11	1.5204	1.5559	1.5934	1.6333	1.6762	1.7228	1.7743	1.8320	1.8984	1.9768	2.0727	2.1958	2.3649	2.6248	3.1315				6.829
12	1.5385	1.5747	1.6130	1.6537	1.6977	1.7456	1.7987	1.8585	1.9277	2.0100	2.1117	2.2442	2.4309	2.7322	3.4128				6.801
13	1.5579	1.5948	1.6339	1.6757	1.7208	1.7701	1.8250	1.8872	1.9596	2.0464	2.1552	2.2994	2.5090	2.8715	3.8967				6.565
14	1.5785	1.6162	1.6562	1.6991	1.7455	1.7964	1.8534	1.9182	1.9943	2.0865	2.2036	2.3626	2.6034	3.0654					6.369
15	1.6003	1.6389	1.6799	1.7240	1.7718	1.8245	1.8837	1.9516	2.0319	2.1305	2.2580	2.4360	2.7214	3.3765					6.302
16	1.6234	1.6629	1.7050	1.7503	1.7997	1.8544	1.9161	1.9876	2.0729	2.1791	2.3193	2.5227	2.8777						6.173
17	1.6476	1.6881	1.7314	1.7781	1.8292	1.8861	1.9508	2.0262	2.1174	2.2329	2.3894	2.6281	3.1062						6.067
18	1.6730	1.7146	1.7591	1.8073	1.8604	1.9198	1.9877	2.0678	2.1660	2.2929	2.4710	2.7630	3.5083						5.966
19	1.6995	1.7422	1.7881	1.8381	1.8933	1.9554	2.0272	2.1128	2.2194	2.3608	2.5686	2.9508							5.865
20	1.7272	1.7711	1.8185	1.8704	1.9279	1.9932	2.0694	2.1615	2.2785	2.4387	2.6902	3.2608							5.764
21	1.7560	1.8013	1.8503	1.9042	1.9644	2.0334	2.1146	2.2145	2.3446	2.5306	2.8537								5.669
22	1.7859	1.8327	1.8835	1.9397	2.0029	2.0760	2.1633	2.2728	2.4198	2.6433	3.1088								5.585
23	1.8170	1.8653	1.9182	1.9769	2.0436	2.1215	2.2161	2.3376	2.5075	2.7911									5.495
24	1.8492	1.8993	1.9544	2.0160	2.0866	2.1702	2.2737	2.4106	2.6136	3.0124									5.411
25	1.8827	1.9347	1.9922	2.0571	2.1323	2.2226	2.3372	2.4949	2.7503	3.3851									5.327
26	1.9174	1.9715	2.0318	2.1004	2.1809	2.2796	2.4084	2.5958	2.9494										5.248
27	1.9533	2.0098	2.0732	2.1461	2.2330	2.3420	2.4900	2.7241	3.2879										5.164
28	1.9906	2.0497	2.1167	2.1946	2.2893	2.4115	2.5867	2.9070											5.086
29	2.0293	2.0914	2.1624	2.2464	2.3507	2.4906	2.7080	3.2171											5.007
30	2.0695	2.1350	2.2108	2.3020	2.4186	2.5835	2.8783												4.935
31	2.1114	2.2621	2.3623	2.1807	2.4952	2.6988	3.1611												4.856
32	2.1549	2.2288	2.3170	2.4285	2.5845	2.8580													4.783
33	2.2005	2.2796	2.3761	2.5027	2.6941	3.1183													4.710
34	2.2482	2.3336	2.4406	2.5883	2.8429														4.632
35	2.2984	2.3914	2.5122	2.6920	3.0801														4.559
36	2.3514	2.4541	2.5939	2.8300															4.481
37	2.4078	2.5229	2.6912	3.0439															4.408
38	2.4683	2.6002	2.8173																4.335
39	2.5339	2.6903	3.0057																4.251
40	2.6064	2.8030																	4.167
41	2.6886	2.9620																	4.077
42	2.7864																		3.982
43	2.9130																		3.875
44	3.0670																		3.752

HD

$\langle R^{-2} \rangle^{-1/2}$

TABLE XI

V \ J	0	1	2	3	4	5	6	7	8	9	10	11	12	13	14	15	16	17	18	19	20	21	U(MAX)
0	-36748.1	-33754.1	-30879.3	-28121.5	-25479.1	-22950.8	-20536.0	-18234.6	-16046.8	-13973.8	-12017.4	-10180.1	-8465.7	-6878.9	-5426.1	-4114.9	-2955.5	-1960.0	-1144.6	-529.1	-138.5	-1.1	0.0
1	-36688.4	-33696.5	-30823.7	-28068.0	-25427.5	-22901.3	-20488.5	-18189.0	-16003.3	-13932.4	-11978.0	-10142.9	-8430.7	-6846.2	-5395.9	-4087.4	-2930.8	-1938.6	-1126.7	-515.4	-129.9	0.3	0.4
2	-36569.1	-33581.4	-30712.8	-27961.1	-25324.7	-22802.5	-20393.7	-18098.2	-15916.5	-13849.7	-11899.5	-10068.7	-8360.9	-6781.1	-5335.7	-4032.5	-2881.7	-1895.8	-1091.2	-488.3	-113.1	4.4	6.8) 2.0
3	-36390.8	-33409.4	-30547.0	-27801.4	-25171.1	-22654.9	-20252.1	-17962.6	-15786.9	-13726.2	-11782.3	-9957.9	-8256.8	-6684.0	-5246.0	-3950.8	-2808.7	-1832.4	-1038.6	-448.4	-88.9	20.	(28.) 5.3
4	-36154.4	-33181.4	-30327.2	-27589.7	-24967.4	-22459.2	-20064.3	-17782.8	-15615.2	-13562.6	-11627.0	-9811.2	-8119.0	-6555.6	-5127.5	-3842.9	-2712.3	-1748.9	-969.8	-396.7	-58.7		10.6
5	-35860.9	-32898.3	-30054.3	-27327.0	-24714.7	-22218.3	-19831.6	-17559.8	-15402.2	-13359.8	-11434.6	-9629.4	-7948.3	-6396.5	-4980.9	-3709.6	-2593.6	-1646.4	-885.7	-334.4	-24.6		18.2
6	-35511.5	-32561.4	-29729.7	-27014.4	-24414.0	-21927.6	-19554.4	-17294.7	-15149.0	-13118.8	-11206.0	-9413.6	-7745.8	-6208.1	-4807.3	-3552.0	-2453.6	-1526.0	-787.8	-263.2	10.2		28.0
7	-35107.9	-32172.2	-29354.6	-26653.3	-24066.7	-21594.0	-19236.6	-16988.7	-14856.9	-12840.8	-10942.4	-9165.0	-7512.7	-5991.3	-4607.9	-3371.4	-2293.6	-1389.1	-677.6	-185.2	41.	(19.2)	40.8
8	-34651.6	-31732.3	-28930.8	-26245.3	-23674.5	-21217.3	-18873.5	-16643.2	-14527.3	-12527.2	-10645.3	-8884.9	-7250.3	-5747.6	-4384.1	-3169.3	-2115.2	-1237.5	-557.0	-102.9	80.	(47.)	55.8
9	-34144.6	-31243.5	-28460.0	-25792.2	-23238.9	-20799.1	-18472.8	-16260.0	-14161.8	-12179.7	-10316.2	-8574.8	-6960.2	-5478.6	-4137.6	-2947.2	-1920.1	-1072.9	-428.4	-20.1			74.5
10	-33588.9	-30707.9	-27944.0	-25295.8	-22761.7	-20341.2	-18034.1	-15840.6	-13761.9	-11799.7	-9956.7	-8236.5	-6644.0	-5185.8	-3859.9	-2706.9	-1710.1	-897.7	-294.5	57.	6(0.2)		96.3
11	-32986.6	-30127.4	-27385.1	-24758.0	-22245.0	-19845.5	-17559.3	-15387.0	-13329.6	-11389.2	-9568.6	-7871.5	-6303.4	-4871.0	-3582.9	-2450.3	-1487.5	-714.3	-158.6	123.	(16.)		120.9
12	-32339.9	-29504.3	-26785.2	-24181.0	-21690.8	-19313.9	-17050.4	-14900.9	-12866.7	-10949.9	-9153.6	-7481.9	-5940.3	-4536.3	-3278.6	-2179.6	-1254.5	-525.4	-24.9	197.	(78.)		148.9
13	-31651.2	-28840.8	-26146.5	-23566.9	-21101.1	-18748.5	-16509.3	-14384.4	-12375.1	-10483.8	-8713.7	-7069.4	-5556.7	-4183.4	-2959.2	-1897.0	-1013.8	-334.4	100.2				181.5
14	-30922.8	-28139.3	-25471.4	-22917.9	-20478.0	-18151.3	-15938.2	-13839.5	-11856.8	-9992.8	-8251.0	-6636.1	-5154.5	-3814.6	-2626.7	-1604.9	-768.3	-145.2	205.	(11.)			217.4
15	-30157.2	-27402.0	-24762.0	-22236.2	-19823.8	-17524.6	-15339.0	-13268.2	-11313.9	-9479.0	-7767.3	-6184.0	-4735.9	-3432.3	-2283.6	-1306.1	-521.2	37.0	305.	(72.)			256.4
16	-29356.7	-26631.3	-24020.8	-21524.1	-19140.6	-16870.4	-14713.9	-12672.6	-10748.4	-8944.4	-7264.8	-5715.2	-4303.1	-3037.9	-1932.4	-1003.5	-276.4	204.	1(0.1)				300.5
17	-28523.8	-25829.5	-23249.8	-20783.7	-18430.7	-16190.9	-14065.1	-12054.8	-10162.3	-8391.1	-6745.5	-5231.8	-3858.2	-2634.8	-1575.8	-700.3	-38.7	342.	(18.)				348.7
18	-27660.8	-24999.1	-22451.6	-20017.3	-17696.1	-15488.2	-13394.5	-11416.9	-9557.8	-7821.1	-6211.6	-4736.2	-3403.6	-2225.1	-1216.7	-400.5	185.4						402.0
19	-26770.1	-24142.3	-21628.2	-19227.2	-16939.0	-14764.4	-12704.4	-10760.9	-8937.0	-7236.6	-5665.3	-4230.5	-2941.7	-1811.7	-858.4	-108.5	383.	7(1.8)					459.3
20	-25854.2	-23261.4	-20781.9	-18415.3	-16161.7	-14021.7	-11996.7	-10089.0	-8301.8	-6639.7	-5108.7	-3717.0	-2475.0	-1397.4	-504.6	169.7	546.	(44.)					521.3
21	-24915.2	-22358.5	-19914.9	-17584.0	-15366.1	-13262.0	-11273.5	-9403.1	-7654.5	-6032.5	-4544.1	-3198.1	-2006.3	-985.4	-159.8	424.	8(0.1)						588.9
22	-23955.4	-21436.0	-19029.3	-16735.3	-14554.3	-12487.5	-10537.0	-8705.4	-6997.0	-5417.2	-3973.6	-2678.2	-1538.4	-579.3	170.5	638.	(16.)						661.6
23	-22976.9	-20495.8	-18127.2	-15871.2	-13728.4	-11700.2	-9788.9	-7997.8	-6331.4	-4795.9	-3399.8	-2154.1	-1074.4	-183.5	477.9								739.7
24	-21981.8	-19540.1	-17213.6	-14993.7	-12890.2	-10901.9	-9031.4	-7282.3	-5659.8	-4170.9	-2824.9	-1634.6	-617.9	196.7	745.	7(4.9)							823.5
25	-20972.3	-18670.8	-16281.4	-14104.7	-12041.7	-10094.6	-8266.3	-6561.0	-4984.4	-3544.4	-2251.6	-1120.6	-173.1	553.6	969.	(72.)							913.2
26	-19950.2	-17589.9	-15341.6	-13206.1	-11184.8	-9280.2	-7495.6	-5835.8	-4307.2	-2918.7	-1682.5	-615.7	254.9	872.	9(1.5)								1009.2
27	-18917.4	-16599.1	-14392.9	-12299.7	-10321.3	-8460.6	-6721.2	-5108.7	-3630.4	-2296.4	-1120.7	-123.9	658.7	1136.	(49.)								1111.5
28	-17875.7	-15600.4	-13437.1	-11387.3	-9453.0	-7637.5	-5945.0	-4381.8	-2956.2	-1680.0	-569.5	349.6	1025.	6(0.5)									1220.4
29	-16826.9	-14595.3	-12476.1	-10470.7	-8581.7	-6812.8	-5168.9	-3657.2	-2287.2	-1072.5	-32.8	798.1	1331.	(34.)									1336.1
30	-15772.7	-13585.7	-11511.3	-9551.4	-7709.0	-5988.2	-4394.9	-2937.0	-1625.7	-477.0	484.3	1209.	5(0.2)										1458.9
31	-14714.7	-12573.1	-10544.4	-8631.2	-6836.7	-5165.7	-3624.9	-2223.4	-974.6	102.5	975.2	1558.	(25.)										1589.1
32	-13654.3	-11558.9	-9577.1	-7711.6	-5966.4	-4346.9	-2860.9	-1519.0	-337.0	661.2	1428.	4(0.2)											1726.7
33	-12593.2	-10544.9	-8610.8	-6794.3	-5099.9	-3533.8	-2105.1	-826.4	283.3	1192.5	1818.	(20.)											1872.4
34	-11532.7	-9532.3	-7647.0	-5880.8	-4238.8	-2728.3	-1359.8	-148.6	881.8	1685.	4(0.1)												2026.3
35	-10474.2	-8522.6	-6687.3	-4972.7	-3384.9	-1932.4	-627.7	510.7	1451.8	2115.	(17.)												2188.7
36	-9419.1	-7517.2	-5733.0	-4071.6	-2540.0	-1148.4	88.5	1147.1	1982.	6(0.1)													2359.9
37	-8368.6	-6517.4	-4785.6	-3179.1	-1706.0	-378.5	785.1	1754.2	2449.	(15.)													2540.4
38	-7324.0	-5524.6	-3846.6	-2296.8	-885.0	374.3	1458.0	2321.	5(0.1)														2730.5
39	-6286.5	-4540.1	-2917.5	-1426.7	-79.3	1106.8	2100.8	2825.	(15.)														2930.5
40	-5257.4	-3565.3	-1999.8	-570.4	708.7	1814.7	2703.	4(0.1)															3140.9
41	-4237.9	-2601.5	-1095.2	269.7	1475.7	2492.3	3242.	(14.)															3362.3
42	-3229.1	-1650.1	-205.3	1091.4	2217.7	3129.	5(0.1)																3595.1
43	-2232.3	-712.5	667.8	1891.7	2929.2	3704.	(13.)																3839.8
44	-1248.7	209.6	1522.1	2666.9	3600.	7(0.1)																	4097.1
45	-279.6	1114.5	2354.8	3411.9	4211.	(12.)																	4367.6
46	673.5	2000.3	3162.6	4118.	1(0.1)																		4651.7
47	1609.2	2864.7	3941.0	4766.	2(9.9)																		4950.4
48	2525.9	3704.9	4682.	4(0.1)																			5265.2
49	3421.5	4516.8	5370.	5(6.9)																			5597.1
50	4293.9	5294.	4(0.1)	5993.	(79.)																		5947.2
51	5139.8	6025.	6(3.7)																				6317.3
52	5955.2	6694.	(52.)																				6709.4
53	6731.	9(1.1)																					7126.8
54	7456.	(22.)																					7573.9
55	8133.	(100.)																					8056.9
56	8791.	(230.)																					8593.2

D_2

$E(v,J)$

TABLE XII

V \ J	0	1	2	3	4	5	6	7	8	9	10	11	12	13	14	15	16	17	18	19	20	21
0	767.7	2204.4	3523.7	4728.2	5819.8	6799.4	7666.6	8420.2	9057.1	9573.6	9962.7	10216.6	10323.2	10267.3	10030.3	9588.2	8907.8	7949.1	6652.1	4950.1	2747.0	178.0
1	767.2	2202.8	3521.1	4724.6	5815.3	6793.9	7660.1	8412.7	9048.5	9563.8	9951.6	10204.1	10309.0	10251.1	10011.8	9566.8	8883.0	7919.6	6616.4	4905.7	2687.6	149.9
2	766.1	2199.7	3515.9	4717.5	5806.2	6782.9	7647.1	8397.6	9031.2	9544.1	9929.4	10179.0	10280.5	10218.7	9974.8	9524.1	8833.1	7860.4	6544.9	4816.5	2567.0	
3	764.5	2195.0	3508.2	4706.9	5792.7	6766.5	7627.6	8375.1	9005.4	9514.8	9896.2	10141.3	10237.9	10170.1	9919.3	9459.8	8758.2	7771.2	6436.8	4681.2	2380.8	
4	762.3	2188.7	3498.0	4692.8	5774.7	6744.6	7601.8	8345.0	8971.0	9475.7	9851.9	10091.2	10181.0	10105.3	9845.1	9373.9	8657.9	7651.6	6291.4	4497.8	2120.2	
5	759.7	2181.0	3485.3	4675.2	5752.3	6717.3	7569.5	8307.7	8928.2	9426.9	9796.7	10028.6	10109.9	10024.2	9752.2	9266.2	8531.9	7501.0	6107.4	4263.3	1765.5	
6	756.5	2171.7	3470.1	4654.2	5725.5	6684.7	7531.0	8263.0	8877.0	9368.6	9730.6	9953.6	10024.7	9926.9	9640.6	9136.4	8379.7	7318.2	5882.9	3972.7	1357.6	
7	752.9	2161.0	3452.5	4629.8	5694.5	6646.9	7486.4	8211.1	8817.5	9300.8	9653.6	9866.3	9925.3	9813.2	9509.9	8984.3	8200.6	7102.2	5615.4	3618.3		
8	748.7	2148.8	3432.5	4602.2	5659.2	6604.0	7435.6	8152.1	8749.8	9223.6	9565.9	9766.6	9811.7	9683.1	9360.0	8809.3	7993.8	6851.4	5301.3	3186.3		
9	744.0	2135.2	3410.2	4571.3	5619.9	6556.1	7378.9	8086.1	8674.0	9137.1	9467.6	9654.7	9683.9	9536.5	9190.4	8611.0	7758.0	6563.4	4935.3	2647.4		
10	738.9	2120.2	3385.6	4537.4	5576.6	6503.2	7316.3	8013.2	8590.3	9041.4	9358.6	9530.4	9541.7	9373.2	9000.9	8388.4	7491.6	6235.4	4509.4	1993.8		
11	733.4	2103.9	3358.9	4500.4	5529.3	6445.6	7247.9	7933.6	8498.7	8936.7	9239.1	9393.9	9385.2	9192.8	8790.8	8140.8	7192.7	5863.1	4009.8			
12	727.4	2086.3	3330.0	4460.4	5478.2	6383.2	7174.0	7847.4	8399.4	8822.8	9109.1	9245.0	9214.0	8995.2	8559.3	7866.6	6858.5	5440.1	3408.4			
13	720.9	2067.5	3299.1	4417.5	5423.4	6316.3	7094.5	7754.7	8292.4	8700.1	8968.5	9083.8	9028.1	8779.6	8305.7	7564.0	6485.4	4956.8	2681.1			
14	714.1	2047.5	3266.2	4371.9	5365.1	6244.9	7009.7	7655.6	8177.9	8568.5	8817.4	8909.9	8827.0	8545.5	8028.8	7230.6	6068.5	4396.9	1796.3			
15	706.9	2026.3	3231.4	4323.6	5303.3	6169.2	6919.6	7550.2	8055.8	8428.0	8655.6	8723.2	8610.4	8291.9	7727.0	6862.9	5600.1	3733.0				
16	699.3	2004.0	3194.8	4272.8	5238.0	6089.3	6824.3	7438.7	7926.3	8278.6	8483.2	8523.5	8377.8	8017.6	7398.4	6456.4	5068.0	2896.5				
17	691.4	1980.7	3156.4	4219.4	5169.5	6005.3	6724.0	7321.0	7789.5	8120.2	8299.8	8310.2	8128.3	7721.1	7039.8	6004.4	4450.4	1974.8				
18	683.1	1956.4	3116.3	4163.6	5097.9	5917.3	6618.7	7197.3	7645.2	7952.8	8105.2	8082.9	7860.9	7400.7	6647.3	5497.2	3708.4					
19	674.5	1931.1	3074.6	4105.5	5023.1	5825.4	6508.5	7067.4	7493.6	7776.1	7899.0	7840.9	7574.2	7053.9	6214.8	4918.3	2732.8					
20	665.6	1904.9	3031.3	4045.2	4945.4	5729.6	6393.6	6931.6	7334.4	7589.9	7680.7	7583.3	7266.1	6677.3	5733.5	4237.1						
21	656.4	1877.8	2986.6	3982.7	4864.7	5630.0	6273.8	6789.6	7167.5	7393.9	7449.6	7309.0	6934.5	6265.8	5189.4	3385.6						
22	646.9	1849.9	2940.4	3918.1	4781.2	5526.6	6149.2	6641.4	6992.7	7187.6	7205.0	7016.2	6576.0	5811.5	4558.0	2323.8						
23	637.2	1821.2	2892.8	3851.4	4694.8	5419.5	6019.7	6487.0	6809.7	6970.4	6945.7	6702.8	6186.5	5302.0	3788.2							
24	627.2	1791.7	2843.8	3782.7	4605.7	5308.6	5885.3	6326.1	6618.0	6741.5	6670.3	6365.5	5759.5	4715.9	2763.1							
25	617.0	1761.5	2793.6	3712.0	4513.8	5194.0	5745.8	6158.4	6417.0	6499.9	6377.0	6000.3	5284.1	4011.7								
26	606.6	1730.5	2742.1	3639.4	4419.1	5075.6	5601.1	5983.6	6206.1	6244.3	6062.9	5601.4	4741.7	3087.1								
27	595.9	1698.9	2689.3	3564.8	4321.5	4953.2	5450.8	5801.1	5984.5	5972.9	5724.2	5159.6	4096.0									
28	585.0	1666.6	2635.2	3488.3	4221.1	4826.7	5294.7	5610.3	5750.7	5683.5	5355.3	4659.0	3262.0									
29	574.0	1633.5	2580.0	3409.8	4117.7	4695.9	5132.5	5410.4	5503.3	5372.5	4947.9	4068.1	2263.2									
30	562.7	1600.0	2523.4	3329.2	4011.2	4560.5	4963.5	5200.2	5240.1	5035.2	4488.1	3314.5										
31	551.3	1565.7	2465.6	3246.5	3901.5	4420.1	4787.0	4978.4	4958.2	4663.6	3949.0	2345.1										
32	539.6	1530.7	2406.4	3161.6	3788.2	4274.3	4602.0	4743.1	4653.3	4245.3	3267.4											
33	527.8	1495.0	2345.9	3074.3	3671.2	4122.5	4407.3	4491.7	4318.6	3756.4	2357.8											
34	515.7	1458.7	2283.9	2984.5	3549.9	3963.9	4201.2	4220.3	3942.6	3142.9												
35	503.5	1421.6	2220.4	2892.0	3424.0	3797.4	3981.4	3923.1	3504.2	2306.7												
36	491.0	1383.7	2155.2	2796.4	3292.8	3621.6	3744.6	3590.2	2955.7													
37	478.3	1344.9	2088.2	2697.4	3155.4	3434.6	3486.0	3202.9	2205.9													
38	465.4	1305.2	2019.1	2594.5	3010.8	3233.5	3196.8	2719.6														
39	452.2	1264.5	1947.8	2487.0	2857.3	3014.2	2861.2	2054.8														
40	438.7	1222.7	1873.8	2374.1	2692.7	2769.5	2443.4															
41	424.9	1179.5	1796.7	2254.6	2513.5	2486.3	1870.2															
42	410.8	1134.9	1716.0	2126.8	2314.0	2135.2																
43	396.2	1088.5	1630.8	1988.2	2083.8	1655.1																
44	381.1	1040.1	1540.0	1834.3	1800.0																	
45	365.5	989.1	1441.8	1657.6	1413.7																	
46	349.3	935.0	1333.3	1441.0																		
47	332.2	876.8	1209.6	1148.4																		
48	314.1	812.9	1060.0																			
49	294.8	740.6	860.9																			
50	273.6	654.7																				
51	249.9	543.5																				
52	222.2	427.9																				
53	187.9																					
54	149.1																					

D_2

$\langle E - U(R) \rangle$

TABLE XIII

V \ J	0	1	2	3	4	5	6	7	8	9	10	11	12	13	14	15	16	17	18	19	20	21	R(MAX)
0	1.4345	1.5021	1.5716	1.6432	1.7173	1.7942	1.8744	1.9584	2.0471	2.1413	2.2423	2.3516	2.4716	2.6052	2.7570	2.9333	3.1447	3.4088	3.7598	4.2733	5.2011	11.038	∞
1	1.4356	1.5032	1.5727	1.6444	1.7185	1.7955	1.8757	1.9598	2.0486	2.1429	2.2440	2.3535	2.4737	2.6076	2.7597	2.9366	3.1488	3.4141	3.7674	4.2859	5.2316	10.187	14.246
2	1.4378	1.5055	1.5750	1.6468	1.7210	1.7980	1.8784	1.9627	2.0516	2.1461	2.2475	2.3573	2.4779	2.6124	2.7652	2.9431	3.1569	3.4248	3.7827	4.3115	5.2958		11.216
3	1.4410	1.5088	1.5785	1.6503	1.7247	1.8019	1.8824	1.9669	2.0561	2.1509	2.2527	2.3630	2.4842	2.6195	2.7735	2.9530	3.1692	3.4411	3.8062	4.3511	5.4012		9.915
4	1.4454	1.5132	1.5831	1.6551	1.7296	1.8070	1.8878	1.9725	2.0621	2.1573	2.2596	2.3705	2.4926	2.6291	2.7846	2.9663	3.1859	3.4632	3.8383	4.4066	5.5647		9.177
5	1.4507	1.5188	1.5887	1.6609	1.7357	1.8134	1.8945	1.9796	2.0696	2.1653	2.2682	2.3800	2.5032	2.6411	2.7985	2.9832	3.2070	3.4914	3.8799	4.4806	5.8282		8.806
6	1.4571	1.5254	1.5956	1.6680	1.7430	1.8210	1.9024	1.9880	2.0785	2.1749	2.2786	2.3914	2.5159	2.6556	2.8155	3.0036	3.2328	3.5263	3.9322	4.5778	6.1304		8.329
7	1.4646	1.5330	1.6035	1.6762	1.7515	1.8298	1.9117	1.9978	2.0889	2.1861	2.2908	2.4048	2.5308	2.6726	2.8354	3.0279	3.2636	3.5686	3.9968	4.7057			8.062
8	1.4730	1.5417	1.6124	1.6855	1.7611	1.8399	1.9223	2.0090	2.1008	2.1989	2.3046	2.4201	2.5480	2.6923	2.8586	3.0562	3.3000	3.6190	4.0764	4.8790			7.900
9	1.4825	1.5514	1.6225	1.6959	1.7720	1.8512	1.9342	2.0215	2.1142	2.2133	2.3203	2.4374	2.5674	2.7147	2.8851	3.0889	3.3424	3.6789	4.1746	5.1310			7.453
10	1.4929	1.5622	1.6335	1.7073	1.7839	1.8637	1.9473	2.0354	2.1290	2.2292	2.3377	2.4567	2.5893	2.7399	2.9152	3.1262	3.3916	3.7500	4.2975	5.4774			7.381
11	1.5043	1.5739	1.6457	1.7199	1.7970	1.8774	1.9617	2.0507	2.1453	2.2468	2.3570	2.4781	2.6135	2.7681	2.9491	3.1687	3.4485	3.8349	4.4561				7.267
12	1.5166	1.5866	1.6588	1.7335	1.8111	1.8922	1.9773	2.0673	2.1631	2.2661	2.3781	2.5017	2.6404	2.7995	2.9871	3.2170	3.5146	3.9372	4.6733				7.038
13	1.5298	1.6002	1.6729	1.7481	1.8264	1.9082	1.9942	2.0852	2.1823	2.2870	2.4011	2.5274	2.6699	2.8342	3.0297	3.2719	3.5917	4.0630	4.9748				6.852
14	1.5439	1.6148	1.6879	1.7638	1.8427	1.9254	2.0123	2.1046	2.2031	2.3096	2.4261	2.5556	2.7023	2.8727	3.0774	3.3345	3.6825	4.2231	5.4143				6.814
15	1.5589	1.6302	1.7040	1.7804	1.8602	1.9437	2.0317	2.1252	2.2254	2.3339	2.4531	2.5861	2.7379	2.9153	3.1309	3.4064	3.7912	4.4373					6.605
16	1.5747	1.6466	1.7209	1.7981	1.8786	1.9631	2.0523	2.1473	2.2493	2.3601	2.4822	2.6194	2.7767	2.9625	3.1911	3.4897	3.9246	4.7546					6.567
17	1.5914	1.6638	1.7388	1.8167	1.8982	1.9837	2.0742	2.1707	2.2747	2.3881	2.5137	2.6554	2.8193	3.0149	3.2593	3.5877	4.0958	5.1530					6.405
18	1.6089	1.6819	1.7576	1.8364	1.9187	2.0055	2.0974	2.1956	2.3018	2.4181	2.5475	2.6945	2.8659	3.0733	3.3373	3.7054	4.3295						6.324
19	1.6272	1.7009	1.7773	1.8570	1.9404	2.0284	2.1218	2.2220	2.3307	2.4502	2.5839	2.7370	2.9174	3.1388	3.4279	3.8517	4.6930						6.276
20	1.6463	1.7207	1.7979	1.8785	1.9631	2.0524	2.1476	2.2499	2.3614	2.4845	2.6232	2.7833	2.9742	3.2130	3.5349	4.0436							6.133
21	1.6662	1.7413	1.8194	1.9010	1.9869	2.0777	2.1748	2.2795	2.3939	2.5212	2.6656	2.8339	3.0376	3.2981	3.6654	4.3206							6.057
22	1.6869	1.7628	1.8418	1.9246	2.0117	2.1042	2.2033	2.3107	2.4286	2.5605	2.7115	2.8895	3.1088	3.3975	3.8320	4.7232							5.981
23	1.7083	1.7851	1.8651	1.9491	2.0377	2.1320	2.2334	2.3437	2.4655	2.6028	2.7614	2.9510	3.1898	3.5168	4.0624								5.900
24	1.7305	1.8092	1.8893	1.9746	2.0648	2.1611	2.2650	2.3786	2.5048	2.6482	2.8159	3.0197	3.2834	3.6664	4.4197								5.814
25	1.7534	1.8321	1.9144	2.0011	2.0931	2.1916	2.2983	2.4156	2.5469	2.6975	2.8758	3.0973	3.3946	3.8674									5.733
26	1.7772	1.8569	1.9405	2.0287	2.1226	2.2235	2.3334	2.4548	2.5919	2.7509	2.9423	3.1864	3.5317	4.1718									5.657
27	1.8016	1.8825	1.9675	2.0574	2.1534	2.2570	2.3704	2.4966	2.6404	2.8095	3.0170	3.2913	3.7124										5.585
28	1.8269	1.9090	1.9955	2.0872	2.1856	2.2922	2.4095	2.5412	2.6929	2.8741	3.1023	3.4191	3.9789										5.514
29	1.8529	1.9363	2.0244	2.1182	2.2191	2.3291	2.4509	2.5890	2.7501	2.9462	3.2020	3.5849	4.3397										5.442
30	1.8797	1.9646	2.0545	2.1505	2.2543	2.3680	2.4950	2.6405	2.8130	3.0282	3.3225	3.8238											5.371
31	1.9073	1.9938	2.0856	2.1841	2.2910	2.4091	2.5420	2.6964	2.8829	3.1234	3.4769	4.1736											5.309
32	1.9358	2.0240	2.1179	2.2191	2.3297	2.4526	2.5926	2.7576	2.9618	3.2377	3.6959												5.242
33	1.9651	2.0551	2.1514	2.2557	2.3703	2.4989	2.6472	2.8253	3.0530	3.3829	4.0269												5.176
34	1.9953	2.0874	2.1863	2.2939	2.4132	2.5483	2.7067	2.9015	3.1619	3.5860													5.109
35	2.0264	2.1207	2.2225	2.3340	2.4586	2.6016	2.7723	2.9890	3.2992	3.8985													5.052
36	2.0585	2.1553	2.2603	2.3762	2.5070	2.6594	2.8458	3.0929	3.4895														4.985
37	2.0917	2.1912	2.2998	2.4208	2.5589	2.7229	2.9298	3.2231	3.7814														4.923
38	2.1259	2.2284	2.3412	2.4680	2.6150	2.7936	3.0289	3.4019															4.861
39	2.1613	2.2673	2.3848	2.5185	2.6763	2.8741	3.1523	3.6764															4.799
40	2.1979	2.3078	2.4308	2.5727	2.7441	2.9685	3.3204																4.737
41	2.2360	2.3503	2.4797	2.6316	2.8209	3.0850	3.5761																4.675
42	2.2755	2.3949	2.5319	2.6965	2.9103	3.2422																	4.618
43	2.3167	2.4420	2.5884	2.7693	3.0198	3.4788																	4.556
44	2.3599	2.4922	2.6500	2.8534	3.1655																		4.494
45	2.4051	2.5459	2.7186	2.9551	3.3822																		4.433
46	2.4529	2.6041	2.7969	3.0885																			4.371
47	2.5037	2.6680	2.8901	3.2836																			4.309
48	2.5581	2.7399	3.0091																				4.237
49	2.6170	2.8236	3.1786																				4.171
50	2.6819	2.9271																					4.099
51	2.7552	3.0676																					4.023
52	2.8416	3.2264																					3.947
53	2.9504																						3.851
54	3.0839																						3.751

D_2

$\langle R \rangle$

TABLE XIV

V \ J	0	1	2	3	4	5	6	7	8	9	10	11	12	13	14	15	16	17	18	19	20	21	R(MAX)
0	1.4414	1.5219	1.6036	1.6869	1.7721	1.8597	1.9502	2.0442	2.1426	2.2462	2.3563	2.4745	2.6031	2.7450	2.9046	3.0883	3.3061	3.5752	3.9287	4.4402	5.3585	11.781	∞
1	1.4425	1.5230	1.6047	1.6880	1.7733	1.8610	1.9515	2.0456	2.1441	2.2478	2.3580	2.4764	2.6052	2.7474	2.9074	3.0916	3.3102	3.5805	3.9362	4.4525	5.3887	10.442	14.246
2	1.4447	1.5252	1.6070	1.6904	1.7758	1.8635	1.9542	2.0485	2.1471	2.2510	2.3615	2.4802	2.6094	2.7522	2.9130	3.0982	3.3184	3.5912	3.9514	4.4777	5.4522		11.216
3	1.4479	1.5286	1.6105	1.6940	1.7795	1.8674	1.9583	2.0528	2.1516	2.2559	2.3668	2.4860	2.6158	2.7594	2.9213	3.1081	3.3307	3.6074	3.9746	4.5168	5.5569		9.915
4	1.4522	1.5330	1.6151	1.6987	1.7844	1.8725	1.9637	2.0584	2.1577	2.2623	2.3738	2.4937	2.6243	2.7691	2.9325	3.1215	3.3474	3.6294	4.0064	4.5713	5.7200		9.177
5	1.4576	1.5385	1.6207	1.7046	1.7905	1.8789	1.9704	2.0655	2.1652	2.2704	2.3825	2.5032	2.6350	2.7812	2.9466	3.1385	3.3685	3.6576	4.0476	4.6442	5.9858		8.806
6	1.4640	1.5451	1.6276	1.7117	1.7978	1.8866	1.9784	2.0740	2.1742	2.2801	2.3930	2.5148	2.6479	2.7959	2.9637	3.1590	3.3944	3.6923	4.0993	4.7399	6.2691		8.329
7	1.4714	1.5528	1.6355	1.7199	1.8064	1.8955	1.9878	2.0839	2.1848	2.2914	2.4053	2.5283	2.6630	2.8131	2.9838	3.1835	3.4253	3.7343	4.1632	4.8658			8.062
8	1.4799	1.5615	1.6444	1.7292	1.8161	1.9056	1.9984	2.0952	2.1968	2.3043	2.4193	2.5438	2.6804	2.8330	3.0072	3.2119	3.4616	3.7845	4.2417	5.0366			7.900
9	1.4893	1.5712	1.6545	1.7396	1.8269	1.9170	2.0103	2.1078	2.2103	2.3189	2.4352	2.5613	2.7001	2.8557	3.0340	3.2447	3.5040	3.8440	4.3386	5.2864			7.453
10	1.4997	1.5819	1.6656	1.7511	1.8389	1.9295	2.0236	2.1218	2.2252	2.3350	2.4528	2.5809	2.7222	2.8812	3.0643	3.2822	3.5532	3.9146	4.4597	5.6196			7.381
11	1.5111	1.5936	1.6777	1.7637	1.8520	1.9433	2.0381	2.1372	2.2417	2.3529	2.4724	2.6026	2.7468	2.9097	3.0984	3.3249	3.6100	3.9986	4.6158				7.267
12	1.5234	1.6063	1.6908	1.7773	1.8662	1.9582	2.0538	2.1540	2.2597	2.3723	2.4937	2.6264	2.7739	2.9414	3.1368	3.3734	3.6759	4.0998	4.8299				7.038
13	1.5366	1.6200	1.7050	1.7920	1.8816	1.9743	2.0708	2.1721	2.2792	2.3935	2.5171	2.6526	2.8039	2.9766	3.1797	3.4284	3.7527	4.2241	5.1225				6.852
14	1.5507	1.6346	1.7201	1.8077	1.8980	1.9916	2.0891	2.1916	2.3002	2.4164	2.5424	2.6811	2.8367	3.0155	3.2277	3.4911	3.8429	4.3821	5.5440				6.814
15	1.5657	1.6500	1.7361	1.8244	1.9155	2.0100	2.1087	2.2125	2.3228	2.4411	2.5698	2.7121	2.8727	3.0585	3.2815	3.5630	3.9508	4.5925					6.605
16	1.5816	1.6664	1.7531	1.8422	1.9341	2.0296	2.1295	2.2348	2.3469	2.4676	2.5994	2.7458	2.9120	3.1061	3.3421	3.6462	4.0829	4.9019					6.567
17	1.5983	1.6837	1.7711	1.8609	1.9538	2.0504	2.1516	2.2586	2.3728	2.4961	2.6313	2.7823	2.9551	3.1590	3.4106	3.7439	4.2520	5.2824					6.405
18	1.6158	1.7018	1.7899	1.8806	1.9745	2.0723	2.1750	2.2838	2.4003	2.5265	2.6656	2.8220	3.0024	3.2179	3.4888	3.8609	4.4816						6.324
19	1.6341	1.7208	1.8097	1.9013	1.9963	2.0955	2.1998	2.3106	2.4295	2.5591	2.7026	2.8652	3.0544	3.2839	3.5794	4.0060	4.8345						6.276
20	1.6532	1.7407	1.8304	1.9230	2.0192	2.1198	2.2259	2.3389	2.4607	2.5939	2.7425	2.9121	3.1119	3.3586	3.6863	4.1956							6.133
21	1.6731	1.7613	1.8520	1.9457	2.0432	2.1453	2.2534	2.3688	2.4938	2.6312	2.7856	2.9634	3.1760	3.4440	3.8163	4.4671							6.057
22	1.6938	1.7828	1.8745	1.9694	2.0683	2.1721	2.2823	2.4005	2.5290	2.6712	2.8322	3.0198	3.2478	3.5437	3.9816	4.8541							5.981
23	1.7152	1.8052	1.8979	1.9940	2.0945	2.2003	2.3128	2.4340	2.5665	2.7142	2.8829	3.0821	3.3294	3.6631	4.2089								5.900
24	1.7375	1.8284	1.9222	2.0197	2.1219	2.2297	2.3449	2.4695	2.6065	2.7604	2.9382	3.1516	3.4236	3.8121	4.5554								5.814
25	1.7604	1.8524	1.9475	2.0465	2.1504	2.2606	2.3787	2.5071	2.6493	2.8105	2.9991	3.2300	3.5352	4.0113									5.733
26	1.7842	1.8772	1.9737	2.0743	2.1803	2.2930	2.4143	2.5470	2.6951	2.8649	3.0665	3.3200	3.6724	4.3092									5.657
27	1.8087	1.9030	2.0008	2.1033	2.2114	2.3269	2.4519	2.5895	2.7445	2.9244	3.1422	3.4255	3.8524										5.585
28	1.8340	1.9295	2.0290	2.1334	2.2440	2.3626	2.4917	2.6349	2.7979	2.9900	3.2285	3.5539	4.1149										5.514
29	1.8600	1.9570	2.0582	2.1647	2.2780	2.4001	2.5339	2.6836	2.8562	3.0633	3.3292	3.7197	4.4649										5.442
30	1.8869	1.9854	2.0885	2.1973	2.3136	2.4396	2.5787	2.7361	2.9202	3.1465	3.4507	3.9564											5.371
31	1.9145	2.0147	2.1198	2.2313	2.3509	2.4814	2.6266	2.7930	2.9913	3.2429	3.6056	4.2963											5.309
32	1.9430	2.0450	2.1524	2.2667	2.3901	2.5257	2.6781	2.8554	3.0716	3.3585	3.8236												5.242
33	1.9724	2.0764	2.1862	2.3037	2.4314	2.5728	2.7338	2.9244	3.1642	3.5048	4.1467												5.176
34	2.0027	2.1088	2.2214	2.3425	2.4749	2.6232	2.7945	3.0020	3.2746	3.7078													5.109
35	2.0339	2.1424	2.2580	2.3832	2.5212	2.6775	2.8614	3.0911	3.4134	4.0144													5.052
36	2.0660	2.1772	2.2962	2.4260	2.5704	2.7365	2.9363	3.1967	3.6044														4.985
37	2.0992	2.2133	2.3362	2.4712	2.6233	2.8012	3.0220	3.3287	3.8922														4.923
38	2.1336	2.2508	2.3781	2.5192	2.6805	2.8734	3.1230	3.5090															4.861
39	2.1690	2.2899	2.4222	2.5705	2.7430	2.9556	3.2485	3.7811															4.799
40	2.2058	2.3308	2.4688	2.6257	2.8123	3.0519	3.4186																4.737
41	2.2440	2.3737	2.5184	2.6858	2.8907	3.1708	3.6733																4.675
42	2.2836	2.4187	2.5715	2.7519	2.9821	3.3305																	4.618
43	2.3250	2.4664	2.6288	2.8263	3.0939	3.5674																	4.556
44	2.3683	2.5171	2.6916	2.9123	3.2425																		4.494
45	2.4138	2.5715	2.7615	3.0163	3.4607																		4.433
46	2.4619	2.6304	2.8414	3.1527																			4.371
47	2.5129	2.6954	2.9367	3.3504																			4.309
48	2.5676	2.7685	3.0586																				4.237
49	2.6270	2.8538	3.2311																				4.171
50	2.6925	2.9595																					4.099
51	2.7666	3.1029																					4.023
52	2.8542	3.2657																					3.947
53	2.9646																						3.851
54	3.0998																						3.751

D_2

$\langle R^2 \rangle^{1/2}$

TABLE XV

J \ v	0	1	2	3	4	5	6	7	8	9	10	11	12	13	14	15	16	17	18	19	20	21	R(MAX)
0	1.4138	1.4394	1.4660	1.4937	1.5227	1.5532	1.5856	1.6201	1.6573	1.6977	1.7421	1.7916	1.8477	1.9125	1.9892	2.0825	2.2006	2.3577	2.5836	2.9497	3.7145	8.5650	∞
1	1.4149	1.4406	1.4672	1.4949	1.5240	1.5545	1.5869	1.6215	1.6588	1.6992	1.7437	1.7934	1.8496	1.9147	1.9916	2.0853	2.2040	2.3621	2.5900	2.9606	3.7435	8.6452	14.246
2	1.4171	1.4428	1.4695	1.4973	1.5264	1.5571	1.5896	1.6243	1.6617	1.7023	1.7470	1.7969	1.8535	1.9189	1.9965	2.0910	2.2109	2.3711	2.6028	2.9829	3.8049		11.216
3	1.4203	1.4461	1.4729	1.5009	1.5301	1.5609	1.5936	1.6285	1.6661	1.7069	1.7520	1.8022	1.8593	1.9254	2.0037	2.0995	2.2213	2.3847	2.6226	3.0176	3.9064		9.915
4	1.4246	1.4506	1.4775	1.5056	1.5350	1.5660	1.5989	1.6340	1.6719	1.7131	1.7586	1.8093	1.8670	1.9339	2.0135	2.1109	2.2353	2.4031	2.6496	3.0664	4.0647		9.177
5	1.4300	1.4561	1.4832	1.5115	1.5411	1.5724	1.6055	1.6409	1.6792	1.7208	1.7668	1.8182	1.8767	1.9447	2.0257	2.1254	2.2531	2.4267	2.6847	3.1320	4.3202		8.806
6	1.4364	1.4627	1.4901	1.5186	1.5484	1.5799	1.6134	1.6492	1.6879	1.7300	1.7766	1.8288	1.8883	1.9576	2.0405	2.1429	2.2748	2.4558	2.7290	3.2189	4.6841		8.329
7	1.4439	1.4704	1.4980	1.5267	1.5569	1.5887	1.6226	1.6588	1.6980	1.7407	1.7880	1.8411	1.9018	1.9728	2.0579	2.1635	2.3006	2.4911	2.7840	3.3348			8.062
8	1.4523	1.4791	1.5070	1.5360	1.5665	1.5987	1.6330	1.6697	1.7095	1.7529	1.8011	1.8553	1.9174	1.9903	2.0780	2.1876	2.3311	2.5332	2.8520	3.4944			7.900
9	1.4618	1.4888	1.5170	1.5464	1.5773	1.6099	1.6447	1.6820	1.7224	1.7666	1.8158	1.8712	1.9349	2.0100	2.1008	2.2152	2.3665	2.5833	2.9367	3.7311			7.453
10	1.4722	1.4996	1.5281	1.5579	1.5892	1.6223	1.6576	1.6955	1.7366	1.7818	1.8320	1.8889	1.9545	2.0322	2.1267	2.2467	2.4075	2.6429	3.0439	4.0979			7.381
11	1.4836	1.5113	1.5402	1.5704	1.6021	1.6358	1.6716	1.7103	1.7522	1.7984	1.8499	1.9084	1.9762	2.0568	2.1557	2.2824	2.4549	2.7143	3.1844				7.267
12	1.4959	1.5240	1.5532	1.5839	1.6161	1.6504	1.6869	1.7263	1.7692	1.8165	1.8695	1.9298	2.0001	2.0841	2.1881	2.3228	2.5099	2.8010	3.3810				7.038
13	1.5091	1.5376	1.5673	1.5984	1.6312	1.6661	1.7034	1.7436	1.7875	1.8361	1.8907	1.9531	2.0262	2.1142	2.2242	2.3687	2.5742	2.9087	3.6754				6.852
14	1.5232	1.5521	1.5823	1.6140	1.6474	1.6829	1.7209	1.7622	1.8072	1.8572	1.9136	1.9784	2.0547	2.1473	2.2644	2.4209	2.6501	3.0479	4.1730				6.814
15	1.5382	1.5676	1.5982	1.6305	1.6645	1.7008	1.7397	1.7819	1.8283	1.8798	1.9382	2.0057	2.0857	2.1837	2.3093	2.4807	2.7415	3.2393					6.605
16	1.5540	1.5839	1.6151	1.6479	1.6827	1.7197	1.7596	1.8030	1.8507	1.9040	1.9646	2.0352	2.1195	2.2238	2.3597	2.5500	2.8548	3.5395					6.567
17	1.5707	1.6010	1.6328	1.6663	1.7018	1.7397	1.7807	1.8252	1.8745	1.9298	1.9930	2.0670	2.1562	2.2682	2.4166	2.6317	3.0023	3.9973					6.403
18	1.5881	1.6191	1.6515	1.6857	1.7220	1.7608	1.8029	1.8488	1.8998	1.9572	2.0233	2.1013	2.1963	2.3174	2.4816	2.7304	3.2103						6.324
19	1.6064	1.6379	1.6710	1.7059	1.7431	1.7830	1.8262	1.8737	1.9265	1.9864	2.0557	2.1384	2.2402	2.3723	2.5569	2.8543	3.5607						6.276
20	1.6255	1.6576	1.6914	1.7271	1.7652	1.8062	1.8508	1.8998	1.9548	2.0174	2.0905	2.1785	2.2884	2.4343	2.6462	3.0200							6.133
21	1.6454	1.6781	1.7126	1.7492	1.7883	1.8305	1.8765	1.9274	1.9847	2.0504	2.1278	2.2220	2.3419	2.5052	2.7557	3.2700							6.057
22	1.6660	1.6994	1.7347	1.7722	1.8124	1.8559	1.9035	1.9564	2.0163	2.0855	2.1679	2.2696	2.4017	2.5880	2.8972	3.6912							5.981
23	1.6874	1.7215	1.7577	1.7961	1.8375	1.8824	1.9318	1.9869	2.0497	2.1230	2.2113	2.3218	2.4695	2.6877	3.0984								5.900
24	1.7095	1.7445	1.7815	1.8210	1.8636	1.9101	1.9614	2.0191	2.0852	2.1632	2.2583	2.3799	2.5477	2.8137	3.4405								5.814
25	1.7324	1.7682	1.8062	1.8468	1.8908	1.9390	1.9924	2.0529	2.1229	2.2063	2.3097	2.4452	2.6405	2.9861									5.733
26	1.7560	1.7927	1.8317	1.8736	1.9191	1.9691	2.0250	2.0886	2.1630	2.2529	2.3663	2.5200	2.7555	3.2635									5.657
27	1.7804	1.8180	1.8582	1.9014	1.9486	2.0006	2.0592	2.1264	2.2060	2.3035	2.4296	2.6077	2.9090										5.585
28	1.8056	1.8442	1.8855	1.9302	1.9792	2.0336	2.0952	2.1666	2.2521	2.3591	2.5016	2.7149	3.1451										5.514
29	1.8315	1.8712	1.9138	1.9601	2.0111	2.0680	2.1331	2.2093	2.3021	2.4207	2.5854	2.8550	3.5236										5.442
30	1.8582	1.8991	1.9431	1.9912	2.0443	2.1042	2.1731	2.2551	2.3566	2.4903	2.6866	3.0633											5.371
31	1.8857	1.9278	1.9734	2.0234	2.0790	2.1421	2.2157	2.3045	2.4169	2.5708	2.8169	3.4110											5.309
32	1.9140	1.9575	2.0048	2.0569	2.1153	2.1822	2.2611	2.3581	2.4845	2.6672	3.0058												5.242
33	1.9432	1.9881	2.0373	2.0917	2.1533	2.2245	2.3098	2.4171	2.5622	2.7899	3.3248												5.176
34	1.9732	2.0198	2.0710	2.1281	2.1932	2.2695	2.3626	2.4830	2.6546	2.9644													5.109
35	2.0041	2.0525	2.1060	2.1661	2.2353	2.3177	2.4205	2.5582	2.7709	3.2588													5.052
36	2.0360	2.0864	2.1424	2.2059	2.2799	2.3696	2.4847	2.6470	2.9341														4.985
37	2.0689	2.1214	2.1803	2.2477	2.3275	2.4263	2.5576	2.7578	3.2053														4.923
38	2.1029	2.1578	2.2199	2.2919	2.3786	2.4889	2.6431	2.9112															4.861
39	2.1380	2.1957	2.2615	2.3389	2.4341	2.5596	2.7488	3.1637															4.799
40	2.1743	2.2351	2.3052	2.3891	2.4951	2.6419	2.8935																4.737
41	2.2120	2.2763	2.3515	2.4433	2.5635	2.7428	3.1272																4.675
42	2.2511	2.3195	2.4008	2.5026	2.6425	2.8788																	4.618
43	2.2919	2.3650	2.4537	2.5687	2.7383	3.0940																	4.556
44	2.3345	2.4132	2.5112	2.6442	2.8655																		4.494
45	2.3791	2.4647	2.5746	2.7347	3.0621																		4.433
46	2.4262	2.5203	2.6464	2.8523																			4.371
47	2.4762	2.5809	2.7310	3.0293																			4.309
48	2.5295	2.6486	2.8380																				4.247
49	2.5872	2.7267	2.9924																				4.171
50	2.6504	2.8221																					4.099
51	2.7215	2.9519																					4.023
52	2.8046	3.1176																					3.947
53	2.9086																						3.851
54	3.0429																						3.751

D_2

$\langle R^{-2} \rangle^{-\frac{1}{2}}$

TABLE XVI

v \ J	0	1	2	3	4	5	6	7	8	9	10	11	12	13	14	U(MAX)
0	-36117.5	-31955.4	-28028.8	-24332.6	-20863.9	-17621.6	-14607.1	-11824.3	-9280.5	-6987.1	-4960.8	-3224.6	-1810.6	-763.1	-143.2	0.0
1	-35999.0	-31842.8	-27922.0	-24231.5	-20768.4	-17531.8	-14523.0	-11746.1	-9208.4	-6921.6	-4902.4	-3174.0	-1768.9	-732.2	-126.1	1.1
2	-35763.1	-31618.7	-27709.4	-24030.3	-20578.5	-17353.1	-14355.8	-11590.7	-9065.2	-6791.4	-4786.3	-3073.6	-1686.6	-671.6	-93.5	5.3
3	-35411.9	-31285.1	-27393.0	-23730.8	-20295.9	-17087.5	-14107.2	-11359.7	-8852.6	-6598.3	-4614.4	-2925.4	-1565.6	-583.5	-49.0	13.6
4	-34948.6	-30845.1	-26975.8	-23336.1	-19923.4	-16737.4	-13779.9	-11055.7	-8573.0	-6344.7	-4389.2	-2731.8	-1408.8	-471.5	1.0	26.3
5	-34377.2	-30302.5	-26461.4	-22849.6	-19464.6	-16306.4	-13377.1	-10682.0	-8229.8	-6034.0	-4113.9	-2496.5	-1220.1	-340.4	47.0(17.0)	44.4
6	-33702.4	-29662.0	-25854.4	-22275.7	-18923.7	-15798.5	-12902.9	-10242.5	-7826.7	-5670.0	-3792.7	-2223.7	-1004.2	-196.7		67.5
7	-32929.7	-28928.8	-25159.9	-21619.3	-18305.3	-15218.4	-12361.8	-9741.6	-7368.3	-5257.2	-3430.1	-1918.4	-767.3	-49.3		97.7
8	-32065.2	-28108.7	-24383.3	-20885.8	-17614.7	-14571.1	-11758.7	-9184.3	-6859.4	-4800.5	-3031.5	-1586.4	-516.3	86.3(1.5)		133.5
9	-31115.1	-27207.7	-23530.6	-20080.8	-16857.5	-13862.1	-11098.9	-8575.8	-6305.3	-4305.5	-2602.5	-1234.3	-260.2	201. (52.)		176.9
10	-30086.0	-26232.3	-22608.0	-19210.4	-16039.3	-13096.9	-10388.0	-7921.7	-5711.6	-3777.9	-2149.5	-869.7	-10.7			228.0
11	-28984.7	-25189.0	-21621.6	-18280.7	-15166.3	-12281.3	-9631.8	-7227.6	-5084.2	-3224.0	-1679.6	-501.6	211.4(2.3)			286.2
12	-27818.1	-24084.3	-20577.9	-17297.6	-14244.2	-11421.3	-8835.9	-6499.5	-4429.2	-2650.4	-1200.6	-141.2	393. (71.)			353.6
13	-26592.8	-22924.6	-19483.1	-16267.3	-13279.0	-10522.7	-8006.4	-5743.4	-3753.1	-2064.3	-721.4	195.5				430.8
14	-25315.4	-21716.4	-18343.3	-15195.9	-12276.7	-9591.3	-7149.2	-4965.4	-3062.3	-1473.4	-252.9	477. (17.)				516.4
15	-23992.5	-20465.9	-17164.6	-14089.2	-11243.1	-8633.0	-6270.1	-4171.8	-2364.0	-886.6	190.4					613.1
16	-22630.2	-19179.1	-15952.9	-12953.0	-10183.8	-7653.5	-5375.3	-3369.2	-1665.9	-314.3	582.0(2.8)					720.3
17	-21234.4	-17861.8	-14713.8	-11792.8	-9104.5	-6658.7	-4470.7	-2564.5	-976.5	229.6	898. (94.)					838.9
18	-19811.0	-16519.5	-13452.7	-10614.1	-8010.6	-5654.1	-3562.7	-1764.9	-305.9	722.4(0.5)						969.6
19	-18365.4	-15157.6	-12174.9	-9422.0	-6907.6	-4645.5	-2657.8	-978.7	332.6	1123. (58.)						1112.9
20	-16902.5	-13781.0	-10885.4	-8221.8	-5800.7	-3638.9	-1762.9	-215.6	918.0(0.2)							1269.3
21	-15427.4	-12394.7	-9589.0	-7018.4	-4695.3	-2640.4	-886.0	511.5	1405. (40.)							1439.7
22	-13944.7	-11003.1	-8290.5	-5816.7	-3597.0	-1656.6	-36.4	1182.8(0.1)								1624.8
23	-12458.6	-9610.6	-6994.4	-4621.6	-2511.4	-694.9	773.7	1753. (31.)								1825.1
24	-10973.3	-8221.6	-5705.1	-3438.3	-1444.8	235.7	1524.9(0.1)									2042.0
25	-9492.7	-6840.1	-4427.2	-2271.9	-404.0	1123.6	2173. (27.)									2275.7
26	-8020.6	-5470.1	-3165.1	-1128.1	602.5	1949.8(0.1)										2527.7
27	-6560.7	-4115.7	-1923.7	-13.3	1563.6	2671. (26.)										2798.8
28	-5116.3	-2780.7	-708.0	1064.6	2461.0(0.1)											3090.1
29	-3691.1	-1469.5	476.1	2095.1	3253. (25.)											3403.2
30	-2288.5	-186.5	1621.6	3061.3(0.2)												3739.2
31	-912.2	1063.0	2719.0	3924. (24.)												4099.9
32	434.1	2273.1	3752.6(0.2)													4487.1
33	1746.0	3435.5	4687. (21.)													4902.4
34	3018.5	4537.0(0.1)														5349.3
35	4245.1	5549. (14.)														5831.0
36	5416.2(0.1)															6351.5
37	6513.2(6.0)															6916.7
38	7513. (81.)															7537.0
39	8456.(266.)															8229.0

$H_2(\Delta'')$

$E(v,J)$

TABLE XVII

FOOTNOTES

1. a) D. L. S. McElwain and H. O. Pritchard, J. Am. Chem. Soc. 91, 7693 (1969); b) ibid, 92, 5027 (1970).

2. a) R. E. Roberts, R. B. Bernstein, and C. F. Curtiss, Chem. Phys. Lett. 2, 366 (1968); b) ibid, J. Chem. Phys. 50, 5163 (1969); c) R. E. Roberts and R. B. Bernstein, Chem. Phys. Lett. 6, 282 (1970).

3. R. J. Le Roy and R. B. Bernstein, "Shape Resonances and Rotationally Predissociating Levels: The Atomic Collision Time-Delay Functions and Quasibound Level Properties of $H_2(X\ ^1\Sigma_g^+)$", University of Wisconsin Theoretical Chemistry Institute report WIS-TCI-427 (1971), to be published.

4. a) W. Kołos and L. Wolniewicz, J. Chem. Phys. 41, 3663 (1964); b) ibid, 43, 2429 (1965); c) ibid, 49, 404 (1968).

5. L. Wolniewicz, J. Chem. Phys. 45, 515 (1966).

6. J. K. Cashion, J. Chem. Phys. 45, 1037 (1966).

7. J. D. Poll and G. Karl, Can. J. Phys. 44, 1467 (1966).

8. T. G. Waech and R. B. Bernstein, J. Chem. Phys. 46, 4905 (1967).

9. R. J. Le Roy and R. B. Bernstein, J. Chem. Phys. 49, 4312 (1968).

10. G. Herzberg and A. Monfils, J. Mol. Spectry. 5, 482 (1960).

11. W. C. Stwalley, Chem. Phys. Lett. 6, 241 (1970).

12. G. Herzberg, J. Mol. Spectry. 33, 147 (1970).

13. In addition to the above references, see: a) R. A. Buckingham and E. Gal, Adv. At. Molec. Phys. 4, 37 (1968), and references therein; b) J. W. Fox and E. Gal, Proc. Phys. Soc. (London) 90,

55 (1967); c) A. C. Allison, Chem. Phys. Lett. 3, 371 (1969); d) M. E. Gersh and R. B. Bernstein, Chem. Phys. Lett. 4, 221 (1969).

14. E. R. Cohen and J. W. DuMond, Rev. Mod. Phys. 37, 537 (1965).

15. An improved value of the electron mass has been reported[16] which is $0.73 \times 10^{-3}\%$ smaller than the value in Table I. However, the errors this imputes in reported eigenvalues are negligible, having a maximum of 0.075 cm^{-1}.[9]

16. B. N. Taylor, W. H. Parker and D. N. Langenberg, Rev. Mod. Phys. 41, 375 (1969).

17. Comparisons of several criteria for determining the quasibound level energies and of divers means of estimating their widths are presented in Ref.(3). The time-delay function $\tau_d(E,d)$ and a means of computing it are also described there.

18. Of course, in reality the quadratures need only be performed out to a finite R_+ which is sufficiently large that $\Psi_{v,J}(R)$ is negligible for $R > R_+$.

19. R. J. Le Roy, University of Wisconsin Theoretical Chemistry Institute report WIS-TCI-429G (1971).

20. a) J. W. Cooley, Math. Computation 15, 363 (1961); b) J.K. Cashion, J. Chem. Phys. 39, 1872 (1963); c) R. N. Zare and J. K. Cashion, University of California Radiation Laboratory report UCRL-10881 (1963).

21. It is believed that the Ref.(9) estimates of the non-adiabatic corrections to the eigenvalues are slightly large, which implies that Δ'' underestimates the necessary corrections to the KW potential.

9. PERMEABILITY OF ONE-DIMENSIONAL POTENTIAL BARRIERS

All of the techniques and results discussed above have basically been concerned with the exact description (within the framework of the Born-Oppenheimer or adiabatic approximations) of the relative nuclear motion of pairs of isolated atoms. On the other hand, useful, though approximate results for much more complicated systems may sometimes be obtained by assuming that they too may be effectively reduced to one mathematical dimension. This is the framework of the present chapter. The work presented below will be published in the Transactions of the Faraday Society, Volume 66, pp. 2997-3006 (1970).

Permeability of One-Dimensional Potential Barriers

BY R. J. LE ROY*

Theoretical Chemistry Institute and Chemistry Dept., University of Wisconsin, Madison, Wisconsin 53706

AND

K. A. QUICKERT † AND D. J. LE ROY

Lash Miller Chemical Laboratories, University of Toronto, Toronto 181, Ontario, Canada

Received 13*th April* 1970

A numerical method is described for computing the exact permeability (tunnelling probability) for any one-dimensional potential barrier. It is used to test the validity of the widely-used approximate formulae for the tunnelling factors for truncated parabolic barriers. The method is also used to calculate tunnelling factors for the $H+H_2$ exchange reaction, using the theoretical potential surface of Shavitt, Stevens, Minn and Karplus, and it is shown that standard Eckart and parabolic barrier approximations can yield considerable error.

Evaluation of the probability of transmission for a particle impinging on a potential barrier has long been an important problem in the theoretical treatment of chemical reaction rates. The early use of tunnelling corrections is discussed by Glasstone, Laidler and Eyring.[1] Their usefulness in interpreting the results of proton transfer reactions has been reviewed by Caldin,[2] and their application to the hydrogen exchange reactions is discussed by Johnston.[3]

While the potential barrier in a chemical reaction is in general multi-dimensional, a widely-used approximation has been to consider the reaction as motion along a one-dimensional (1-Dim) "reaction coordinate" which is orthogonal to all other modes of motion of the interacting species. In this approximation, estimates of barrier transmission rates have usually been obtained after approximating the exact potential by a model 1-Dim barrier of one of two analytic forms for which exact analytic tunnelling probabilities are known: an Eckart barrier,[4] or an infinite parabolic barrier.[5] An exact tunnelling probability expresson has also been derived [6] for a third potential form, the infinite double anharmonic barrier, $V(x) = V_0[1-(x/a-a/x)^2]$; however, this result has not yet been applied to chemical problems. Although the result for the parabolic potential is for an infinite barrier, it has been widely used for truncated parabolas,[2] probably because of the convenient analytic expression obtained for the tunnelling factor in the high-temperature limit.[7] The Eckart potential,[4] on the other hand, is finite, and the potential and its first derivative are everywhere continuous; however, while its exact transmission probability is known analytically, the tunnelling factors cannot be obtained in closed form.‡

* present address: Dept. of Physics, University of Toronto, Toronto 181, Ontario, Canada.

† present address: Institut für Physikalische Chemie, Universität Göttingen, 34 Göttingen, Bürgerstrasse 50, West Germany.

‡ A table of Eckart tunnelling factors for a wide range of potential parameter values and reduced temperatures is given in ref. (3), p. 44. Johnston (private communication, 1969) computed this table using the correct transmission probability expression and not his [3] eqn (2-22), in which the last term should be $\pi^2/4$, not $2\pi^2/16$.

Despite the convenience of using the analytic [7] or tabulated [3] results for the two main model barriers mentioned above, these potentials will rarely accurately represent a reasonable 1-Dim cut through an actual potential surface. Furthermore, the analytic tunnelling probabilities can not take account of the change in the asymptotic reduced mass between reagents and products which arises in many chemical situations. An additional problem associated with the use of Bell's formulae [7] for parabolic barriers is the unknown effect of truncating the barrier at a finite height on the transmission probability, and hence on his approximate expressions for the tunnelling factor.

In the next section, a simple numerical procedure is presented for determining exact transmission coefficients for any 1-Dim potential barrier. This approach is tested by comparing its predictions to the exact analytic results for an Eckart barrier.[4] The numerical method is then applied to truncated parabolic barriers to examine the validity of Bell's approximations. Finally, the usefulness of the exact 1-Dim method is demonstrated by applying it to the calculation of tunnelling factors for the $H+H_2$ exchange reaction.

SCATTERING BY A ONE-DIMENSIONAL BARRIER

EXACT BARRIER PASSAGE PROBABILITY

Many elementary quantum mechanics texts derive the exact transmission probability for a rectangular barrier,[8] and the present treatment is qualitatively the same.* The Schrödinger equation describing 1-Dim potential scattering may be written in the dimensionless form

$$d^2\psi(y)/dy^2 + B_y[\bar{E} - \bar{V}(y)]\psi(y) = 0, \qquad (1)$$

where

$$y = x/a,\ \bar{E} = E/V_0,\ \bar{V}(y) = V(x)/V_0,$$

and

$$B_y = 2\mu V_0 a^2/\hbar^2 = 20.746\ 59\mu[\text{a.m.u.}]V_0[\text{kcal/mol}]\ (a[\text{Å}])^2.$$

In general, the energy and length scaling factors V_0 and a may be chosen completely arbitrarily; however, it is usually convenient to associate them with the barrier height and width. In the present discussion, the coordinate x along the reaction path is

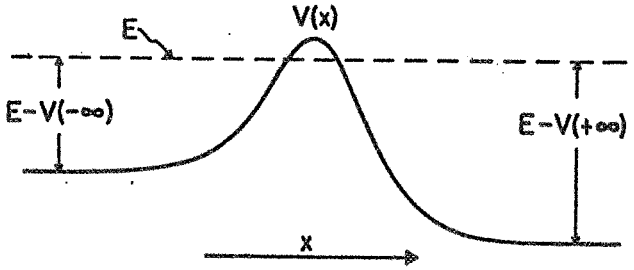

FIG. 1.—Schematic potential barrier.

defined such that $x \simeq -\infty$ corresponds to reagents and $x \simeq +\infty$ to products. The potential $V(x)$ is everywhere finite and approaches constant values in the limits $x \simeq \pm\infty$ (see fig. 1). E is the translational energy of the colliding particles. In

*A. Kuppermann has pointed out that a method similar to that described here was previously presented and used in a study of the Shottky effect.[9]

general, the effective reduced mass μ may vary along the reaction coordinate, and the asymptotic reduced mass of the reagents may differ from that of the products.[10] However, this may readily be taken account of by introducing a variable mass $\mu = \mu(y)$ into eqn (1), or alternatively by scaling the reaction coordinate appropriately while holding μ fixed.[11] When this question arose here the latter approach was used, and hence μ is assumed to be a constant in the rest of the derivation.

For "reagents", the solution of eqn (1) may be asymptotically expressed as a linear combination of plane waves incident on and reflected from the barrier, i.e., for $y \simeq -\infty$:

$$\psi(y) = A_I \exp(i\alpha_- y) + A_R \exp(-i\alpha_- y), \tag{2}$$

where $\alpha_- = \{B_y[\bar{E} - \bar{V}(-\infty)]\}^{\frac{1}{2}}$. Similarly, particles which tunnel past the barrier to form products may be described asymptotically by a plane wave moving away from the barrier, i.e., for $y \simeq +\infty$:

$$\psi(y) = A_T \exp(i\alpha_+ y), \tag{3}$$

where $\alpha_+ = \{B_y[\bar{E} - \bar{V}(+\infty)]\}^{\frac{1}{2}}$. The probability of barrier passage is the ratio of the transmitted to the incident flux:

$$\kappa(\bar{E}) = \frac{v_+}{v_-}\left|\frac{A_T}{A_I}\right|^2,$$

where v_+ and v_- are respectively the asymptotic velocities of products (+) and reagents (−). For fixed μ, $v_+/v_- = \alpha_+/\alpha_-$, and hence

$$\kappa(\bar{E}) = \frac{\alpha_+}{\alpha_-}\left|\frac{A_T}{A_I}\right|^2. \tag{4}$$

To facilitate computation of $\kappa(\bar{E})$ it is convenient to expand $\psi(y)$ in terms of its real and imaginary parts:

$$\psi(y) = \phi_1(y) + i\phi_2(y),$$

Comparing this with eqn (3) shows that for products, at $y \simeq +\infty$:

$$\begin{aligned} \phi_1(y) &= A_T \cos(\alpha_+ y), \\ \phi_2(y) &= A_T \sin(\alpha_+ y). \end{aligned} \tag{5}$$

Starting from this boundary condition with an arbitrary choice of A_T (most conveniently, $A_T \equiv 1$), the two independent solutions $\phi_1(y)$ and $\phi_2(y)$ may be numerically integrated through the barrier to the reagent boundary condition at $y \simeq -\infty$. There they may be decomposed into

$$\begin{aligned} \phi_1(y) &= C_1 \cos(\alpha_- y) + D_1 \sin(\alpha_- y), \\ \phi_2(y) &= C_2 \cos(\alpha_- y) + D_2 \sin(\alpha_- y). \end{aligned} \tag{6}$$

Comparing eqn (2) and (6), values of A_I and A_R are obtained in terms of values of the solution functions $\phi_1(y)$ and $\phi_2(y)$ at adjacent integration mesh points y_1 and y_2. Substituting them into eqn (4) yields

$$\begin{aligned} \kappa(\bar{E}) = 4(\alpha_+/\alpha_-)\sin^2[\alpha_-(y_2 - y_1)] \mid A_T \mid^2 \{&[\phi_1(y_1)]^2 + [\phi_1(y_2)]^2 + [\phi_2(y_1)]^2 + \\ &[\phi_2(y_2)]^2 - 2[\phi_1(y_1)\phi_1(y_2) + \phi_2(y_1)\phi_2(y_2)]\cos[\alpha_-(y_2 - y_1)] + \\ &2[\phi_1(y_1)\phi_2(y_2) - \phi_1(y_2)\phi_2(y_1)]\sin[\alpha_-(y_2 - y_1)]\}^{-1}. \end{aligned} \tag{7}$$

This is the desired result. The exact numerical integration of eqn (1) and the practical application of the boundary conditions are discussed below.

The above method was tested by applying it to a symmetric Eckart barrier, $\bar{V}(y) = 1/\cosh^2(y)$, for which the exact $\kappa(\bar{E})$ function is known analytically.[4] For barriers with B_y values ranging from 2 to 200, it was found that single precision numerical integration yielded $\kappa(\bar{E})$ accurate to within 1×10^{-5}, for $\bar{E} = 0.1$, 1.0, and 2.0. This confirms the validity of the present approach.

INTEGRATION OF EQN (1) AND APPLICATION OF BOUNDARY CONDITIONS

The Numerov method [12] is a very efficient technique for the numerical integration of a homogeneous linear second-order differential equation without first derivatives, such as eqn (1).[13] One restriction on its use is that it assumes that the potential function $\bar{V}(y)$ is smooth, since when it is not an inordinately small increment of integration is required to yield reasonable accuracy. In the latter situation a self-starting technique such as the Runge-Kutta-Gill (RKG) method [14] is more appropriate. The RKG procedure requires more arithmetic, and one more function evaluation per integration step than does the Numerov method. However, when calculating the solution at a given point the latter utilizes the solution at the *two* previous mesh points, while the former requires the solution and its first derivative only at the adjacent previous point. Thus, if RKG is used and the integration mesh chosen so that mesh points lie at any potential slope discontinuities, the numerical integration is in no way affected by the existence of such discontinuities. In the present work, the RKG procedure was used in the calculations for truncated parabolic barriers, as they have discontinuous first derivatives at $y = \pm 1$ (see below). The Numerov method was used in all other cases.

For either algorithm the accuracy of the integration improves with decreasing increment Δy until a lower bound is reached beyond which the theoretical improvement in the numerical accuracy is exceeded by the accumulated machine round-off error. The optimum increment of integration as a function of particle and barrier size is approximately given by

$$\Delta y = \Delta x/a = F/(B_y)^{\frac{1}{2}},$$

where the height of the barrier is used as V_0 in the calculation of B_y. The value of the numerical constant F depends on the integration algorithm and the number of significant digits of machine accuracy. On the 8-digit computer used in the present work, $F = 0.18$ was appropriate for Numerov integration, and $F = 0.07$ for the RKG algorithm.

For potentials with a finite range, such as truncated parabolic barriers, application of the boundary conditions eqn (2) and (3) presents no difficulties. On the other hand, realistic potentials which reach their asymptotic values only in the limits $y \simeq \pm\infty$ can only be integrated over a finite interval, and hence the exact boundary conditions are never achieved. In the present work, the ends of this finite interval, y_- and y_+, were defined as the smallest values of $|y|$ for which the first-order WKB convergence criterion (see, e.g., pp. 112-115 of ref. (8*a*)) was smaller than a chosen critical value. Thus, they are the solutions of

$$\left| [\alpha(y)]^{-2} \frac{d}{dy}\alpha(y) \right| = Z,$$

where $\alpha(y) = \{B_y[\bar{E} - \bar{V}(y)]\}^{\frac{1}{2}}$ and Z is the chosen convergence criterion. It was found here that $Z = 1.0 \times 10^{-5}$ yielded values of $\kappa(\bar{E})$ within 1×10^{-5} of the exact analytic barrier passage probabilities for Eckart barriers of different sizes. A Fortran listing of the subroutine used to integrate eqn (1) to yield $\kappa(\bar{E})$ is given in the appendix to ref. (15).

THE TUNNELLING FACTOR $\Gamma(T)$

The tunnelling factor is the ratio of the quantum mechanical to the classical barrier-crossing rate for particles with a Boltzmann distribution of initial kinetic energies relative to the barrier. In reduced units analogous to those of eqn (1), it may be written as [3]

$$\Gamma(\bar{T}) = \frac{1}{\bar{T}}\int_0^\infty \kappa(\bar{E}) \exp\left(\frac{1-\bar{E}}{\bar{T}}\right) d\bar{E} \tag{8}$$

where $\bar{T} = kT/V_0$, and V_0 is the barrier height. After obtaining $\kappa(\bar{E})$ values over a range of energies by the method presented above, eqn (8) may be integrated numerically. This quantity is in effect an observable and is the point of comparison between theoretical and experimental estimates of tunnelling.

APPLICATION TO PARABOLIC BARRIERS

The potential form which appears to have been most widely used to account for tunnelling in chemical processes [2] is the truncated parabola:

$$\begin{aligned} \bar{V}(y) &= 1-y^2 \qquad \text{for } -1 \leqslant y \leqslant 1 \\ &= 0 \qquad\quad \text{for } |y| < 1, \end{aligned} \tag{9}$$

where particles may impinge on the barrier with energies $\bar{E} > 0$. In the present discussion, the energy and length scaling factors V_0 and a used in B_y always signify the barrier height, and the half-width at its base. It is apparent that in this case the transmission probability function $\kappa(\bar{E})$ is completely defined by the corresponding value for B_y, since eqn (1) is precisely the same for all barriers with different heights and widths, but the same B_y.

It will be convenient to replace B_y by the previously used [2, 7] and equivalent reduced parameter

$$\beta = \pi(B_y)^{\frac{1}{2}} = 14.309\,46\,(\mu[\text{a.m.u.}]V_0[\text{kcal/mol}])^{\frac{1}{2}}a[\text{Å}] = 2197.524V_0[\text{kcal/mol}]/\nu[\text{cm}^{-1}]$$

where ν is the characteristic frequency of the harmonic oscillator potential obtained on inverting the parabolic barrier.* The reduced temperature $\bar{T}$ used here is equivalent to the previously used [2, 7] reduced variable $\alpha = 1/\bar{T}$. In the following discussion, particular combinations of temperature, and particle mass and barrier size are characterized by values of $\bar{T}$ and β. For given choices of these quantities, exact values of $\kappa(\beta,\bar{E})$ and $\Gamma(\beta,\bar{T})$ were calculated by the numerical method presented above.

*While consideration of eqn (1) suggests that B_y is a more "natural" parameter, previous work with truncated parabolas [2, 7] used β, which is a natural parameter in Bell's [7] approximate analytic tunnelling factor expressions.

The exact transmission probability [5] for particles impinging on an *infinite* parabolic barrier: $\bar{V}(y) = 1-y^2$, where $-\infty < y < +\infty$, is

$$\kappa_\infty(\beta,\bar{E}) = \{1+\exp[\beta(1-\bar{E})]\}^{-1}, \tag{10}$$

where $\bar{E}$ and β are as defined above, and $\bar{E}$ may range to $\pm\infty$. A widely used approximation has been to assume that the transmission coefficient for a *finite* parabolic barrier may be accurately represented by eqn (10). This question is examined in fig. 2 where the ratios of approximate (from eqn (10)) to exact numerical (κ_{ex}) transmission coefficients are plotted against $\bar{E}$ for barriers of different sizes (different β). The error inherent in the use of $\kappa_\infty(\beta,\bar{E})$ for finite barriers increases with decreasing β, and for the particle and barrier sizes considered, eqn (10) becomes satisfactory

only for energies above the top of the barrier ($\bar{E}>1$). However, in all cases it is significantly in error at low values of $\bar{E}$, and this will affect the tunnelling factors at low temperatures.

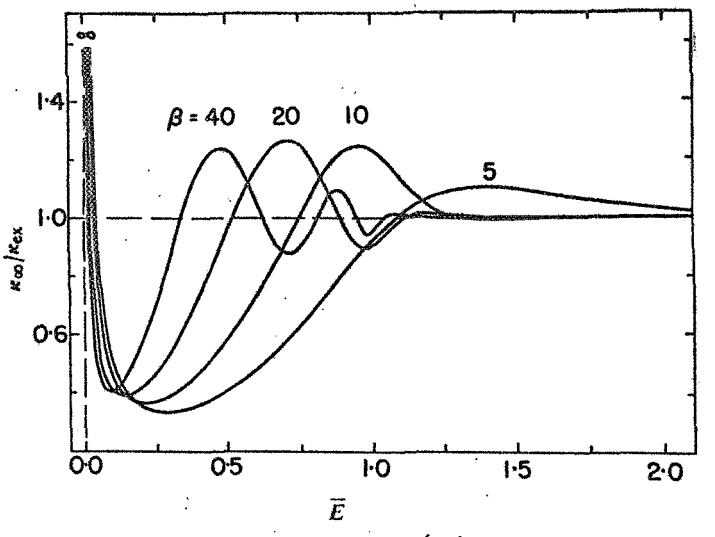

FIG. 2.—Ratios of approximate (κ_∞) to exact numerical (κ_{ex}) transmission probabilities for truncated parabolic barriers, as a function of the reduced energy $\bar{E}$. The barrier maxima correspond to $\bar{E} = 1$.

Bell's [7] widely used formulae for the tunnelling factors for truncated parabolic barriers are based on eqn (10). On substituting it into eqn (8) he obtained an analytic approximation for the resulting integral, yielding

$$\Gamma^{I}_{\infty}(\beta,\bar{T}) = \frac{\pi/\beta\bar{T}}{\sin(\pi/\beta\bar{T})} - \frac{\exp(1/\bar{T}-\beta)}{\beta\bar{T}-1}\times \left\{1-\left(\frac{1-\beta\bar{T}}{1-2\beta\bar{T}}\right)e^{-\beta}+\left(\frac{1-\beta\bar{T}}{1-3\beta\bar{T}}\right)e^{-2\beta}-\ldots\right\}. \quad (11)$$

Although individual terms in this expansion have singularities at integer values of $1/\beta\bar{T}$, there is exact mutual cancellation of such terms so that the sum remains finite and eqn (11) is defined for all values of $\beta\bar{T}$.* Bell also noted [7] that in the high

* In Bell's original treatment [7] he unnecessarily [2] restricted the use of eqn (11) to $\beta\bar{T}>1$.

temperature region where

$$\left|\frac{\exp(1/\bar{T}-\beta)}{\beta\bar{T}-1}\right| \ll 1,$$

$\Gamma^{I}_{\infty}(\beta,\bar{T})$ becomes

$$\Gamma^{II}_{\infty}(\beta,\bar{T}) = \frac{\pi/\beta\bar{T}}{\sin(\pi/\beta\bar{T})}, \quad (12)$$

which has been used widely.[2, 10] The accuracies of these approximate formulae are illustrated in fig. 3, where their predictions are compared to the exact numerical values $\Gamma_{ex}(\beta,\bar{T})$; the solid curves used eqn (11) for Γ_∞, and the broken curves eqn (12). The breaks in the solid curves at integer values of $1/\beta\bar{T}$ are a reminder that two of the terms in the full expansion of right side of eqn (11) are singular at each of these points.

the

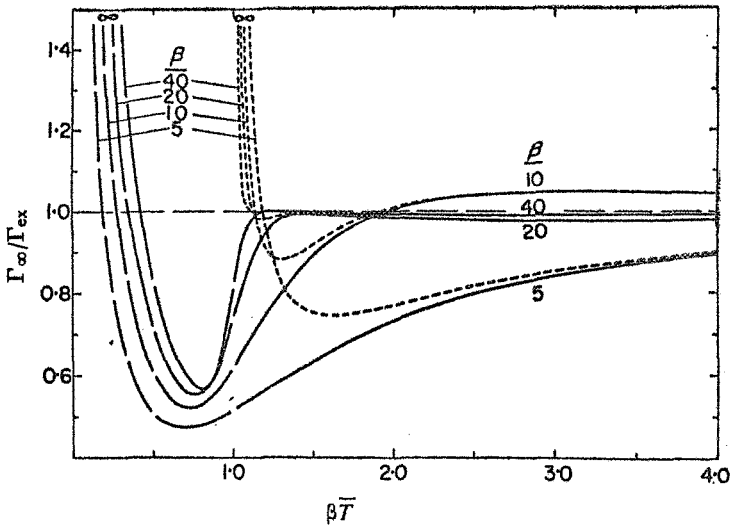

FIG. 3.—Ratios of approximate (Γ_∞) to exact numerical (Γ_{ex}) tunnelling factors for truncated parabolic barriers. The solid curves were obtained by using eqn (11) for Γ_∞, and the broken curves, eqn (12). The breaks in the former for $\beta\bar{T} \leqslant 1$ correspond to the points at which pairs of terms in eqn (11) blow up (i.e., where $1/\beta\bar{T}$ is an integer).

The effects shown in fig. 3 reflect the trends seen in fig. 2, the errors in the approximate formulae increasing with decreasing β and $\bar{T}$. For all barriers, the simple approximate formula Γ^{II}_∞ is as good as the more general expression Γ^{I}_∞ *wherever* the latter is reasonably accurate. For the larger barriers ($\beta \gtrsim 20$), this appears to include virtually all $\bar{T} > 1/\beta$. On the other hand, for all barrier sizes, none of the approximate formulae are at all reliable for $\bar{T} < 1/\beta$.* In addition to Γ^{I}_∞ and Γ^{II}_∞, this includes eqn (7) and (10) in Bell's paper,[7] which were suggested for use in this region. The former, proposed for $\bar{T} < 1/\beta$, yields curves of $\Gamma_\infty/\Gamma_{ex}$ which are identical to those for Γ^{I}_∞ from $\beta\bar{T} = 0$ to approximately their minima, and then rise to infinity at $\beta\bar{T} = 1$. The latter, designed for $\bar{T} \approx 1/\beta$, yields negative values of $\Gamma_\infty/\Gamma_{ex}$ for all $\bar{T}$ outside a very narrow interval about $\bar{T} = 1/\beta$, and even in this interval it is significantly less accurate than is Γ^{I}_∞.

*In addition to the results shown in fig. 3, a calculation for $\beta = 80$ showed that its $\Gamma^{I}_\infty/\Gamma_{ex}$ curve has a minimum of 0.57 at $\beta\bar{T} = 0.84$, while for all $\beta\bar{T} \gtrsim 1.05$ it is within 1 % of unity.

To put the present results in perspective it is helpful to consider Caldin's [2] table VII, which contains most of the reliable data on the dimensions of energy barriers for proton transfer reactions. For all of the cases presented there $\beta \gtrsim 30$, and the temperatures corresponding to $\beta\bar{T} = 1$ range between 130 and 250 K. Since most of the results were obtained using Γ^{II}_∞ (eqn (12)),[2] the experimental data for these cases must have corresponded to $\beta\bar{T} > 1$, and fig. 3 suggests that their derived barrier parameter should be reasonably accurate. However, the present results clearly demonstrate that in those cases for which eqn (11) had to be used (where $\beta\bar{T} \lesssim 1$), the reported barrier parameters are probably unreliable.

Another situation in which Bell's [7] approximate formulae have been used is in calculating tunnelling corrections to the rates of the isotopic $H+H_2$ exchange reactions. Weston [16] fitted a parabola to the reaction path at the saddle point of a Sato [17] potential surface for collinear collisions, and used Bell's formulae [7] to estimate

the tunnelling through it. This parabolic barrier was 8.0 kcal/mol high and had $\beta = 11.64$, so that $T = 1/\beta$ corresponded to 340°K. Using the present method it was found that Weston's [16] predicted tunnelling factors at 1000, 500, and 295 K are respectively 6 % larger, and 6 and 35 % smaller than the exact tunnelling factors for his barrier.

APPROXIMATION OF BARRIERS BY ECKART AND PARABOLIC FUNCTIONS RESULTS FOR $H + H_2$

This section examines the validity of approximating an actual barrier with a convenient analytic function, by considering the tunnelling contribution to the rate of the simple hydrogen exchange reaction. Here the exact 1-Dim barrier is taken as the minimum potential path on the potential surface for collinear collisions. A number of treatments have previously estimated the amount of tunnelling in this system using Eckart [3, 10, 18-20] or parabolic [10, 16] approximations to the actual potential barrier.

The potential surface used here is the one reported by Shavitt, Stevens, Minn and Karplus,[21] scaled by a factor of 0.89 as recommended by Shavitt.[19] The method of obtaining the present 1-Dim barrier from the low-energy path on this surface is described elsewhere.[11] Fig. 4 shows the actual energy barrier so obtained, curve A, and five approximations to it. Curves E_1 and P_1 are respectively Eckart and parabolic potentials with both the same height and curvature (second derivative) at the maximum as the "exact" barrier. Similarly, curves E_2 and P_2 are Eckart and parabolic barriers chosen to have the same height, and the same width at half maximum as the actual curve. The additional curve, S, is the Eckart function Shavitt [19] used in estimating tunnelling factors for this case. His potential had the same curvature at the maximum as the actual barrier, and was "selected by inspection to give a good fit to the *ab initio* barrier over as much of its upper part as possible". The constant reduced mass used with these potentials is $\mu = M_H/3 = 0.335\,94$ a.m.u.

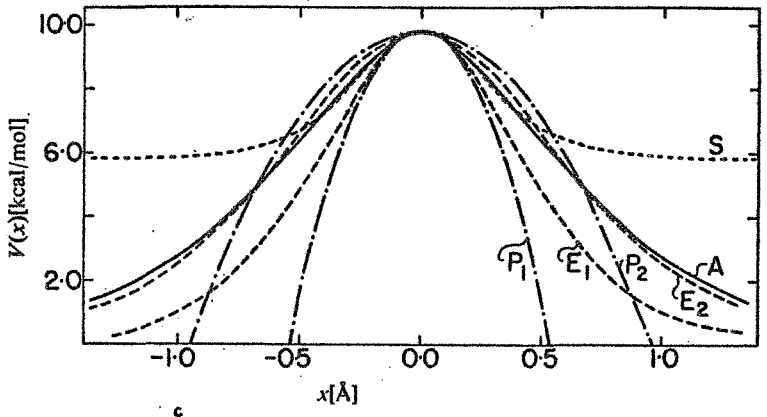

FIG. 4.—Comparison of actual theoretical 1-Dim potential barrier for collinear $H+H_2$ collisions (curve A) with analytic approximations to it. Curves P_1 and P_2 are truncated parabolas corresponding to $\beta = 14.74$ and 24.84, respectively, while curves E_1 and E_2 are Eckart functions, $V(x) = V_0/\cosh^2(x/a)$, with $a = 0.566$ and 0.768 Å respectively. E_1 and P_1 have the same curvature at the maximum as does curve A, while E_2 and P_2 have the same width at half maximum. Curve S is the Eckart function with which Shavitt [19] approximated the barrier for this case.

Fig. 5 shows the calculated tunnelling factors for these potentials as a function of temperature; the curves are labelled as in fig. 4. The total computer time required

to generate curve A was less than 1 min on an IBM-7094. As might be expected, the present Eckart tunnelling factors (curves E_1 and E_2) are closer to the exact values than are the parabolic results. However, none of the present approximate barriers yields tunnelling factors that are good, especially at low temperatures. On the other hand, the manner in which the approximate results straddle curve A (in fig. 5) suggests that their main source of error lies in the criteria used to fit the approximate barriers to the actual one. This is confirmed by the fact that Shavitt's Eckart function [19] yielded tunnelling factors in remarkable agreement with the present exact values, despite the large differences between his barrier and the actual one. Furthermore, it seems certain that systematic variation of the two free Eckart parameters could yield even better agreement with curve A. By comparison, it was found that no truncated parabola would yield tunnelling factors in good agreement with curve A over the whole temperature range shown. The best fit of this sort (corresponding to $\beta \simeq 19$) had $\Gamma(T)$ values which were significantly too small at high temperatures and too large at low. Thus, while the tunnelling factors for the $H+H_2$ case are insensitive to the nature of an approximating barrier except near its maximum, they are *very* sensitive to its shape in this region. In any case, exact numerical computations of $\Gamma(T)$ should be used whenever the shape of the barrier is known.

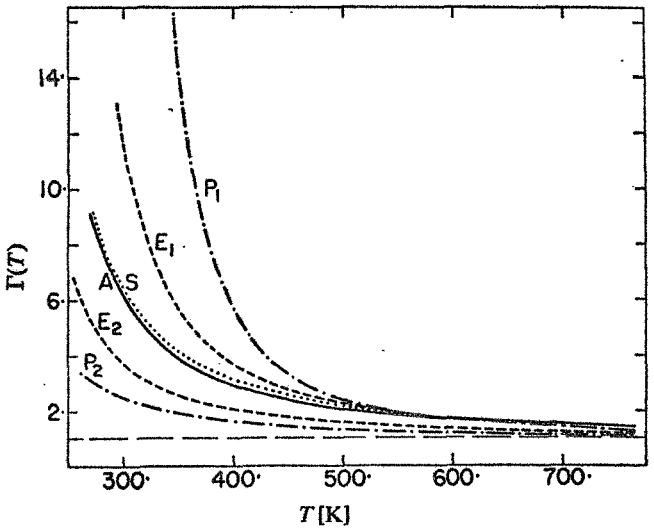

FIG. 5.—Tunnelling factors for the potentials shown in fig. 4, labelled in the same manner. The broken horizontal line lies at unity.

CONCLUDING REMARKS

A method has been presented for calculating the exact transmission probabilities and tunnelling factors for any 1-Dim potential barrier. It has been used to determine the region of validity of Bell's [7] approximate expressions for the tunnelling factors for truncated parabolic barriers. It has also been used elsewhere [11] to help correlate with theory some new experimental measurements of the relative rates of the exchange reactions $H+H_2$ and $H+D_2$.

The systems in which Bell's [7] formulae are appropriate are precisely those in which there is relatively little barrier transmission except at energies close to and above its maximum. This insensitivity of such results to the nature of the potential except near its maximum is further illustrated by the success of Shavitt's [19] approximation for the $H+H_2$ tunnelling, discussed in the preceding section. This suggests

that if experimental results may be accurately explained using eqn (11) or (12) for values of β and $\bar{T}$ for which these expressions accurately reflect the appropriate truncated parabola (e.g., $\beta \gtrsim 20$ and $\bar{T} > 1/\beta$), then the truncated parabola so obtained accurately approximates the shape and height of the actual 1-Dim potential barrier near its maximum.

The above quantitative confirmation of the validity of eqn (11) and (12) for large barrier situations (negligible tunnelling at low energies) will be reassuring to experimentalists who have been interpreting their data using these expressions. Also, the present method offers a way of treating cases where tunnelling is important at energies well below the barrier maximum, but for which the Eckart functions results are not sufficient. However, the whole of the present approach is based on the strong assumption that a multi-dimensional problem may be meaningfully represented in 1-Dim. The validity of this approximation has been examined by Truhlar and Kuppermann.[22]

This work was supported in part by National Aeronautics and Space Administration Grant NGL 50–002–001. The authors are also grateful to the National Research Council of Canada for support, and for the award of scholarships to two of us (R. J. L. and K. A. Q.). In addition, we thank Dr. R. L. Le Roy for helpful comments on the manuscript, and R. J. L. gratefully acknowledges the encouragement of Prof. R. B. Bernstein.

[1] S. Glasstone, K. J. Laidler and H. Eyring, *The Theory of Rate Processes* (McGraw-Hill, New York, 1941).
[2] E. F. Caldin, *Chem. Rev.*, 1969, 69, 135.
[3] H. S. Johnston, *Gas Phase Reaction Rate Theory* (Ronald Press, New York, 1966).
[4] C. Eckart, *Phys. Rev.*, 1930, 35, 1303.
[5] (*a*) E. C. Kemble, *The Fundamental Principles of Quantum Mechanics* (McGraw-Hill, New York, 1937), §21j; (*b*) L. D. Landau and E. M. Lifschitz, *Quantum Mechanics-Non Relativistic Theory*, 2nd ed. (Pergamon Press, London, 1965), p. 176.
[6] K. A. Quickert and D. J. Le Roy, *J. Chem. Phys.*, 1970, 52, 856.
[7] R. P. Bell, (*a*) *Trans. Faraday Soc.*, 1959, 55, 1; (*b*) the discussion in chap 11 of *The Proton in Chemistry* (Cornell University Press, Ithaca, New York, 1959).
[8] (*a*) E. Merzbacher, *Quantum Mechanics* (John Wiley & Sons, New York, 1961), pp. 91-93; (*b*) W. Kauzmann, *Quantum Chemistry* (Academic Press Inc., New York, 1957), pp. 195-198; (*c*) A. S. Davydov, *Quantum Mechanics*, (Pergamon Press, Toronto, 1965), § 26; (*d*) see also pp. 38-47 in ref. (3).
[9] G. G. Belford, A. Kuppermann, and T. E. Phipps, *Phys. Rev.*, 1962, 128, 524.
[10] D. J. Le Roy, B. A. Ridley and K. A. Quickert, *Disc. Faraday Soc.*, 1967, 44, 92.
[11] (*a*) K. A. Quickert, *Ph.D. Thesis* (University of Toronto, 1970); (*b*) K. A. Quickert and D. J. Le Roy,
[12] see e.g., R. W. Hamming, *Numerical Methods for Scientists and Engineers* (McGraw-Hill, New York, 1962), p. 215.
[13] (*a*) J. W. Cooley, *Math. Computations*, 1961, 15, 363; (*b*) J. K. Cashion, *J. Chem. Phys.*, 1963, 39, 1872.
[14] S. Gill, *Proc. Cambr. Phil. Soc.*, 1951, 47, 96.
[15] R. J. Le Roy, K. A. Quickert, and D. J. Le Roy, *University of Wisconsin Theoretical Chemistry Institute Report* WIS-TCI-384 (1970).
[16] R. E. Weston, Jr., *J. Chem. Phys.*, 1959, 31, 892.
[17] S. Sato, *J. Chem. Phys.*, 1955, 23, 592 and 2465.
[18] I. Shavitt, *J. Chem. Phys.*, 1959, 31, 1359.
[19] I. Shavitt, *J. Chem. Phys.*, 1968, 49, 4048.
[20] E. M. Mortensen, *J. Chem. Phys.*, 1968, 48, 4029.
[21] I. Shavitt, R. M. Stevens, F. L. Minn and M. Karplus, *J. Chem. Phys.*, 1968, 48, 2700.
[22] (*a*) D. G. Truhlar, *Ph.D. Thesis* (California Institute of Technology, 1970); (*b*) D. G. Truhlar and A. Kuppermann, *J. Chem. Phys.*, 1970, 52,

APPENDIX A: DISSOCIATION ENERGIES OF DIATOMIC MOLECULES FROM VIBRATIONAL SPACINGS OF HIGHER LEVELS: APPLICATION TO THE HALOGENS

This appendix contains a preliminary account of the work discussed in Sections 3.1 and 3.2; it is reprinted from Chemical Physics Letters, Volume 5, pp. 42-44 (North-Holland Publishing Company, Amsterdam, 1970).

Volume 5, number 1 CHEMICAL PHYSICS LETTERS 15 February 1970

DISSOCIATION ENERGIES OF DIATOMIC MOLECULES FROM VIBRATIONAL SPACINGS OF HIGHER LEVELS: APPLICATION TO THE HALOGENS *

ROBERT J. LEROY ** and RICHARD B. BERNSTEIN
Theoretical Chemistry Institute and Chemistry Department, University of Wisconsin, Madison, Wisconsin 53706, USA

Received 22 December 1969

The distribution of vibrational levels near the dissociation limit D, governed mainly by the long-range part of the potential, can be WKB-approximated to yield a simple expression which permits accurate determination of D. Improved ground-state dissociation energies are presented for Cl_2, Br_2 and I_2.

1. INTRODUCTION

Since its introduction 44 years ago, the Birge–Sponer (BS) extrapolation procedure has been widely used (mostly in its original form) to evaluate dissociation limits (D) of diatomic molecules from vibrational spectroscopic data [1]. The main difficulty in its application arises from the curvature generally exhibited in the "tails" of BS plots near the dissociation limit, which give rise to uncertainty in the extrapolation. The present communication reports a better, WKB-based method (derived and more fully discussed elsewhere [2]) which takes proper account of this curvature.

The new procedure has been applied to the halogens [2], yielding ground state D_0 values with much smaller uncertainties than heretofore obtainable. These results are presented in section 3.

2. METHOD

For highly excited vibrational levels lying close to the dissociation limit D, the potential $V(R)$ through their outer turning points may be well represented by an inverse-power functionality

$$V(R) = D - C_n/R^n. \qquad (1)$$

Differentiating the WKB eigenvalue expression with respect to energy, approximating the exact potential by eq. (1), and integrating (neglecting the small contribution to the exact integral from the region of the inner turning point), one obtains

$$\frac{dE(v)}{dv} = \hbar\sqrt{\frac{2\pi}{\mu}}\,\frac{\Gamma\left(1+\frac{1}{n}\right)}{\Gamma\left(\frac{1}{2}+\frac{1}{n}\right)}\,\frac{n}{C_n^{1/n}}\,[D-E(v)]^{\left(\frac{n+2}{2n}\right)}$$

$$= K_n[D-E(v)]^{\left(\frac{n+2}{2n}\right)}. \qquad (2)$$

Here $E(v)$ is the rotationless ($J=0$) energy of level v, μ the reduced mass, $\Gamma(x)$ the gamma function, and K_n a collection of constants; $dE(v+\frac{1}{2})/dv$ is very nearly $\Delta G_{v+\frac{1}{2}}$, the conventional BS ordinate. Eq. (2) requires (as is generally observed) positive (upward) curvature in BS plots for energies near enough to the dissociation limit for eq. (1) to be appropriate.

In practical applications it is convenient to use the integrated form of eq. (2); for $n \neq 2$ this becomes‡

* Work supported by National Science Foundation Grant GB-16665 and National Aeronautics and Space Administration Grant NGL 50-002-001.

** National Research Council of Canada Postgraduate Scholar.

‡ Expressions analogous to eq. (3) have also been obtained [2, 3] for the $n = 2$ case, and for a potential with an exponential long-range tail.

$$E(v) = D - [(v_D - v)H_n]^{\left(\frac{2n}{n-2}\right)}, \qquad (3)$$

where

$$H_n \equiv \left(\frac{n-2}{2n}\right) K_n \ .$$

Here v_D is an integration constant; for cases of $n > 2$ it can be identified as the "effective" (non-integer) vibrational index at the dissociation limit (i.e., $E(v_D) = D$).

Determination of D (together with n, C_n, and v_D) using eq. (3) requires at least four (preferably more) vibrational energies. The best approach is to carry out a non-linear least-squares fit of experimental eigenvalues to eq. (3), to yield a "best" set of parameters. However, typical non-linear regression programs* require fairly accurate initial trial values of the unknowns to ensure convergence to the "best" final values. Suitable starting values for n and v_D may be obtained by fitting the data to the following *linear* expression, obtained from eq. (3):

$$\frac{dE(v)/dv}{d^2E(v)/dv^2} = -\left(\frac{n-2}{n+2}\right)(v_D - v). \qquad (4)$$

Using these n and v_D values, eq. (3) becomes linear in the new variable

$$w \equiv \left[\left(\frac{n-2}{2n}\right)(v_D - v)\right]^{\left(\frac{2n}{n-2}\right)},$$

$$E(v) = D - wK_n^{\left(\frac{2n}{n-2}\right)}. \qquad (3')$$

Fitting the data to eq. (3') then yields trial values of D and K_n. The full set of parameters now serves as the trial set for the refined non-linear least-squares fit to eq. (3) which yields the "best" parameter values. In principle, eqs. (4) and (3') are just as accurate as eq. (3). However, in practice, the prior smoothing of experimental energies to obtain the derivatives in eq. (4) introduces some error, so that the subsequent fit to eq. (3) is slightly more reliable.

3. RESULTS. GROUND-STATE DISSOCIATION ENERGIES OF THE HALOGENS

Application of the present method to spectroscopic data for Cl_2, Br_2, and I_2, together with conclusions regarding the nature of the long-range forces, are discussed in detail elsewhere [2,3]. Attention here is restricted to the values obtained for the ground ($X\,^1\Sigma_g^+$) state dissociation energies.

The experimental data are the band origins for transitions between the $v'' = 0$ level of the ground electronic state and highly excited vibrational levels (v') of the $B\,^3\Pi_{0u}^+$ state. Fitting these to eq. (3) by the numerical methods discussed in section 2, yielded the dissociation limits D for the B-states. Subtracting from D the accurately known $^2P_{1/2} - {}^2P_{3/2}$ atomic spin-orbit splitting (ΔE) yielded values of D_0 for the ground ($X^1\Sigma_g^+$) states.

3.1. *Chlorine*

The most extensive measurements are for $^{35,35}Cl_2$ [4]. The present analysis of these data places D some 2.85(±0.15) cm^{-1} above the highest observed level, $v' = 31$ (cf. the experimenters' value: 3.1(±2) cm^{-1} [4]. Subtracting from D the ΔE of 882.50 cm^{-1} [5,6] yields a dissociation energy of D_0 = 19 997.25(±0.15) cm^{-1} (see table 1).

3.2. *Bromine*

For each of the pure isotopic species $^{79,79}Br_2$ and $^{81,81}Br_2$, energies of four adjacent vibrational levels very near the B-state dissociation limits have been reported [7]. Analysis by the present method yielded binding energies of 5.24(±0.17) cm^{-1} and 6.96(±0.22) cm^{-1}, respectively, for the highest observed level of each species, $v' = 53$‡.

‡ It has been found [3] that the experimenters' [7] vibrational assignments for the four levels near the dissociation limit should be increased by one.

Table 1
Results for the halogens[a)]

Species	v'_H	$B\,^3\Pi_{0u}^+$ state $D - E(v'_H)$ (cm^{-1})	$X\,^1\Sigma_g^+$ state D_0 (eV)
$^{35,35}Cl_2$	31	2.85 ± 0.15 (3.1 ± 2.0) [4]	2.479 367 ± 0.000 019
$^{79,79}Br_2$	53	5.24 ± 0.17 (2.7 ± 0.5) [7]	1.970 69 ± 0.000 04
$^{81,81}Br_2$	53	6.96 ± 0.22 (4.1 ± 0.5) [7]	1.970 95 ± 0.000 05
$^{127,127}I_2$	72	19.6 ± 1.1 (12.6) [9]	1.542 49 ± 0.000 14

a) The values in parentheses are the previous best estimates of these binding energies. The uncertainties in the present results correspond to a 95% statistical confidence limit. The energy conversion factor was taken from ref. [16].

* The present computations employed the University of Wisconsin Computing Center's subroutine GASAUS.

These values are significantly greater than the 2.7(± 0.5) and 4.1(± 0.5) cm^{-1}, respectively, obtained [7] from extrapolations of limiting curves of dissociation. Subtracting ΔE = = 3685.2(± 0.3) cm^{-1} [8] from the thus-obtained D values yields:

$$D_0(^{79,79}Br_2) = 15\,894.5(\pm 0.3_4)\ cm^{-1},$$

and

$$D_0(^{81,81}Br_2) = 15\,896.6(\pm 0.3_7)\ cm^{-1}.$$

The zero-point shift is in good accord with the more-directly obtained value of 2.029(± 0.013) cm^{-1} from ref. [7].

3.3. *Iodine*

For the case of $^{127,127}I_2$, the data [9] for the highest observed levels of the B-state are relatively less accurate. The present analysis yields a binding energy for the uppermost recorded level, $v' = 72^*$, of 19.6(± 1.1) cm^{-1} (considerably greater than the experimenter's estimate [9] of 12.6 cm^{-1}).

Using ΔE = 7603.15 cm^{-1} [5, 12] one obtains D_0 = 12 440.9(± 1.1) cm^{-1}. This value differs significantly with the previously recommended one of 12 452.5(± 1.5) cm^{-1} [13]; the source of the discrepancy is discussed elsewhere [14].

4. CONCLUSIONS

A new method has been described for extrapolating beyond the highest observed vibrational levels of a diatomic molecule to determine its dissociation limit. On the basis of the available evidence [2, 3], it appears to be more reliable than the utilization either of the limiting curve of dissociation** or of a BS extrapolation. For levels near the dissociation limit for which the BS plot shows positive curvature, its use should supersede that of the conventional Birge–Sponer extrapolation.

Table 1 summarizes the results of applying the present method to the determination of the halogen dissociation energies. Binding energies of the highest observed B-state vibrational levels (v'_H) are also tabulated and compared with previously reported values.

*It has been found [10, 11] that the vibrational numbering of ref. [9] should be decreased by one.

**See, for example, ref. [15].

REFERENCES

[1] R. T. Birge and H. Sponer, Phys. Rev. 28 (1926) 259;
R. T. Birge, Trans. Faraday Soc. 25 (1929) 707;
A. G. Gaydon, Dissociation energies, 3rd Ed. (Chapman and Hall, London, 1968) ch. 5.
[2] R. J. LeRoy and R. B. Bernstein, Univ. Wisconsin Theoret. Chem. Inst. Rept. WIS-TCI-362 (1969), to be published in J. Chem. Phys. See Section 3.1.
[3] R. J. LeRoy and R. B. Bernstein, Univ. Wisconsin Theoret. Chem. Inst. Rept. WIS-TCI-369 (1970). Section 3.2.
[4] A. E. Douglas, Chr. Kh. Møller and B. P. Stoicheff, Can. J. Phys. 41 (1963) 1174.
[5] C. Moore, Natl. Bur. Std. (US), Circ. 467 (1958) Vol. 3.
[6] S. Avellén, Arkiv Fysik 8 (1954) 211.
[7] J. A. Horsley and R. F. Barrow, Trans. Faraday Soc. 63 (1967) 32.
[8] J. L. Tech, J. Res. Natl. Bur. Std. A 67 (1963) 505.
[9] W. G. Brown, Phys. Rev. 38 (1931) 709.
[10] J. I. Steinfeld, R. N. Zare, L. Jones, M. Lesk and W. Klemperer, J. Chem. Phys. 42 (1965) 25.
[11] R. L. Brown and T. C. James, J. Chem. Phys. 42 (1965) 33.
[12] C. C. Kiess and C. H. Corliss, J. Res. Natl. Bur. Std. A 63 (1959) 1.
[13] R. D. Verma, J. Chem. Phys. 32 (1960) 738.
[14] R. J. LeRoy, J. Chem. Phys., to be published. See Section 6.
[15] G. Herzberg, Spectra of diatomic molecules, 2nd Ed. (Van Nostrand, Princeton, 1950).
[16] B. N. Taylor, W. H. Parker and D. N. Langenberg, Rev. Mod. Phys. 41 (1969) 375.

APPENDIX B: RECOMBINATION OF IODINE ATOMS IN DILUTE SOLUTIONS OF ARGON

The rate constants reported in this section are analyzed according to a mechanism which assumes thermal equilibrium between I and Ar atoms, and molecular I-Ar. Fitting the mechanism to the experimental data yielded an estimate of this equilibrium constant and its temperature dependence. Following the discussion of Section 4.2 (above), these are used to determine approximately the depth and minimum position of the I-Ar potential well. It should be noted, however, that the values obtained are probably somewhat large, since the expression used for the equilibrium constant[1] treats the quasibound levels of the diatomic[2] as unbound, while in fact they will make a significant contribution to the equilibrium population of I-Ar.[3]

The work presented below is reprinted from the Proceedings of the Royal Society of London, Series A, Volume 316, pp. 81-96 (1970).

FOOTNOTES:

1. S. K. Kim, J. Chem. Phys. 46, 123 (1967).
2. See Chapter 7.
3. D. E. Stogryn and J. O. Hirschfelder, J. Chem. Phys. 31, 1531 (1959).

Proc. Roy. Soc. Lond. A. 316, 81–96 (1970)
Printed in Great Britain

Recombination of iodine atoms in dilute solutions of argon†

BY G. BURNS, R. J. LEROY,‡ D. J. MORRISS§ AND J. A. BLAKE‖
Lash Miller Chemical Laboratories, University of Toronto, Toronto 181, *Ontario, Canada*

(*Communicated by R. G. W. Norrish, F.R.S.—Received* 30 *June* 1969 —*Revised* 17 *November* 1969)

The reaction $2I + Ar \rightarrow I_2 + Ar$ was studied at 298, 323 and 423 K by flash photolysis. The overall rate constant, k_{obs}, for this reaction is a linear function of $[I_2]/[Ar]$, but below $[I_2]/[Ar] \sim 10^{-4}$, the relation becomes non-linear and k_{obs} falls below extrapolated values. The fall-off is explained in terms of a mechanism involving an IAr intermediate:

$$I + Ar \rightleftharpoons IAr$$
$$IAr + I \rightarrow I_2 + Ar.$$

The equilibrium separation in such an IAr complex is 0.55 nm and the binding energy is 6.3 kJ mol^{-1} (1.5 kcal mol^{-1}). This mechanism predicts the onset of the fall-off in agreement with the available experimental data. Moreover, the temperature dependence of this onset and the temperature dependence of the recombination rate constant from 298 to 1500 K are also satisfactorily explained.

In addition to the above, the new mechanism yields quantitative agreement between our new rate constants and those reported previously. These combined data for 298 K yield a value of $3.00\ (\pm 0.16) \times 10^9$ l^2 mol^{-2} s^{-1} for the rate constant for the reaction

$$2I + Ar \rightarrow I_2 + Ar,$$

and one of $1.00(\pm 0.09) \times 10^{12}$ l^2 mol^{-2} s^{-1} for $2I + I_2 \rightarrow 2I_2$.

Several other mechanisms are also considered, including some previously suggested in the literature. It is shown that none of these explains satisfactorily *all* the experimental data. However, *most* of the available experimental data could be explained, if it were assumed that the recombination proceeds via an unobserved electronically excited I_2, formed from two $^2P_{\frac{1}{2}}$ atoms, with a potential well 21 to 29 kJ mol^{-1} deep (5 to 7 kcal mol^{-1}).

INTRODUCTION

The termolecular recombination of iodine atoms in the presence of a third body, M:

$$2I + M \rightarrow I_2 + M, \quad (1)$$

$$d[I_2]/dt = k_{obs}[I]^2[M] \quad (2)$$

was studied by Rabinowitch & Wood (1936), using a photostationary method, and by Christie, Harrison, Norrish & Porter (1955), Strong, Chien, Graf & Willard

† This work was presented, in part, at the Toronto Meeting of the American Physical Society: *Bull. Am. phys. Soc.* II, 12, 638 (1967), and, in part, at the Meeting of the American Chemical Society, Atlantic City, September 1968.

‡ Present address: Theoretical Chemistry Institute, University of Wisconsin, Madison, Wisconsin 53706, U.S.A.

§ Present address: Department of Chemical Technology, Ryerson Polytechnical Institute, Toronto, Ontario, Canada.

‖ Present address: Department of Food Science, University of Toronto, Toronto 181, Ontario, Canada.

(1957), Bunker & Davidson (1958), Engleman & Davidson (1960), Kramer, Hanes & Bair (1961) and Porter & Smith (1961), all of whom used flash photolysis. Rabinowitch (1937) suggested that such recombination proceeds via an I–M complex. If more than one third body (M_i) contributes to the reaction, Rabinowitch's mechanism may be generalized as follows:

$$I + M_i \underset{k_{-3i}}{\overset{k_{3i}}{\rightleftharpoons}} IM_i, \tag{3}$$

$$IM_i + I \xrightarrow{k_{4i}} I_2 + M_i, \tag{4}$$

$$IM_i + IM_j \xrightarrow{k_{5ij}} I_2 + M_i + M_j, \tag{5}$$

$$d[I_2]/dt = \sum_{i=1}^{N} k_{4i}[I][IM_i] + \sum_{i=j}^{N}\sum_{j=1}^{N} k_{5ij}[IM_i][IM_j]. \tag{6}$$

Assuming that equilibria (3) are maintained, equation (6) reduces to

$$d[I_2]/dt = \sum_{i=1}^{N} k_{4i}K_{3i}[I]^2[M_i] + \sum_{i=j}^{N}\sum_{j=1}^{N} k_{5ij}K_{3i}K_{3j}[I]^2[M_i][M_j], \tag{7}$$

where $K_{3i} = k_{3i}/k_{-3i}$ is the equilibrium constant for reaction (3).

The experimental rate constant k_{obs} (equation (2)) has usually been obtained by optically monitoring the concentration of I_2 following the flash. In this case, the apparent iodine atom concentration is

$$[I]_{app} = [I] + \sum_{i=1}^{N} [IM_i] = [I]\left(1 + \sum_{i=1}^{N} K_{3i}[M_i]\right), \tag{8}$$

where $[I]_{app}$ is twice the concentration of dissociated molecular iodine (i.e.

$$d[I_2]/dt = -\tfrac{1}{2}\, d[I]_{app}/dt.$$

Replacing [I] in equation (2) by $[I]_{app}$, and combining the result with equation (7), one obtains

$$\begin{aligned} k_{obs} &= (d[I_2]/dt)\,[I]_{app}^{-2}\,[M_1]^{-1} \\ &= \left(1 + \sum_{i=1}^{N} K_{3i}[M_i]\right)^{-2}\left(k_{4,1}K_{3,1} + \sum_{i=2}^{N} k_{4i}K_{3i}[M_i]/[M_1] \right. \\ &\qquad \left. + \sum_{i=j}^{N}\sum_{j=1}^{N} K_{3j}k_{5ij}K_{3i}[M_i][M_j]/[M_1]\right), \end{aligned} \tag{9}$$

where M_1 is the diluent gas which is present in large excess.

In the past, it has usually been implicitly assumed that concentrations of IM_i complexes are negligible compared with the iodine atom concentration, and that $K_{3i}[M_i] \ll 1$ for all i. The contribution of (5) also was usually neglected. In this case, since in most experiments the only third bodies available were molecular iodine and a single diluent gas, equation (9) reduces to

$$\left.\begin{aligned} k_{obs} &= k_{4M}K_{3M} + k_{4I_2}K_{3I_2}[I_2]/[M], \\ &= k_M + k_{I_2}[I_2]/[M]. \end{aligned}\right\} \tag{10}$$

Equation (10) has been verified for various M over an appreciable range of $[I_2]/[M]$ ratios (Christie *et al.* 1955). However, Christie *et al.* (1955) and Kramer *et al.* (1961) observed that if the $[I_2]/[M]$ ratio is less than about 2×10^{-4}, k_{obs} falls below the extrapolation of results obtained at higher concentration ratios. Moreover, Christie (1962) deduced the existence of the fall-off from the results of Bunker & Davidson (1958). Since fall-off occurs at low dilution ratios, it cannot be ascribed to the thermal effects described by Burns & Hornig (1960) and by Burns (1967). Christie *et al.* (1955) suggested that the fall-off could be attributed to the formation of metastable iodine molecules which are deactivated only by collisions with $I_2(^1\Sigma_g^+)$. However, they made no attempt to identify the metastable iodine.

The present work was undertaken to investigate this low concentration ratio fall-off and to determine the nature of the intermediate that would account for its existence.

Experimental

The iodine recombination reaction in argon was investigated in two conventional flash photolysis apparatuses. The reaction vessel of apparatus I was double-walled, constructed of quartz tubing, 167 cm long, and had a 35 mm diameter. The flash lamp, also made of quartz tubing, was 175 cm long and had a 9 mm diameter. The flash was generated by discharging through the lamp a 10 μF capacitor, at typically 15 kV. The lamp and the reaction vessel were mounted parallel within a polished aluminium reflector. The reflector was wrapped in heating tape and asbestos insulation. The reaction vessel could be heated to 450 K; the temperature fluctuation along the length of the cell was less than 2 K. A greaseless vacuum system was constructed for these experiments; Teflon type stopcocks were used in the vacuum system.

Flash photolysis apparatus II was similar, though physically smaller. A single walled reaction vessel and flash lamp were mounted in a furnace; the portions of the vacuum system containing iodine were enclosed in an oven which could be heated to 1200 K. Greaseless stopcocks were used in these portions of the vacuum system.

The recombination was monitored using a quartz incandescent lamp, collimating lenses and an RCA 931-A-photomultiplier tube. The analyzing beam was rendered monochromatic using an interference filter and a Corning no. 3387 cut-off filter. This combination of filters had a transmission peak at 487 nm with a peak half-width of 7 nm. The amplified output of the photomultiplier was displayed on an oscilloscope and photographed. Four to seven photographs were taken and combined to obtain one value of the rate constant. A second photomultiplier monitored the drift in intensity of the analysing light. The response time of the photomultiplier circuits was better than 1.5 μs.

The iodine molecule concentration was determined from the optical transmission of the cell before and after filling with an I_2–Ar gas mixture; for this purpose, the decadic extinction coefficient was determined for each apparatus. In these determinations, an ice bath was used to produce a standard iodine vapour pressure. The vapour pressure–temperature relation of Gillespie & Fraser (1936) was used.

Results

To obtain k_{obs}, the data were reduced according to the integrated form of equation (2). For ratios $[I_2]/[Ar] > 10^{-4}$ ('high ratio' results), the values of k_{obs} (shown in

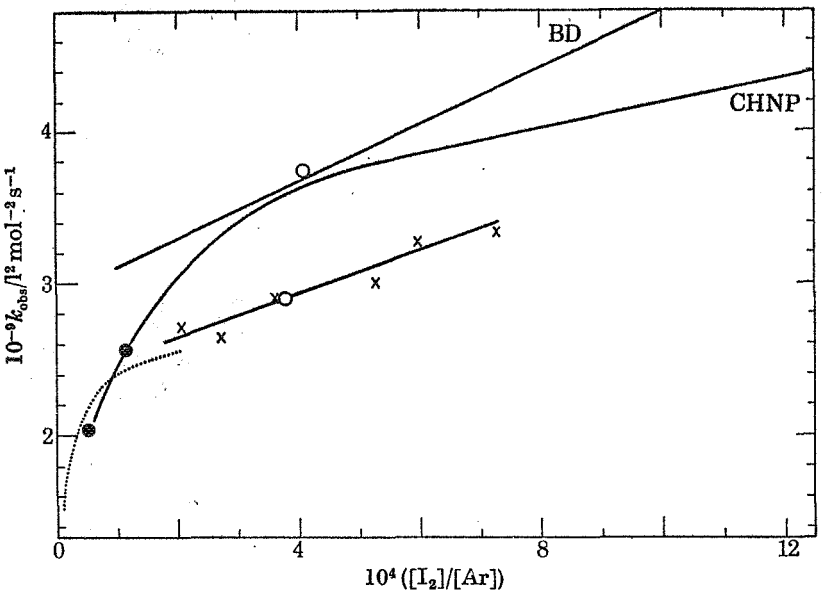

FIGURE 1. Recombination rate constants, k_{obs}, against $[I_2]/[Ar]$ at room temperature: BD, Bunker & Davidson (1958); CHNP, Christie *et al.* (1955); ○, Strong *et al.* (1957); ●, Kramer *et al.* (1961); ..., this work-apparatus 1; ×, this work-apparatus 2.

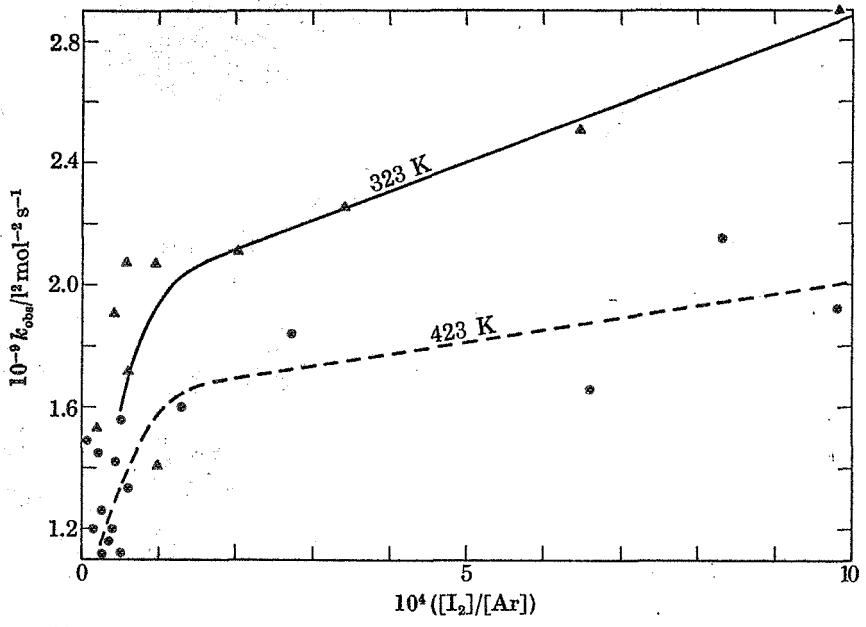

FIGURE 2. Recombination rate constants, k_{obs}, against $[I_2]/[Ar]$ at 323 K (▲) and 423 K (●), obtained from apparatus I.

figures 1 and 2) were a linear function of $[I_2]/[Ar]$, as predicted by equation (10). The values of k_{Ar} and k_{I_2}, defined as the intercept and slope of this linear plot, agree well with those in the literature (see table 1) except that the present values of k_{Ar} at 298 and 323 K are somewhat lower than those of previous investigators. However, this discrepancy may be partially explained in terms of the mechanism which accounts for the low concentration ratio fall-off. This mechanism will be described later in this paper.

TABLE 1. SUMMARY OF RESULTS ON RECOMBINATION OF IODINE ATOMS IN Ar AND I_2, INTERPRETED ACCORDING TO EQUATION (10)

T/K	$10^{-9}\,k_{Ar}/l^2\,mol^{-2}\,s^{-1}$	$10^{-12}\,k_{I_2}/l^2\,mol^{-2}\,s^{-1}$	Reference
298	$3{\cdot}3 \pm 0.36$	0.85	Christie *et al.* (1955)
	2.9 ± 0.3	1.9 ± 0.2	Bunker & Davidson (1958)
	2.4 ± 0.1	1.4 ± 0.2	This work, apparatus II
323	3.15	0.973 ± 0.1‡	Engleman & Davidson (1960)
	2.99 ± 0.15†	1.07 ± 0.18†	Engleman & Davidson (1960)
	1.9 ± 0.1	1.0 ± 0.1	This work, apparatus I
423	1.84	0.227 ± 0.053‡	Engleman & Davidson (1960)
	1.66 ± 0.05†	0.143 ± 0.038†	Engleman & Davidson (1960)
	1.6 ± 0.1	0.38 ± 0.2	This work, apparatus I

† Calculated from data obtained by Bunker & Davidson (1958).
‡ Obtained from measurements in excess of He.

TABLE 2. k_{obs}, $[I_2]$ AND [Ar] ROOM TEMPERATURE, APPARATUS I

$10^9\,k_{obs}/l^2\,mol^{-2}\,s^{-1}$	$10^5[I_2]/mol\,l^{-1}$	$10^2[Ar]/mol\,l^{-1}$
	no filter used	
1.70	0.067	8.01
1.62	0.077	7.79
1.67	0.096	7.97
1.48	0.150	6.49
1.77	0.139	5.83
1.77	0.169	6.11
1.84	0.134	4.23
2.08	0.155	4.25
2.13	0.219	4.21
2.32	0.228	3.58
2.39	0.254	2.40
2.44	0.373	1.67
	$K_2Cr_2O_7$ filter solution used	
1.78	0.075	7.77
1.69	0.083	7.89
2.00	0.148	7.91
2.05	0.199	7.86
1.87	0.181	7.15
2.11	0.158	7.89
2.27	0.214	5.41
1.96	0.332	7.87
2.13	0.369	5.68
2.27	0.284	3.95
2.13	0.390	4.12
2.49	0.823	3.94

Room temperature rate constants for $[I_2]/[Ar] < 10^{-4}$ ('low ratio' results) fall below the linear extrapolation from those at higher ratios, in agreement with the findings of previous investigators (table 2 and figures 1 and 2).

Discussion

The rate constant drop-off at low concentration ratios (figures 1 and 2) may be explained in terms of the participation of an intermediate species in the reaction process. In this section several possible intermediates are considered; however, it is shown that only one of these can successfully account for *all* of the experimental observations.

Participation of $I_2(B\,^3\Pi_{0u}^+)$

It was pointed out by Nikitin (1966) that the low $[I_2]/[Ar]$ fall-off may be due to the participation of electronically excited iodine molecules. Such molecules may be formed either from ground state atoms ($^2P_{\frac{3}{2}}$) or from excited iodine atoms ($^2P_{\frac{1}{2}}$). The recombination of excited atoms with ground state atoms into attractive states, one of which ($B\,^3\Pi_{0u}^+$) is known, may take place. It has been argued by Snider (1966) that these $B^3\Pi_{0u}^+$ molecules deactive to the ground state only upon collision with other I_2. Thus, at low $[I_2]/[Ar]$, this route for recombination would be ineffective and the fall-off would occur. Snider also pointed out that this mechanism is not in disagreement with the data of Christie *et al.* (1955). However, Steinfeld & Klemperer (1965) found that $B\,^3\Pi_{0u}^+$ molecules predissociate very readily on collision with inert gases. Therefore deactivation via collision with I_2 could not be important. Moreover, the radiative lifetime of $B^3\Pi_{0u}^+$ state is of the order of a microsecond, which is three orders of magnitude shorter than the typical recombination time. For these reasons, $B\,^3\Pi_{0u}^+$ state cannot account for the observed fall-off.

Participation of excited $I(^2P_{\frac{1}{2}})$ atoms

Another possible explanation of the fall-off involves direct participation of $I(^2P_{\frac{1}{2}})$ atoms:

$$I(^2P_{\frac{1}{2}}) + I_2 \rightarrow I(^2P_{\frac{3}{2}}) + I_2. \qquad (11)$$

Alternatively, $I(^2P_{\frac{1}{2}})$ atoms may participate in the overall recombination reaction via electronically excited I_2, other than $^3\Pi_{0u}^+$,

$$I(^2P_{\frac{1}{2}}) + I_2(^1\Sigma_g^+) \rightarrow I_2(\text{elec. excited}) + I(^2P_{\frac{3}{2}}) \rightarrow I_2(^1\Sigma_g^+) + I(^2P_{\frac{3}{2}}) \qquad (12)$$

in a reaction which precedes the recombination. The fall-off would then be observed at low $[I_2]/[Ar]$. Experiments suitable for testing the validity of this mechanism were carried out by Christie *et al.* (1955), who flash photolysed I_2 in Ar, using a potassium dichromate filter solution in a double walled photolysis reaction vessel. This filter limited the wavelength of the photolysing light reaching the reaction mixture, so that the $B\,^3\Pi_{0u}^+$ iodine molecules, formed in the photolysis were at least 800 cm^{-1} below the dissociation limit of the state. In this case the $B\,^3\Pi_{0u}^+$ molecules predissociate to give two $^2P_{\frac{3}{2}}$ atoms, thus effectively preventing the production of $I(^2P_{\frac{1}{2}})$.

Christie *et al.* (1955) found that the use of the potassium dichromate filter solution did not affect the magnitude of the rate constants. Unfortunately, only one experiment was performed in the fall-off region; it suggested that a mechanism involving reactions (11) and (12) cannot account for the abnormally small rate constants at low $[I_2]/[Ar]$. We extended the range of the Christie *et al.* (1955) experiments and obtained twenty-one rate constant measurements in the 'low-ratio' region. In eleven of these, a potassium dichromate filter solution was used; in the remainder, no filter was used. The results (table 2) indicate that the rate constants in the fall-off region may be lower by about 10 % if a filter solution is not used. However, such a discrepancy is almost within experimental error. Therefore, it is concluded that while reactions (11) and (12) may contribute they are not the main cause of the observed fall-off. This conclusion is in agreement with direct measurements of the $I(^2P_{\frac{1}{2}})$ relaxation rate due to $I(^2P_{\frac{1}{2}}) - I_2$ collisions, reported by Donovan & Husain (1965).

Participation of vibrationally excited $I_2(X\,^1\Sigma_g^+)$

To explain the fall-off at low $[I_2]/[M]$, Christie (1962) proposed the following mechanism:

$$I + I + M \rightarrow I_2^\dagger + M, \tag{13}$$

$$I_2^\dagger + I_2 \rightarrow 2I_2, \tag{14}$$

where $I_2^\dagger$ is a vibrationally excited ground state ($^1\Sigma_g^+$) iodine molecule. According to this mechanism, the relaxation (14) becomes the rate determining step at low $[I_2]/[M]$ ratios. However, Shields (1960) showed that vibrational relaxation of $I_2(^1\Sigma_g^+)$ is much too fast to cause the fall-off in k_{obs} at concentration ratios of the order of 10^{-4}. The theoretical analyses of Nikitin (1962) and Snider (1966) also preclude an explanation involving reactions (13) and (14), which will not be further discussed here.

Participation of electronically excited I_2 *produced from two* $^2P_{\frac{3}{2}}$ *atoms*

An alternative explanation of the fall-off involves the participation of electronically excited molecules, I_2^*, produced from atoms in the *ground* electronic state (i.e. two $I(^2P_{\frac{3}{2}})$ atoms). For the experimental situation where only I_2 and a single inert gas M are present as third bodies, this mechanism may be written as

$$I + I + M \xrightarrow{k_{15}} I_2 + M, \tag{15}$$

$$I + I + I_2 \xrightarrow{k_{16}} I_2 + I_2, \tag{16}$$

$$I + I + M \underset{k_{-17}}{\overset{k_{17}}{\rightleftharpoons}} I_2^* + M, \tag{17}$$

$$I + I + I_2 \underset{k_{-18}}{\overset{k_{18}}{\rightleftharpoons}} I_2^* + I_2, \tag{18}$$

$$I_2^* + I_2 \xrightarrow{k_{19}} 2I_2. \tag{19}$$

If more than one excited state is involved, reactions (17), (18) and (19) are repeated for each state. This mechanism is particularly interesting because it would imply

that in the fall-off region the internal (electronic) distribution function of I_2 differs, during recombination, from the equilibrium distribution function (Nikitin 1966).

Assuming a steady state in I_2^* and the approximations inherent in equation (10), the following expression for k_{obs} is obtained:

$$k_{obs} = k_{15} + (k_{16} + Kk_{19})\,[I_2]/[M] - \frac{(Kk_{19}\,[I_2]/[M])^2}{k_{17} + (k_{18} + Kk_{19})\,[I_2]/[M]}$$

$$= k_{15} + k_{16}[I_2]/[M] + \frac{Kk_{19}\,(k_{17} + k_{18}[I_2]/[M])\,([I_2]/[M])}{k_{17} + (k_{18} + Kk_{19})\,[I_2]/[M]}, \tag{20}$$

where

$$K = k_{17}/k_{-17} = k_{18}/k_{-18}. \tag{21}$$

The mechanism (15) to (19) explains the fall-off at low $[I_2]/[M]$ provided that k_{16} and k_{18} are very much smaller than Kk_{19}. Then for the special case of very small values of $[I_2]/[M]$

$$k_{obs} \approx k_{15} + Kk_{19}[I_2]/[M], \tag{22}$$

and for large $[I_2]/[M]$ such that $Kk_{19}\,[I_2]/[M] \gg k_{17}$,

$$k_{obs} \approx k_{15} + k_{17} + (k_{16} + k_{18})\,[I_2]/[M]. \tag{23}$$

Values of the four independent parameters k_{15}, $k_{16} + k_{18}$, k_{17} and Kk_{19} were derived for the best fit of equation (20) at room temperature, for the special case M = Ar, using the data of Christie *et al.* (1955). These data were used rather than our own (table 1), because while the latter are more abundant at very small $[I_2]/[Ar]$ values, the former extend to much higher concentration ratios, and hence reach both high and low asymptotic regions. If the mechanism (15) to (19) is valid, the constants obtained should apply equally well to both sets of data.

It was found that the experimental differences between our work and those of Christie *et al.* are appreciable at higher $[I_2]/[Ar]$ (figure 1). On the other hand, the Kk_{19} value obtained from our data (table 1) agrees well with that obtained from the Christie *et al.* data. This value of Kk_{19}, 1.6 $(\pm 0.7) \times 10^{13}\,l^2\,mol^{-2}\,s^{-1}$, quantitatively relates the nature of the I_2^* internuclear potential which determines K, to the effective collision diameter buried in k_{19}.

The I_2^* mechanism may now be tested by considering its predictions with respect to four factors. These are: (1) the nature of the internuclear potential for the I complex, (2) the dependence of the ratio at which fall-off begins, $([I_2]/[M])_{dev}$, on the nature of the third body M, (3) the temperature dependence of $([I_2]/[M])_{dev}$, and (4) the apparent inconsistencies (shown in figure 1) between the experimental results obtained in different laboratories.

Chang (1967) has used perturbation theory to calculate moderately long-range interaction energies for pairs of degenerate atoms for non-resonant cases. His results show that of the sixteen molecular states formed from pairs of ground $^2P_{\frac{3}{2}}$ iodine atoms, at least seven other than the ground $X\,^1\Sigma_g^+$ state are attractive.

These are the single degenerate $^3\Pi_{0u}^-$ state, and the doubly Ω-degenerate $^3\Pi_{1u}$, $^3\Pi_{1g}$ and $^3\Pi_{2u}$ states. Of these, only the first two are optically accessible from the ground state and only the $^3\Pi_{1u}$ has been observed (Brown 1931).

Calculations were carried out to determine the parameters of the I_2^* internuclear potential which would account for the fall-off, while giving a reasonable collision diameter for reaction (19). The equilibrium constant was evaluated for a number of well depths (E) and equilibrium separations (R_{eq}) for I_2^*, using the expression Kim (1967)† obtained from Hill's (1955) partition function integrals:

$$K = \frac{64}{45}\frac{R_{eq}^3}{\sqrt{2}}\left[\pi\left(\frac{E}{kT}\right)^3\right]^{\frac{1}{2}}\frac{g_M}{g_A^2}F\left(\frac{E}{kT}\right), \tag{24}$$

where g_M/g_A^2, the ratio of molecular to atomic degeneracies, is taken to be 2/16, and $F(E/kT)$ is the generalized hypergeometric series (Erdelyi 1953):

$$_2F_2(1, 1; 7/4, 9/4; E/kT). \tag{25}$$

Expression (24) assumes a Lennard-Jones (12–6) interaction potential for I_2^*.

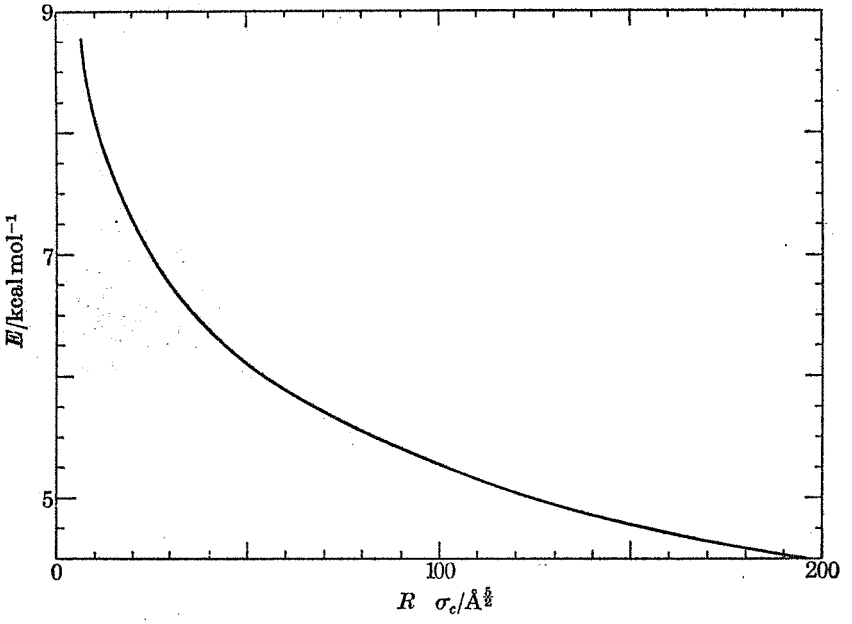

FIGURE 3. Plot of $\sigma_c R_{eq}^{\frac{2}{3}}$ for electronically excited iodine, I_2^*, against the interaction well depth, E. The curve was obtained by combining the fitted value of Kk_{19} with equation (24) and with the kinetic theory hard sphere collision frequency.

The calculated equilibrium constants were combined with the derived value of Kk_{19} to give corresponding values for k_{19}. From each value of k_{19}, the hard sphere collision diameter σ_c for reaction (19) was calculated assuming zero activation energy and unit probability factor. In figure 3, $\sigma_c R_{eq}^{\frac{2}{3}}$ is plotted against E, showing the possible combinations of collision diameter, equilibrium separation and well depth

† Modified for homonuclear molecules by multiplication by a statistical factor of ½.

for I_2^*. It follows from this plot that for a reasonable value of σ_c the value of E should be somewhere between 21 and 29 kJ mol^{-1} (5 and 7 kcal mol^{-1}). This is three times the 7.5 kJ mol^{-1} (1.8 kcal) depth of the potential well of $A^3\Pi_{1u}$, the only observed (Brown 1931) excited I_2^* state which dissociates to two $^2P_{\frac{1}{2}}$ atoms. However, Chang's (1967) calculations show that at long range the $^3\Pi_{1g}$ and $^3\Pi_{2u}$ states are respectively 2 and $3\frac{1}{2}$ times more strongly attractive than $A^3\Pi_{1u}$. Hence, one of these states will probably have the 21 to 29 kJ mol^{-1} well depth required of an acceptable I_2^* complex. We therefore conclude that this mechanism (equations (15) to (19)) makes an acceptable prediction for the nature of the internuclear potential of I_2^*.

As a check on equation (24), the equilibrium constant K for formation of I_2^* in the $A\ ^3\Pi_{1u}$ state was calculated directly. The internal partition function was based on vibrational energies observed by Brown (1931) and rotational constants calculated from formulae given by Herzberg (1950). This yielded $K = 0.0851\,\text{mol}^{-1}$, only 20% larger than the corresponding $0.0721\,\text{mol}^{-1}$ value generated from expression (24). This concurs with the conclusion that the 7.5 kJ (1.8 kcal) mol^{-1} deep $A\ ^3\Pi_{1u}$ state cannot be the main cause of the drop off.

Condition (2) can now be further tested by considering the asymptotic forms of expression (20) for very large and very small concentration ratios. An approximate value of $([I_2]/[M])_{dev}$ may be obtained by solving equations (22) and (23) for their point of intersection

$$\left(\frac{[I_2]}{[M]}\right)_{dev} \approx \frac{k_{17}}{K k_{19}}. \tag{26}$$

Since the relative efficiencies of various third bodies depend principally on the stability of the intermediate IM complex, it seems reasonable to assume that the relative efficiencies are independent of the final iodine electronic state formed. Thus k_{15} and k_{17} would show the same dependence on the choice of third body M, and hence $k_{17} \propto k_M$, where k_M is the experimentally obtained intercept of equation (23). Therefore, (26) becomes

$$([I_2]/[M])_{dev} \propto k_M. \tag{27}$$

Christie (1962) has noted just such a linear relation between the experimental values of $([I_2]/[M])_{dev}$ and k_M. Moreover, the linear relation (27) predicts that the fall-off should be observed with helium as third body at values of $[I_2]/[He]$ which are smaller than those used by Christie *et al.* (1955). Thus, from this viewpoint, the data of Christie *et al.* supports this mechanism (equations (15) to (19)). However, the mechanism fails to explain the difference between the 298 K value of $([I_2]/[Ar])_{dev}$ obtained by Christie *et al.* (1955), i.e. 4×10^{-4}, and that reported here, i.e. 1×10^{-4} (see figure 1).

The temperature dependence of $([I_2]/[M])_{dev}$ may be determined by rearrangement of equation (26) to yield

$$\left(\frac{[I_2]}{[M]}\right)_{dev} \approx \frac{k_{-17}}{k_{19}}. \tag{28}$$

Assuming that k_{19} has zero activation energy and that k_{-17} has an activation energy equal to the well depth of the internuclear interaction in I_2^* (i.e. 21 to 29 kJ mol^{-1}),

equation (28) predicts a twofold increase in $([I_2]/[M])_{dev}$ as temperature is increased from 298 to 323 K, and a 10 to 20-fold increase in $([I_2]/[M])_{dev}$ as temperature is increased from 298 to 423 K. Although the data of this work at 323 and 423 K are somewhat scattered, it appears that this prediction is not fulfilled; the onset of the fall-off appears to be roughly independent of T (figures 1 and 2).

The fourth requirement of the mechanism, that it explain the discrepancies which figure 1 shows to exist among the results obtained in different laboratories, is also not fulfilled. This mechanism does not suggest any route by which the diverse sets of data can be made self-consistent.

The mechanism involving electronically excited I_2^* can explain the fall-off only if it is assumed that I_2^* is deactivated very efficiently by $I_2(^1\Sigma_g^+)$, so that the deactivation by inert gas is a slower process by a factor of 10^{-5}. Theoretical studies by Nikitin (1966) support such an assumption. However, Steinfeld & Klemperer (1965) found that $I_2(^1\Sigma_g^+)$ was only *ca.* seven times more efficient than Ar in the electronic de-excitation of $I_2(^3\Pi_{0u}^+)$.

Participation of intermediate IM *complex*

An alternative explanation for the low-ratio fall-off has been proposed by Troe & Wagner (1967), who measured the dissociation rate constant for iodine in argon in high pressure (*ca.* 10 MN m^{-2}; 100 atm) shock waves. They observed a transition in the dissociation rate constant from bimolecular to unimolecular with increasing argon pressure. They suggest that the recombination rate constant should undergo a similar transition from third to second order, and by extrapolating their results to room temperature they predict that the transition argon concentration would be approximately 70 mmol l^{-1}. A similar effect has been observed by Porter, Szabo & Townsend (1962) for iodine atom recombination in high pressures of nitric oxide chaperon.

In this case, the mechanism is that given by equations (3) to (5), where I_2 and a single inert gas M are the only chaperons present for the cases experimentally considered. Furthermore, since the absolute concentrations of I_2 used experimentally are always quite small, it is safe to assume that $K_{3I_2}[I_2] \ll 1$. In this case, (9) becomes

$$k_{obs} = \frac{K_{3M}k_{4M} + K_{3I_2}k_{4I_2}[I_2]/[M] + K_{3M}^2 k_{5M-M}[M]}{(1+K_{3M}[M])^2}. \quad (29)$$

The room temperature data of this work (both apparatuses) and the data of Christie *et al.* (1955) and of Strong *et al.* (1957) for M = Ar were fitted to (29) using a Hooke & Jeeves (1961) pattern search method. The best fit was obtained with a negative value of $K_{3M}^2 k_{5M-M}$, indicating that the effect of reaction (5) was less than the experimental scatter in the data.† The data were then fitted to an expression which neglected reaction (5):

$$k_{obs} = \frac{K_{3M}k_{4M} + K_{3I_2}k_{4I_2}[I_2]/[M]}{(1+K_{3M}[M])^2}. \quad (30)$$

† Furthermore, a fit with the four parameters constrained to be positive yielded an insignificantly small value of $K_{3M}^2 k_{5M-M}$ which had a very large uncertainty.

TABLE 3. RATE AND EQUILIBRIUM CONSTANTS AT ROOM TEMPERATURE

These values are obtained for M = Ar from a fit of equation (30) to 58 experimental k_{obs}; the fit had a standard error of ± 10 %.

$K_{3Ar}/l\,mol^{-1}$	$3.18(\pm 0.63)$
$K_{3Ar}k_{4Ar}/l^2\,mol^{-2}\,s^{-2}$	$3.00(\pm 0.16)\times 10^9$
$K_{3I_2}k_{4I_2}/l^2\,mol^{-2}\,s^{-2}$	$1.00(\pm 0.09)\times 10^{12}$
$k_{4Ar}/l\,mol^{-1}\,s^{-1}$	0.94×10^9
$k_{4I_2}/l\,mol^{-1}\,s^{-1}$	1.7×10^9
$K_{3I_2}/l\,mol^{-1}$	6×10^2

The results of this fit are listed in table 3 along with calculated values for K_{3I_2} and k_{4I_2}. The latter were obtained by assuming that the steric factor for k_{4I_2} (unity) was twice that for k_{4Ar}. The standard error of the fit was ± 10 %; a total of 58 points were fitted. This agreement contrasts with the discrepancies in these results when

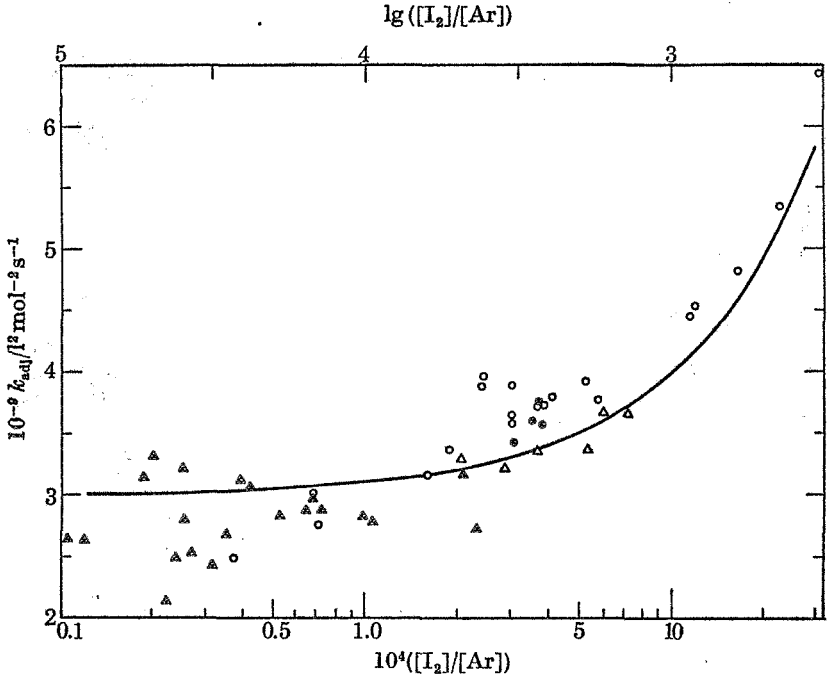

FIGURE 4. Plot of $k_{adj} = k_{obs}(1 + K_{3Ar}[Ar])^2$ against lg ([I_2]/[Ar]) at 298 K. Data as in figure 1 and table 2; the curve is obtained by substituting the constants of table 3 into equation (30). ◉, Strong *et al* (1957); ○, Christie *et al.* (1955); ▲, this work—apparatus 1; △, this work—apparatus 2; ——, best curve.

they are treated according to (10) (see figure 1). In figure 4, $k_{adj} = k_{obs}(1 + K_{3Ar}[Ar])^2$ is plotted against log ([I_2]/[Ar]); the experimental points and the curve represented by the parameters of table 3 are shown. It was not possible to apply this analysis to the data of Bunker & Davidson (1958), since the individual values of [I_2] and [Ar] were not available.

Calculations were carried out to determine the plausibility of the numerical values of table 3. The value of $k_{4\mathrm{Ar}}$ was used to obtain the hard sphere collision diameter for reaction (4). The activation energy was assumed to be zero; a probability factor of 0.5 and an electronic degeneracy factor of $\frac{1}{16}$ for reaction (4) were also assumed. The calculated value, 0.23 nm, is reasonable in view of the approximations made.

The experimental value of $K_{3\mathrm{Ar}}$ was applied to expression (24)† to yield the combination of values of well depth, E, and equilibrium separation, R_{eq} for the I–Ar interaction, which combination corresponds to the experimental equilibrium constant. These are plotted in figure 5.

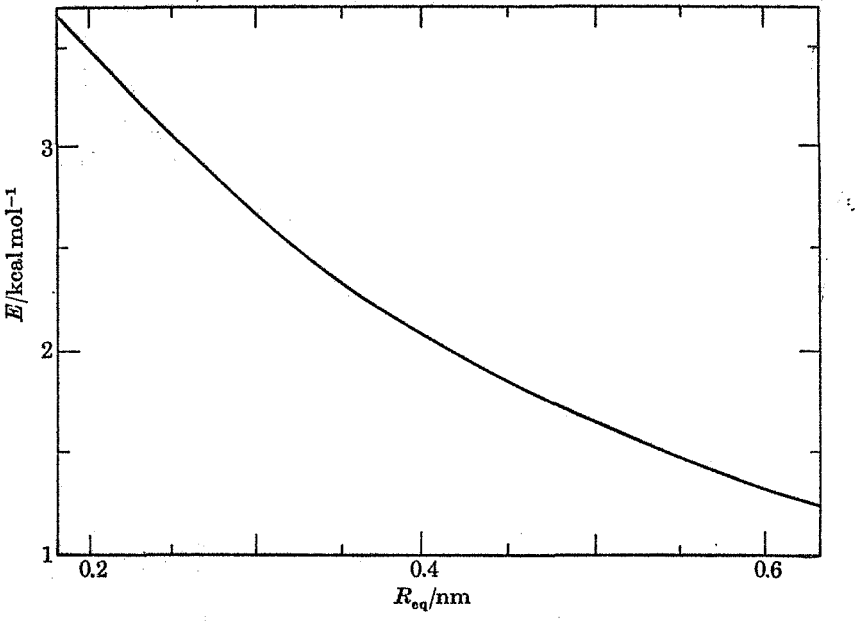

FIGURE 5. I–Ar Interaction potentials: combinations of E (well depth) and R_{eq} (equilibrium separation) which, on substitution into equation (24)† yield the derived (table 3) value of $K_{3\mathrm{Ar}}$.

Finally, the calculated value of $K_{3\mathrm{I}_2}$ was substituted into equation (10), and it was found that the assumption, that $K_{3\mathrm{I}_2}[\mathrm{I}_2] \ll 1$, is justified over the experimental range of $[\mathrm{I}_2]$.

As an additional test, the temperature dependence of k_{Ar} (defined by equation (10) as $k_{\mathrm{Ar}} = K_{3\mathrm{Ar}} k_{4\mathrm{Ar}}$) is predicted by this mechanism. Since reaction (4) is unlikely to have any activation energy, the temperature dependence of $k_{4\mathrm{Ar}}$ was assumed to be $T^{\frac{1}{2}}$. Also the temperature dependence of $K_{3\mathrm{Ar}}$ may be determined from equation (24) for any of the 'suitable' potentials illustrated by figure 5. The resulting temperature dependence of k_{Ar} for two such I–Ar potentials is shown in figure 6

† Multiplied by a statistical factor of 2 for heteronuclear molecules, and with $g_{\mathrm{M}}/g_{\mathrm{A}}^2$ replaced by $g_{\mathrm{IM}}/g_{\mathrm{I}}g_{\mathrm{M}} = 1$.

along with available experimental data. Values are scaled relative to the 298 K value given in table 3. This shows that an I–Ar interaction potential 6.3 kJ (1.5 kcal) mol^{-1} deep with an equilibrium separation of 0.55 nm can account for both the negative temperature dependence of k_{Ar} and the apparent low concentration ratio fall-off.

The IM mechanism may be further tested by considering its predictions with respect to the four factors treated in the discussion of the I_2^* mechanism.

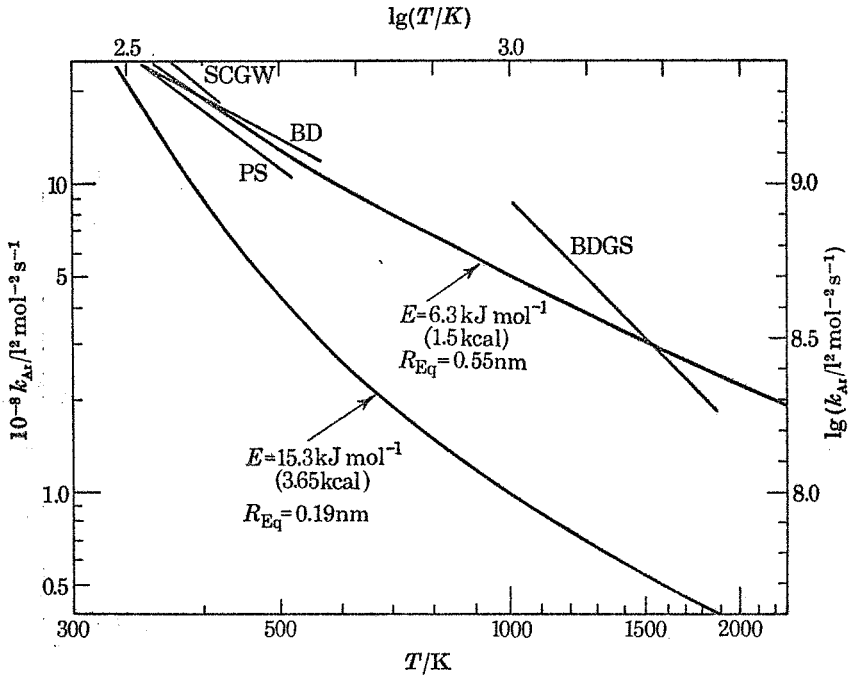

FIGURE 6. Temperature dependence of k_{Ar} for two possible I–Ar interaction potentials. The experimental curves are : SCGW, Strong *et al.* (1957); BD, Bunker & Davidson (1958); PS, Porter & Smith (1961); BDGS, Britton, Davidson, Gehman & Schott (1955).

The first of these involves the plausibility of the internuclear potential required by the intermediate IM species. This interaction potential is some five times deeper than that calculated for van der Waals' forces between argon and xenon (1.25 kJ mol^{-1}; 0.3 kcal mol^{-1}), which is iodine's neighbour in the periodic table. This appears quite reasonable to us.

Inspection of expression (30) indicates that the fall-off will begin, not at a critical concentration ratio, but at some critical third body concentration; i.e. when $K_{3M}[M]$ ceases to be negligible compared with unity. Thus for various third bodies, the critical third body concentration $[M]_{dev}$ is proportional to $1/K_{3M}$. If similar I_2 concentrations are used in all experiments, as was done in the work of Christie *et al.* (1955), we may therefore write

$$([I_2]/[M])_{dev} \propto K_{3M}.$$

Furthermore, assuming that k_{4M} will change only slightly for different third bodies M, the equation (1) definition of k_M yields

$$[I_2]/[M]_{dev} \propto K_{3M} k_{4M} = k_M.$$

This is the approximate relation noted by Christie (1962). Hence, the IM mechanism correctly predicts the M dependence of $([I_2]/[M])_{dev}$.

The value of $[M]_{dev}$, as stated previously, is proportional to $1/K_{3M}$. As the temperature increases, K_{3M} will decrease; thus $[M]_{dev}$ will increase. Again assuming that similar I_2 concentrations are used at all temperatures, this mechanism predicts a decrease in $([I_2]/[M])_{dev}$ with increasing temperature. However, in this case the temperature dependence is relatively small because the potential well of the IAr complex is only about 6.3 kJ mol^{-1} deep. Temperature increases from 298 to 323 K or 423 K respectively, would invoke 18 % and 50 % decreases in $([I_2]/[Ar])_{dev}$, which is well within the experimental uncertainty (see figures 1 and 2).

The final test of the IM mechanism is whether or not it accounts for the discrepancies, shown in figure 1, between experimental values of k_{obs} obtained in different laboratories. A cursory examination of figure 4 shows this to be the case.

The above arguments have shown that taking account of the steady state concentration of IM intermediate is the only way of explaining the low concentration ratios drop-off which agrees with *all* the experimental observations. In addition, this mechanism explains the observed negative temperature dependence of the experimental rate constants and predicts the depth and minimum position of the IAr potential well.

This work was supported in part by the National Research Council of Canada, by the Defence Research Board of Canada, grant no. 9530–34, and by the Directorate of Chemical Sciences, U.S. Air Force Office of Scientific Research, grant no. 506-64, 66 and 69. Acknowledgement is also made to the donors of the Petroleum Research Fund, administered by the American Chemical Society for partial support of this research. Three of us (J. A. Blake, R. J. LeRoy and D. J. Morriss) held graduate fellowships granted by the Government of the Province of Ontario, Canada.

Note added in proof, 17 *November* 1969. Christie *et al.* (1955) have reported room temperature recombination rate constants for each of the other inert gases: He, Ne, Kr, and Xe. These sets of data were fitted in turn to equation (30), with $K_{3I_2} k_{4I_2}$ held fixed at the value given in table 3 (1.0×10^{12} l^2 mol^{-2} s^{-2}). The results are presented in table 4, where $k_M = K_{3M} k_{4M}$. There were too few experimental points to allow K_{3M} to be determined with precision, and for M = He and for one of the fits with M = Ne, K_{3M} was arbitrarily set equal to 1.0.

TABLE 4. RATE AND EQUILIBRIUM CONSTANTS AT ROOM TEMPERATURE FOR M = He, Ne, Kr AND Xe

M	$K_{3M}/l^2\ mol^{-2}\ s^{-1}$	$10^{-9}\ k_M/l^2\ mol^{-2}\ s^{-1}$
He	(1.0)	1.0 (± 0.2)
Ne	(1.0)	1.4 (± 0.2)
	0.1 (± 6.0)	1.3 (± 0.3)
Kr	7.3 (± 4.6)	4.4 (± 0.5)
Xe	5.4 (± 2.3)	5.4 (± 0.3)

The results listed in tables 3 and 4 were obtained using the University of Wisconsin Computing Centre nonlinear regression library GASAUS.

REFERENCES

Britton, D., Davidson, N., Gehman, W. & Schott, G. 1956 *J. Chem. Phys.* **25**, 804.
Brown, W. G. 1931 *Phys. Rev.* **38**, 1187.
Bunker, D. L. & Davidson, N. 1958 *J. am. Chem. Soc.* **80**, 5085.
Burns, G. 1967 *Can. J. Chem.* **45**, 2369.
Burns, G. & Hornig, D. F. 1960 *Can. J. Chem.* **38**, 1702.
Chang, T. Y. 1967 *Rev. mod. Phys.* **39**, 911.
Christie, M. I., Harrison, A. G., Norrish, R. G. W. & Porter, G. 1955 *Proc. Roy. Soc. Lond.* A **231**, 446.
Christie, M. I. 1962 *J. am. Chem. Soc.* **84**, 4066.
Donovan, R. J. & Husain, D. 1965 *Nature, Lond.* **206**, 171.
Engleman, Jr. R. & Davidson, N. R. 1960 *J. am. Chem. Soc.* **82**, 4770.
Erdelyi, A. (Editor) 1953 *Higher transcendental functions*, vol. 1, 182. New York: McGraw-Hill.
Gillespie, L. J. & Fraser, L. H. D. 1936 *J. am. Chem. Soc.* **58**, 2260.
Herzberg, G. 1950 *Molecular spectra and molecular structure*, pp. 106–108. Princeton. Van Nostrand.
Hill, T. L. 1955 *J. Chem. Phys.* **23**, 617.
Hooke, R. & Jeeves, T. A. 1961 *J. Ass. comput. Mach.* **8**, 212.
Kramer, H. H., Hanes, M. H. & Bair, E. J. 1961 *J. Opt. Soc. Am.* **51**, 775.
Kim, S. K. 1967 *J. Chem. Phys.* **46**, 123.
Nikitin, E. E. 1962 *Kinet. Katal.* **3**, 830.
Nikitin, E. E. 1966 *Theory of thermally induced gas phase reactions* p. 128. Bloomington: Indiana University Press.
Porter, G., Szabo, Z. G. & Townsend, M. G. 1962 *Proc. Roy. Soc. Lond.* A **270**, 493.
Porter, G. & Smith, J. A. 1961 *Proc. Roy. Soc. Lond.* A **261**, 28.
Rabinowitch, E. 1937 *Trans. Faraday, Soc.* **33** 283.
Rabinowitch, E. & Wood, W. C. 1936 *J. Chem. Phys.* **4**, 497.
Shields, F. D. 1960 *J. Acoust. Soc. Am.* **32**, 180.
Snider, N. S. 1966 *J. Chem. Phys.* **45**, 3299.
Steinfeld, J. I. & Klemperer, W. 1965 *J. Chem. Phys.* **42**, 3475.
Strong, R. L., Chien, J. C. W., Graf, P. E. & Willard, J. E. 1957 *J. Chem. Phys.* **26**, 1287.
Troe, J. & Wagner, H. G. 1967 *Z. phys. Chem.* N.F. **55**, 326.

VOCABULARY REVIEW FORM

NO.:

SUBJECT TERM: Nuclear Potential

STI DIVISION ACTION: ☐ APPROVED ☐ DISAPPROVED

COMMENTS:

☒ ADD AS A NEW TERM: ☒ POSTABLE ☐ NONPOSTABLE
☐ ADD OR DELETE CROSS REFS. AS SHOWN BELOW.
☐ CHANGE SPELLING FROM:

☐ DELETE
☐ DELETE AND TRANSFER TO:

☐ CHANGE TERM TYPE (Specify)

SUGGESTED BY: ☒ AIAA ☐ FACILITY ☐ L. C.
~~AIAA~~ NEN ☐ OTHER:

DATE: 31 March 71

SIGNATURE:

IN LIEU TERM: Potential Energy

DATE:

SCOPE NOTES (SN):

CATEGORIES:

USE (U) [Add or Delete]:

USED FOR (UF) [Add or Delete]:

BROADER TERMS (BT) [Add or Delete]:

either NT or RT to Potential energy,

RELATED TERMS (RT) [Add or Delete]:

NARROWER TERMS (NT) [Add or Delete]:

depending on which deffinition you like

DEFINITION:

COMMENTS:

ITEM ACCESSION NO.:	ISSUE	CATEGORY
N71-19737	09	24

TEST 6801.1

N71-19747

VOCABULARY REVIEW FORM

NO.:

SUBJECT TERM: Potential Barriers

STI DIVISION ACTION:
☐ APPROVED ☐ DISAPPROVED

COMMENTS:

☒ ADD AS A NEW TERM: ☒ POSTABLE ☐ NONPOSTABLE
☐ ADD OR DELETE CROSS REFS. AS SHOWN BELOW.
☐ CHANGE SPELLING FROM:

☐ DELETE
☐ DELETE AND TRANSFER TO:

☐ CHANGE TERM TYPE (Specify)

SUGGESTED BY: ☐ AIAA ☒ FACILITY ☐ L. C.
NEN ☐ OTHER:

DATE: 1 April 71

SIGNATURE:

DATE:

IN LIEU TERM: Coulomb Potential

SCOPE NOTES (SN):

CATEGORIES:

USE (U) [Add or Delete]:

USED FOR (UF) [Add or Delete]:

BROADER TERMS (BT) [Add or Delete]:

RELATED TERMS (RT) [Add or Delete]:

Coulomb Potential
nuclear physics
nuclear potential
nuclear chemistry

NARROWER TERMS (NT) [Add or Delete]:

DEFINITION:

COMMENTS:

ITEM ACCESSION NO.:	ISSUE	CATEGORY
N71-19737	09	24

TEST 6801.1

N71-19747